laboratori nazionali di frascati

2002 ANNUAL REPORT

$$\frac{\Gamma(K_S \to \pi^+\pi^-(\gamma))}{\Gamma(K_S \to \pi^0\pi^0)} = 2.236 \pm 0.003_{STAT} \pm 0.015_{SYST}$$

Phys. Lett. B 538, (2002) 21-28

$$BR(K_S \to \pi e \nu) = (6.91 \pm 0.34_{STAT} \pm 0.15_{SYST}) \cdot 10^{-4}$$

Phys. Lett. B 535, (2002) 37-42

KLOE ▮ 2002 PHYSICS PAPERS

$$BR(\phi \to \pi^0\pi^0\gamma) = (1.09 \pm 0.03_{STAT} \pm 0.05_{SYST}) \cdot 10^{-4}$$

Phys. Lett. B 537, (2002) 21-27

$$BR(\phi \to a_0\,\gamma \to \eta\,\pi^0\gamma) = (7.4 \pm 0.7) \cdot 10^{-5}$$

Phys. Lett. B 536, (2002) 209-216

$$\frac{\Gamma(\phi \to \eta'\gamma)}{\Gamma(\phi \to \eta\,\gamma)} = (4.70 \pm 0.47_{STAT} \pm 0.31_{SYST}) \cdot 10^{-3}$$

$q_{\eta'} = (41.8^{+1.7}_{-1.6})^\circ$ Phys. Lett. B 541, (2002) 45-51

The LNF Beam Test Facility (BTF)

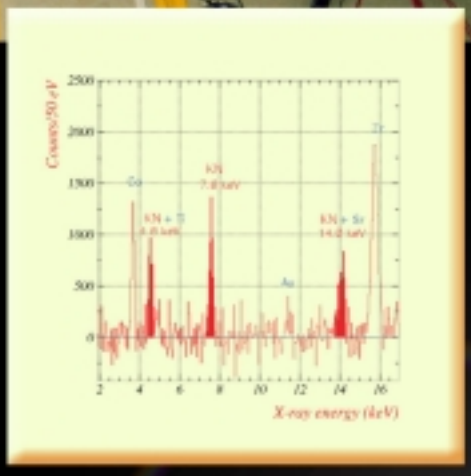

DEAR ▮ WORLD-FIRST MEASUREMENT OF THE KAONIC NITROGEN SPECTRUM

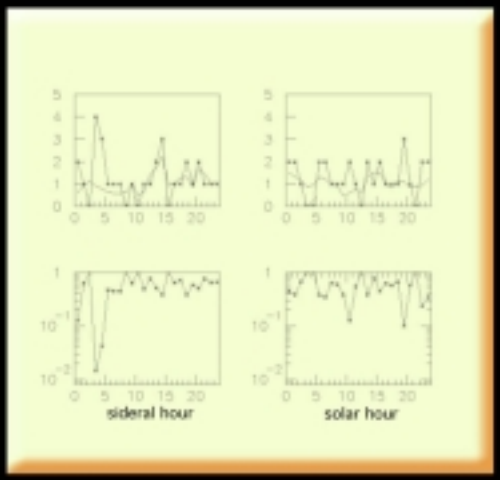

NAUTILUS ▮ COINCIDENCES WITH EXPLORER

Front Cover

The two top right figures list the physics papers published in 2002 by the KLOE Collaboration (see page 25). The central photoshows the new LNF Beam Test Facility (BTF, see page 172). The bottom right figure reports the measurement of thekaonic nitrogen spectrum by the DEAR experiment (see page86). The bottom left figure shows the coincidences recorded by Nautilus and Explorer (see page 65).

Inside Cover

Aerial view of the Laboratori Nazionali di Frascati dell'INFN.

Back Cover

Elementary school children visiting LNF

Cover artwork by: Claudio Federici

istituto nazionale di fisica nucleare

laboratori nazionali di frascati

2002
ANNUAL REPORT

LNF-03/010 (IR)
June 10, 2003

Editor
Simone Dell'Agnello

Technical Editor
Luigina Invidia

Published by
SIS-Pubblicazioni
P.O.Box 13 – I–00044 Frascati (Italia)

Available at www.lnf.infn.it/rapatt

Sergio Bertolucci
LNF Director

Lucia Votano
Head, Research Division

Pantaleo Raimondi
Head, Accelerator Division

LNF Scientific Coordinators

Maria Curatolo
Particle Physics

Marco Ricci
Astroparticle Physics

Valeria Muccifora
Nuclear Physics

Calogero Natoli
Theory and Phenomenology

Francesco Celani
Techn. and Interdisciplinary Research

ACKNOWLEDGMENTS

I would like to thank Luigina Invidia, for her hard work and her relentless effort to complete the project within the planned yearly deadline. Many thanks also to Claudio Federici, who created the cover page and shot the photos, for his graphics skills. I am also grateful to Sergio Bertolucci and Stefano Bianco for their many helpful suggestions and encouragments.

Finally, I want to thank the authors of the reports included in this book, for the interesting scientific contributions they gave to INFN.

Simone Dell'Agnello
Editor

Laboratori Nazionali di Frascati dell'INFN

2002 ANNUAL REPORT

CONTENTS

5 — Technological and Interdisciplinary Research

6 — Accelerator Physics

ATLAS

A. Antonelli, M. Antonelli, M. Beretta, S. Bertolucci, H. Bilokon, S. Braccini,
E. Capitolo (Tecn.), V. Chiarella, M. Curatolo, B. Dulach, B. Esposito (Resp.),
G. Felici, M.L. Ferrer, P. Laurelli, W. Liu, G. Maccarrone, A. Martini, G. Nicoletti,
G. Pileggi (Tecn.), B. Ponzio (Tecn.), V. Russo (Tecn.), A. Sansoni, Y. Zhang

1 Introduction

The ATLAS experiment [1)] is one of the two general purpose experiments at the LHC at CERN. It has been designed to exploit the full physics potential of the LHC, with excellent performances in the detection and measurement of jets, electrons, muons, photons, and missing transverse energy. A world wide collaboration of more than 150 institutions is committed in the realization of this detector of unprecedented size and complexity. After an intense Research and Development (R&D) phase, aimed at the development of appropriate detection devices able to cope with the complexity of the events, the rate of interaction, the background conditions and the radiation environment, the construction of the ATLAS detector started and the completion is foreseen for the end of the year 2006.

The Frascati group has given an important contribution to the design and development of the precision tracking chambers of the ATLAS muon spectrometer [2, 3)] and has taken the commitment of the construction of the Barrel Middle Large (BML) chambers, which represent about 10% of the chambers. The ATLAS muon spectrometer has been designed to achieve very good momentum resolution in stand-alone mode. It consists of super-conducting toroids, instrumented with very high precision tracking chambers, the so-called MDT (Monitored Drift Tubes) chambers, and RPC and TGC chambers for triggering. The MDT chambers are large area (about 5000 m^2) high precision (about 80 μm intrinsic resolution) detectors, based on the assembly of high-pressure drift tubes. Two multi-layers of tubes are glued on the two sides of a support structure, called "spacer". The design project requires the wires to be positioned at less than 20 micron r.m.s. precision. The Frascati group has contributed with the design of the assembly jig (Fig. 1), necessary to achieve such a mechanical precision, and the design of a fully automated wiring machine (Fig. 2). Also an automated leak test station (Fig. 3) and a wire tension-meter (Fig. 4) have been designed and built by the Frascati group.

2 Activity in the year 2002

The production of the BML MDT chambers [4)]for the ATLAS Muon Spectrometer has proceeded successfully, with the assembly of 37 chambers in the coarse of the year 2002. The achieved production is above the goal set for the year. At the end of the year 2002 the total number of chambers produced was 53. This represents 56% of the production, to be compared with the 45% milestone value set for the end of the year 2002.

A new technique for the assembly of the spacer, proposed and implemented by the Frascati group, was developed for simplifying and speeding-up the production (Fig. 5). The new tools were designed and realized in the first months of the year and with their adoption the production rate went up from 1 chamber per 7 working days to 1 chamber per 6 working days.

The mechanical precision of the assembly of the BML chambers, which has to comply with the challenging specification of better than 20 μm rms on the wire positioning, was monitored continuously during the assembly procedure with the monitoring systems, based on optical sensors and incorporated in the precision assembly tools (Fig. 6).

Figure 1: *The high precision jig for the positioning of the tubes.*

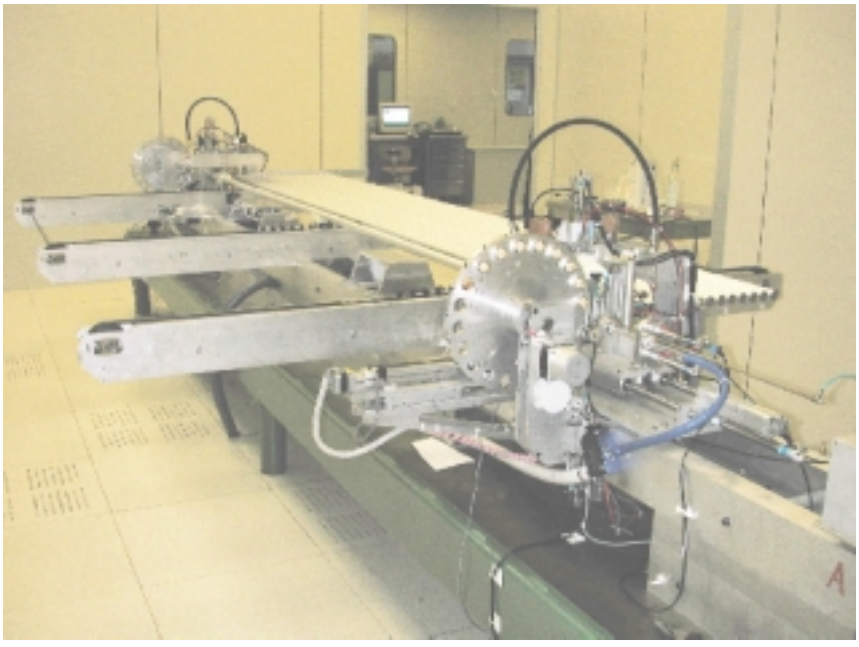

Figure 2: *The "Tub-o-matic" fully automated wiring machine.*

Figure 3: *The gas leak test station based on a helium spectrometer.*

Figure 4: *The wire tension meter (WTM) station.*

A sample of BML chambers has been checked by means of a x-ray tomography scan at CERN. The tomography measurements show a precision on the positioning of the wires well below 20 μm, confirming the results achieved with the measurements of 3 chambers in 2001 and 1 chamber in 2000. All the phases of the construction of the MDT chambers are done at LNF, including tube wiring and tube testing. About 12000 tubes were wired and tested in the year 2002. The test of the MDT chambers and of the related systems (alignment, DAQ, DCS) was performed on the muon beam H8 at CERN [5]. A set up reproducing two barrel towers of the Atlas muon precision tracking chambers was realized, fully equipped with the alignment sensors, read-out with the so-called DAQ-1 system and monitored with the DCS (Fig. 7). The Frascati group contributed two BML chambers fully equipped and took care of the installation and setting up of the chambers. Together with the other muon groups, the LNF group participated in DAQ setting up and in the data collection and analysis. The resolution of a BML chamber is shown in Fig. 8. This first system test was successful. It provided important results on the detector itself, on the alignment systems, on the operation and performance of the electronics and DAQ.

In the year 2002 also the cosmic ray test station in Frascati was put in operation (Fig. 9). A program of measurements was started to study the gas mixture and the features of the gas distribution systems. A typical TDC spectrum and a reconstructed muon track are shown in Fig. 10 and Fig. 11.

After the "bare" chambers have been assembled, they need to be equipped with the gas distribution system, the Faraday cage and the electronics. These operations are done in parallel with the main production line dedicated to the chamber assembly. The gas distribution system is complex, composed of many pieces (gas bar, connectors, tubelets, O-rings, etc.). All the assembly operations are manpower and time consuming. The gas tightness specification is very stringent, i.e. 2×10^{-8} bar·l/s per tube. The chambers are operated at 3 bar absolute pressure and this leak rate corresponds typically to a pressure drop of less than 1 mbar per day. Great care is required in the various assembly operations needed and very sensitive leak test methods have to be applied, based on a helium detector. The certification is done by means of the measurement of the pressure drop over 1-2 days. In the first half of the year 2002 10 chambers have been equipped and certified to be within the Atlas specifications. Unfortunately the brass tubelets of the gas system were found to have some probability to develop cracks with time and give rise to large leaks in chambers previously certified. For this reason the collaboration has decided to replace all the brass tubelets and to adopt stainless steel tubelets. Therefore the equipping of the chambers has been stopped and will be resumed as soon as the stainless steel tubelets will become available.

While the MDT chambers track with high precision the muons, the trigger on muons is provided by RPC chambers. MDTs and RPCs are to be mounted in one station by common supports and the MDT-RPC station will be mounted as a whole on the Atlas detector. In the case of the MDT BML chambers, which are under responsibility of the LNF group, each MDT chamber has to be packed between two RPC chambers. The common supports for the BML chambers have been designed by the Frascati group in close contact with RPC groups. Prototypes of the common supports have been realized and a first test of the mechanical assembly of RPC and MDT has been made in Frascati (Fig. 12). The test was successful and provided important indications for the tools to be developed for the assembly in series of MDT and RPC to be started at CERN in 2003.

Since November 2002, the Frascati group is represented with 1.5 FTE in the Trigger/DAQ subsystem. Activity in the data acquisition field was already done in particular for what concerns the MDT test station in Frascati and the active participation to the test beam at CERN. The new involvement is related to software development in the DataFlow activity. DataFlow is the DAQ component that transports acquired data from the read-out system to the storage devices. The model implemented by the DataFlow group has to be integrated in order to be used at the next test beam at CERN.

Figure 5: *The set-up for the construction of the spacers. The new spacer is glued upon a high precision structure, based of two identical spacers built on a precision granite table.*

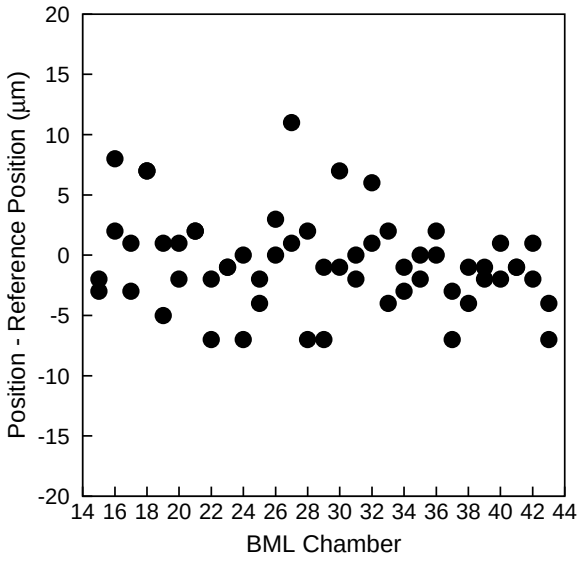

Figure 6: *The positioning of the chamber with respect to the granite table is measured with high precision during the construction and compared with reference values. The measurements put in evidence a high precision and an excellent reproducibility.*

Figure 7: *The set-up of the H8 test beam at CERN showing the two fully equipped BML chambers produced at the LNF.*

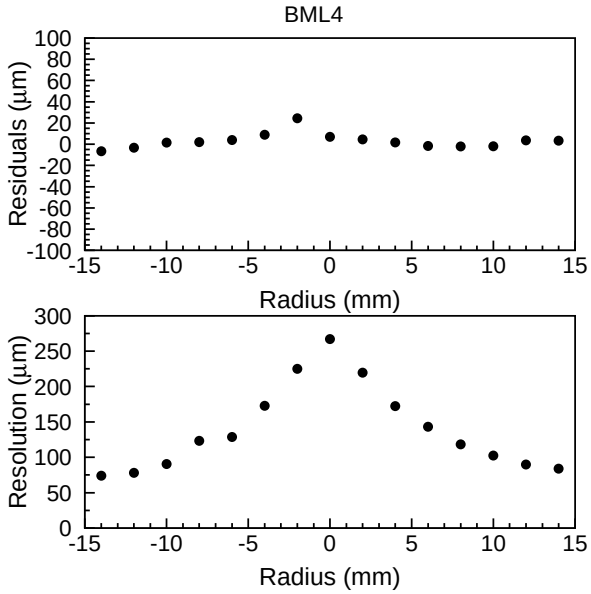

Figure 8: *The residuals and the resolution as a function of the radius of hits in the drift tubes for a BML chamber measured on the muon beam H8 at CERN.*

Figure 9: *The cosmic ray stand in Frascati.*

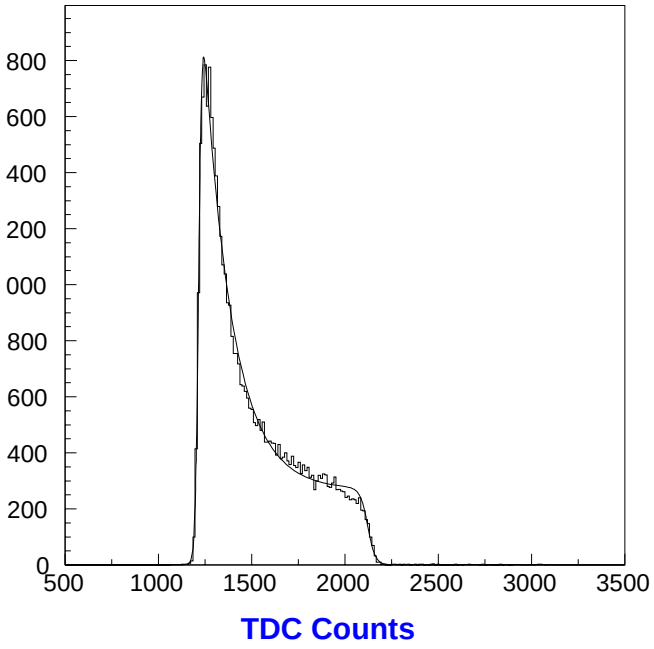

Figure 10: *A typical drift tube TDC spectrum registered at cosmic ray stand in Frascati.*

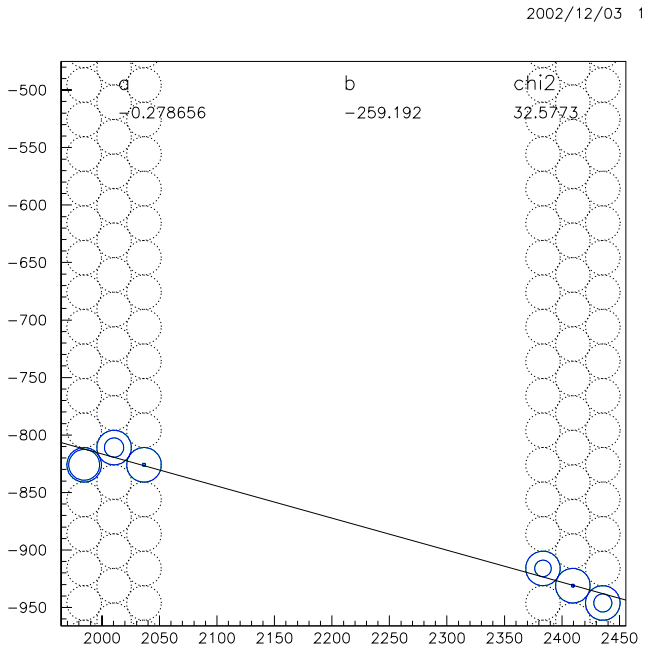

Figure 11: *A reconstructed cosmic muon track at cosmic ray stand in Frascati.*

Figure 12: *The MDT RPC integration realized by the common supports designed at the LNF.*

During 2002 the activity of the Frascati group in this field was dedicated to install the acquisition software in the PC farm of Group I, to measure performances and to acquire the required knowledge to be able to integrate it with new components. The program for 2003 is to develop an interface allowing the monitoring of full events built at the end on the acquisition chain. The group programs also to collaborate in the "muon detector slice" to be installed in Rome I, in particular in the porting of algorithms developed for the second level trigger into the DAQ related processes.

The group participated in the analysis and software work, not only on test beam and cosmic ray station data, but also in the framework of the Atlas Data Challenge. A production of simulation and reconstruction jobs with the Atlas software package was run on a PC farm at LNF.

3 Program of activity for the year 2003

In the year 2003 the MDT chamber production will continue and the chamber equipping work will restart. Toward the end of the year the preassembly of MDT and RPC stations will start at CERN, and the final test will be done, in order to make the chambers "ready for installation". The test beam activity and the measurements on the LNF cosmic ray station will continue and complete MDT-RPC stations will be tested. The work on the trigger DAQ area will proceed, as well as the offline software and analysis work.

References

1. ATLAS, Detector and physics performance, Technical Design Report, CERN/LHCC/99-14 and CERN/LHCC/99-15, May 1999.

2. ATLAS Muon Spectrometer, Technical Design Report, CERN/LHCC/97-22, May 1997.

3. H. Bilokon *et al*, ATL-MUON-95-081;
   P. Benvenuto *et al*, ATL-MUON-97-152;
   A. Ackermann *et al*, ATL-MUON-97-153;
   S. Cerioni *et al*, ATL-MUON-99-007.

4. S. Braccini, *on behalf of the ATLAS Frascati Group*, "Monitored Drift Tube Chamber Production at Laboratori Nazionali di Frascati", proceedings of the 7th International Conference on Advanced Technology and Particle Physics, Como, Italy, October 2001.

5. G. Avolio *et al.*, "First results of the 2001 MDT chambers beam test", ATL-COM-MUON-2001-022.

BaBar

F. Anulli(Ass.), R. Baldini Ferroli, A. Calcaterra, L. Daniello(Tecn.), R. de Sangro
G. Finocchiaro, P. Patteri, I. Peruzzi(Resp.), M. Piccolo, A. Zallo

1 Introduction

BaBar (in fig. 1) is the experiment running at the SLAC asymmetric B-factory PEP-II; the physics program is centered on, but not limited to, the study of the CP violation effects in the decay of neutral B mesons. The B system is the best suited to study CP violation because the expected effects are large, should appear in many final states and, most importantly, can be directly related to the Standard Model parameters. The large data sample now being collected has already allowed significant advances in a large number of topics in B, charm and top quark physics.

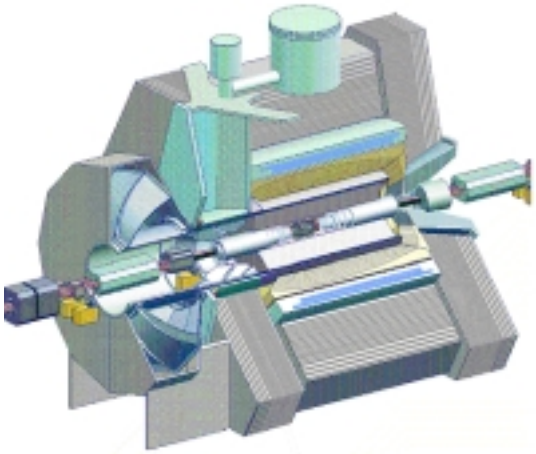

Figure 1: The BaBar Detector.

2 Activity

PEP-II is a two-ring e^+e^- storage ring, colliding 9 GeV electrons with 3.1 GeV positrons, energies chosen to maximize the production of B mesons. The c.m. energy corresponds to the mass of the $\Upsilon(4S)$ resonance which decays 50% in B^+B^-, 50% in $B^0\ \overline{B}^0$. The energy asymmetry is necessary in order to boost the B mesons momentum, so that the decay length can be measured with the accuracy needed to prove the CP violation effects. During the year 2002 additional $32fb^{-1}$ have been delivered by PEP-II, bringing the total data sample recorded by BaBar to $94fb^{-1}$. Data taking was suspended at the end of July 2002 for upgrades to PEP-II (new RF stations and a new section of vacuum chamber) and improvements to the detector (mainly to the Silicon Vertex Tracker and Instrumented Flux Return), and data taking resumed in Mid-November.

The PEP-II startup after the long shutdown was very encouraging, and by the end of December 2002 the machine was ready to take advantage of the numerous accelerator improvements. The plans for an upgrade to $10^{34}fb^{-1}$ and beyond are being actively addressed.

The BaBar Collaboration includes about 560 physicists, with contributions from 76 Institutions in 10 countries in North America, Europe, and Asia. Approximately half of the group are

physicists from U.S. Universities and Laboratories, with the largest foreign contribution coming from Italy, with 12 INFN Institutions and more than 90 people.

The BaBar detector has been designed primarily for CP studies, but it is also serving well for the other physics objectives of the experiment. The asymmetry of the beam energies is reflected in the detector design: the apparatus is centered 37 cm ahead of the collision point, along the direction of the high-energy beam, to increase forward acceptance. All services are placed on the opposite side of the detector, in order to minimize multiple scattering in the forward direction.

The momentum of the charged tracks is obtained from the curvature in a solenoidal field of 1.5 T and is measured in a low mass Drift Chamber. Different species of hadrons are identified in the DIRC, a dedicated device of a novel kind, based on the detection of Čerenkov light. Excellent photon detection and electron identification is provided by a CsI crystals electromagnetic calorimeter.

Muons and neutral hadrons are identified in the iron magnet's yoke, where a total thickness of 65 cm of Fe plates has been segmented in 18 slabs of graded thickness (from 2 to 10 cm) and instrumented with Resistive Plate Counters. This system, made of a 6-sided barrel, 2 endcaps and a double cylindrical layer inside the magnet coil, is called Instrumented Flux Return, or IFR. The final ingredient in the CP asymmetry measurements, the distance between the two decay vertices, is measured by a state of the art vertex detector, with five layers of double sided silicon strips.

The year 2002 has seen all Institutions participating to the IFR, including Frascati, involved in an effort to improve muon detection efficiency in the Forward Endcap, where a combination of harder momentum particles and less absorption material (60 cm of Fe) with respect to the Barrel (65 cm) posed performance limitations. This was solved by installing an additional 10 cm thick Fe plate with a new detector layer, and substituting 5 layers of inner detector with 5 layers of 2.54 cm thick brass. A new series of detectors was also added, to improve muon efficiency in the transition region ($\theta \approx 45^\circ$) betwen the Barrel and the Endcap. These new detectors are placed beyond 20 cm thick Fe structural parts of the magnet.

At the same time, the IFR group proceeded to the substitution of some detectors in the FE that had deteriorated because of excessive overheating. All RPC's in the FE, good and bad, were substituted with new-generation RPC's, characterized by less linseed oil and better curing of it. The effects of this new fabrication technique will be assessed during 2004, when the moment and opportunity will come to confront with a similar problem, affecting detectors in the Barrel.

In this perspective, the Frascati group has operated during the first 6 months of 2002 a test setup at the RPC factory (fig. 2), with the capability to read out cosmic rays passing a stack of 10 finished IFR chambers of the "new" type; the expected impact point on each one being predicted by two additional trigger chambers.

Data from this test setup were analyzed at LNF, obtaining efficiency plateaux and detailed 2d efficiency maps for a total of ≈ 100 4m^2 finished endcap chambers before shipment to SLAC. A summary of the efficiency data was stored on an online database for future reference, and in fig. 3 is shown a sample of a 2d efficiency plot.

Members of the Frascati group had also both hardware and softare related responsabilities inside the collaboration. Concerning the former, a member of the group was in 2002 *IFR Operation Manager*, whose main job is to coordinate activities in order to guarantee stable and reliable operation of the detector during data taking. Other responsabilities in the group included the integration of physics and analysis code in the general softare frame of BaBar (the *Physics Contact* role), and the responsibility of the production of the experiment's *skims* (the categories in which events at the end of offline reconstruction are tagged), which is another central role in BaBar.

Figure 2: The LNF testing facility at the RPC factory.

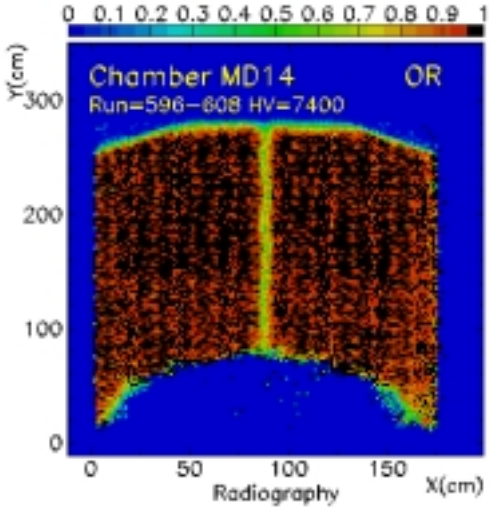

Figure 3: A 2d efficiency map.

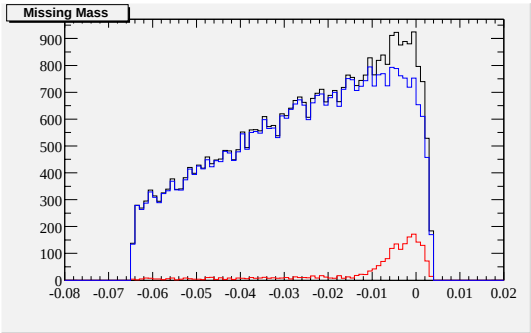

Figure 4: Missing mass of D^*D^* candidates in Monte Carlo events: all events(black), true $B^0 \to D^*D^*$ events(red) and background(blue).

3 Physics Results

In 2002 BaBar has improved its measurement of $\sin(2\beta)$, more than doubling the sample of events used: the latest 2002 value [4], obtained from 88×10^6 $B\overline{B}$ events is $(0.741 \pm 0.067(stat.) \pm 0.034(syst.)$; this measurement is still statistically limited. Measurement of CP-violating asymmetries have been published also in channels with non-charmed B^0 decays [3] and in charged B decays to charmonium [5]. Other important BaBar results include measurements of B meson lifetimes [8] and branching fractions [9, 11] for poorly known or rare decay modes.

In Frascati, analyses have been dedicated to three topics: measurements of the branching fraction and CP asymmetry of the $B^0 \to D^{*+}D^{*-}$ decay, measurement of the branching fraction of the $B^0 \to D^{*+}D_s^{*-}$ decay, and study of states characterized by high-momentum photons emitted from the electron lines (Initial State Radiation, ISR).

Concerning the former, study of the time evolution of the CP asymmetry for these decays allows one to measure a value for $\sin(2\beta)$ independent from the one obtained using the so-called *golden* modes, *e.g.* $B^0 \to J/\psi K_S$, hence its interest.

The analysis of $(B^0 \to D^{*+}D^{*-})$ with complete reconstruction of the B^0 state has already been published [6] and the measurement, being $\approx 2.3\sigma$ away from the *golden* one, calls for a method to reduce the statistical error and confirm (or deny) the discrepancy.

The interest of the Frascati analysis lies in the increase in statistics allowed by use of partially reconstructed events (to be weighted against the increased backgrounds): in this work, only one of the two D^* is identified, via its decay to $D^0\pi^{\pm}$. This completely reconstructed D^* is then combined with a low-momentum pion: assuming that both particles come from a B^0 decay, one can compute the mass of the missing particle. The events in which a B^0 actually decayed in D^*D^* will be signalled in the missing mass plot by an accumulation centered at the D^0 mass, while backgrounds will be more or less randomly distributed. A very preliminary result of the missing mass plot is shown in fig. 4: the black histogram is the superposition of background (blue) and signal (red) events.

The group is now analyzing the Monte Carlo sample, to optimize the selection of events versus the S/B ratio, and is working on the determination of the contribution of background events to the measurement error on $\sin(2\beta)$.

The $B^0 \to D^{*+}D_s^{*-} \to D^0\pi^+D_s^-\gamma$ is also studied with a partial reconstruction technique, this time combining a completely reconstructed D^* meson with a soft photon. The interest of such a decay channel stems not only from testing the factorisation hypothesis in B^0 decays, but also from the possibility, comparing with former measurements of the $B^0 \to D^{*+}D_s^{*-}$ branching

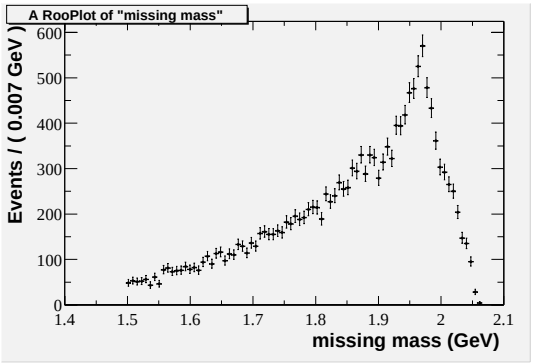

Figure 5: Missing mass of $D^* D_s^*$ candidates in $20 fb^{-1}$ data.

fraction, to extract the $D_s^+ \to \phi\pi^+$ branching fraction in a model independent way. A plot of the missing mass recoling againts the $D^* - \gamma$ system in $20 fb^{-1}$ of data collected at the $\Upsilon(4S)$ is shown in fig. 5.

For the ISR studies, the $K_s K\pi$, $K^+K^-\pi^0$, $K^+K^-\eta$ final states, accompanied by an emitted ISR hard photon, have been measured by BaBar from threshold up to 4.5 GeV/c^2. These processes are dominated by the I=0, $\Phi'(1.68$ GeV/c$^2)$ state decaying mainly through $K^*(892)$ production. The high statistics of this measurement have made possible to extract the I=1 contribution, obtain the first measurement of the $\phi\eta$ process and put a limit on the $\phi\pi^0$ production.

The $K^+K^-\eta$ invariant mass for ϕ candidates with mass in the range 1005-1035 Mev/c^2 is shown in fig. 6, in which the background has been estimated by scaling the $\gamma\gamma$ sidebands below and above the η, using a linear interpolation.

References

1. F. Anulli *et al.*, "The Babar Instrumented Flux Return Performance: Lessons Learned," Nucl. Instrum. Meth. A **494**, 455 (2002).

2. F. Anulli *et al.*, "Resistive Plate Chamber Performance In The Babar IFR System," IEEE Trans. Nucl. Sci. **49**, 888 (2002).

3. B. Aubert *et al.*, "Measurements of branching fractions and CP-violating asymmetries in $B^0 \to \pi^+\pi^-, K^+\pi^-, K^+K^-$ decays," Phys. Rev. Lett. **89**, 281802 (2002)

4. B. Aubert *et al.*, "Measurement of the CP-violating asymmetry amplitude $\sin(2\beta)$," Phys. Rev. Lett. **89**, 201802 (2002)

5. B. Aubert *et al.*, "Study of $B^\pm \to J/\psi\pi^\pm$ and $B^\pm \to J/\psi K^\pm$ decays: Measurement of the ratio of branching fractions and search for direct CP-violating charge asymmetries," Phys. Rev. D **65**, 091101 (2002).

6. B. Aubert *et al.*, "Measurement of the branching fraction and CP content for the decay $B^0 \to D^{*+}D^{*-}$," Phys. Rev. Lett. **89**, 061801 (2002)

7. B. Aubert *et al.*, "Search for T and CP violation in B^0–$\overline{B}^0$ mixing with inclusive dilepton events," Phys. Rev. Lett. **88**, 231801 (2002)

8. B. Aubert *et al.*, "Measurement of the B^0 lifetime with partially reconstructed $B^0 \to D^{*-}\ell^+\nu_l$ decays," Phys. Rev. Lett. **89**, 011802 (2002) [Erratum-ibid. **89**, 169903 (2002)]

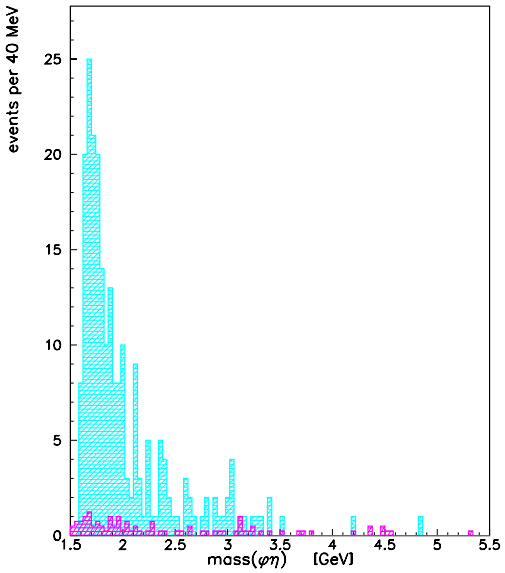

Figure 6: The $K^+K^-\eta$ invariant mass.

9. B. Aubert *et al.*, "Measurement of D_s^+ and D_s^{*+} production in B meson decays and from continuum e^+ e^- annihilation at $\sqrt{s} = 10.6$ GeV," Phys. Rev. D **65**, 091104 (2002)

10. B. Aubert *et al.*, "A study of time dependent CP-violating asymmetries and flavor oscillations in neutral B decays at the $\Upsilon(4S)$," Phys. Rev. D **66**, 032003 (2002)

11. B. Aubert *et al.*, "Search for the rare decays $B \to K\ell^+\ell^-$ and $B \to K^*\ell^+\ell^-$," Phys. Rev. Lett. **88**, 241801 (2002)

CDF II

M. Barone (Ass.), M. Cordelli (Resp.), S. Dell'Agnello, F. Happacher (Ass. Ric.), S. Miscetti, A. Sansoni, I. Sfiligoi (Art. 23)

1 Introduction

With the installation of the new Main Injector, the TeVatron has been upgraded to achieve a $p\bar{p}$ collision energy up to 1.98 TeV in the centre of mass system; moreover, the design of the whole accelerator complex aims to increase L, the instantaneous luminosity, delivered to the experiments, up to $2 \times 10^{32}\ cm^{-2}s^{-1}$ ($vs.\ 1.6 \times 10^{31}$ of Run I). During Run IIa (officially begun in march 2001 and that will end in 2005) we expect to integrate 2 fb^{-1} of data. As the end of year 2002 the CDF II experiment has collected ~ 120 pb^{-1}, with peak instantaneous luminosities the TeVatron up to $4 \times 10^{31}\ cm^{-2}s^{-1}$.

It should be noted that CDF II has declared the beginning of the "physics" data taking to be December 2001, at the end of an intense and successfull commissioning phase.

One of the main ingredients to reach high L consists in increasing the number of p and $\bar{p}$ bunches (N_b); this reflects in the shortening of the time interval between two adjacent bunch crossings, thus requiring the upgrade of the CDF II detector. CDF II essential components, like the central tracking chamber, the silicon secondary vertex detector and the forward regions of the calorimeter nedeed to be built *ex novo*. The central electromagnetic and hadronic calorimeters are the only devices, together with most of the muon chambers, that are still working properly in the new Run after the renewal of all the Front-End electronics; indeed the integration time of charge signals has to be completed within the 132 ns window of the new machine clock (during Run I this was 3.5 μs).

The CDF II group of the Frascati laboratory, has the responsibility of the commissioning, calibration and continuted maintenance of the steel-scintillator hadronic calorimeters covering $|\eta| < 1.36$ (the central hadron, CHA, built by INFN-Frascati and the wall hadron, WHA built by INFN-Pisa). Thus, our primary duty is the energy calibration, which we accomplish with the following methods:

- to set the absolute energy scale we use, a ^{137}Cs source system; this procedure relies on the test beam of '83 - '85 that used π's with energy greater than 10 GeV;
- we use also Minimum Ionizing Particle (MIP) energy deposition, in a sample of muons from J/Ψ's and W/Z's decays, to cross-calibrate the detector towers;
- the N_2 laser system is run periodically to track the gains of the photomultipliers (PMs) and as a quick tool to check the functionality of the PM-ADMEM chain.

Stricly related to the above, INFN-Frascati has the responsibility of the slow control of the HV of CHA, WHA and of the central hadron calorimeter (CEM) located in front of the hadronic compartment. These three detectors share a common, camac-controlled hardware which is 20 years old. The slow control system has been significantly improved with respect to Run I: (i) the PM HV readout does not induce noise in the CEM unlike Run I; (ii) the PM HV readout and monitoring is done every hour (rate limited by the low speed of the serial readout, which is an ancestor of the modern CAENET), much more ofter than in Run I; (iii) the monitoring and control application has been ported to the CDF II online software environment; the HV data, including the warning and alarms, are stored into a GUI-driven database in the local PC running Windows NT/2000 and are

used by the shift crew; data are then uploaded to an ORACLE v9 database (on a UNIX host) for permanent storage and for offline reconstruction. In addition, the bulk power supplies which feed HV to the PMs are monitored which in a much faster rate, about 1 Hz, to provide a trigger-inhibit and stop the experiment data acquisition in case the HV goes out of the tolerance range (± 2 Volt). The slow control system was commissioned in 2000 has performed with full functionality and no problems also during all 2002.

The group has also an important committment in the calorimeter timing project, both for the hadron and electromagnetic sectors. The timing system in the hadronic calorimeters (CHA, WHA, PHA), HADTDC, is fully working since the year 2002. Our responsability are described in section 3

2 Setting of the Energy Scale

2.1 ^{137}Cs Sources

An important activity carried on during 2002 has been the re-establishment of the absolute calorimeter energy scale. In order to correct for light yield losses of the scintillator, due to aging phenomena, we have acquired a set of runs with Cs^{137} sources with the magnetic field on and off. These runs consists on pulling the sources inside the calorimeter and recording the current output, I, from the PM's. This system runs in front of the scintillator plane located approximately at shower maximum, thus irradiating few of the scintillator/absorber layers of the calorimeter. We monitor aging phenomena of the scintillator together with PM gain variations, by comparing present response with the one recorded in conjunction with the original test beam calibration with pions and muons (early 80's). We compute the Linear Energy Response

$$LER = \frac{^{137}Cs(test-beam)e^{-\Delta t/\tau}}{^{137}Cs(today)}$$

for the CHA and WHA calorimeters towers and we correct for these factors the raw ADMEM counts.

2.2 Minimum Ionizing Particles

The ^{137}Cs sources technique has two drawbacks:

- not all scintillator planes are irradiated;
- since we monitor I, it is not sensitive to any possible loss of charge, Q, in the shorter integration gate of Run II.

For these reasons we look at the energy deposition of Minimum Ionizing Particles (Mip's) to monitor the energy response of the hadronic calorimeter. At the Tevatron energies muons are Mip's, so that for our studies clean samples of μ's from J/Ψ or W/Z decays are considered. First of all we looked at μ's from the ~ 81 pb^{-1} dimuon trigger sample collected in Run Ib; we focused on the CHA towers and we determined the necessary statistics to determine the peaks of μ's hadronic energy, HadE, distributions with enough precision. We splitted the sample into two subset of ~ 40 pb^{-1} and we found that the tower by tower peak is determined with a precision of around $\sim 1.5\%$. This is shown in Figure 1. Run I vs Run II Mip peaks comparison showed a $\sim 10\%$ difference. In Figures 2 and 3 we show the HadE distribution for μ's from J/Ψ decays impinging the CHA detector. The plot in Figure 3 has been obtained after correcting by a $\sim 10\%$ factor the raw hadronic energy of the muons; in this way the mean of the Run II distribution has been equalized to the ~ 1.70 GeV we had in Run I.

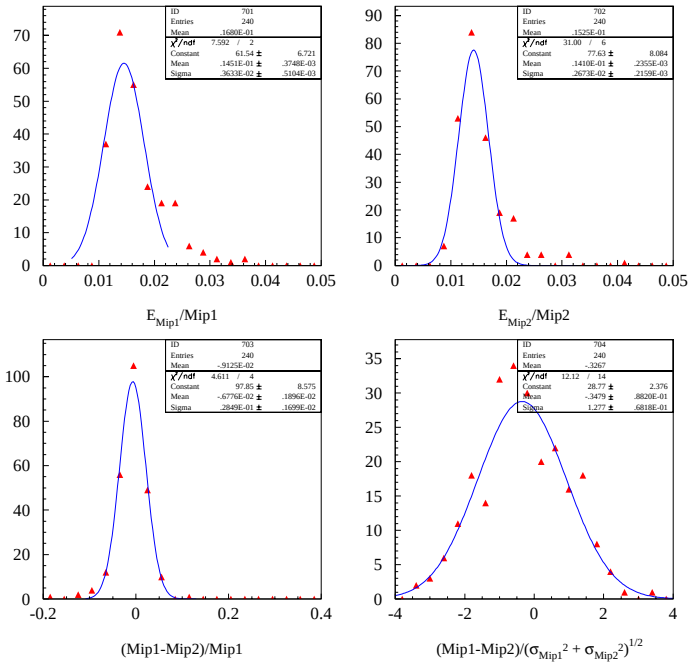

Figure 1: *Run I μ's from J/Ψ. Tower by tower Mip's peak determination precision for two $\sim 40pb^{-1}$ subsets of the sample.*

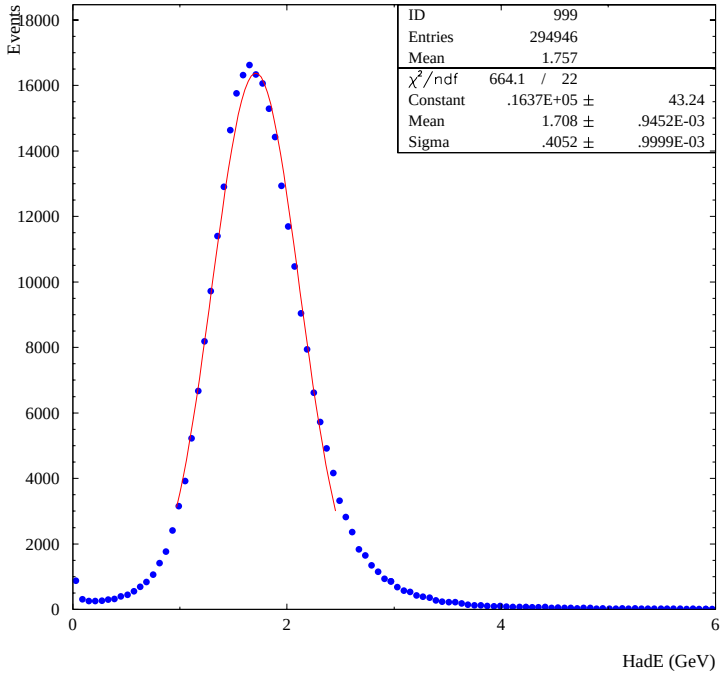

Figure 2: *Run I HadE deposition in CHA.*

2.3 N_2 Laser

The ageing mechanichs of the ^{137}Cs source drives make this calibration method difficult for some towers; therefore we decided to take sources runs once per year, only when there is a long shut-

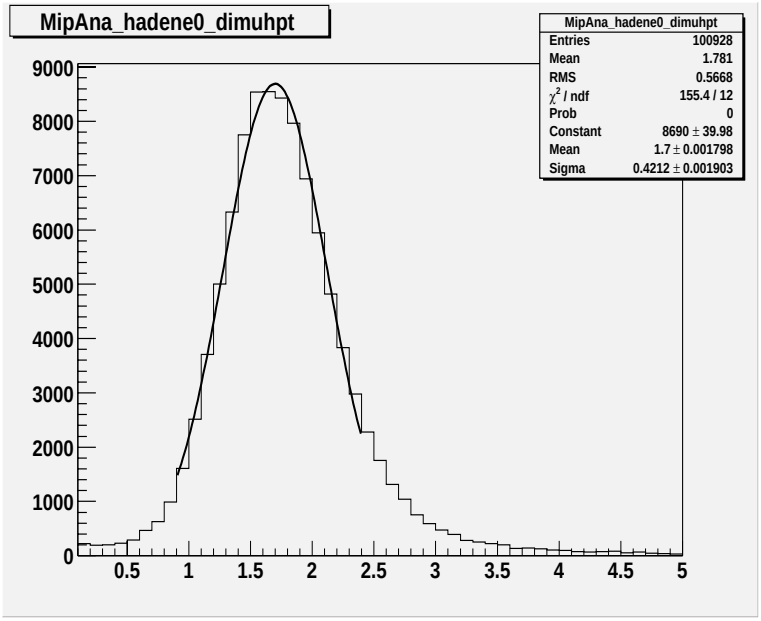

Figure 3: *Run II HadE deposition in CHA.*

down that would allow us to access the CDF II detector and fix sources that could get stuck inside the detector. The laser system represents a more indirect by safer method to follow the trend of (only) the PM gains.

The laser system consists of a N_2 laser whose light is carried in front of the photocathode of each CHA/WHA PM through quartz fibers. There are six main bundles of fibers going separately to the four CHA arches (NE, NW, SE, SW) and the two WHA sides (East and West); each bundle is then splitted and distributed to every wedge and then to every PM. Since the laser light has a $\sim 10\%$ variation in the amplitude from run to run, we need to have a reference to normalize it; this is achieved using six sets of four reference photomultipliers; each set measures the light amplitude coming from the fiber bundle relative to one of the calorimeter arches. While comparing two laser runs, the mean of the adc counts of each tower, belonging to a certain arch, has to be scaled by the ratio of the two laser signal amplitudes recorded by its relative reference PM's set.

In Run II, the 132 ns acquisition gate of the FrontEnd electronics makes difficult to collect the whole laser pulses in the ADMEM buffer; this is due to a lenght difference between the fibers that reflects into a time spread of the arrival time of the light to the PM's of ± 30 ns; so that, given a fixed trigger signal coming from the free running laser, if a certain set of channels are in time there are others for which part of the signal is lost. In Run I the ~ 3.5 μs gate was large enough not to affect the system. We performed a careful study to overcome the problem. First of all we started acquiring laser runs using a wider acquisition buffer, called Myron Mode; it consists of recording the FrontEnd electronic information in the previous buffer to the triggered one and in two subsequent ones, four buffers in total. This is shown in Figure 4. In these way we could study where the laser pulses were falling. Then using the TDC information of the towers we determined the relative delays only due to the fiber lenght. These delays have then been used to modify the ADMEM acquisition delay and in this way we succeded to have the whole calorimeter acquired in one buffer when the laser is firing. In Figure 5 we show the fractional energy deposited in each

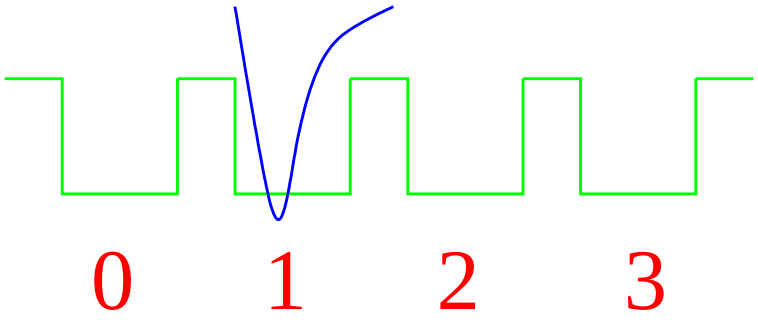

Figure 4: *Myrone Mode acquisition scheme.*

buffer for channels belonging to one CHA arch; it can be seen that, apart from pedestals, there is no leakage in the buffers other than the second (trigger buffer); $\sim 100\%$ of the energy is collected in the trigger buffer.

We developed a C++ consumer program in the AC++ CDF II standard software framework to analyze laser runs. Figure 6 shows the comparison between two laser runs taken a month apart for half of the CHA. The comparison is between the mean of ADC counts distributions (black histogram) before the reference PM rescaling and after the normalization (red and green distibutions use slightly different normalization techniques). It can be noticed that the method keeps track of the light output variations. We found that PM gain fluctuations are of the order of $\sim 2\%$; a few channels (especially in WHA) drift more than this value and are constantly monitored.

3 Calorimeter Timing

The hardware committment of the Frascati group has been the realization of the fast discriminators VME boards, the transition boards to the crates; the group played an important role in the commissioning of the whole system and has the responsibility of the t_0 calibrations, slewing corrections and check of the discriminator thresholds. Every 5-10 pb^{-1} we look at collision data and provide these calibration constants. For this pourpose we developed a C++ consumer in the AC++ CDF II framework.

Run IIb upgrades of CDF II include the increasing of the readout of the central and plug electromagnetic calorimeters (CEM, PEM) to add tower timing information. Having time information in the electromagnetic sectors would significantly improve the potential of the CDF II detector to do physics in samples with photons in the final state in two ways: it would reduce the cosmic ray backgrounds in searches with photons in the final state and would be an handle to identify prompt photons in unusual events like $ee\gamma\gamma$ $\not\!\!E_T$.

The year 2002 was devoted to study the feasibility of the project. The hardware is similar to that used in the hadron TDC system; the only difference being that in the CEM sector we don't have the 'last dynode" output in the photomultipliers, but only the anode signal. To overcome this problem we are going to use purely inductive splitters that pick up a small fraction of the anode signal, without changing the collected charge in a noticeable way, that is then sent to the discriminator boards.

The Frascati group has realized two prototypes of ASD boards and TB boards; during the last long access we have been able to instrument the system for 30 PEM towers and we tried these inductive "pick up" for two CEM channels. The whole chain is working, we have spare TDC

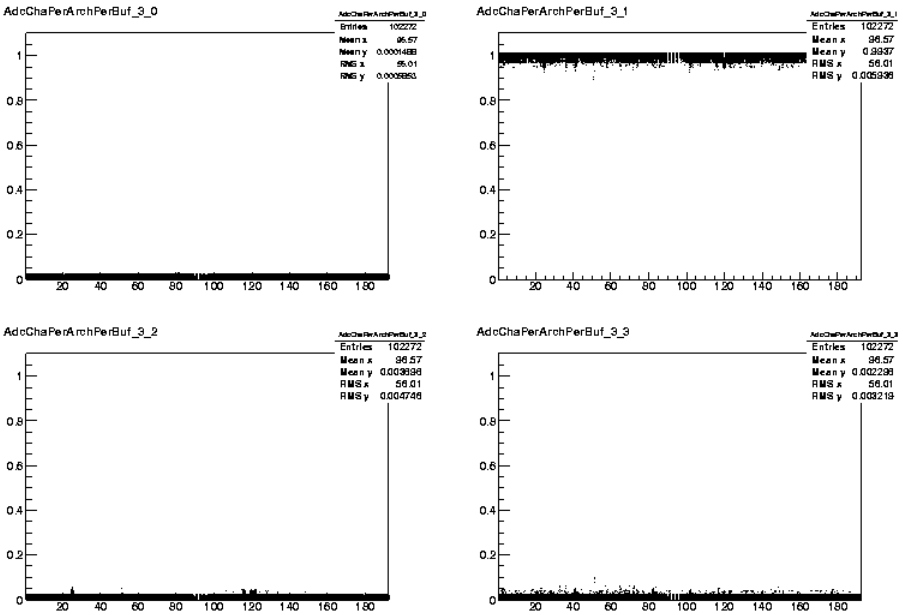

Figure 5: *Laser run. Fractional energy deposition per buffer for one CHA arch.*

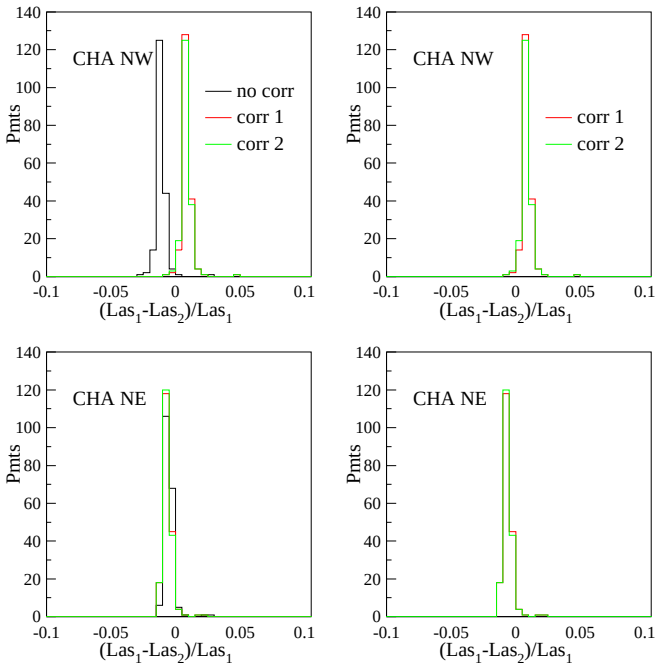

Figure 6: *Laser run. Comparison between two laser runs, before end after light amplitude normalization, for CHA north arches.*

boards we are reading out and we obtained good results. The EMTiming project seems to be easy to implement and therefore we will start its implementation during year 2003, before Run IIb.

Talks 2002

1 "CDF II Integrated Calorimetry Environment", presented by S. Dell'Agnello for the CDF2 Collaboration, Proceedings of the "10th International Conference on Calorimetry in Particle Physics" (Caltech, Pasadena, California (USA), 25-29 March 2002), WORLD SCIENTIFIC, 563-569 (2003).

Pubblications 2002

1. D. Acosta *et al.* [CDF Collaboration], "Cross section for forward J/ psi production in pp collisions at s =1.8 TeV," Phys. Rev. D **66**, 092001 (2002).

2. D. Acosta *et al.* [CDF Collaboration], "Search for long-lived charged massive particles in anti-p p collisions at s**1/2 = 1.8-TeV," Phys. Rev. Lett. **90**, 131801 (2003) [arXiv:hep-ex/0211064].

3. D. Acosta *et al.* [CDF Collaboration], "Search for a W' boson decaying to a top and bottom quark pair in 1.8-TeV p anti-p collisions," Phys. Rev. Lett. **90**, 081802 (2003) [arXiv:hep-ex/0209030].

4. D. Acosta *et al.* [CDF Collaboration], "Search for radiative b-hadron decays in p anti-p collisions at s**(1/2) = 1.8-TeV," Phys. Rev. D **66**, 112002 (2002) [arXiv:hep-ex/0208035].

5. D. Acosta *et al.* [CDF Collaboration], "Search for radiative b-hadron decays in p anti-p collisions at s**(1/2) = 1.8-TeV," FERMILAB-PUB-02-146-E.

6. D. Acosta *et al.* [CDF Collaboration], "Momentum distribution of charged particles in jets in dijet events in p anti-p collisions at s**(1/2) = 1.8-TeV and comparisons to perturbative QCD predictions," FERMILAB-PUB-02-096-E.

7. D. Acosta *et al.* [CDF Collaboration], "Measurement of the ratio of b quark production cross sections in anti-p p collisions at s**(1/2) = 630-GeV and s**(1/2) = 1800-GeV," Phys. Rev. D **66**, 032002 (2002) [arXiv:hep-ex/0206019].

8. D. Acosta *et al.* [CDF Collaboration], "Branching ratio measurements of exclusive B+ decays to charmonium with the Collider Detector at Fermilab," Phys. Rev. D **66**, 052005 (2002).

9. D. Acosta *et al.* [CDF Collaboration], "Limits on extra dimensions and new particle production in the exclusive photon and missing energy signature in p anti-p collisions at s**(1/2) = 1.8-TeV," Phys. Rev. Lett. **89**, 281801 (2002) [arXiv:hep-ex/0205057].

10. T. Affolder *et al.* [CDF Collaboration], "Charged jet evolution and the underlying event in proton-antiproton collisions at 1.8 TeV," Phys. Rev. D **65**, 092002 (2002).

11. D. Acosta *et al.* [CDF Collaboration], "Measurement of B meson lifetimes using fully reconstructed B decays produced in p anti-p collisions at s**(1/2) = 1.8-TeV," Phys. Rev. D **65**, 092009 (2002).

12. D. Acosta *et al.* [CDF Collaboration], "Search for new physics in photon lepton events in p anti-p collisions at s**(1/2) = 1.8-TeV," Phys. Rev. Lett. **89**, 041802 (2002) [arXiv:hep-ex/0202044].

13. D. Acosta *et al.* [CDF Collaboration], "Comparison of the isolated direct photon cross sections in p anti-p collisions at s**(1/2) = 1.8-TeV and s**(1/2) = 0.63-TeV," Phys. Rev. D **65**, 112003 (2002) [arXiv:hep-ex/0201004].

E831 FOCUS

R. Baldini-Ferroli, L. Benussi (Ass.), M. Bertani, S. Bianco (Resp.)
F.L. Fabbri, M. Giardoni, A. Zallo

FOCUS (Experiment 831 at Fermilab, www-focus.fnal.gov) studies photoproduction and decays of charm mesons and baryons at Fermilab. In FOCUS, a forward multi-particle spectrometer is used to measure the interactions of high energy photons on a segmented BeO target. The FOCUS detector is a large aperture, fixed-target spectrometer with excellent vertexing, particle identification, and reconstruction capabilities for photons and π^0's. FOCUS is a considerably upgraded version of a previous experiment, E687, and it amply surpassed the goal of collecting ten times the E687 sample of fully reconstructed charm decays, i.e. a sample of over 1 million fully reconstructed charm particles in the three major decay modes: $D^0 \to K^-\pi^+$, $K^-\pi^+\pi^-\pi^+$ and $D^+ \to K^-\pi^+\pi^+$. The FOCUS Italian groups (Milano, Pavia and Frascati) hold full responsibility for the μ-strip detector, the Hadron calorimetry, and the Outer em calorimetry respectively, and coordinate about half of the software-related projects. The Frascati group also coordinates the calorimetry working group, and is responsible for the first level selection process in physics analyses utilizing em calorimetry.

1 Activity during year 2002

The activity of the Frascati FOCUS group in 2002 has been focussed on the data analysis, and presentation of results at conferences. The data analysis studies of the Frascati group were centered on spectroscopy. Along with the traditional ensemble of studies focussed on the spectroscopy of orbitally and radially excited charm mesons, a new line of research was open on the study of the spectroscopy of light quark mesons diffractively photoproduced.

Heavy Quark Symmetry and Heavy Quark Effective Theory predict a rich spectrum for the excited charm mesons. FOCUS presented precise new measurements of D_2^* masses and widths. Evidence for an insofar unobserved broad state (possibly the D_0^* as predicted by HQET) at mass 2427MeV and width 200MeV was also shown. Work continued on the search for radial excitations. Publication of these results was finalized.Results were presented at HQL2k2 (Vietri, Italy).

Light quark diffractive physics is a surprise for a heavy quark experiment. Thanks to a dedicated trigger FOCUS has collected a very significant sample of diffractive events, thus starting studies of interest in hadronic physics and predictions of χQCD. During 2001, FOCUS published evidence in E687 data for a narrow dip structure in diffractive photoproduction of the 6π final state. When interpreted as a new resonance interfering with the diffractive continuum, the structure has $1.911 \pm 0.004\,\mathrm{Gev/c^2}$ mass and $29 \pm 11\,\mathrm{Mev/c^2}$ width. In 2002 we showed preliminary evidence for a confirmation signal in FOCUS data, at a mass and width compatible with the E687 published result. We also showed evidence for diffractively photoproduced $\phi\eta$, $\phi\eta'$, ϕf_0 events, studied the q^2 evolution, and investigated a relationship via dispersion relations to the controversial values of the branching ratios $\Gamma(\phi \to \eta\gamma)/\Gamma(\phi \to f_0\gamma)$. Results were presented at ICHEP02 (Amsterdam, The Netherlands), and MESON 2002 (Krakow, Poland).

1.1 Conference Organization and IAC Memberships

During 2002, members of the FOCUS Frascati group have participated in the organization of the conference *Frontier Science 2002: The physics of D, B and CP*, Frascati, Italy, October 2002. Members of the Frascati group served in International Advisory Committees of the following conferences: 11th Conference On Calorimetry In High Energy Physics (CALOR 2001), 1st Int. Conf.

on Heavy Quarks and Leptons (HQL2K2), 22nd Physics In Collision Conference (PIC02).

1.2 Seminars

1. S. Bianco, New FOCUS Results, Notre Dame University, S.Bend (Indiana) USA, November 2002.

2 Outlook

The activity in 2003 will be focussed in searching for radial excitations, including channels with γ and π^0 in the final state. In the light quark sector, we plan to continue the study to seek confirmation of the six pion structure found out of a larger data sample, and to finalize the study f_0 production and $\eta - \eta'$ mixing from our diffractive sample.

3 Conference Talks in 2002

1. S. Bianco, Light-Quark Spectroscopy Results from FOCUS and E687, ICHEP02 Amsterdam (The Netherlands), July 2002, arXiv:hep-ex/0212028.
2. A. Zallo, Light quark results from FOCUS, MESON2002, Kracow, Poland, 2002.
3. L. Benussi, Charm Meson Spectroscopy, invited talk at HQL2k2, Vietri, Italy, June 2002.

References

1. J. M. Link *et al.* [FOCUS Collaboration], arXiv:hep-ex/0211056.
2. J. M. Link *et al.* [FOCUS Collaboration], Phys. Lett. B **545** (2002) 50 [arXiv:hep-ex/0208027].
3. J. M. Link *et al.* [FOCUS Collaboration], Phys. Lett. B **544** (2002) 89 [arXiv:hep-ex/0207049].
4. J. M. Link *et al.* [Focus Collaboration], Phys. Lett. B **541** (2002) 211 [arXiv:hep-ex/0206069].
5. J. M. Link *et al.* [Focus Collaboration], branching ratios," Phys. Lett. B **541** (2002) 243 [arXiv:hep-ex/0206056].
6. J. M. Link *et al.* [FOCUS Collaboration], Phys. Lett. B **541** (2002) 227 [arXiv:hep-ex/0206049].
7. J. M. Link *et al.* [FOCUS Collaboration], Phys. Lett. B **540** (2002) 25 [arXiv:hep-ex/0206013].
8. J. M. Link *et al.* [FOCUS Collaboration], arXiv:hep-ex/0204023.
9. J. M. Link *et al.* [FOCUS Collaboration], Phys. Lett. B **537** (2002) 192 [arXiv:hep-ex/0203037].
10. J. M. Link *et al.* [FOCUS Collaboration], Phys. Lett. B **535** (2002) 43 [arXiv:hep-ex/0203031].
11. J. M. Link *et al.* [FOCUS Collaboration], Phys. Rev. Lett. **88** (2002) 161801 [arXiv:hep-ex/0202001].

KLOE

The KLOE-LNF Collaboration:
A. Antonelli, M. Antonelli, G. Bencivenni, S. Bertolucci, F. Bossi, P. Campana (Resp),
G. Capon, P. Ciambrone, P. De Simone, S. Dell'Agnello, A. Denig (bors.CEE),
M. Dreucci (Ass), G. Felici, M. L. Ferrer, G. Finocchiaro, C. Forti, A. Franceschi,
S. Giovannella (art.23), G. Lanfranchi, J. Lee-Franzini (art.23), Lu Feng (B.str),
W. Mei (art.23), S. Miscetti, M. Moulson (art.23), F. Murtas, A. Nedosekin (art.23),
M. Palutan (art.23), L. Passalacqua, V. Patera (Ass), P. Santangelo, B. Sciascia (ass.ric),
A. Sciubba (Ass), I. Sfiligoi (art.23), T. Spadaro (ass.ric), P. Valente (art.23)

The KLOE-LNF Technical Staff:
M. Anelli, A. Balla, E. Capitolo, M. Carletti, A. Ceccarelli
G. Corradi, U. Denni, A. Di Virgilio, G. Fortugno, M.A. Frani, G. Paoluzzi,
G. Papalino, M. Santoni, A. Saputi, A. Rutili

1 Introduction

DAΦNE, the Frascati ϕ-factory [1], is an e^+e^- collider working at the ϕ resonance peak. The ϕ meson, produced practically at rest, decays with a probability of 33.8% into a K_SK_L pair. DAΦNE collisions are thus a source of nearly monochromatic, back-to-back K_S-K_L beams.

The KLOE experiment [2] is primarily designed to study CP and CPT violation in the K^0-$\overline{K}^0$ system. The unique feature of KLOE is the possibility to perform these studies by measuring the interference patterns in the relative time distributions of the K_SK_L pair decays (the pair is produced in a $J^{PC} = 1^{--}$ quantum state) into various final states [3]. Another complementary and more traditional way to measure $\Re(\epsilon'/\epsilon)$ at KLOE is the double ratio method based on the relation:

$$\frac{R_L}{R_S} \simeq 1 + 6\Re(\epsilon'/\epsilon) \tag{1}$$

where

$$R_{S,L} = \frac{BR(K_{S,L} \to \pi^+\pi^-)}{BR(K_{S,L} \to \pi^0\pi^0)} \tag{2}$$

As an example of the statistics needed for these studies, the measurement of $\Re(\epsilon'/\epsilon)$ with an accuracy $O(10^{-4})$, considering the double ratio method for simplicity, requires an integrated luminosity of about 10 fb^{-1}. This corresponds, at the design luminosity $L = 5 \cdot 10^{32}$ cm^{-2} s^{-1}, to about two years of running.

Since its commissioning in 1999, DAΦNE performance has been continously improving. In 1999 the KLOE integrated luminosity was $\sim$ 2pb^{-1}, while during year 2000 it exceeded 20pb^{-1}. In year 2001 the DAΦNE luminosity reached $5 \cdot 10^{31}$ cm^{-2} s^{-1} and KLOE collected $\sim$ 180pb^{-1}, the vast majority of which in the last three months. In year 2002 other $\sim$ 300 pb^{-1} have been written on tape in less than 5 months of data taking.

Of relevance also is the effort performed by the DAΦNE team in reducing the machine background inside KLOE. Cleaner data taking conditions have been obtained in 2002 with respect to the previous year. This is fundamental for the control of systematic effects which can affect precision measurements.

Even though the statistics of the current data set is not adequate for the precision studies of fundamental symmetries, however it is suitable for the study of other topics, which are part of the KLOE physics program. The analysis of the year 2000 data, carried on during the following

year, has resulted in the publication of five physics papers in the early 2002. Since most of these analysis are statistically limited, a substantial improvement of these results can be obtained with the use of the entire data sample. Published results and prospects for improvements are discussed in the following.

2 The KLOE detector

The KLOE detector, shown in Fig.1, consists mainly of a large volume drift chamber surrounded by an electromagnetic calorimeter. A superconducting coil provides a 0.52 T solenoidal magnetic field.

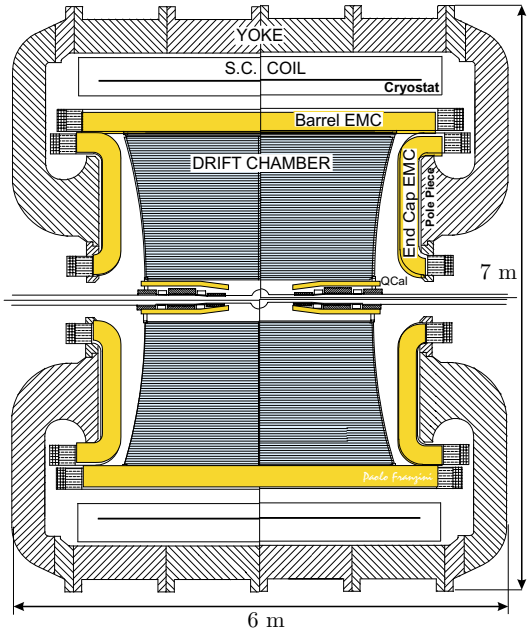

Figure 1: Schematic view of the KLOE detector.

The fine sampling lead-scintillating fiber calorimeter [4] consists of 24 barrel modules with 4.3 m active length and 23 cm thickness ($\sim 15X_0$) and 2×32 C-shaped end-cap modules of various lengths and same thickness as barrel modules, with photomultiplier read-out at both sides. The solid angle coverage is 98%. The energy resolution measured using $e^+e^- \to e^+e^-\gamma$ events is $\sigma_E/E = 5.7\%/\sqrt{E(\mathrm{GeV})}$. The time resolution measured using $e^+e^- \to e^+e^-\gamma$ and $e^+e^- \to 2\gamma$ events is $\sigma_t = 54$ ps$/\sqrt{E(\mathrm{GeV})} \oplus 50$ ps, after the subtraction of the finite bunch-lenght effect.

The tracking detector is a 4 m diameter and 3.3 m long cylindrical drift chamber [5] with a total of ~ 52000 wires, of which ~ 12000 are sense wires, in an all-stereo geometry. In order to minimize multiple scattering and K_L regeneration and to maximize detection efficiency of low energy photons, the chamber works with a helium based gas mixture and its walls are made of light materials (mostly carbon fiber composites). The momentum resolution for tracks produced at large polar angle is $\sigma_p/p \leq 0.4\%$ while spatial resolutions are $\sigma_{r,\phi} \approx 150\mu$ m and $\sigma_z \approx 2$mm.

3 Tagging of K_S decays

As specified above, DAΦNE is an exceptional source of monocrhomatic and well tagged K_S mesons, allowing for precision measurements of its dominant branching ratios as well as for the study of its more rare decays. At KLOE a K_S is tagged by identifying the interactions of the K_L in the calorimeter. In fact about 50% of the produced K_L's in $\phi \to K_S K_L$ events reach the calorimeter before decaying; their associated interactions (called "K_L-crash") are identified by a high-energy ($E \geq 200$ MeV), neutral (i.e. not associated to any track in the event) and delayed (the interaction time of a K_L with $\beta \sim 0.218$ is delayed of ≈ 30 ns with respect to the one due to a $\beta = 1$ particle coming from the interaction region) cluster in the calorimeter.

The position of the K_L-crash, exploiting the two body decay kinematics, provides the momentum of the K_S. Moreover in about 40% of the events the K_L-crash alone indipendently satisfies the trigger conditions, thus facilitating the trigger efficiency studies.

4 BR($K_S \to \pi^+\pi^-$)/BR($K_S \to \pi^0\pi^0$)

The measurement of $R_S = BR(K_S \to \pi^+\pi^-)/BR(K_S \to \pi^0\pi^0)$ constitutes a part of the double ratio method for measuring $\Re(\epsilon'/\epsilon)$.

In the sample of K_L-crash events the $K_S \to \pi^+\pi^-$ decay is identified by requiring the presence of two tracks of opposite charge coming from the interaction region (IR) which satisfy loose cuts on momentum, p, and polar angle, θ. These cuts define the acceptance for the decay; the corresponding efficiency is obtained from Monte Carlo simulation (MC). The single-track reconstruction efficiency in bins of (p, θ) is obtained directly from subsamples of $K_S \to \pi^+\pi^-$ events themselves.

The $K_S \to \pi^0\pi^0$ decay is identified by requiring the presence of at least three "prompt" clusters (i.e. originated by photons coming from the IR: $|T_{cl} - R/c| \leq 5\sigma_t$, where R and T_{cl} are the measured distance from the IR and the time of the cluster, respectively) which satisfy cuts on energy and polar angle.
The photon detection efficiency is evaluated from a sample of $\phi \to \pi^+\pi^-\pi^0$ events, in which the kinematic variables of one photon can be constrained by the detection of the two pions and the other photon in the event.

In both $\pi^+\pi^-$ and $\pi^0\pi^0$ cases, the probability that the K_S (K_L-crash) detection fully or partially satisfies the trigger conditions can be evaluated using events in which the K_L-crash (K_S) alone triggers. Thus the trigger efficiency is evaluated as the combined probability of K_S and K_L-crash to satisfy the trigger conditions.

The published KLOE result is [6]:

$$R_S = 2.236 \pm 0.003_{\text{stat}} \pm 0.015_{\text{syst}} \tag{3}$$

This result has a statistical significance never reached before by a single measurement and has to be compared to the world average [7] $2.197 \pm 0.026_{\text{stat}} \pm 0.013_{\text{syst}}$.

The analysis of the full data sample is well under way. The systematic error will be further reduced, partly because the error on some efficiencies are currently dominated by the statistics of control samples, and partly because of an improved selection of K_L-crash events in 2001-2002 data.

5 Study of $K_S \to \pi e \nu$ decays

Assuming CPT and the $\Delta S = \Delta Q$ rule, the $K_S \to \pi e \nu$ branching ratio is calculated from the equality $\Gamma(K_S \to \pi e \nu) = \Gamma(K_L \to \pi e \nu)$. Using the measured values of BR($K_L \to \pi e \nu$) and τ_S/τ_L [7], BR($K_S \to \pi e \nu$) $= (6.70 \pm 0.07) \cdot 10^{-4}$ is obtained.

At KLOE the $K_S \to \pi e\nu$ events are selected in the sample of K_L-crash events by requiring the presence of a vertex with two tracks of opposite charge in the IR. The observation of the K_L-crash determines the momentum of the K_S. The invariant mass at the vertex is calculated assuming both tracks are from pions, and the total momentum at the vertex is calculated in the K_S rest frame. Loose preselection cuts, which mainly eliminate $K_S \to \pi^+\pi^-$ events, are imposed on these quantities. The preselection efficiency is evaluated by the MC.

The $K_S \to \pi e\nu$ decay is identified by making the correct π/e assignment to the two tracks. In order to use time-of-flight π/e identification, both tracks from the vertex must be associated to calorimeter clusters. The difference $\delta_t(m) = T_{cl} - L/c\beta(m)$ is calculated for each track by using the measured cluster time, the track length L, and by applying the mass hypotheses $m = m_e$ or $m = m_\pi$ to derive the velocity β from the track momentum. In order to be independent from the absolute time zero determination, the difference $\Delta = \delta_t(m)_1 - \delta_t(m)_2$ is evaluated. For the correct mass assignment, this difference is expected to be around zero. Therefore a cut at $|\Delta| \leq 1$ ns is applied to select the signal. In the end, events are kinematically constrained at the K_S vertex finding the neutrino energy E_{miss} and momentum P_{miss}. The difference of these two variables is plotted in Fig. 2. The observed peak around zero is due to the $K_S \to \pi e\nu$ decays, while the residual $K_S \to \pi^+\pi^-$ background populates the region above zero. The histogram corresponds to $\sim 17\text{pb}^{-1}$ of data of year 2000, while crosses are the results of a fit to the sum of the MC spectra for signal and background events. The free parameters of the fit are the independent normalizations of the signal and background distributions, and the finite MC statistics has been taken into account in the likelihood function. As a result of the fit, 627 ± 30 signal events are observed.

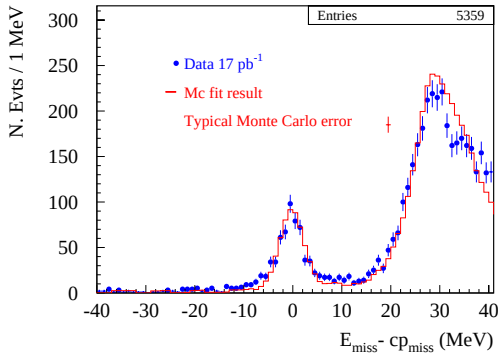

Figure 2: Spectrum of $E_{miss} - P_{miss}$ for $K_S \to \pi e\nu$ candidate events; data (crosses) are compared to MC (solid histogram).

The vertex reconstruction, π/e identification and trigger efficiencies can be evaluated from a clean and unbiased sample of $K_L \to \pi e\nu$ events in which the K_L decays near the IR, thus simulating a $K_S \to \pi e\nu$ decay. The track-cluster association efficiency is evaluated using proper samples of $\phi \to \pi^+\pi^-\pi^0$, $K_S \to \pi^+\pi^-$ and $K_L \to \pi e\nu$ events. Therefore from these events the probability that a given particle (π^+, π^-, $\mu^\pm$ or $e^\pm$) reaching the calorimeter deposits enough energy to register a cluster and that the track and cluster are then correctly associated can be obtained. The final result is obtained by normalizing the number of signal events to the number of $K_S \to \pi^+\pi^-$ events in the same data set and using the present experimental value for $\text{BR}(K_S \to \pi^+\pi^-)$.

Based on year 2000 data, KLOE has published [8]:

$$\text{BR}(K_S \to \pi e\nu) = (6.91 \pm 0.34_{\text{stat}} \pm 0.15_{\text{syst}}) \cdot 10^{-4} \tag{4}$$

in agreement with the expectation of the $\Delta S = \Delta Q$ rule. The relative uncertainty on the KLOE

measurement is less than a third of that on the only previously existing measurement [9].

Data of year 2001 and 2002 have been also preliminarly analysed. Based on a statistics corresponding to an integrated luminosity of ~ 170 pb^{-1}, an improved determinatation of the above branching ratio is

$$\mathrm{BR}(K_S \to \pi e \nu) = (6.76 \pm 0.12_{\mathrm{stat}} \pm 0.10_{\mathrm{syst}}) \cdot 10^{-4} \tag{5}$$

Assuming CPT, from this result one can determine a limit for the parameter $Re(x_+)$, which describes the departure from the $\Delta S = \Delta Q$ rule:

$$Re(x_+) = (2.2 \pm 5.3_{\mathrm{stat}} \pm 3.5_{\mathrm{syst}}) \cdot 10^{-3} \tag{6}$$

One can also test CPT conservation by measuring K_L and K_S charge asymmetries in semileptonic decays, defined as:

$$\delta_{\mathrm{L,S}} = \frac{\Gamma^+_{\mathrm{L,S}} - \Gamma^-_{\mathrm{L,S}}}{\Gamma^+_{\mathrm{L,S}} + \Gamma^-_{\mathrm{L,S}}} \tag{7}$$

where $\Gamma^{+(-)}_{\mathrm{L,S}}$ are the decay widths for K_{LS} decays to a positively (negatively) charged lepton. It can be shown that the quantity $\delta_{\mathrm{S}} - \delta_{\mathrm{L}}$ measures the amount of CPT violation either in the decay or in the kaon mixing matrix [10]. At present, while δ_{L} is known with an absolute error of about 70 parts per million [11], δ_{S} has never been measured.

The procedure for signal extraction and efficiency determination described above, can be applied separately for the two charge states, taking into account the differences in π^+ and π^- interaction in the calorimeter, thus allowing for the measurement of the charge asymmetry. The KLOE preliminary measurement is:

$$\delta_S = (1.9 \pm 1.7_{\mathrm{stat}} \pm 0.6_{\mathrm{syst}}) \cdot 10^{-2} \tag{8}$$

6 BR($K_L \to \gamma\gamma$)/BR($K_L \to \pi^0\pi^0\pi^0$)

The measurement of $\Gamma(K_L \to \gamma\gamma)$ is a good test for Chiral Perturbation Theory, and helps in constraining the value of the CKM matrix parameter ρ if combined with $\Gamma(K_L \to \mu\mu)$. A recent measurement by the NA48 Collaboration [12] gives $\Gamma(K_L \to \gamma\gamma)/\Gamma(K_L \to \pi^0\pi^0\pi^0) = (2.81 \pm 0.01_{\mathrm{stat}} \pm 0.02_{\mathrm{syst}}) \cdot 10^{-3}$.

At KLOE $K_L \to \gamma\gamma$ and $K_L \to \pi^0\pi^0\pi^0$ decays are selected by looking for a neutral vertex in events tagged by a $K_S \to \pi^+\pi^-$ decay. The K_L decay vertex is required to be identified whithin the fiducial volume (FV) defined by the conditions: $30 \geq r_t(cm) \leq 170$, $|z|(cm) \leq 140$. Although the efficiency of the tag slightly depends on the K_L decay channel, it is shown to be the same for the two channels of interest, thus cancels out in the ratio.

The K_L flight direction is determined by the reconstructed decay kinematics of the accompanying K_S. Its decay vertex is then considered found if at least three (for $K_L \to \pi^0\pi^0\pi^0$) or exactly two (for $K_L \to \gamma\gamma$) neutral clusters are observed in the calorimeter with times compatible with those expected for photons produced on a point along that direction. In the case of the more rare $K_L \to \gamma\gamma$ decay, the two photons are also required to satisfy the associated two body decay kinematics. The efficiency of the selection in the FV is $\geq 99\%$ for $K_L \to \pi^0\pi^0\pi^0$ and $\sim 90\%$ for $K_L \to \gamma\gamma$ events. The ability for finding the neutral vertex in the FV is also checked on data with the use of $K_L \to \pi^+\pi^-\pi^0$ decays.

Using data from 312 pb^{-1} collected in 2001 and 2002, KLOE measures preliminarly:

$$\Gamma(K_L \to \gamma\gamma)/\Gamma(K_L \to \pi^0\pi^0\pi^0) = (2.80 \pm 0.03_{\mathrm{stat}} \pm 0.02_{\mathrm{syst}}) \cdot 10^{-3} \tag{9}$$

in excellent agreement with the above mentioned NA48 result.

7 BR($\phi \to \eta'\gamma$)

The branching ratio of the decay $\phi \to \eta'\gamma$ is particularly interesting since its value can probe the $|s\overline{s}\rangle$ and gluonium content of the η' [14, 15, 16]. In particular, the ratio of its value to the one of $\phi \to \eta\gamma$ can be related to the $\eta - \eta'$ mixing parameters and determine the mixing angle in the flavor basis φ_P, offering an important point of comparison for the description of the $\eta - \eta'$ mixing in chiral perturbation theory [17].

The decay chains considered are:

- $\phi \to \eta'\gamma$ with $\eta' \to \pi^+\pi^-\eta$ and $\eta \to \gamma\gamma$
- $\phi \to \eta\gamma$ with $\eta \to \pi^+\pi^-\pi^0$ and $\pi^0 \to \gamma\gamma$

In both cases the final state is $\pi^+\pi^-\gamma\gamma\gamma$, resulting in several systematic errors cancellation in the measurement of the ratio BR($\phi \to \eta'\gamma$)/BR($\phi \to \eta\gamma$). For both channels events are selected requiring the presence of three prompt photons and two tracks of opposite charge with a vertex near the IR. Then a preliminary kinematic fit is performed requiring total energy and momentum conservation, the constraint $\beta = 1$ for all photons, without any invariant mass constraint on intermediate particles. Simple kinematic cuts eliminate the background mainly due to $\phi \to \pi^+\pi^-\pi^0$ events in which a spurious cluster is present, and to $\phi \to K_S K_L \to \pi^+\pi^-\pi^0\pi^0$ events in which one photon is lost.

The energy spectrum of the photons gives no combinatorial problem: the radiative photon is the hardest one in $\phi \to \eta\gamma$ events ($E_{rad} \simeq 363$ MeV), while is the softest in $\phi \to \eta'\gamma$ events ($E_{rad} \simeq 60$ MeV), the other two photons being generated in π^0 and η decays, respectively. Hence η' events are disentangled from η background by proper cuts on the energy spectrum of the two hardest photons γ_1 and γ_2.

The distribution of the invariant mass of $\pi^+\pi^-\gamma_1\gamma_2$ for the $\phi \to \eta'\gamma$ events is shown in Fig.3, where a small residual background is observed in the η' peak region. The shape of the background is obtained from sidebands of the signal region in the γ_1 and γ_2 energy distribution. The number of signal events, as obtained from the simple fit shown in Fig.3, is $120 \pm 12_{\rm stat} \pm 5_{\rm syst}$. The ratio BR($\phi \to \eta'\gamma$)/BR($\phi \to \eta\gamma$) is obtained by normalizing to the number of $\phi \to \eta\gamma$ observed events and correcting for detection efficiency taken from MC.

The KLOE published result is [13]:

$$\frac{\mathrm{BR}(\phi \to \eta'\gamma)}{\mathrm{BR}(\phi \to \eta\gamma)} = (4.7 \pm 0.47_{\rm stat} \pm 0.31_{\rm syst}) \cdot 10^{-3} \tag{10}$$

from which the corresponding value for the mixing angle can be extracted [15, 17]:

$$\varphi_P = (41.8^{+1.9}_{-1.6})^\circ \tag{11}$$

Making use of BR($\phi \to \eta\gamma$) value from Ref. [7], it is obtained:

$$\mathrm{BR}(\phi \to \eta'\gamma) = (6.10 \pm 0.61_{\rm stat} \pm 0.43_{\rm syst}) \cdot 10^{-5} \tag{12}$$

which is the most accurate measurement to date. The value obtained disfavours a very large gluonium content of η'.

The η' channel has been searched for also in the final state with seven photons and two charged tracks, produced by the two following decay chains:

- $\phi \to \eta'\gamma$; $\eta' \to \eta\pi^+\pi^-$; $\eta \to \pi^0\pi^0\pi^0$

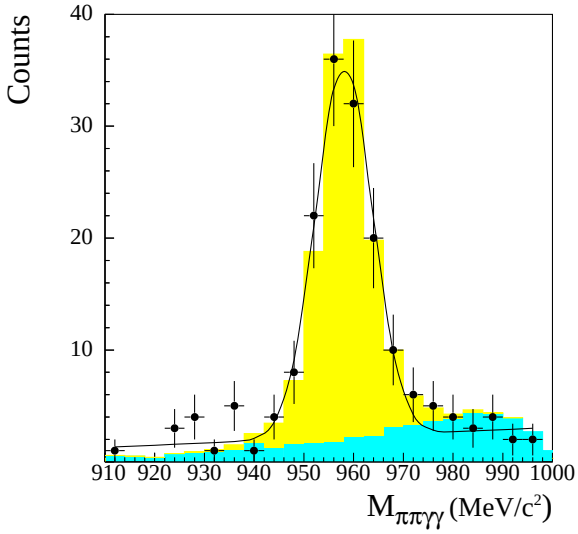

Figure 3: The $\pi^+\pi^-\gamma_1\gamma_2$ invariant mass distribution for candidate events $\phi \to \eta'\gamma$. The darker shaded area represents the residual background. The continuous line is the result of a gaussian plus linear fit.

- $\phi \to \eta'\gamma$; $\eta' \to \eta\pi^0\pi^0$; $\eta \to \pi^+\pi^-\pi^0$

  Using data of the year 2000 run, KLOE measures preliminarly:

$$\mathrm{BR}(\phi \to \eta'\gamma) = (7.05 \pm 0.50_{\mathrm{stat}} \pm 0.53_{\mathrm{syst}}) \cdot 10^{-5} \tag{13}$$

in agreement with the published result (12). This is the first time that such final state has been observed, to date.

8 Study of $\phi \to \pi^0\pi^0\gamma$ and $\phi \to \eta\pi^0\gamma$

Several models proposed to explain the nature of the f_0 and a_0 mesons: ordinary $q\overline{q}$ meson, $q\overline{q}q\overline{q}$ state, $K\overline{K}$ molecule, make different predictions of $\mathrm{BR}(\phi \to f_0\gamma)$, $\mathrm{BR}(\phi \to a_0\gamma)$ and their ratio [18]. Therefore a precise measurement of $\mathrm{BR}(\phi \to f_0\gamma)$ and $\mathrm{BR}(\phi \to a_0\gamma)$ would clarify the interpretation on the nature of these mesons. Up to now only the VEPP-2M experiments have studied these decays [19, 20].

At KLOE the following decay chains are considered:

- $\phi \to f_0\gamma$ with $f_0 \to \pi^0\pi^0$
- $\phi \to a_0\gamma$ with $a_0 \to \eta\pi^0$ and $\eta \to \gamma\gamma$

In both cases the final state is 5γ's. Several backgrounds are present: the main contributions come from the resonant process $\phi \to \rho^0\pi^0$ with $\rho^0 \to \pi^0\gamma$ or $\rho^0 \to \eta\gamma$, and the continuum process $e^+e^- \to \omega\pi^0$ with $\omega \to \pi^0\gamma$ or $\omega \to \eta\gamma$. Also the process $\phi \to \sigma(500)\gamma$ is taken into account, where

Table 1: Results of the fits to f_0 and a_0 parameters. See text for details.

f_0	Fit A	Fit B
χ^2/ndf	109.5/34	43.2/33
M_{f_0} (MeV)	962 ± 4	973 ± 1
$g^2_{f_0KK}/(4\pi)$ (GeV^2)	1.29 ± 0.14	2.79 ± 0.12
$g^2_{f_0KK}/g^2_{f_0\pi\pi}$	3.22 ± 0.29	4.00 ± 0.14
$g_{\phi\sigma\gamma}$	-	0.060 ± 0.008
a_0		
χ^2/ndf	27.2/25	
$g^2_{a_0KK}/(4\pi)$ (GeV^2)	0.40 ± 0.04	
$g_{a_0\eta\pi}/g_{a_0KK}$	1.35 ± 0.09	
Br$(\phi \to \rho^0\pi^0 \to \eta\pi^0\gamma)$	$(0.5 \pm 0.5) \times 10^{-5}$	

$\sigma(500) \to \pi^0\pi^0$ is the scalar meson recently observed at FNAL by the E791 Collaboration [21] There are also contributions from the 3γ's final states in which two clusters are spurious, and from 7γ's final state in which two clusters are lost.

The events are identified by requiring five prompt photons within loose acceptance cuts. Then a preliminary kinematic fit is performed requiring total energy and momentum conservation with the additional constraint $\beta = 1$ for all photons, thus refining the measured cluster positions, energies, and times. The best photon pairing is then obtained assuming each one of the possible decays, e.g. $\phi \to \pi^0\pi^0\gamma$, $\phi \to \eta\pi^0\gamma$, and $e^+e^- \to \omega\pi^0$. For each of them, a second kinematic fit is then performed with additional constraints on the masses of intermediate η's and π^0's. Finally the $\phi \to \pi^0\pi^0\gamma$ and $\phi \to \eta\pi^0\gamma$ events are isolated by means of cuts on kinematic variables and on the χ^2 probability values obtained in the second series of kinematic fits.

The overall detection efficiency is obtained by tuning the MC to reproduce the observed $M_{\pi^0\pi^0}$ and $M_{\eta\pi^0}$ invariant mass distributions in case of $\phi \to \pi^0\pi^0\gamma$ and $\phi \to \eta\pi^0\gamma$ events, respectively. The background in the $M_{\pi^0\pi^0}$ and $M_{\eta\pi^0}$ distributions is estimated using the MC and the cross section values for various processes directly measured by KLOE. The background from misreconstructed 3γ's final state events is estimated by embedding accidental cluster distributions obtained directly from data into MC generated events.

KLOE published results are [22]:

$$\mathrm{BR}(\phi \to \pi^0\pi^0\gamma) = (1.09 \pm 0.03_{\mathrm{stat}} \pm 0.05_{\mathrm{syst}}) \cdot 10^{-4} \tag{14}$$

and [23]

$$\mathrm{BR}(\phi \to \eta\pi^0\gamma) = (8.51 \pm 0.51_{\mathrm{stat}} \pm 057_{\mathrm{syst}}) \cdot 10^{-5} \tag{15}$$

In order to disentangle the various contributions, the data have been fitted to theoretical mass spectra obtained from the following model: (a) the coupling of ϕ to $S(0^{++})\gamma$ is assumed to occur through a charged kaon loop, (b) the scalar propagator with finite width corrections is used, (c) the $\phi \to \rho^0\pi^0$ parametrization is taken from VDM calculations. Two different fits have been tried on the $\pi^0\pi^0$ mass spectrum, after background subtraction: without (Fit A) and with (Fit B) $\phi \to \sigma(500)\gamma$; the $\sigma(500)$ has been parametrized as a fixed width Breit-Wigner ($M_\sigma = 478$ MeV, $\Gamma_\sigma = 324$ MeV [21]) and a point-like $\phi - \sigma\gamma$ coupling has been assumed. The free parameters of the fits are: the f_0 mass, the coupling $g^2_{f_0KK}/(4\pi)$, the ratio $g^2_{f_0KK}/g^2_{f_0\pi\pi}$, the Br$(\phi \to \rho^0\pi^0 \to \pi^0\pi^0\gamma)$

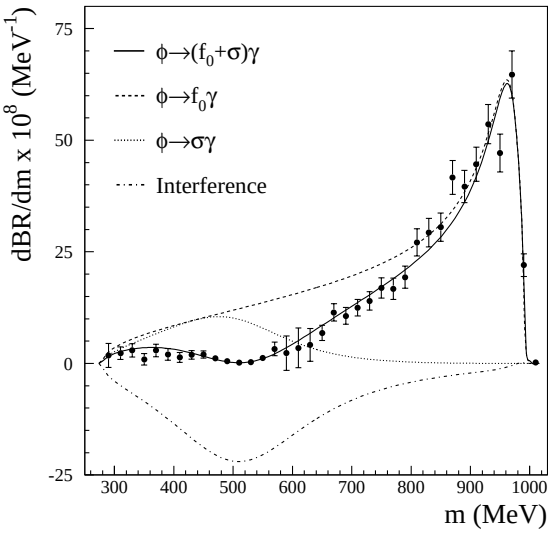

Figure 4: Differential branching ratio for $\phi \to \pi^0\pi^0\gamma$ events, as a function of m, the invariant mass of the two π^0 system. Fit (B) is shown as a solid line; individual contributions are also shown.

and $g_{\phi\sigma\gamma}$ (only for Fit B). The parameter values are listed in tab.1, the $\phi \to \rho^0\pi^0$ contribution turns out to be negligible for both fits. Fit A gives a large χ^2, while Fit B shows a good agreement with the experimental data. In fig.4 the differential decay rate is plotted, as a function of the invariant mass of the $2\pi^0$ system, together with the various contributions from Fit B; the depletion of the mass spectrum below 700 MeV is produced by a large negative interference between f_0 and σ.

For $\phi \to \eta\pi^0\gamma$, a combined fit of the two mass spectra, after background subtraction, has been performed, by fixing their relative normalization to the ratio $\mathrm{Br}(\eta \to \gamma\gamma)/\mathrm{Br}(\eta \to \pi^+\pi^-\pi^0)$. The free parameters are: the coupling $g^2_{a_0KK}/(4\pi)$, the ratio $g_{a_0\eta\pi}/g_{a_0KK}$ and $\mathrm{Br}(\phi \to \rho^0\pi^0 \to \eta\pi^0\gamma)$ (tab.1). The mass of the a_0 is not free, it has been fixed to the PDG value M_{a_0}=984.8 MeV. By integrating the theoretical curve over the fit results, the a_0 contribution can be evaluated:

$$BR(\phi \to a_0\gamma \to \eta\pi^0\gamma) = (7.4 \pm 0.7) \times 10^{-5} \tag{16}$$

The f_0 parameters are compatible with the $q\overline{q}q\overline{q}$ model, while the a_0 ones disagree with that model.

The final state corresponding to $\phi \to \eta\pi^0\gamma, \eta \to \pi^+\pi^-\pi^0$ decay consists of two charged tracks from the interaction point and five prompt photons. This signature is unique among all of the possible final states, so that it is less affected from background with respect to the five photons one. The analysis scheme is very similar to that of the five photons sample. In the same data set, 196 events have been selected, with an estimated background of 4±4 events. From this decay chain

$$Br(\phi \to \eta\pi^0\gamma) = (7.96 \pm 0.60 \pm 0.40) \times 10^{-5} \tag{17}$$

can be extracted, in good agreement with the result of the five photon sample (15).

9 Study of $\phi \to \pi^+\pi^-\pi^0$ decays

The decay of the ϕ mesons to three pions is dominated by the $\rho\pi$ intermediate state through the equally probable $\rho^+\pi^-$, $\rho^-\pi^+$, $\rho^0\pi^0$ states. Further contributions are the direct term and the $\omega\pi$ term, where the ω decays to $\pi^+\pi^-$. Introducing the two Dalitz variables $X = T^+ - T^-$ and $Y = T^0$ where $T^{+,-,0}$ are the kinetic energies of the pions in the centre of mass system, the Dalitz plot distribution $D(X,Y)$ is expressed in terms of the three contributing amplitudes as:

$$D(x,y) \propto |\vec{p}^{\,CM}_{\pi^+} \times \vec{p}^{\,CM}_{\pi^-}|^2 |A_{\rho\pi} + A_{\rm dir} + A_{\omega\pi}|^2 \tag{18}$$

where $\vec{p}^{\,CM}_{\pi^\pm}$ are the $\pi^\pm$ momenta in the CM and $A_{\rho\pi}$, $A_{\rm dir}$ and $A_{\omega\pi}$ are the amplitudes described above.

At KLOE, $\phi \to \pi^+\pi^-\pi^0$ are selected by looking for two opposite charge tracks coming from the interaction point with a polar angle $\theta > 40^\circ$. The missing mass at the vertex, computed making use of the measured quadrimomenta of the charged pions and the known quadrimomentum of the ϕ, is required to be whithin ± 20 MeV of the nominal π^0 mass. Moreover, two photons of energy larger than 10 MeV and polar angle larger than 20° are required in the calorimeter. The cosine of the angle $\theta_{\gamma\gamma}$ between the two photons in the π^0 reference frame is required to be lower than -0.98.

With the above selection criteria, a sample of 2 millions of events is selected in a data set of 16 pb^{-1} collected in the fall of 2000. The contamination of the background in the above sample is negligible ($< 10^{-5}$). The Dalitz plot of this data sample is shown in fig.5.

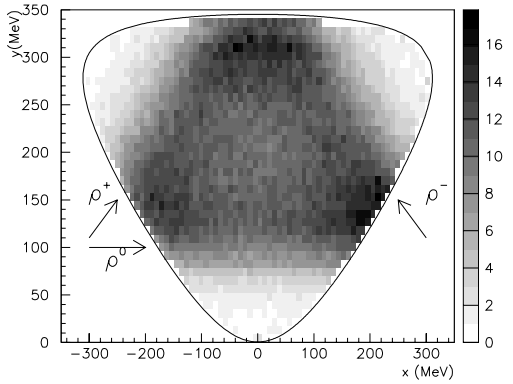

Figure 5: Distribution of the number of events corrected for the efficiency and divided by $|\vec{p}^{\,CM}_{\pi^+} \times \vec{p}^{\,CM}_{\pi^-}|$ for 1.98 millions selected $\phi \to \pi^+\pi^-\pi^0$ decays. Three broad bands corresponding to the three charge states are indicated. The kinematical boundary is also shown.

Trigger and selection efficiencies are evaluated as function of the position whithin the Dalitz plot, making use of a full Monte Carlo simulation of the detector with corrections based on several control data sample. The overall efficiency ranges between 20 and 30%. The uncertainty on the efficiency is dominated by Monte Carlo statistics and is of the order of 1% in each bin.

The fits to the Dalitz plot are done using a standard binned χ^2 technique. Three different fits have been performed: (a) a fit assuming CPT invariance and no isospin violations ($M_{\rho^0} = M_{\rho^+} = M_{\rho^-}$ and $\Gamma_{\rho^0} = \Gamma_{\rho^+} = \Gamma_{\rho^-}$), (b) a fit assuming CPT invariance but allowing isospin violation ($M_{\rho^+} = M_{\rho^-}$ and $\Gamma_{\rho^+} = \Gamma_{\rho^-}$), (c) and finally a fit allowing also for CPT violation. In all of the

Table 2: Fit results. Masses and widths are in MeV. The amplitudes are scaled in such a way that a_ρ=1. ϕ_d and ϕ_ω are in radians. χ^2 values and probabilities of the fits are given in the first raw.

parameter	fit(a)	fit(b)	fit(c)
χ^2 $[p(\chi^2)]$	1939 [12%]	1914 [21%]	1902 [26%]
M_{ρ^0}	$775.8 \pm 0.5 \pm 0.3$	$775.9 \pm 0.5 \pm 0.5$	$775.9 \pm 0.6 \pm 0.5$
M_{ρ^+}		$775.5 \pm 0.5 \pm 0.4$	$776.3 \pm 0.6 \pm 0.7$
M_{ρ^-}			$774.8 \pm 0.6 \pm 0.4$
Γ_{ρ^0}	$143.9 \pm 1.3 \pm 1.1$	$147.3 \pm 1.5 \pm 0.7$	$147.4 \pm 1.5 \pm 0.7$
Γ_{ρ^+}		$143.7 \pm 1.3 \pm 1.2$	$144.7 \pm 1.4 \pm 1.2$
Γ_{ρ^-}			$142.9 \pm 1.3 \pm 1.4$
a_d	$0.78 \pm 0.09 \pm 0.13$	$0.72 \pm 0.09 \pm 0.05$	$0.71 \pm 0.09 \pm 0.05$
ϕ_d	$2.47 \pm 0.08 \pm \pm 0.08$	$2.43 \pm 0.10 \pm 0.08$	$2.43 \pm 0.10 \pm 0.08$
$a_\omega \times 10^3$	$7.1 \pm 0.6 \pm 0.8$	$9.0 \pm 0.7 \pm 0.7$	$9.0 \pm 0.7 \pm 0.3$
ϕ_ω	$-0.22 \pm 0.11 \pm 0.04$	$-0.10 \pm 0.10 \pm 0.05$	$-0.10 \pm 0.10 \pm 0.07$

fits the following are free parameters: modulus and phase of the direct term a_d and ϕ_d, modulus and phase of the coefficient of the $\omega\pi$ term, and an overall normalization factor. The results of the fits are shown in table2

Fit (a) converges to an acceptable χ^2 probability, showing that the experimental distribution is in agreement with a model neglecting any possible CPT and Isospin violations. The values of the ρ mass are significantly larger and the widhts are significantly lower with respect to the PDG averages, but are closer to recent results [25, 26, 27].

We observe significant contributions from the direct term and from the $\omega\pi$ term, the coefficients a_d and a_ω are significantly different from 0. If we define the weight of each contribution α ($\alpha = \rho\pi$, dir and $\omega\pi$) as

$$I_\alpha = \int dxdy|A_\alpha|^2 / \int dxdy|A_{tot}|^2 \tag{19}$$

we get the following weights (A_{dir} and A_{tot} are taken from fit c. $A_{\rm tot}$ is the sum of three amplitudes given in eq. 18):

$$I_{\rho\pi} = 0.937 \tag{20}$$

$$I_{\rm dir} = 8.5 \times 10^{-3} \tag{21}$$

$$I_{\omega\pi} = 2.0 \times 10^{-4} \tag{22}$$

The sum of the three weights is not equal to one, due to a sizeable interference term between $A_{\rho\pi}$ and $A_{\rm dir}$ accounting for about 6% of the total. From $I_{\omega\pi}$, neglecting interference, we get the cross section for the non resonant process $e^+e^- \to \omega\pi^0$ with $\omega \to \pi^+\pi^-$ at $W = 1019.4$ MeV.

$$\sigma(e^+e^- \to \omega\pi^0 \to \pi^+\pi^-\pi^0) = I_{\omega\pi} \times \sigma(e^+e^- \to \pi^+\pi^-\pi^0) = 92 \pm 15 \text{ pb} \tag{23}$$

The ratio of this cross-section to the value $\sigma(e^+e^- \to \omega\pi^0 \to \pi^0\pi^0\gamma) = 0.46 \pm 0.01 \pm 0.03$ nb obtained by KLOE in the 5 photons analysis [22] gives:

$$R = \frac{\text{BR}(\omega \to \pi^+\pi^-)}{\text{BR}(\omega \to \pi^0\gamma)} = 0.20 \pm 0.04 \tag{24}$$

which compares well with the value 1.7/8.7=0.20±0.03 from [7].

10 Talks by LNF authors in year 2002

G. Lanfranchi, The KLOE electromagnetic calorimeter, Inst. for colliding beams physics, Novosibirsk
V. Patera, Recent results from KLOE at DAΦNE, Moriond Workshop
B. Sciascia, KLOE perspectives in K_{l3} decays, CKM Workshop, CERN
S. Dell'Agnello, La camera a deriva di KLOE, Incontri di fisica, PARMA
P. Valente, Recent results from KLOE, Meson 2002, Cracow
M. Palutan, KLOE results, STORI02, Uppsala
S. Miscetti, Recent results from KLOE, SLAC Summer Institute
S. Giovannella, KLOE results on radiative decays, PANIC02, Osaka
S. Giovannella, KLOE results on radiative decays, Garniano
G. Capon, KLOE results, SIF, Alghero
A. Denig, KLOE results, RADCOR02, Kloster Banz
M. Antonelli, KLOE results, Seminar Marseille
T. Spadaro, KLOE results on K_S semileptonic decays, Frontier Science 2002, Frascati

11 KLOE papers in year 2002

1. KLOE Collaboration, *The KLOE electromagnetic calorimeter*, Nucl. Inst. Meth. A 482, 363-385 (2002).
2. KLOE Collaboration, *The QCAL tile calorimeter of KLOE*, Nucl. Inst. Meth. A 483, 649-659 (2002).
3. KLOE Collaboration, *The tracking detector of the KLOE experiment*, Nucl. Inst. Meth. A 488, 1-23 (2002).
4. KLOE Collaboration, *The trigger system of the KLOE experiment*, Nucl. Inst. Meth. A 492, 134-146 (2002).
5. KLOE Collaboration, *Measurement of the branching ratio of the decay* $K_S \to \pi e \nu$, Phys. Lett B 535, 37-42 (2002).
6. KLOE Collaboration, *Study of the decay* $\phi \to \eta\pi^0\gamma$ *with the KLOE detector*, Phys. Lett B 536, 209-216 (2002).
7. KLOE Collaboration, *Study of the decay* $\phi \to \pi^0\pi^0\gamma$ *with the KLOE detector*, Phys. Lett B 537, 21-27 (2002).
8. KLOE Collaboration, *Measurement of* $\Gamma(K_S \to \pi^+\pi^-/\Gamma(K_S \to \pi^0\pi^0)$, Phys. Lett B 538, 21-26 (2002).
9. KLOE Collaboration, *Measurement of* $\Gamma(\phi \to \eta'\gamma)/\Gamma(\phi \to \eta\gamma)$ *and the pseudoscalar mixing angle*, Phys. Lett B 541, 45-51 (2002).

References

1. S. Guiducci et al, Proceedings of PAC99, New York, March 1999

2. KLOE collaboration, *KLOE: a general purpose detector for DAΦNE*, LNF-92/019 (IR) (1992); KLOE collaboration, *The KLOE detector - technical proposal*, LNF-93/002 (IR) (1993)

3. G. D'Ambrosio, G. Isidori and A. Pugliese, "CP and CPT measurements at DAΦNE", in L. Maiani, G. Pancheri and N. Paver eds., *The second DAΦNE physics handbook*, LNF, Frascati, (1995)

4. KLOE Collaboration, Nucl. Inst. Meth. A 482, (2002) 363-385

5. KLOE Collaboration Nucl. Inst. Meth. A 488, (2002) 1-23

6. KLOE Collaboration, Phys. Lett B 538, (2002) 21-26

7. Particle Data Group, K. Hagiwara et al., Phys. Rev. D66 (2002) 010001

8. KLOE Collaboration Phys. Lett B 535, (2002) 37-42

9. R. R. Akhmetshin et al., Phys. Lett. B456 (1999) 90

10. L. Maiani, "CP and CPT violation in neutral kaon decays", in: L. Maiani, G. Pancheri, N. Paver eds., *The second DAΦNE physics handbook* , LNF, Frascati (1995)

11. A. Alavi-Harati *et al.*, Phys. Rev. Lett. 88 (2002) 52

12. A. Lai et. al, Phy. Lett. B551 (2003) 7

13. KLOE Collaboration, Phys. Lett B 541, (2002) 45-51

14. J. L. Rosner, Phys. Rev D27 (1983) 1101

15. A. Bramon, R. Escribano and M.D. Scadron, Eur. Phys. J. C7 (1999) 271

16. E. Kou, Phys. Rev. D63 (2001) 054027

17. T. Feldmann, Int. J. Mod. Phys. A15 (2000) 159

18. F. E. Close and A. Kirk, Phys. Lett. B515 (2001) 13 and references therein

19. R. R. Akhmetshin et al., Phys. Lett. B462 (1999) 380

20. M. N. Achasov et al., Phys. Lett. B479 (2000) 53; M. N. Achasov et al., Phys. Lett. B485 (2000) 349

21. E. M. Aitala et al., Phys. Rev. Lett. 86 (2001) 770

22. KLOE Collaboration, Phys. Lett B 537, (2002) 21-27

23. KLOE Collaboration Phys. Lett B 536, (2002) 209-216

24. M. N. Achasov V. V. Gubin, Phys. Rev. D63 (2001) 094007

25. R. Barate et al., Zeit. Phys. C76 (1997) 15

26. R.R. Akhmetshin et al., Phys. Lett. B527 (2002) 161

27. M. N. Achasov et al., Phys. Rev. D65 (2002) 03002

LHCb

M. Alfonsi (Laur.), M. Anelli (Tecn.), G. Bencivenni, C. Bloise, F. Bossi, P. Campana,
G. Capon, M. Carletti (Tecn.), P. de Simone, C. Forti, A. Franceschi, G. Lanfranchi, F. Murtas,
L. Passalacqua, V. Patera (Ass.), M. Poli Lener (Laur.), A. Sciubba(Resp.Ass.)

In collaboration with the "Servizio di Automazione":
U. Denni, M.A. Frani, A. Saputi.

In collaboration with the "Servizio di Elettronica":
A. Balla, F. Bertino, P. Ciambrone, G. Corradi, G. Felici,
G. Paoluzzi, G. Papalino, D. Riondino, M. Santoni.

1 Introduction

The LNF group of LHCb operates on the **muon subdetector** with responsibilities on detectors (WPC and GEM), electronics and mechanics. In 2002 all the projects have been finalized with the production of several prototypes. In 2003 the detector production will start and a test of the electronics chain will be performed.

2 Multiwire Proportional Chambers

LHCb-LNF has the responsibility for the construction of $\sim 1/4$ of the MWPCs of the muon detector. Depending on the position inside the detector, there are different chamber dimensions with different readout: anode pads, cathode pads, anode & cathode pads.

We designed, collaborating with the Ferrara group, all the details of 10 different chambers types (with active dimensions ranging from 29×35 cm^2 to 27×130 cm^2). With these characteristics 444 chambers will be assembled and tested, half in LNF, half in Ferrara. The same design will be applied to the remaining 456 chambers that will be built at CERN and in S.Petersbourg.

2.1 Brief description of MWPC

The MWPC chambers of the LHCb muon detector must fulfill stringent requirements on time response: for triggering purpose $\sim 95\%$ minimum efficiency must be exploited in 20 ns. Each chamber is constituted by 4 layers assembled as two independent bigaps with hardwired-OR of the readout. In each 5 mm gap there are 30 microns gold plated tungsten wires stretched at about 60 grams. The filling mixture is $Ar/CO_2/CF_4$ (40/40/20).

To obtain more stable working conditions of the chambers, the CERN group performed some measurements [1)] on a small prototype with a wire pitch increased to 2 mm. Since wider plateau at reduced high voltage has been obtained without any appreciable loss on timing performances of a double gap, this wire spacing is now being adopted in the chamber production.

2.2 Main goals reached in 2002

PANELS

The chamber **panels** are obtained injecting a rigid polyurethanic foam (ESADUR 120) between two FR4 printed circuit boards. In addition to a small preliminary mould also one of the two final moulds (one for wide panels and one for high panels) have been constructed. With this final mould, several big panels ($\sim 140 \times 35\ cm^2$) have been produced and showed to satisfy the most critical requirements: thickness and planarity are constant within $\pm 50 \mu m$.

Several **mechanical tests** have been caried out on panels to study their resistance to tensile, compression, flexural strenghts. Before the tests, some panels were irradiated with a powerful Co^{60} at Calliope facility at ENEA-Casaccia [2)], with a dose of $1 Mrad$, corresponding to ~ 10 LHC years. The facility consists of a high intensity (∼25,000 Curie) ^{60}Co source emitting γ of 1.25 MeV average energy. The tests proved [3)] that the panels are very robust and are not affected by this radiation dose.

After production of tens of panels, we verified that both **moulds** still respects geometrical tolerances (in particular the planarity).

CONSTRUCTION OF CHAMBER PROTOTYPES

The first **big chamber prototype** (with active area $\sim 130 \times 27\ cm^2$) have been constructed and tested at a CERN beam (october 2002). The prototype performance were satisfactory : high efficiency ($\sim 99\% for HV > 3.1 kV$), low crosstalk ($\sim 2\%$), low cluster size (1.08 on average at 220 mV threshold and HV=3.1 kV), and good time resolution (3.6 ns at 220 mV, HV=3.1 kV).

DESIGN AND ENGINEERING OF CHAMBER PROTOTYPES

Moving toward the production line, several improvements have been done both on the production tools (new **vacuum system** of the mould, new **foam injectors**) and in the chamber design (dimensions slightly changed, new gas and HV distributions).

AGING TEST OF CHAMBER PROTOTYPES

An **aging test** has been performed on a small chamber quadrigap prototype (with active area $\sim 20 \times 25\ cm^2$) at Calliope facility at ENEA-Casaccia [2)]. We monitored the current in the 4 gaps (A,B,C,D) of the test chamber and in the 4 gaps of a similar monitor chamber.

The current in each gap is related to the high voltage (V) and the gas temperature (T) and pressure (P), according to the formula:

$$I = K \cdot e^{\alpha\ V\ T/P}$$

where α is the amplification coefficient. To take into account all the temperature and pressure variations of the gas mixture, the ratio of the amplification coefficients of test chamber divided the average amplification coefficient of the monitor chamber have been computed for each gap:

$$R^i = /[ln(I_T^i) - ln(K_T^i)]/[ln(I_M) - ln(K_M)] = \alpha_T^i/\alpha_M$$

These ratios are shown in Fig.1. They are constant within $\sim 1\%$. Over a test duration of ~ 90 hours, we integrated ~ 50 mC/cm of wire, without any appreciable deterioration.

CLEAN ROOM AND TOOLING

A **clean room** dedicated to the WPC and GEM production has been commissioned and will be operating in 2003. Several equiments have already been built/ordered in order to instrument the

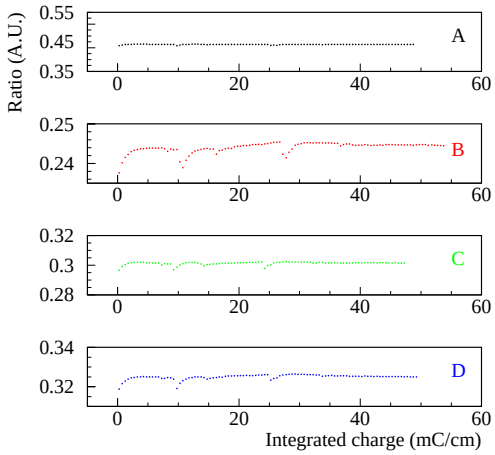

Figure 1: Ratio R^i (see text) for each gap of the test chamber over the same coefficient obtained from the average current of the four gaps of the monitor chamber, as function of the integrated charge.

area (tables, wiring machine, soldering machine, GEM assembly tools, etc.) and will be installed as soon as the room will be ready.

3 Triple GEM detectors

For the innermost part (R1, $\sim 3\text{m}^2$ area) of the first muon station (M1) of the LHCb experiment the LNF group, in collaboration with INFN-Cagliari, proposes a detector based on Gas Electron Multiplier (GEM) technology. The requirements [4] for the detector are: a rate capability of $\sim$ 500 kHz/cm^2; each station must have an efficiency of $\sim$ 96% in a 20 ns time window (two independent detector layers per station, logically OR-ed, are foreseen); the cluster size, i.e. the number of adjacent detector pads fired when a track crosses the detector, should not be larger than 1.2, for a 10$\times$25 mm^2 pad size; a radiation hardness of $\sim$ 6 C/cm^2 in 10 years of operation (for a gain of $\sim 10^4$).

3.1 Brief description of GEM

The GEM [6] consists of a thin (50 μm) kapton foil, copper clad on each side, chemically perforated by a high density of holes having bi-conical structure, with external (internal) diameter of 70 μm (50 μm) and a pitch of 140 μm.

In safe condition, gains up to $10^4 \div 10^5$ are reachable using multiple structures, realized assembling more than one GEM at close distance one to each other.

For the R&D we used 10$\times$10 cm^2 triple-GEM detectors. The construction of detector prototypes required the development and realization of a special tool for the stretching of the GEM foils. The detailed description of the detector mechanics and the assembly tools is reported in [7], [8].

The readout anode was segmented in forty, 10×25 mm^2, pads connected to KLOE-VTX chip based pre-amplifiers [8], [9].

3.2 Testbeam results

The results that are shown in this report have been obtained analysing the data collected in two different beam tests.

The first one was performed with an $Ar/CF_4/iso\text{-}C_4H_{10}$ =65/28/7 gas mixture (named A in the following), which is characterized by high ionization yield ($\sim$ 17 electron-ion pairs/cm) and large drift velocity ($\sim$ 11 cm/μs) at low drift fields E_d ($\sim$ 2 kV/cm), thus optimizing either time performances or electron transparency of the detector [7].

An isobutane-less gas mixture, $Ar/CO_2/CF_4$ =45/15/40 (B), non flammable and in principle without polimerization problems, has been also considered in the second beam test. The gas mixture B exhibits ionization yield and drift velocity at $E_d \sim 3$ kV/cm comparable with those of the isobutane gas mixture, and should give similar time performance. Time resolutions better than 5 ns (r.m.s.), corresponding to about 99% efficiency in a 20 ns time window, are obtained with the studied gas mixtures, considerably improving the performance obtained with the standard Ar/CO_2=70/30 gas mixture (9.7 ns r.m.s., [7] [8]). The $Ar/CO_2/CF_4$ (45/15/40) and the isobutane based gas mixtures have been compared with the $Ar/CO_2/CF_4$ =60/20/20 (C) with which we obtained [7] a time resolution of about 6 ns (r.m.s.).

The requirement of 96% for the muon detection efficiency is largely fulfilled, as shown in the upper plot of Fig. 2, with two detectors logically OR-ed pad by pad. We define the starting points of the efficiency plateaux for the different gas mixtures, as the operating voltages for which the efficiency is greater than 96%: $\sim$1000 V for the gas mixture A, $\sim$1245 V for B and $\sim$1190 V for C. They roughly correspond to a single detector efficiency (in 20 ns time window) between 85% and 90%, and an effective gain of the order of $3\times10^3 \div 10^4$.

Discharge studies [11] have been performed with several detectors with our standard triple-GEM geometry: 3/1/2/1 mm respectively for the drift, first and second transfer and induction gaps. The detectors have been irradiated with a low energy hadrons flux up to 300 MHz (pions with 7% of protons of the πM1 test beam at PSI). The discharge probability is defined as the ratio between the observed frequency of discharges and the incident particle rate.

The measurement has been performed by monitoring and acquiring the currents drawn by the various GEM electrodes. In particular, the discharge counting has been performed detecting the current spikes on the pads, corresponding to the OR of the discharges on the three GEM foils.

During the PSI test each detector integrated without any damage or aging effect about 5000 discharges, corresponding to a discharge probability of 10^{-12} in 10 years at LHCb. This limit defines the end of the efficiency plateau. Following this definition, the gas mixture C shows a plateau length of $\sim$45 V. On the contrary, the operation of the detector with the gas mixtures A and B, looks to be very stable: the plateaux length is of the order of $\sim$75 V (see Fig. 2).

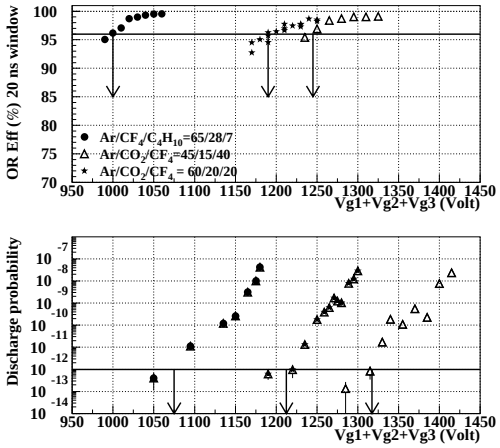

Figure 2: Efficiency in 20 ns time window for two detectors logically OR-ed compared with the discharge probability per incident particle.

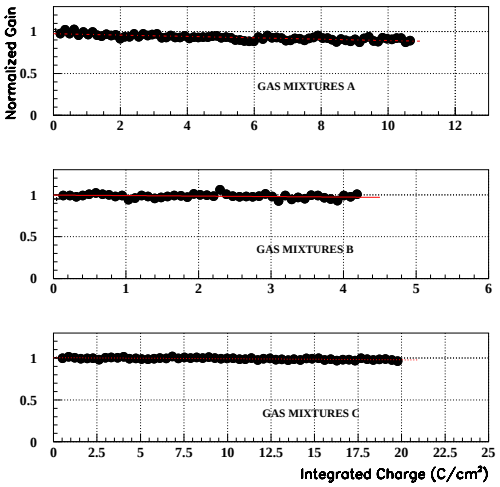

Figure 3: Normalized gain as a function of the accumulated charge for the three gas mixtures.

3.3 Aging studies

The **local aging properties** were investigated [12] exposing the detector to a collimated high intensity 5.9 keV X-rays. The detector was operated with the studied gas mixtures. The X-ray flux was ∼50 MHz/cm^2 and the irradiated area about 1 mm^2. Ambient parameters (temperature, relative humidity and atmospheric pressure) variations have been corrected by a second low irradiated triple-GEM detector used as reference chamber, installed on the same gas line downstream the high irradiated chamber.

The results are shown in Fig. 3 respectively for the gas mixture (A) at an effective gain of $\sim 1{\times}10^4$, for the gas mixture (B) at an effective gain of $\sim 6{\times}10^3$ and for the gas mixture (C) at an effective gain of $\sim 2{\times}10^4$. After accumulating ∼10.5 C/cm^2 (gas mixture A), ∼4.2 C/cm^2 (gas mixture B) and ∼20 C/cm^2 (gas mixture C), corresponding respectively to about 16 years (A), 11 years (B) and 15 years (C) of normal operation at LHCb experiment, only negligible gain changes were observed. Less than 5% for the isobutane-less gas mixtures, whilst slightly larger, less than 10%, for the isobutane based gas mixture.

To study the aging properties in more realistic conditions, a preliminary **large area irradiation test** has been performed in december at the Calliope Facility of the ENEA-Casaccia [2]. The test lasted only fews days and was intented as a pilot run in view of an extensive (∼1 month) and exhaustive aging test of the detector. The chamber (10×10 cm^2 size) was placed at about 4.5 m from the source, corresponding to a dose rate of ∼10 Gy/hour and operated with the $Ar/CO_2/CF_4$ (45/15/40) gas mixture at a $\Sigma V_{GEM} = 1280$ V, resulting in a gas gain of $\sim 6{\times}10^3$. Under this conditions the specific current drawn by the detector was about 10 nA/mm^2, 100 μA on the whole detector. The detector exhibits no aging after accumulating a charge of about 0.22 C/cm^2, corresponding to ∼7 months of normal operation in M1R1 at LHCb.

4 Electronics

The LHCb-LNF group is in charge for the development of the main components of the front-end electronics chain: the **Intermediate Boards** (IB) and the **Off Detector Electronics** (ODE) boards. Depending on the region, signals from some detectors are ORed on the chambers itself by the front-end electronics or signals from different chambers are ORed on the off detector electronics by the IB system.

The IB system is made of 152 two boards, the Intermediate Board and the Transition Board (TB). Both boards have been designed to minimize the different types of layout required to match the detector geometry. The IB has been implemented using radiation tolerant programmable logic because of the 10 krad of radiation dose foreseen near the detector. One single layout with three programmable devices fits all chamber geometries, while three different layouts are required for the TB. The IBs were also required to maintain the input-output time delay difference within 2 ns for all signals. Each board (6U) can manage up to 192 LVDS input signals and 60 output signals.

The ODE boards receive the signals directly from the front-end electronics or from the IB system, synchronizes these signals with the bunch crossing frequency and send them to the trigger system via high frequency (1,6 GB) optical links. Each of 148 6U boards can manage up to 192 LVDS input signals and 12 optical link outputs. ODE board includes the Level-0 logic as well; formatted data are sent to Level-1 trigger and to the experiment DAQ through a (further) dedicated optical link. A CAN interface manages the communications with the experiment ECS. Because the huge number of input channels per boards (192 LVDS) and the very strict requirements on timing performances for optical link connections (less than 20 ps on clock jitter) a multilayer (10) approach was used to design the board. A mother board / daughter cards design has been used to match the detector geometry.

5 Chamber supporting structure

LHCb-LNF has the responsibility for the construction of the 10 **movable walls** that will support the chambers in between the iron absorbers of the muon filter. A full scale (4,5×7,5 m^2) light aluminum structure with the dimensions of the second station (M2) was installed in the KLOE assembly hall during April 2002 to show the feasability of the project. The prototype is now used to study the chambers fixing and positioning procedure, the integration of the chambers in the system (MWPC and GEM), the routing of the cables (for signals, power supply and pulse and control signals), and the gas piping.

In the meanwhile it is going on, together with the CERN group, the optimization of the dimensions and the positioning of the racks for the electronics and of the platforms around the detector since they must both move togheter with the supporting structure without interfere with other systems (some elements of the cryogenics and the RICH). The choice among several almost completed solutions is being performed in order ot reduce the cost of the system with the aim to finalize the project before the end of 2003.

6 List of Conference Talks by LNF Authors in Year 2001

- **Performance of a triple-GEM detector for high rate charged particle triggering** International Conference on Instrumentation for Colliding Beam Physics, Novosibirsk, Russia, February 28 - March 6, 2002;

- **Advances in triple GEM detectors operation for high rate particle triggering** PSD6, The Sixt International Conference on Position Sensitive Detectors, Leicester, UK, September 9-13, 2002;

- **Triple GEM detector operation for high rate particle triggering** 8^{th} Topical Seminar on Innovative Particle and Radiation Detectors, 21-24 October 2002, Siena - Italy;

- **Advances in triple GEM detectors operation for high rate particle triggering** IEEE Conference, Norfolk - Virginia, USA, November 3-11, 2002.

References

1. LHCb Collaboration, "LHCb: Addendum to muon system technical design report", CERN LHCC MUON 2003-002, LHCb TDR 4 Addendum 1, 15 January 2003.

2. S. Baccaro, A. Festinesi, B. Borgia, "Gamma and neutron irradiation facilities at ENEA-Casaccia Center (Rome)", Report **CERN-CMS/TN, 95-192** (RADH), 1995.

3. G. Auriemma *et al.*, "Sandwich panels for the MWPC of the LHCb muon system: mechanical properties before and after irradiation", Internal Note **LHCb MUON-2003-011**.

4. LHCb Collaboration, "LHCb: muon system technical design report", **CERN LHCC MUON 2001-010**, LHCb TDR 4, 28 May 2001.

5. M. Anelli *et al.*, "Test of a double gap MWPC for the region 3 of the LHCb muon system", Internal Note **LHCb MUON-2001-120**.

6. F. Sauli, Nucl. Instrum. Meth. **A386** (1997) 531.

7. G. Bencivenni et al., Nucl. Instrum. Meth. **A478** (2002) 245.

8. G. Bencivenni et al., Nucl. Instrum. Meth. **A488** (2002) 493.

9. R.J. Yarema et al., IEEE Trans. Nucl. Sci., **39**, No. 4, 742(1992).

10. G. Bencivenni et al., Nucl. Instrum. Meth. **A494** (2002) 156.

11. G. Bencivenni et al., **Advances in triple-GEM detector operation for high-rate particle triggering**, in publication Nucl. Instrum. Meth.

12. Internal Note **LHCb MUON** in preparation.

ICARUS

P. Picchi (Resp.)

1 Introduction

During the year 2002 the activity of the LNF group was devoted to R&D on aspect of ICARUS detector not yet fully defined.

During the year 2003 we intend to continue the R&D on a two-phase (gas and liquid) Argon detector to search for WIMPs. These could be detected through their collisions with normal matter, producing nuclear recoil signals typically in the range of $1 \div 100\ KeV$.

2 Activity(2002)

Being very hard to find large photo-multipliers with MgF_2 window, sensitive to 128 nm light and working at liquid Argon temperature we have tried to deposit a wave-shifter. More tests were performed with different wave-shifters; not satisfactory results were reached concerning the behavior in liquid Argon (poor stability in time and low quantum efficiency).

Using the 50 liter LAr TPC we have started a test concerning the ability to perform data reduction on line.

A VSLI chip, called Daedalus, has been realized and mounted on the digital DAQ board to perform signal detection and zero skipping in real time.

3 Activity(2003)

Large Area Avalanche photodiodes(LAAPD) are of great interest for high efficiency detection of low intensity light pulse from scintillator. Operation at low temperature can be not only a necessity as in the case of LAr, but also a favorable option. In fact, to operate the LAAPD at low temperature has two advantageous effects: 1) the dark current noise decreases dramatically 2) the voltage required to achieve a certain gain became lower.

They can compete successfully with PMT in many applications that require very compact detector packaging, low sensitivity to magnetic field or when low intrinsic radioactivity is required for the low background experiments (search of dark matter).

During this year we will make some preliminary test using a windowless LAAPD, 16 mm in diameter, from Advanced Photonix. This photodiode has low dark current and relatively small capacitance (and a gain up to 1000).

We want to demonstrate experimentally the ability to detect scintillation light in liquid Argon due to ionizing particles by means of LAAPDs with quantum efficiency of about 100% and time resolution of 0.9 ns(FWHM).

We intend also to continue our $R\&D$ on a two phase Argon detector to search for WIMPs.

MACRO

G. Battistoni (Ass.), H. Bilokon, C. Bloise, M. Carboni, V. Chiarella
C. Forti, E. Iarocci (Ass.), A. Marini, A. Mengucci (Tecn.), V. Patera (Ass.)
F. Ronga, A. Sciubba (Ass.), M. Spinetti (Resp. Naz.)

Collaboration with: University of Boston, Caltech, Drexel, Indiana, Michigan and Texas A&M, Infn Sections of Bari, Bologna, Lecce, Napoli, Pisa, Roma, Torino, LNGS, University of L'Aquila and University of Oudja

1 Introduction

MACRO (Monopole, Astrophysics, and Cosmic Ray Observatory) is a large area underground detector optimized to search for the supermassive magnetic monopoles predicted by Grand Unified Theories (GUTs).

The detector allows to perform also observations relevant to particle physics, astrophysics, and cosmic ray physics. These include different studies on atmospheric neutrinos, search for low energy gravitational collapse neutrinos, high energy neutrino astronomy and studies of the high energy underground muon flux relevant to primary cosmic ray composition and origin.

In order to provide redundant and complementary particle identification for rare events like monopoles, MACRO employees three different detector types: liquid scintillation counters, gas filled limited streamer tubes, and Lexan/CR39 nuclear track-etch detectors. The active components (the scintillators and the streamer tubes) measure particle tracks with resolutions of $\sim 0.2^{\circ}$ in angle, $\sim$1 cm in position, $\sim$0.5 ns in time of flight and $\sim$6 MeV in energy loss (for muons). The passive nuclear track detector provides additional information for heavy ionizing particles.

The MACRO detector has dimensions $76.6 \times 12.0 \times 9.3 m^3$, divided longitudinally in six supermodules and horizontally in a lower part (4.8 m high, with absorbers interleaved between tracking planes) and in an upper part (4.5 m high). The total acceptance for isotropic flux is about 10^4 m^{-2} sr^{-1}. The contruction of detector started in October 1987. The main milestones of the MACRO detector construction were: the first supermodule in February 1989, the lower part in June 1991, the upper part in April 1994 and the full electronics and trigger configurations in August 1995. The data taking started immediately after the main milestone were reached with the partial detector while in August 1995 the continuos data taking started with the full detector and trigger configuration.

In December 2000, the data taking was stopped and the detector was dismounted.

All the main goals listed in the 1984 Proposal have been achieved, while for the atmospheric neutrino physics results more significant than expected have been obtained.

Hereafter some results recently reached with the full sample of data are reported.

2 Magnetic monopoles

GUT monopoles are normally expected to have relatively low velocities: around 10^{-4}c if gravitationally bound to the solar system, 10^{-3}c if bound to the galaxy and greater than 10^{-2}c for extragalactic origin. Therefore MACRO has been designed to identify monopole in the whole β range.

Since 1989 and up to December 2000 data have been collected in different detector configurations. Several limits on monopole flux have been derived independently with the three detectors and with various analysis techniques. The limit for relativistic monopoles has been particularly improved intensifying the track-etch development.

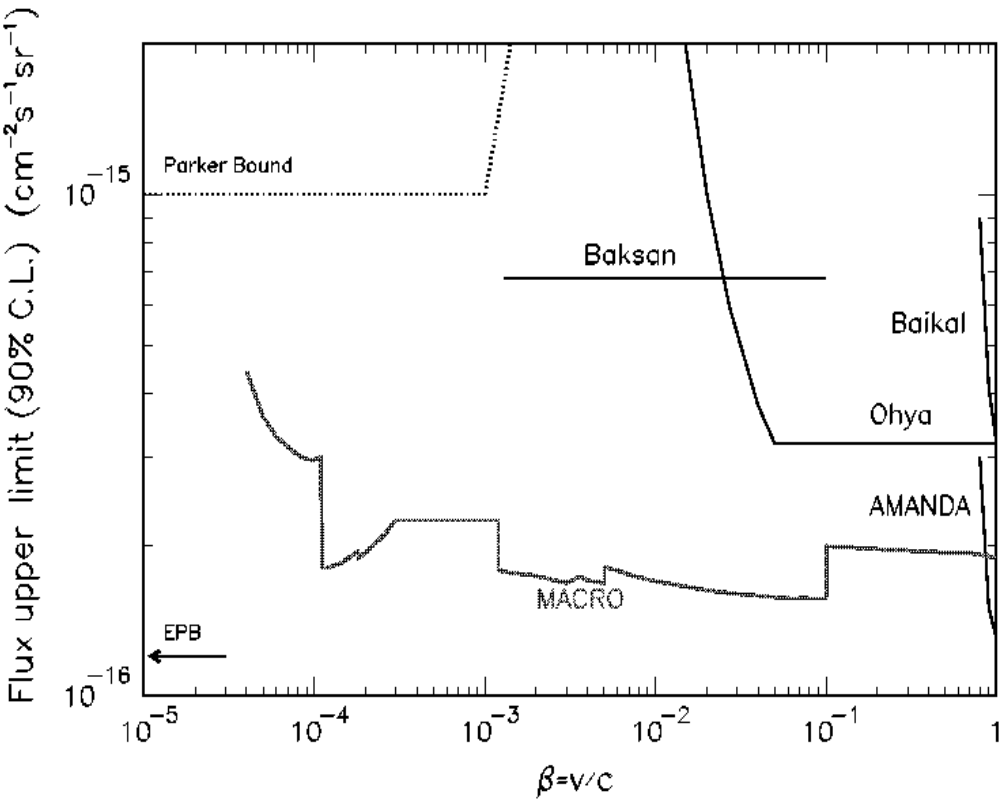

Figure 1: *Magnetic monopole flux upper limits at 90% c.l. obtained by Macro and by other experiments. The limits apply to $g = g_D$ monopole, assuming catalysis cross section smaller than few mb.*

These limits have been combined all together taking properly into account time and spatial overlap. The limit obtained (Fig. 1) is within the range:

$$1.3 \div 1.8 \times 10^{-16}\mathrm{cm}^{-2}\mathrm{sr}^{-1}\mathrm{s}^{-1} \quad \text{for } 10^{-4} < \beta < 1;$$

In the whole β range, the obtained limit is particularly important, being well below the Parker bound ($\sim 10^{-15}\mathrm{cm}^{-2}\mathrm{sr}^{-1}\mathrm{s}^{-1}$) as deduced from the survival of the galactic magnetic field. Moreover, excluding relativistic monopoles, the present limit is the best limit in the literature.

This limit also means that a monopole contribution to dark matter cannot be larger than about 15%.

3 Atmospheric neutrinos

In this field, the results obtained concern the update of statistics up to December 2000 for the standard analysis and the addition of new analysis for extracting more relevant experimental informations from data. In general the whole results obtained by Macro indicate that the anomaly

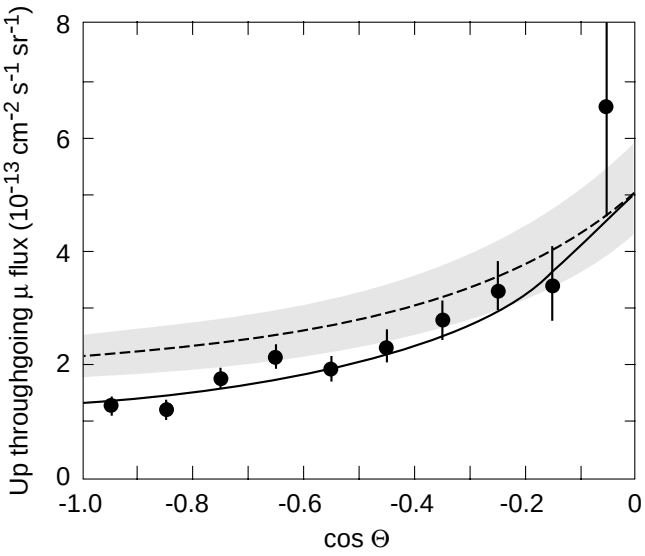

Figure 2: *Zenith angle distribution of upgoing muon events. Data (full dots) are compared with the expected atmospheric neutrino flux without oscillations (dashed line) and with oscillations (continuous line). The shaded area represents the theoretical global uncertainty on the expectations, slightly dependent on the angle.*

already observed in 1993 on the atmospheric neutrino flux (presented at Taup 1993) has the most probable interpretation in a $\nu_\mu - \nu_\tau$ oscillation. The results are based on three event categories:

1. events with through-upgoing muons induced by neutrino interactions in the rock below the detector ($E_{median} \approx 40$ GeV, 863 events) identified through the time of flight between 2-3 scintillator layers (rejection factor about 10^{-7});

2. events induced by neutrino interactions in the lower and dense part of the detector (about 3.5 Kton) with an upgoing muon identified through the time of flight between the upper 2 scintillator layers ($E_{median} \approx 5$ GeV, 161 events);

3. events with muons stopping in the lower and dense part of the detector induced both by upgoing neutrinos interacting in the rock below the detector (about 50%) and by downgoing neutrinos interacting in the lower and dense part of the detector (about 50%); these events are selected through topological cuts ($E_{median} \approx 4$ GeV, 272 events).

From the events of the first category, the angular distribution of atmospheric neutrino flux has been derived as function of zenith angle (see Fig. 2). This result has to be compared with the MC predictions based on the Bartol flux calculations. The theoretical uncertainty on this flux is $\pm 17\%$, slightly dependent on the angle. The simulated flux is reported with and without a $\nu_\mu - \nu_\tau$ oscillation effect: the best-fit probabilities are 66% and 0.2%, respectively. The best fit gives the following parameters:

$$\Delta m^2 = 2.5 \;\; 10^{-3}\,\mathrm{eV}^2; \qquad sin^2\, 2\theta = 1.$$

With these oscillation parameters and with the involved neutrino energies and angles, the angular distribution of the second and third event categories must show a uniform deficit. Coherently, the distribution of the second event category shows a uniform deficit of about 50% while

the distribution of the third event category shows a deficit of about 3/4 of the full flux, being this category a mixture of upgoing and downgoing neutrinos. More precisely, the observed deficits on the three event category are the following:

1. $R_1 = 0.721 \pm 0.026\,(stat) \pm 0.043\,(syst) \pm 0.123\,(theor)$
2. $R_2 = 0.54 \pm 0.04\,(stat) \pm 0.06\,(syst) \pm 0.14\,(theor)$
3. $R_3 = 0.70 \pm 0.04\,(stat) \pm 0.07\,(syst) \pm 0.18\,(theor)$

to be compared, in presence of oscillations using the above quoted parameters, with:

1. $R'_1 = 0.73$
2. $R'_2 = 0.59$
3. $R'_3 = 0.75$

Moreover, another sign of the internal coherence of these results is to look to the ratio between the two ratios of points 2) and 3). In this case, most of the theoretical uncertainties are canceled. The measured value of this ratio is R=0.59 $\pm$ 0.060 (stat) to be compared with 0.59 $\pm$ 0.046 expected in presence of oscillations and with R=0.76 $\pm$ 0.059 expected without oscillations. This last value has a 2% probability to agree with the data.

Another important result has been achieved comparing the data with the ν_μ - ν_τ and a ν_μ - $\nu_{sterile}$ oscillation schemes. The second scheme implies a "matter effect" which deforms the angular distribution of Fig. 2 As a consequence, the expected distribution has the probability reduced from 66% to 8%.

To improve the discrimination power between the two hypotheses, another parameter has been analyzed. This parameter is the ratio between the events collected around the vertical ($-1 < \cos\theta < -0.7$) and those collected around the horizontal ($-0.4 \cos\theta < 0$). The ratio is reported in Fig. 3 as function of the Δm^2. The agreement for the $\nu_\mu - \nu_\tau$ scheme has a probability of 9.4% while for the $\nu_\mu - \nu_{sterile}$ scheme the probability is reduced down to 0.06% disfavoring the $\nu_{sterile}$ solution at 99% c.l.

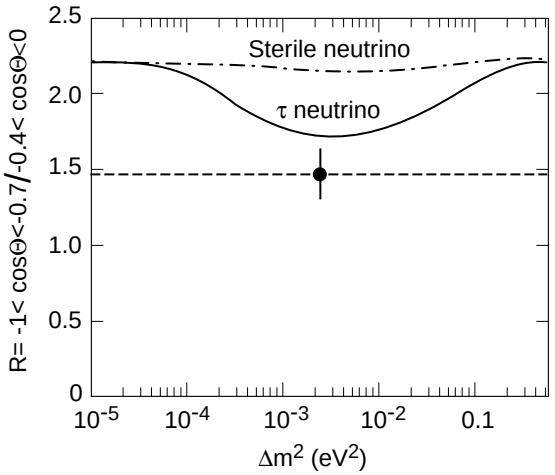

Figure 3: *Ratio between the events collected around the vertical ($-1 < cos\theta < -0.7$) and that collected around the horizontal ($-0.4 < cos\theta < -0$) as function of Δm^2.*

The Multiple Coulomb Scattering (MCS) technique has also been applied to the upthroughgoing events. To this aim, the streamer tubes have been used as drift tubes achieving an overall spatial resolution of 3 mm (including alignments). Seven MCS sensitive variables have been input to a Neural Network whose output allows an estimate of the muon energy up to the saturation point, occurring when MCS is comparable with the detector space resolution. Test with PS and SPS beams at CERN, simulating the whole Macro detector, provided an absolute energy calibration. From the muon energy also the parent neutrino energy can be estimated. The events then have been divided in four subsamples with average neutrino energies of 12, 20, 50 and 102 GeV, respectively (Fig. 4). The comparison of their zenith angle distributions with the predictions of the no oscillations Montecarlo shows a large disagreement at low energies, with a deficit concentrated around the vertical, while the agreement is slowly restored as the neutrino energy increases.

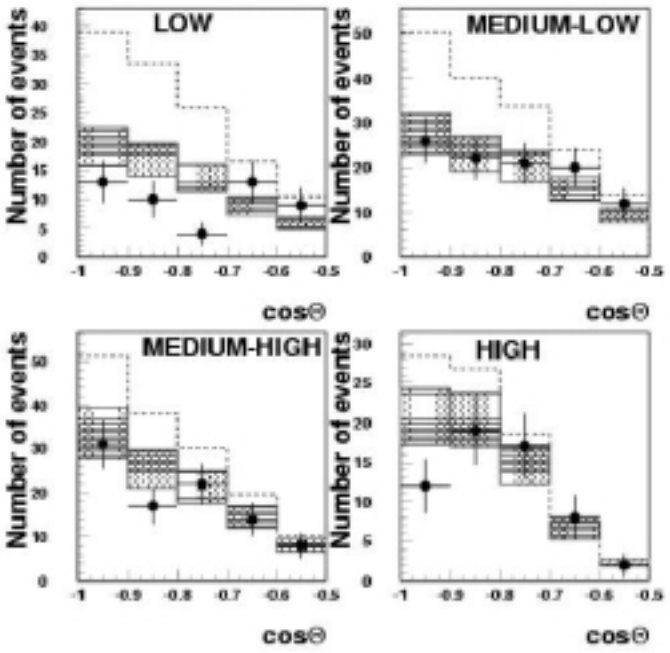

Figure 4: *Angular distribution for upthroughgoing events in the four energy bands centered around 12, 20, 50 and 102 GeV, respectively. The black points with error bars are the data. Dashed lines are the expectations without oscillations. The shaded areas are the expectations with oscillations including theoretical and systematic uncertainties.*

To quantify the significance of the multiple scattering measurement in stand-alone mode, we used the ratio A=N_{low}/N_{high}, where N_{low} and N_{high} are the number of events with E_ν^{rec}<30 GeV and E_ν^{rec}>130 GeV respectively. We considered a 17 % systematic error on this ratio, due to uncertainties in the neutrino flux calculation, neutrino cross section and to experimental systematics. The Monte Carlo prediction in case of no oscillations (Bartol flux) is A'=1.5±0.25(theo.+syst.), while for $\Delta m^2=2.5\times10^{-3}eV^2$ and $\sin^2 2\theta$ =1 the value is A=1.00±0.17(theo.+syst.). The experimental ratio is A^{exp}=0.85±0.16(stat.). The corresponding one sided probability of measuring a value smaller than A^{exp} is 0.75% corresponding to 2.4σ. Finally, the ratio A can be statistically analyzed together with the ratio R quoted in Fig. 3. The combined significance rejecting the no oscillation case in favor of $\nu_\mu - \nu_\tau$ oscillations rises up to 4.7σ. On the contrary, these distributions are well in agreement with the $\nu_\mu - \nu_\tau$.

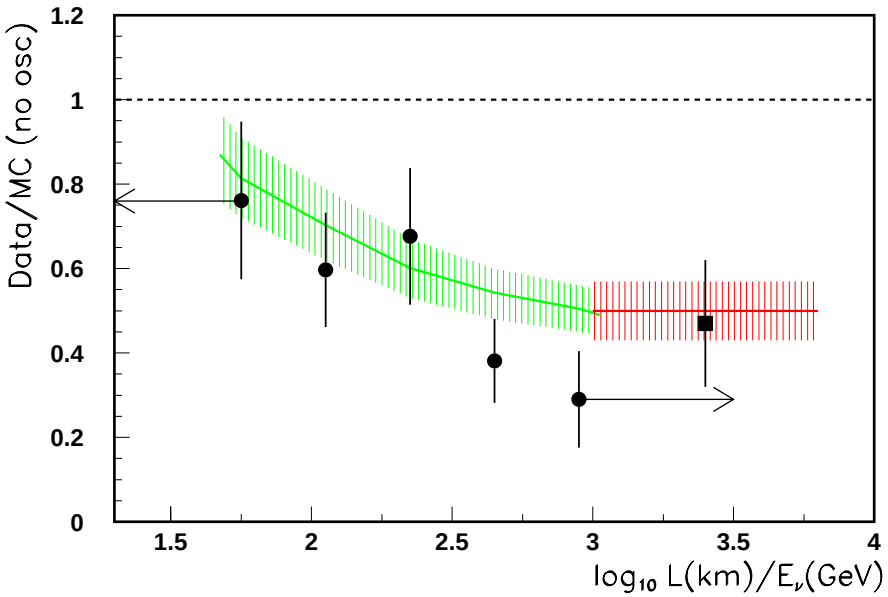

Figure 5: *Data/MC ratio as function of the estimated L/E_ν for the upthrougoing muon sample (black circle) and the semicontained upgoing muons (black square). The shaded regions represent the uncertainties in MC predictions assuming $\Delta m^2 = 2.5\ 10^{-3}\,\mathrm{eV}^2$ and $sin^2\ 2\theta = 1$. The dashed line represents the expectation for no oscillation.*

Further evidence is provided by the parameter L/E, which can be computed using the neutrino zenith angle and its estimated energy on the event by event basis. The distribution in L/E is shown in Fig. 5.

In conclusion, MACRO results for the atmospheric neutrinos has a strong internal coherence pointing towards the $\nu_\mu - \nu_\tau$ oscillation scheme.

4 Search for neutrinos from stellar collapses

A stellar gravitational collapse should results in the emission of a 5-15 MeV electron antineutrino burst of about 10 sec duration. This antineutrino burst, interacting with the 570 tons of liquid scintillator of MACRO, is detected as a positron burst. The live time for observation has been kept close to 97% during the continuos run periods. No burst has been detected over an integrated time of about 8.5 years of observation of our galaxy (about 30% of the mean life of a collapse per galaxy).

5 Moon and Sun shadows

The pointing capability of MACRO, necessary for muon astronomy, is demonstrated by the observed shadows of the Moon and of the Sun, since they act as a shield to the cosmic rays. We used a sample of 45 10^6 muons, looking at the bidimensional density of the events around the directions of the Moon and of the Sun. The bin size is $0.125^\circ x 0.125^\circ$. For the Moon we observe in the bidimensional plot a depletion of events in a cone of 0.25 degree with a statistical significance

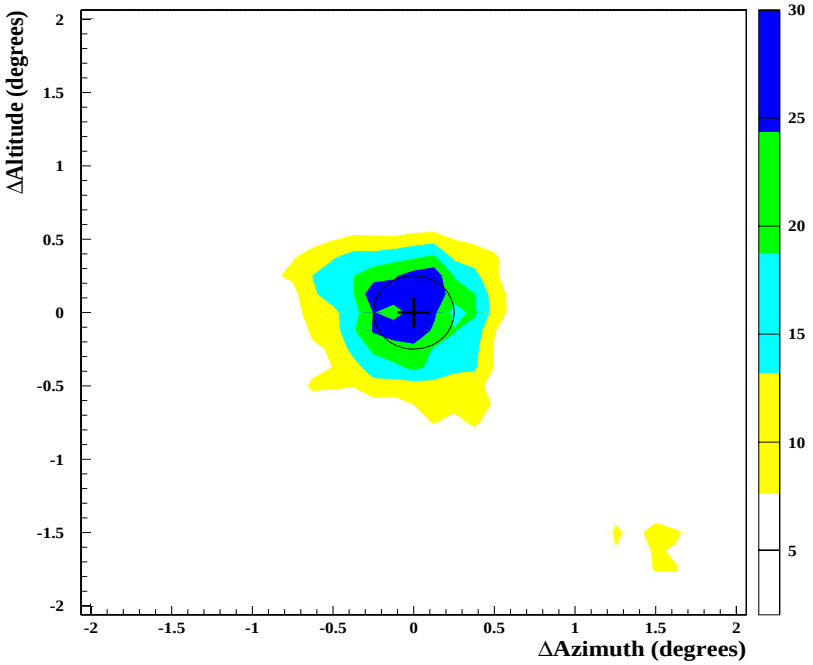

Figure 6: *Moon shadow. Two-dimensional distribution of the muon event density around the Moon direction. The various region of increasing gray scale indicate various levels of deficit in percent. The darkest on the corresponds to the maximum deficit.*

of 5.5 σ (see Fig. 6). The observed slight displacement of the maximum deficit is consistent with the displacement of the primary protons due to the geomagnetic field. We repeated the same analysis for muons in the sun window observing a depletion of events in a cone of 0.25 degree with a statistical significance of 4.5σ (see Fig.7). The larger displacement of the apparent sun position is due to the combined effect of the magnetic field of the Sun and of the Earth.

6 Primary composition studies with MACRO and EASTOP combined events

An importrant feature of the Gran Sasso Laboratory is to have coincidence operation of two large detectors for measuring, on an event-by-event basis, two main physical quantities: the shower energy and number of high energy particles produced in the first stage of the interaction. Two main research lines have been implemented: the first based on the scintillator array ($E_{th} \approx 300$ TeV) and a second based on the Cherenkov light detectors, operating in the 80-250 Tev range. For coincident events of a first line, EASTOP measures the e.m. size of the showers above the surface (at Campo Imperatore), while MACRO measures penetrating muons underground ($E_\mu > 1$ Tev). The purpose of this unique facility is to study the primary Cosmic Ray (CR) composition versus energy, reducing the dependence on the interaction and propagation models. The two detectors operated in coincidence for a live time of 960 days. The number of coincident events is 28160, of which 3752 have shower cores inside the edges of the EASTOP array and shower sizes Ne $> 2\times10^5$; above the CR knee there are still 409 events. The data have been analyzed in terms of the QGSJET interaction model as implemented in CORSIKA shower transport. The considered main experimental features are the muon multiplicity distributions in six different intervals of shower sizes. For each size bin, the muon multiplicity distribution is fitted with a superposition of (i) pure p and Fe components, or (ii) Light (L) and Heavy (H) admixtures containing equal fractions of p and He or Mg and Fe, respectively. This approximation allows to reduce the number of free

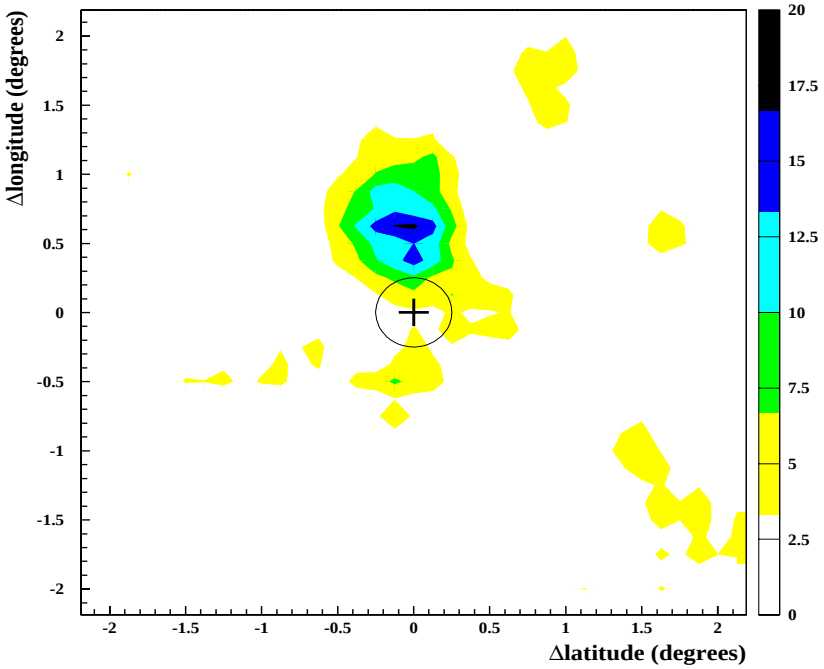

Figure 7: *Sun shadow. Two-dimensional distributions of the muon event density around the Sun direction. The various region of increasing gray scale indicate various levels of deficit in percent. The darkest on the corresponds to the maximum deficit.*

parameters and to stabilize the fitting procedure. In each of the six size bin, we can derive the relative weight of the two components. In Fig. 8 the central four distributions are reported. Two main conclusions can be derived: (i) pure components are escluded since they do not reproduce all the multiplicity distributions; (ii) the L and H component weights pass from about 70% and 30% before the knee to 30% and 70% above the knee, respectively. This is a precise confirmation that the composition changes around the knee, supporting the standard galactic acceleration/propagation models with a rigidity dependent break of the different components.

Significant results have been achieved also for the second research line. In these combined events, the shower axis determined by MACRO muons permits a precise reconstruction of the total amount of Cherenkov light, i.e. the shower energy. The main conclusion is that the three relevant components, Protons, Helium and CNO are measured precisely, clarifying the contradictory experimental results in this energy region.

7 Conclusions

Macro has been a successful experiment both for the achieved results, fulfilling all the physical goals, and technically, since the detector has run about continuosly for 12 years without problems and with very low maintenance.

8 Full list of MACRO publications on referenced Journals from 1989 to 2003

1. MACRO: a large area detector at the Gran Sasso laboratory. MACRO Collaboration, C. De Marzo *et al.*, Nuovo Cimento C**9** (1986) 281-292.

2. The MACRO detector at the Gran Sasso laboratory. MACRO Collaboration, M.Calicchio *et al.*, Nucl. Instr. Methods Phys. Res **A264** (1988) 18-23.

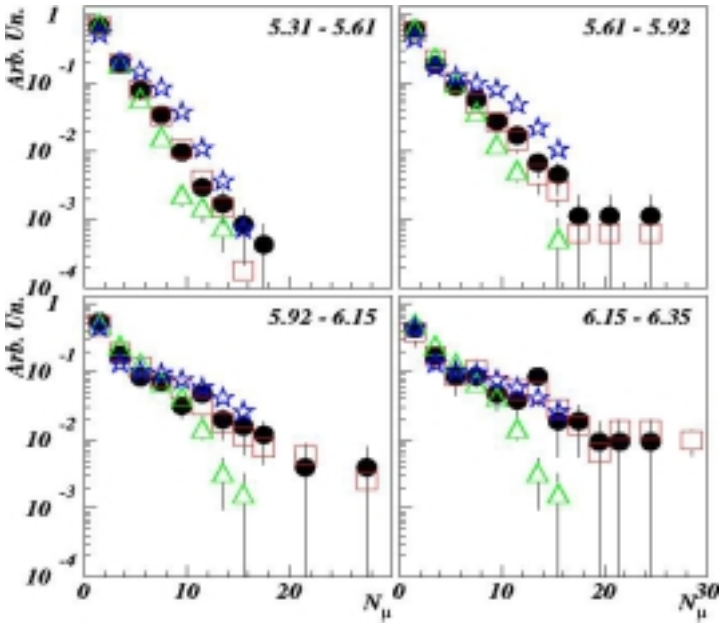

Figure 8: *Distributions of relative frequencies of the detected underground muon multiplicities (black points) together with the predictions for L (open triangles) and H (open stars) admixtures in the QGSJET interaction model and the (L+H) fit (open squares).*

3. Simultaneous observation of the extensive air showers and deep underground muons at the Gran Sasso laboratory. MACRO-EASTOP Collaborations, R.Bellotti *et al.*, M.Aglietta *et al.*, INFN/AE-89/7 (1987). Phys. Rev. **D42** (1990)1396-1403.

4. Study of penetrating cosmic ray muons and search for large scale anisotropy at the Gran Sasso laboratory. MACRO Collaboration, S. Ahlen *et al.*, LNF-90/037 (1990) Phys. Lett. **B249** (1990)149-156.

5. Arrival time distributions of very high energy cosmic ray muons in MACRO. MACRO Collaboration, S.Ahlen *et al.*, LNGS-91/01 (1991), Nucl. Phys. **B370** (1992)432-444.

6. Study of the ultrahigh energy primary cosmic ray composition with the MACRO experiment. MACRO Collaboration, S.Ahlen *et al.*, LNGS-92/25 (1992), Phys. Rev. **D46** (1992)895-902.

7. Measurement of the decoherence function with the MACRO detector at Gran Sasso. MACRO Collaboration, S.Ahlen *et al.*, LNGS-92/29 (1992), Phys. Rev. **D46** (1992)4836-4845.

8. Search for neutrino bursts from collapsing stars with the MACRO detector. MACRO Collaboration, S. Ahlen *et al.*, LNGS-92/32 (1992), Astroparticle Phys. **1** (1992)11-25.

9. Search for nuclearites using the MACRO detector. MACRO Collaboration, S.Ahlen *et al.*, Phys. Rev. Lett. **69** (1992)1860-1863.

10. First supermodule of the macro detector at Gran Sasso MACRO Collaboration, S.Ahlen *et al.*, LNGS 92/34 (1992), Nucl. Inst. Meth. Phys. Res. **A324** (1993)337-362.

11. Muon astronomy with the MACRO detector MACRO Collaboration, S.Ahlen *et al.*, Astrophysical Journal **412** (1993)301-311

12. Search for slow moving magnetic monopoles with the MACRO detector. MACRO Collaboration, S.Ahlen *et al.*, LNGS 93/84 (1993), Phys. Rev. Lett. **72** (1994)608-612.

13. Coincident observation of air Cherenkov light by a surface array and muon bundles by a deep underground detector. GRACE-MACRO Collaborations, M. Ambrosio *et al.* Phys. Rev.**D50** (1994)3046-3058.

14. Study of the primary cosmic ray composition around the knee of the energy spectrum. EASTOP-MACRO Collaborations, M.Aglietta *et al.* Phys. Lett. **B337** (1994)376-382

15. Performance of the MACRO streamer tube system in the search for magnetic monopoles. MACRO Collaboration, M.Ambrosio *et al.*, LNGS 95/11 (1995) Astroparticle Phys. **4** (1995)33-43.

16. Vertical muon intensity measured with MACRO at the Gran Sasso laboratory. MACRO Collaboration, M.Ambrosio *et al.* Phys. Rev. **D52** (1995)3793-3802.

17. Atmospheric neutrino flux measurements using upgoing muons. MACRO Collaboration, M.Ambrosio *et al.* Phys. Lett. **B357** (1995)481-486.

18. The performance of macro liquid scintillator in the search for magnetic monopoles with $10 * *^{-3} < \beta < 1$. MACRO Collaboration, M.Ambrosio *et al.*, INFN-AE 96/22 (1996), Astroparticle Phys. **6** (1997)113-128.

19. High energy cosmic ray physics with the MACRO detector at Gran Sasso: Part I. Analysis methods and experimental results. MACRO Collaboration, M.Ambrosio *et al.*. INFN-AE 96/28 (1996). Phys. Rev. **D56** (1997) 1407.

20. High energy cosmic ray physics with the MACRO detector at Gran Sasso: Part II. Primary spectra and composition. MACRO Collaboration, M.Ambrosio *et al.*, INFN-AE 96/29 (1996), Phys. Rev. **D56** (1997)1418.

21. Seasonal variations in the underground muon intensity as seen by MACRO. MACRO Collaboration, M.Ambrosio *et al.*, INFN-AE 97/05 (1997), Astroparticle Phys. **7** (1997) 109-124

22. Magnetic monopole search with the MACRO detector at Gran Sasso. MACRO Collaboration. M.Ambrosio *et al.*, INFN-AE 97/16 (1997), Phys. Lett. **B406** (1997)249.

23. Real time supernova neutrino burst detection with MACRO. M.Ambrosio *et al.* MACRO Collaboration., INFN-AE 97/44 (1997), Astroparticle Phys. **8** (1998)123.

24. The observation of upgoing charged particles produced by high energy muons in underground detectors. MACRO Collaboration, M.Ambrosio *et al.*, INFN-AE 97/55 (1997), hep-ex/9807032, Astroparticle Phys. **9** (1998)10.5.

25. Measurement of the atmospheric neutrino–induced upgoing muon flux using MACRO. MACRO Collaboration, M.Ambrosio *et al.*, INFN-AE 98/13 (1998); hep-ex/9807005, Phys. Lett. **B434** (1998)451-457.

26. Observation of the shadowing of cosmic rays by the moon using a deep underground detector. MACRO Collaboration, M.Ambrosio*et al.*, INFN-AE 98/14 (1998); hep-ex/9807006, Phys. Rev. **D59**(1999)012003.

27. Measurement of the energy spectrum of underground muons at Gran Sasso with a transition radiation detector. MACRO Collaboration, M.Ambrosio *et al.*, INFN-AE 98/15 (1998); hep-ex/9807009, Astroparticle Phys. **10**(1999)11.

28. Limits on dark matter WIMPs using upward- going muons in the MACRO detector. MACRO Collaboration, M.Ambrosio *et al.* hep-ex/9812020 ; INFN-AE 99/01 (1999), Phys. Rev. **D60** (1999)082002.

29. High statistics measurement of the underground muon pair separation at Gran Sasso. MACRO Collaboration, M. Ambrosio *et al.*, hep-ex/9901027; INFN-AE 99/04 (1999), Phys. Rev. **D60** (1999)032001.

30. Nuclearite search with the MACRO DETECTOR at Gran Sasso. MACRO Collaboration, M.Ambrosio *et al.* hep-ex/9904031, Eur. Phys. J. **C13**(2000)453.

31. Low energy atmospheric muon neutrinos in MACRO. MACRO Collaboration, M.Ambrosio *et al.*, hep-ex/0001044, Phys. Lett. **B478** (2000)5.

32. Search for lightly ionizing particles with the MACRO detector MACRO Collaboration. M. Ambrosio *et al.*, hep-ex/0002029, Phys. Rev. **D62** (2000)052003.

33. Neutrino astronomy with the MACRO detector MACRO Collaboration. M.Ambrosio *et al.*, astro-ph/0002492, Astrophys.J. **546** (2001)1038.

34. Matter effects in upward-going muons and sterile neutrino oscillations. MACRO Collaboration, M.Ambrosio *et al.*, hep-ex/0106049, Phys. Lett. **B517**(2001)59.

35. The MACRO detector at Gran Sasso. MACRO Collaboration, M.Ambrosio *et al.*, Nucl. Instr. Methods Phys .Res **A486** (2002)663-707.

36. A combined analysis technique for the search for fast magnetic monopoles with the MACRO detector. MACRO Collaboration, M.Ambrosio *et al.*, hep-ex/0110083, Astroparticle Phys. **18** (2002)27.

37. Search for diffuse neutrino flux from astrophysical sources with MACRO. MACRO Collaboration, M.Ambrosio *et al.*, astro-ph/0203181, Accepted for publication in Astroparticle Physics.

38. Search for cosmic ray sources using muons detected by the MACRO experiment. MACRO Collaboration, M.Ambrosio *et al.*, hep-ex/0204188, Astropart. Phys. **18** (2003)615.

39. Muon energy estimate through multiple scattering with the MACRO detector MACRO Collaboration, M.Ambrosio *et al.*, physics/0203018, Nucl. Instr. Methods Phys. Res **A492** (2002)376-386.

40. Final results of magnetic monopole searches with the MACRO experiment. MACRO Collaboration, M.Ambrosio *et al.*, Eur. Phys. J. **C25** (2002)511-522.

41. Search for nucleon decays induced by GUT magentic monopoles with the MACRO experiment. MACRO Collaboration, M.Ambrosio *et al.*, Eur. Phys. J. **C26** (2002)163-172.

42. Measurement of the residual energy of muons in the Gran Sasso laboratories; MACRO Collaboration, M.Ambrosio *et al.*, hep-ex/0207043, Accepted for publication on Astroparticle Physics.

43. Search for the sidereal and solar diurnal modulations in the total MACRO muon data set. MACRO Collaboration, M. Ambrosio *et al.* astro-ph/0211119, Accepted for publications on Phys. Rev. D.

44. Moon and Sun shadowing effect in the MACRO detector. MACRO Collaboration, M. Ambrosio *et al.* Submitted to Astropart. Phys.

45. Search for stellar gravitational collapses with the MACRO detector; MACRO Collaboration, M.Ambrosio *et al.*, Submitted to Eur. Phys. J. C.

46. Cosmic ray primary composition around knee with the MACRO and EASTOP detectors; MACRO Collaboration, M.Ambrosio *et al.*, EASTOP Collaboration, M. Aglietta *et al.* In preparation.

47. Primary proton, helium and CNO fluxes around around 100 TeV with the MACRO and EASTOP detectors; MACRO Collaboration, M.Ambrosio *et al.*, EASTOP Collaboration, M. Aglietta *et al.* In preparation.

48. Atmospheric neutrino oscillations from upward throughgoing muon multiple scattering in MACRO, MACRO Collaboration, M. D'Ambrosio *et al.*. Submitted to Phys. Lett. **B6**.

NEMO

M. Cordelli, A. Martini, L. Trasatti (Resp.)

1 Activity

In the framework of an european effort toward the construction of a kilometer cube detector for neutrino astronomy, the NEMO project has studied in detail the best possible sites im the Mediterranean sea, and produced several instruments to study the marine depths. During the year 2002 the group has participated in the ANTARES effort and has been preparing for the Catania Test Site. A pilot project, NEMO Phase 1, has been started to build two towers at the Catania Test Site.

The experiment includes groups from INFN sections of Bari, Bologna, Cagliari, Catania, Genova, LNF, LNS, Messina, Roma1.

The LNF group has continued tests on the prototype of NERONE, an instrument to measure with great accuracy the water transparency using measurements performed at several distances from the source. We reached a depth of 3500 m and we expect to be able to perform a final test at the beginning of 2003. The group is also collaborating with the LNS section of the group for the NEMO Phase 1 controls.

References

1. M. Cordelli, R. Habel, A. Martini, L. Trasatti: NERONE: First Tests in Sea Water, Frascati Report LNF-01 / 029 (NT) (30 novembre 2001).

OPERA

G.F. Bersani, E. Blanco, G. Di Iorio, B. Dulach, A. Franceschi, F. Grianti, A. Paoloni,
M. Spinetti (Resp.), F. Terranova, L. Votano

1 The experiment

The aim of the OPERA experiment [1]. is the observation of $\nu_\mu \rightarrow \nu_\tau$ oscillations in the parameter region indicated by Super-Kamiokande as the explanation of the zenith dependence of the atmospheric neutrino deficit. OPERA is a long baseline experiment to be located at the Gran Sasso Laboratory in the CNGS neutrino beam from the CERN SPS. The detector design is based on a massive lead/nuclear emulsion target. The target is made up of emulsion sheets interleaved with 1mm lead plates and packed into rimovable "bricks" (56 plates per brick). The bricks are located in a vertical support structure making up a "wall". Nuclear emulsions are used as high resolution tracking devices, for the direct observation of the decay of the τ leptons produced in ν_τ charged current interactions. Electronic detectors, positioned after each wall, locate the events in the emulsions. They are made up of extruded plastic scintillator strips read out by wavelenght-shifting fibers coupled with photodetectors at both ends. Magnetised iron spectrometers measure charge and momentum of muons. Each spectrometer consists of a dipolar magnet made of two iron walls interleaved with pairs of precision trackers. The particle trajectories are measured by these trackers, consisting of vertical drift tube planes. Resistive Plate Chambers (RPC) with inclined strips, called XPC, are combined with the precision trackers to provide unambiguous track reconstruction in space. Moreover, planes of RPC's (Inner Tracker) are inserted between the magnet iron plates. They allow a coarse tracking inside the magnet to identify muons and ease track matching between the precision trackers. They also provide a measurement of the tail of the hadronic energy leaking from the target and of the range of muons which stop in the iron. The discovery potential of OPERA originates from the observation of a ν_τ signal with very low background level. The direct observation of $\nu_\mu \rightarrow \nu_\tau$ appearance will constitute a milestone in the study of neutrino oscillations. Opera is an international collaboration (Belgium, China, Croatia, France, Germany, Israel, Italy, Japan, Russia, Switzerland, and Turkey) and the INFN groups involved are Bari, Bologna, LNF (Frascati), LNGS (Gran Sasso), Naples, Padova, Rome and Salerno.

2 Optimization of the experimental apparatus

During 2002 a significant re-optimization of the setup have been carried out after the withdrawal of the CERN group due to the CERN financial crisis and the subsequent budget reduction for the experiment. Moreover, further constraints to the OPERA geometry come from the choice of locating the experiment in the Hall C of LNGS. The detector configuration optimized for Hall C involves two super-modules instead of three, each of 31 walls. The total number of bricks amounts to 206,336 resulting in a target mass of 1766 tons. The modest reduction of the target mass (12.5%) practically does not affect the performance of the detector [2]. The slightly lower geometrical acceptance of the spectrometers (and subsequent increase of charm background) is compensated by the increase of the primary muon efficiency due to the exploitation of dE/dx measurement in emulsion. However, the CERN moratorium on major orders and its effect on other funding agencies imposed on OPERA an unexpected standby position. In spite of the delay accumulated so far for these reasons, the completion of the installation procedure is scheduled for spring 2006, in agreement with the new CNGS startup schedule.

The Changeable Sheet (CS) scheme, which has been put forward in the 2001 Status Report, is now implemented in the design. The CS are emulsion sheets which, through constant automatic "refreshing", have a low density of background tracks. By interfacing the electronic Target Trackers to the lead-emulsion bricks, they permit to reduce by about a factor of two the scanning load and to improve the event location. Finally, a recent proposal aimed at the increase of the CNGS neutrino flux of about 45% through proton loss reduction in the acceleration chain has been approved by CERN. Hence, the physics performance of the CNGS programme has been significantly enhanced.

3 Activities in Frascati

The Frascati group is responsible for the design and construction of the dipolar magnet. It also shares responsibility with INFN Padova and LNGS for the construction and installation of the bakelite RPC planes (Inner Tracker). Frascati and Naples also designed and prototyped the wall support structure housing the lead/emulsion bricks and are taking care of the overall support structure of the experiment in Gran Sasso. Moreover, the group contributes to software development and to the analyses aimed at assessing the performance of the experiment after the completion of the CNGS programme. Finally, since 2002 LNF is involved in the construction of the Brick Assembly Machine (BAM).

3.1 Magnets

In 2000 a full scale prototype of part of the dipole magnet was constructed in Frascati [3]. A full survey of the magnetic properties of this device has been carried out in 2001 [4, 7] in collaboration with the electrical engineering group of LNF. These information have been employed to determine the magnetic field maps of the final spectrometer [5]. Moreover, they have been complemented by experimental tests to assess the impact of the fringe field to the different active detectors of the apparatus (mainly PMT's). The mass production started at the end of 2001. The magnetic properties of each iron heat has been measured to guarantee uniform magnetic response of the spectrometer. At present 70% of the slabs have been produced and machining is in progress. Ordering of yokes and coils has been carried out and they are now in production phase. Drillings in Hall C for the installation of the first magnet are in progress. The system for field monitoring has been designed. It will be based on a set of pick-up coils recording the induced voltage during the ramp-up phase. A detailed computation of the magnetic behavior in the transient regime [8] has been carried out to optimize the size of the coils and the rate of current variation at the ramp-up. Moreover, a full thermal analysis has been commissioned to study the temperature gradient in the region where RPC will be located and the power dissipation in Hall C. A water-based refrigerator system was designed for the lower return yoke; the location and thickness of the thermal insulators for both yokes have been optimized.

3.2 Wall support structure

The wall support structure is made of thin stainless steel vertical bands welded to light horizontal trays where the bricks are positioned with a precision of one millimeter. The structure is suspended through rods and joints from the general support structure and tensioned from the bottom through a spring system. One prototype (full height and 1 m wide) was assembled at the Frascati Laboratory in 2000 and fully tested in 2001. A second prototype (full width and 1 m high) was built and equipped with a more compact tensioning system. It has been sent to LAPP (Annecy) and it was used to test the prototype of the brick manipulator and finalize its design. Finally, a full size prototype has been commissioned to a firm to check the quality of industrial mass production. It

was sent to Gran Sasso in 2002 to test transportation and handling issues. Tendering for mass production has been delayed by the CERN/INFN moratorium. It has been resumed at the end of 2002. The design of the installation tooling and the study for final alignment and survey are in progress.

3.3 Inner trackers

A test facility to be used during mass production is being built at LNGS. Two trigger walls composed of 128 glass RPCs complete with read-out electronics are available together with bakelite RPC strip panels equipped with front-end boards. A push test table has been commissioned and it is presently in use to monitor the quality of the spacer gluing and gas tightness of the detectors. Moreover, the test includes a facility for the simultaneous conditioning of up to 48 RPC. About 70% of the bakelite planes for production have been delivered; they were tested at LNGS and sent to the firm producing the RPC. The mass production started in mid January 2003. The tools for mounting in Hall C have been produced in Padova and tested in Frascati using the prototype of the magnet. The strip design has been finalized and tendering is in progress.
A detailed scan with cosmics has been done at CERN in collaboration with Padova and Frascati. In particular, spatial uniformity and long term variation of response were investigated. Furthermore, a long term run is going on at LNGS with six bakelite RPC (three of them produced according to the final design and procedure). 6 months of data taking at surface, corresponding to 10 years of operation in Hall C, have been accumulated. No efficiency drop has been observed while variations of current were observed only for RPC built according to the old procedures. Tests with different gas flow rates and mixtures are in progress. The tasks concerning the design and construction of the RPC electronics are shared among LNF (strip boards, HV distribution, current monitoring, fast signals for TDC), Padova (front-end boards) and Naples (controller boards interfaced to DAQ) and coordinated by G. Felici (LNF). The design of the strip board has been finalized in December 2002. The prototypes of the current monitoring system have been delivered and are currently under test at LNGS.

3.4 OPERA General layout

A significant work has been carried out to optimize the layout in the two-supermodule configuration, avoiding a complete re-design of the apparatus. In fact, in this configuration the distance between the magnets is unchanged. Thus the main structure remains the same, without the need of restudying the mechanical compatibility of all the detector components, in particular for their installation. The detailed study of the seismic response has been also carried out leading to the design of dumping structures which react only for large earthquakes. This solution has been accepted by LNGS. The upper part of the structure has been optimized to house the front-end electronics so to minimize the cable length and shorten the cabling procedure. The executive drawings are available and the corresponding tenders have been signed. Preliminary drilling in Hall C is in progress and the installation procedure has started in Feb 2003.

3.5 Brick Assembly Machine

Since sept 2002, LNF is involved in the construction of the Brick Assembly Machine. This machine is an automatic system for massive production of the lead-emulsion bricks. The technical specification of the machine is being prepared and the firm pre-selection is in progress. New welding tools, glues and packaging material are under test at CERN and LNF. The LNF technical staff, coordinated by A. Franceschi has being trained for hand-made brick production and subsequent quality checking.

3.6 Software and analysis

An algorithm based on the method used by CDHS has been implemented for muon reconstruction in the OPERA spectrometers. Its performance has been studied both for monochromatic muons and for neutrino interactions. A full simulation keeping into account ambiguities in the drift tubes and the detailed geometry of the apparatus has been carried out in order to cross-check the semi-analytical estimates made at the level of the Proposal. Finally, improvements in the background rate for the $\tau \to \mu$ channel of the order of 30% have been achieved [6].
The sensitivity of the CNGS beam to the sub-dominant $\nu_\mu \leftrightarrow \nu_e$ oscillations in the region indicated by the atmospheric neutrino experiments was investigated [9]. In particular, a revised analysis of the OPERA detector has been carried out and the sensitivity to θ_{13} of ICARUS and OPERA combined was updated. It has been shown that the CNGS beam optimized for ν_τ appearance, will improve significantly (about a factor 5) the current limit of CHOOZ and explore most of the region $\sin^2 2\theta_{13} \simeq \mathcal{O}(10^{-2})$.

References

1. M. Guler *et al.*, OPERA proposal, CERN/SPSC 2000-028, SPSC/P318, LNGS P25/2000
2. Y. Declais, *Status Report of CNGS1*, Talk at the CERN-SPSC Commettee, Sep. 2002.
3. M. Guler *et al.*, *Status report of the OPERA experiment*, CERN/SPSC 2001-025, SPSC/M668, LNGS-EXP 30/2001 Add. 1/01
4. G. Di Iorio et al., *Measurements of the Magnetic Field in the Prototype of the OPERA Spectrometer*, Preprint LNF-01/028.
5. F. Terranova, *Magnetic field maps of the OPERA spectrometer*, Opera Note n.33 (2002).
6. F. Terranova, *A full simulation of charge and momentum reconstruction in the OPERA spectrometers*, Opera Note n.37 (2003).

Conference talks and publications by LNF authors

7. F. Terranova et al., *Ballistic techniques for magnetic field calibration of large iron detectors operating in underground areas.* Talk at the VIII Topical Seminar on Innovative Particle and Radiation Detectors (Siena, 21-24 Oct 2002), to appear in Nucl. Phys. B (Proc. Suppl.).
8. M. Incurvati, F. Terranova, Nucl. Instr. Meth. A500 (2003) 442
9. M. Komatsu, P. Migliozzi, F. Terranova, J. Phys. G29 (2003) 443.

RAP

S. Bertolucci, G.O. Delle Monache, D. Di Gioacchino, V. Fafone, C. Ligi, A. Marini, G. Mazzitelli, G. Modestino, G. Pizzella (Ass.), G. Raffone, F. Ronga (Resp.Naz.), P. Tripodi (Ass.) and P. Valente

Collaboration: INFN and Physics Department, Universitá di Roma Tor Vergata;
Kamerlingh Onnes Laboratory, Leiden University (The Netherlands);
Fundamental Physics Department, Universitat de Barcelona (Spain).

1 Aim of the experiment

The studies [Astone, P. et al., Phys. Rev. Lett.,**84**,14 (2000); Astone, P. et al., Phys.Lett.B,**499**,16 (2001); Astone, P. et al., Phys.Lett.B,**540**,179 (2002)] of the signals due to the interactions of cosmic rays impinging the gravitational wave antenna NAUTILUS have shown that in a run of the detector at thermodynamic temperature $T = 1.5K$ the results are in agreement with the thermo-acoustic model, while in a run at $T = 0.14K$ large signals have been detected at a rate higher than expected.
In the thermo-acoustic model mechanical vibrations originate from the local thermal expansion caused by the warming up due to the energy lost by the particles crossing the material. More precisely, the relation that accounts for the detectable vibrational energy E in the n$-th$ longitudinal mode due to a specific energy loss dW/dx of a particle impinging a cylindrical bar is [cf. for example Liu,G. and Barish,B., Phys.Rev.Lett,**61**,271 (1988) and references therein]:

$$\mathrm{E} = \frac{4\mathrm{k}}{9\pi}\frac{\gamma^2}{\rho \mathrm{L v}^2}(\frac{\mathrm{dW}}{\mathrm{dx}})^2 \mathrm{F_n}(\mathrm{z_0}, \theta_0, \mathrm{l_0})$$

where k is the Boltzmann constant, ρ the density of the bar material, L the length of the bar, v the speed of the sound, γ the Grüneisen parameter of the material and F_n is a function of geometrical parameters related to the particle track.
Simulations have shown that the previous relation, when applied to NAUTILUS, can be approximately reduced to:

$$\mathrm{E} = 7.64\ 10^{-9} \mathrm{W}^2 \mathrm{G}$$

where E is expressed in kelvin, W, in GeV, is the energy released by the particle to the bar and G is a factor of the order of unity. The thermo-acoustic model has been recently verified by an experiment, operated at room temperature only [van Albada,G.D. et al., Rev Sci Instrum., **71**,1345 (2000)], using a small aluminum cylinder and an electron beam.
The results obtained by NAUTILUS suggest that, when the bar is in the superconducting state, a higher efficiency mechanism for the particle energy loss conversion into mechanical energy takes place. In order to clarify these aspects the RAP experiment [LNF-01-027 (2001)] will measure the effect of the passage of an electron beam, provided by the Beam Test Facility of DAΦNE (BTF), in a low temperature mechanical oscillator, constituted by a suspended small cylindrical bar made of the same aluminum alloy as NAUTILUS. Measurements are planned in both normal, to confirm the already obtained results, and superconducting states of the cylindrical bar. The basic parameters of the experimental setup are shown in Table 1.

Table 1: *RAP detector main parameters.*

Test mass	Al5056 cylinder; lenght =585 mm, diameter =205 mm, M =52 kg, resonance frequency 4.6 kHz
Cryostat	Commercial aluminum cryostat; height =3200 mm, diameter =1016 mm
^{3}He-^{4}He dilution refrigerator	Base temperature =100 mK, cooling power at 120 mK =1mW
Suspension	Suspension multistage stainless steel-copper suspension system; overall attenuation at 4 kHz $\simeq$ 150 dB
Read-out	Piezoelectric ceramics + FET amplifier with calibration capabilities
Beam	500 MeV energy e^-, pulsed/single shot operation mode; maximum current per pulse =250 mA
Acquisition	VME based on-line acquisition, sampling rate =100 kHz

2 Activities in the year 2002

The RAP experiment has been preliminarily approved by CSNII and consequently funded in the year 2002.
The LNF group has been involved in the finalization of the constructive details of the experimental setup and, in particular:

- the test mass,
- the suspension,
- the cryogenic and vacuum systems,
- the mechanical structures needed for hosting the cryostat,
- the readout and data acquisition systems.

Mechanical and cryogenic final realization steps have been realized with the DAΦNE Cryogenic Service support.
A test site, needed for the detector initial assembly and commissioning and for the detector housing after the runs on BTF, has been equipped.
The procurement of the detector components has been also made during the year.

3 Planned activities in the year 2003

The scientific planning of the experiments includes runs at various thermodynamic temperatures of the bar (room, cryogenic, ultra-cryogenic).
During the spring 2003 the assembly of the detector will be performed in the test site together with an initial commissioning, in order to be possibly ready to move the detector in the BTF experimental hall by the end of May for a first run with the bar at room temperature.
During the year the insertion of the ^{3}He-^{4}He dilution refrigerator is planned in order to fulfil the experiment milestone recognized by the CSNII for 2003 which foresees the completion of the detector commissioning by the end of the year.

ROG

D. Babusci, F. Campolungo (tecn), V. Fafone, A. Fauth (FAI), G. Giordano,
M. Iannarelli (tecn), R. Lenci (tecn), A. Marini, G. Modestino,
G. Pizzella (resp,ass), L. Quintieri, F. Ronga (resp), E.Turri (tecn),
collaboration with Roma I La Sapienza, Roma 2 Tor Vergata, Leiden

1 Introduction

The ROG (Rivelatore Onde Gravitazionali) group is operating currently two cryogenic gravitational wave bar detectors: Explorer (at CERN) and Nautilus (in Frascati). The main goal of this search is the direct detection of the gravitational waves that could be emitted by astrophysical sources (Supernova, Coalescent Binaries. ecc.). Such detection could be of enormous interest for general relativity and for astrophysics.

Cryogenic resonant-mass detectors were conceived in the '70s with the aim of improving the sensitivity of room temperature Weber detectors by many orders of magnitude, by reducing the temperature of the bar to or below helium temperature (4.2 K) and employing superconducting electronic devices in the readout system.

The principle of operation of resonant-mass detectors is based on the assumption that any vibrational mode of a resonant body that has a mass quadrupole moment, such as the fundamental longitudinal mode of a cylindrical antenna, can be excited by a gravitational wave with non zero energy spectral density at the mode eigenfrequency. The mechanical oscillation induced in the antenna by interaction with the G.W. is transformed into an electrical signal by a motion or strain transducer and then amplified by an electrical amplifier. Unavoidably, Brownian motion noise associated with dissipation in the antenna and the transducer, and electronic noise from the amplifier, limit the sensitivity of the detector.

The sum at the output of the contributions due to the Brownian noise and to the electronic noise gives the total detector noise. This can be referred to the input of the detector (as if it was a GW spectral density) and is usually indicated as $S_h(f)$. This function has a resonant behaviour and can be characterized by its value at the detector resonance frequency f_0 and by its half height width. $S_h(f_0)$ can be written as:

$$S_h(f_0) = \frac{\pi}{8}\frac{KT}{MQL^2}\frac{1}{f_0^3} \tag{1}$$

where T is the antenna temperature, M is the antenna mass, Q is the quality factor of the mode. The half height width of this function gives the bandwidth of a resonant detector. The bandwidth of a resonant detector depends from the mechanical parameters of the detector and from the characteristic of the electronic amplifier and can be written as:

$$\Delta F = \frac{4f_0}{Q}\frac{T}{T_{eff}} \tag{2}$$

where T_{eff} is the noise temperature when the data are filtered to have the maximum signal to noise ratio in the case of delta like signals (like the one expected from supernova). T_{eff} decreases as the noise temperature of the amplifier decreases and as the transducer efficiency increases.

These relations characterize completely the sensitivity of a resonant-mass detector. For instance, the minimum detectable (SNR=1) GW amplitude for a short burst signal lasting for a time τ_g can be written as :

$$h_0 = \frac{2}{\tau_g}\sqrt{\frac{S_h(f_0)}{2\pi\Delta F}} \tag{3}$$

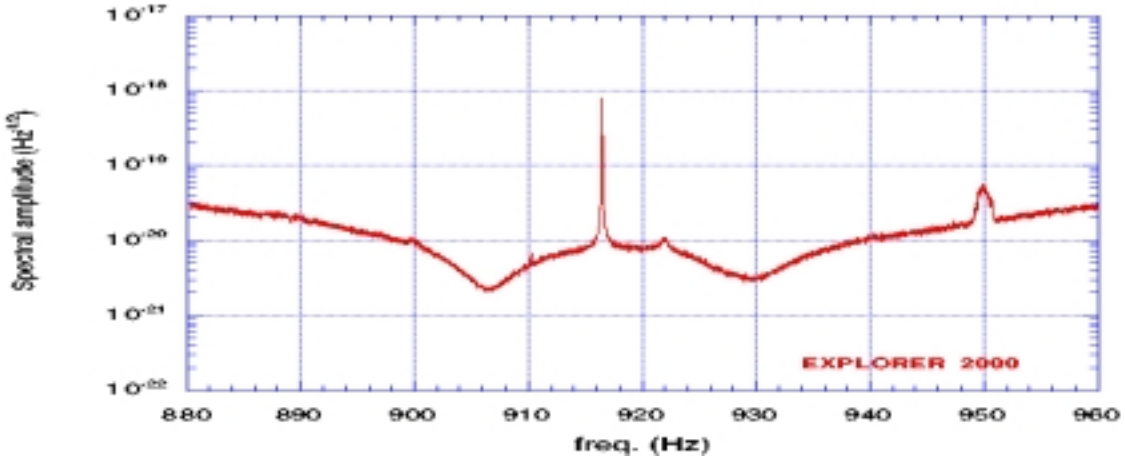

Figure 1: Explorer strain sensitivity with the new trasducer The spectral amplitude is better than $4\,10^{-21}\,\mathrm{Hz}^{-1/2}$ over a band of about 10 hz., The Nautilus strain sensitivity with the improvements done during 2002 will be below $1\,10^{-21}\,\mathrm{Hz}^{-1/2}$

.

2 NAUTILUS and EXPLORER

The ultra cryogenic detector NAUTILUS [1)] is operating at the Frascati INFN National Laboratory since December 1995. It consists of an Al5056 cylindrical bar, 2300 kg in weight and 3 meters in length, cooled to a temperature of 0.1 K by means of a diluition refrigerator, and equipped with a resonant capacitive transducer and a dcSQUID amplifier. Due to the coupling of two resonators (the antenna and the transducer) the resonant frequency f_0 is split in the two frequencies around 908 and 924 hz. Moreover Nautilus is the only detector in the world equipped with a cosmic ray detector.

A shutdown of NAUTILUS was done during 2002 to mount a transducer similar to the one of Explorer. Recently the pulsar originated from the Supernova 1987A has been detected. This pulsar should produce gravitational waves at a frequency of about 935 HZ. The Nautilus alluminium bar was replaced from a bit shorter bar tuned at this frequency [2)].

The Explorer antenna is located in CERN and is very similar to Nautilus, but is cooled only to 2.6 Kelvin [3)]. Explorer has taken data until August 2002. In August 2002 the superconductive circuit connected to the SQUID was damaged. To repair the damage was necessary to warm and to open the antenna. In December 2002 Explorer was again ready to take data. During the 2002 we have completed the installation of the Explorer cosmic ray detector.

The Frascati group has major responsibilities in the maintenance and running of Nautilus (including the production of liquid helium), in the maintenance, building and running of the cosmic ray detectors, in the development of a new superconductive transformer for the signal readout, in the data acquisition and in many items of data analysis.

3 Future

We are studing resonant-mass detectors of spherical shape. A single sphere is capable of detecting gravitational waves from all directions and polarizations and is capable of determining the direction information and tensorial character of the incident wave. A sphere will have a larger mass than

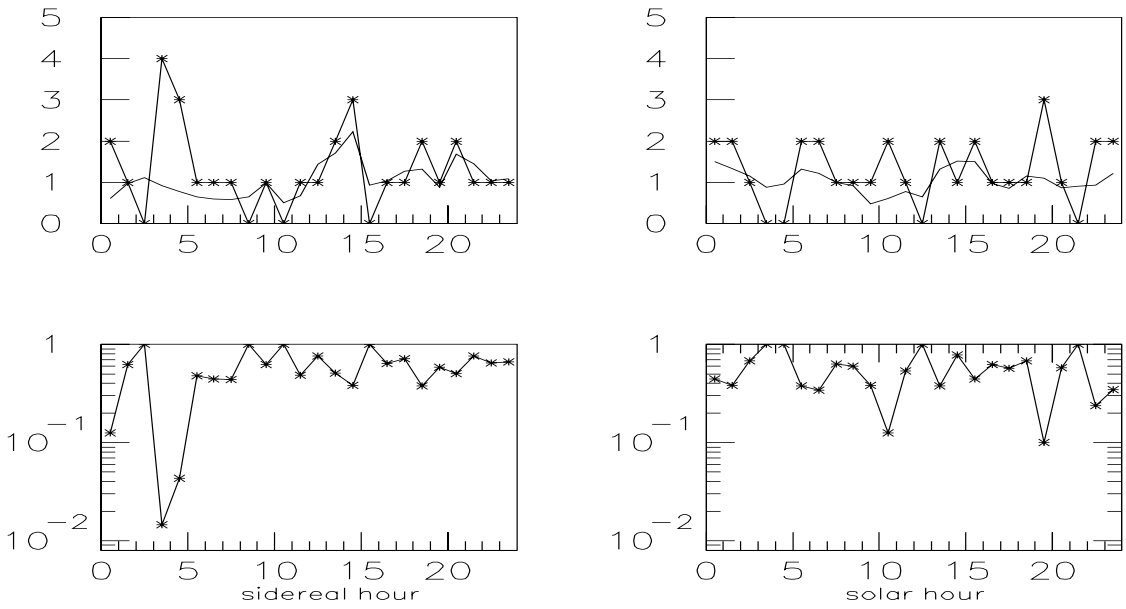

Figure 2: The upper graph on the left shows the number of coincidences n_c indicated with the * and the average number $\bar{n}$ of accidentals versus the sidereal hour. The lower graph on the left shows the Poisson probability to obtain a number of coincidences greater than or equal to n_c. The two graphs on the right show the result using the solar time in hours. We remark that the data points refer to independent sets of events.

the present bars (with the same resonant frequency), translating into an increased cross section and improved sensitivity. Omnidirectionality and source direction finding ability make a spherical detector an unique instrument for gravitational wave astronomy with respect to all present detectors. Studies and measurements essential to define a project of a large spherical detector, 40 to 100 tons of mass, cooled to 10 mK have been made in USA, Italy, Netherland and Brasil. The R/D activity of ROG group is done jointly with the Leiden university group and is related in particular to development of new transducers, the data acquisition and the effect of the cosmic rays.

4 Main analysis results obtained in 2002

The main analyses using the NAUTILUS and EXPLORER data, just published or in progress, are the following:

– A search for monochromatic signal. The present sensitivity of NAUTILUS allows the detection at $SNR = 1$ of a continuous GW signal around 1 khz of amplitude $h \simeq 5\,10^{-26}$ with an observation time of 100 days [4].

–further study of the excitation of NAUTILUS due to the passage of cosmic rays. We have analyzed data with Nautilus at T=1.5 Kelvin. We have seen that at this temperature the experiment is in agreement with theory, and that the anomalous signal detected in the past was due probably to an effect due to the superconductivity of Aluminium [6] [7].

– Search for coincidences with gamma ray bursts [8] [9].

– Search for coincidences between resonant bar detectors [10] [11] [12].

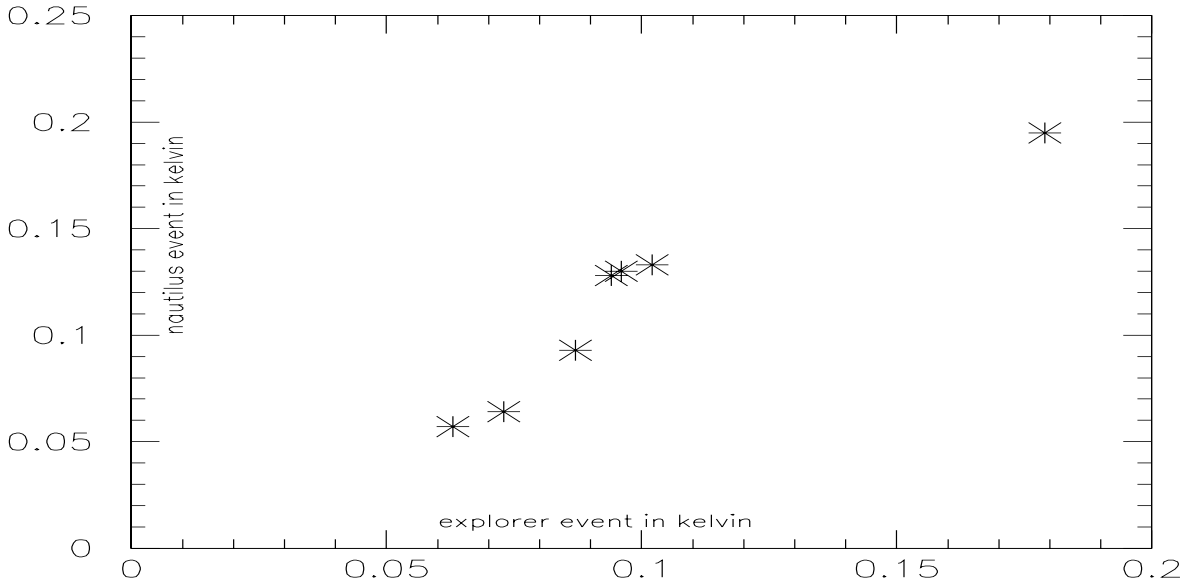

Figure 3: Correlation between the event energies of NAUTILUS with those of EXPLORER for the seven coincidences occurred in the sidereal hour interval 3 to 5. No energy filter was applied.

4.1 Coincidences Nautilus Explorer

In our previous search for coincidences [5)] we took into consideration the non-isotropic response of the detector to a GW burst. We had reasoned that, since extragalactic GW signals should not be detected with the present detectors, possible sources should be located in our Galaxy, or in the Local Group. If any of these sources exist we should expect a more favorable condition of detection when the detectors are oriented with their axes perpendicular to the direction of the potential source, since the bar cross-section is proportional to $sin^4(\theta)$, where θ is the angle between the detector axis and the direction of the line joining it with the source. We did find a small coincidence excess when angle θ with respect to the Galactic Centre was larger than a certain value (see fig.3 of Ref. [5)]).

In the present search for coincidences we extend the previous analysis as follows. We still make use of the directional property of the antenna cross-section. As the Earth rotates around its axis, during the day the detector happens to be variably oriented with respect to a given source at an unknown location. Thus we expect the signal to be modulated during the day; more precisely the modulation is expected to have a period of one or half sidereal day, since the GW sources, if any, are certainly located far outside our Solar system.

The events was selected requiring agreement in time and in energy between signals detected in Explorer and the one detected in Nautilus. Twenty-four categories of events are considered, one per each sidereal hour, the sidereal time referred to a position and orientation halfway between EXPLORER and NAUTILUS (this determines the zero local sidereal time which is not essential for the following considerations). Each category includes coincidences totally independent from those in the other categories. For each category in fig. 2 we report the number n_c of observed coincidences, the average number $\bar{n}$ of accidental coincidences obtained by using the time shifting procedure and, given $\bar{n}$, the probability p that a number $\geq n_c$ of coincidences could have occurred by chance. For comparison we also show a histogram produced with the same procedure using

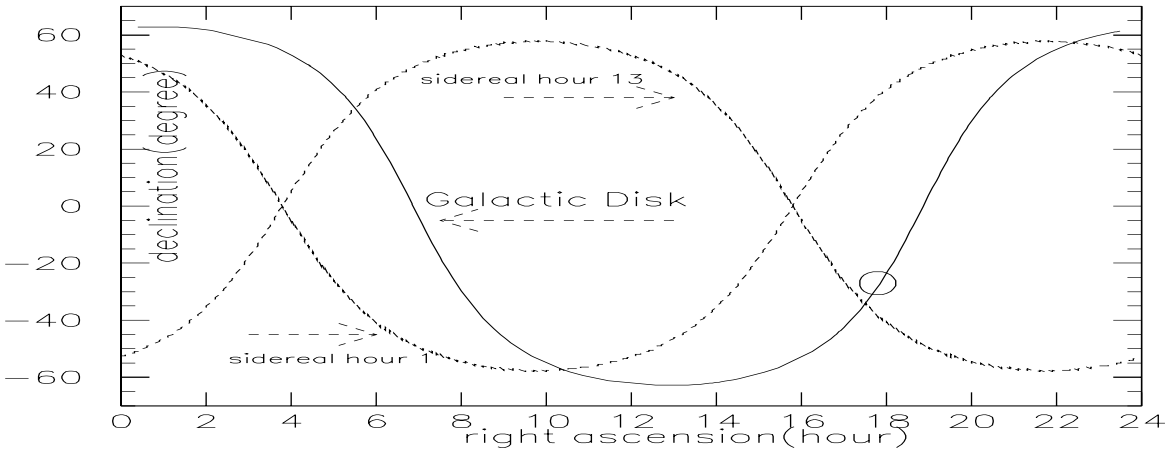

Figure 4: The position of the Galactic Disk and the loci of point sources perpendicular to the detector axis at 1 and 13 sidereal hour in the right ascension-declination plane. At sidereal hour 4.3 the locus tends to coincide with the line of the Galactic Disk. The large circle indicates the location of the Galactic Centre.

solar hours.

One notice a coincidence excess from sidereal hour 3 to sidereal hour 5, which appears to have some statistical significance, as the two largest excesses occur in two neighboring hours (the events in each hour are totally independent from those in a different hour). We have $n_c = 7$ coincidences in this two-hour interval and $\bar{n} = 1.7$. On the contrary, no significant coincidence excess appears at any solar hour.

We proceed now in performing a test, to check if this result is compatible with simultaneous physical excitation of the two detectors of possible non-terrestrial origin. We compare the energies of the coincident events: if the events in EXPLORER and NAUTILUS are due to the same cause we expect their energies to be correlated. This test must be done without applying the energy filter. Without applying the energy filter we still get seven coincidences.

The event energies are very strongly correlated, as shown in fig.3. We also studied the energy correlation of the events of the accidental coincidences and found no correlation. We have verified that, using the cosmic ray detector of NAUTILUS, these events are not due to cosmic ray showers.

At a given sidereal time the intersection of the celestial sphere with the plane perpendicular to the detector axis is a circle. We show in fig.4 two of these circles (i.e., at 1 and at 13 sidereal hours) in the right ascension-declination plane. In the representation of fig.4 the line which indicates the point sources perpendicular to the detector axis (we call this *the line of maximum sensitivity*) moves to the right in the plane of fig.4 with sidereal time. This line intersects the location of the Galactic Centre twice a day (at 4.3 and at 13.6 sidereal hours), and at 4.3 sidereal hour (only once per day) overlaps with the Galactic Disk. This overlapping happens because of the particular orientation of the detectors on the Earth' surface, and does not occur for a different azimuth angle of detector orientation on the Earth' surface. It turns out that the largest number of excess coincidences occurs just when the line of maximum sensitivity of our detectors overlaps with the Galactic Disk, suggesting that GW sources could be located not all in the Galactic Centre but also in other places in the Galactic Disk.

References

1. P. Astone *et al.*, "The gravitational wave detector NAUTILUS operating at T = 0.1-K," Astropart. Phys. 7, 231 (1997).

2. P. Astone *et al.*, "The next science run of the gravitational wave detector NAUTILUS" Classical and Quantum Gravity Volume 19, Number 7 pag 1911, 7 April 2002

3. P. Astone *et al.*, "The EXPLORER gravitational wave antenna: recent improvements and performances" Classical and Quantum Gravity Volume 19, Number 7 pag 1905, 7 April 2002

4. P. Astone *et al.*, "Search for periodic gravitational wave sources with the Explorer detector," arXiv:gr-qc/0011072. Phys.Rev. D65 (2002) 022001

5. P. Astone *et al.*, "Study of coincidences between resonant gravitational wave detectors," Class. Quant. Grav. 18, 243 (2001) [arXiv:gr-qc/0007055].

6. P. Astone *et al.*, "Anomalous signals due to cosmic rays observed by the bar gravitational wave detector NAUTILUS" Classical and Quantum Gravity Volume 19, Number 7 pag 1897, 7 April 2002

7. P. Astone *et al.*, Phys. Lett. B **540**, 179 (2002) [arXiv:gr-qc/0206079].

8. G. Modestino and A. Moleti "On the crosscorrelation between Gravitational Wave Detectors for detecting association with Gamma Ray Bursts" Phys. Rev. D 65, 022005 (2002)

9. P. Astone *et al.*, Phys. Rev. D **66**, 102002 (2002) [arXiv:astro-ph/0206431].

10. P. Astone *et al.*, "Search for gravitational wave bursts by the network of resonant detectors" Classical and Quantum GravityVolume 19, Number 7 1367, 7 April 2002

11. P. Astone, S. D'Antonio and G. Pizzella "Coincidence analysis in gravitational wave experiments" Classical and Quantum Gravity Volume 19, Number 7 pag 1443, 7 April 2002

12. P. Astone *et al.*, Class. Quant. Grav. **19**, 5449 (2002) [arXiv:gr-qc/0210053].

VIRGO

D. Babusci, G. Giordano (Resp.), M. Iannarelli (Tecn.), E. Turri (Tecn.)

1 Introduction

Virgo is a collaboration between Italy (INFN) and France (CNRS) for the construction of an interferometric detector of gravitational waves (GW). The participating laboratories are: LAPP-Annecy, IPN-Lyon, OCA-Nice, LAL-Orsay and ESPCI-Paris for CNRS and Firenze/Urbino, Frascati, Napoli, Perugia, Pisa, Roma for INFN.

The aimed sensitivity should allow to detect, in the frequency range between a few Hz and a few kHz, GW emitted by coalescing binary compact stars, gravitational collapses, spinning neutron stars, or constituting the stochastic GW background.

Virgo will be a recycled (power enhancement factor $\simeq 50$) Michelson interferometer, having in each arm a 3 km Fabry-Perot cavity with finesse of 50. The interferometer (ITF) will be illuminated by a 25 W Nd:YAG laser ($\lambda = 1.064\ \mu m$), stabilized through a monolithic reference cavity and filtered by a high-finesse triangular mode cleaner of 144 m length.

The optical path will be completely under vacuum and all the optical components will be suspended in vacuum by anti-seismic Super Attenuators able to reduce the seismic noise of more than a factor 10^{12} above a few Hz.

The construction of Virgo was planned in two main steps: the realization of the central interferometer (CITF) completed by end 2000, and the realization of the 3 km arms full ITF, foreseen to end within 2003.

2 Responsibility of the Frascati Group

The Frascati group has the responsibility of the "linear alignment", that is the system providing the informations about the misalignment of the ITF mirrors during the standard operation of Virgo. It will employ 8 quadrant photodiodes (QPHD) placed on the beams emerging from the ITF; demodulating the up-down and left-right differencies, the misalignments status will be derived.

3 CITF commissioning

The operation of the CITF started soon after its completion and ended in July 2002.

The CITF consisted of all the Virgo final components in the central area, including the 144 m mode cleaner. It operated as a simple recycled Michelson interferometer where the arm end mirrors were installed at the place of the input mirrors of the future 3 km Fabry-Perot cavities. Its commissioning allowed to set up and test all the detection and control systems that will be used in Virgo, and, in particular, the linear alignement system developed in Frascati, was fully installed and operated.

During the commissioning several engineering runs were done. The aim of these runs was to periodically test the progresses achieved by operating the CITF continuosly for a few days. Figure (1) shows the achieved sensitivity in the various engineering runs: E0 and E1 refer to a simple Michelson configuration, while the others refer to a recycled Michelson configuration. Only in E4 the real injection system was used, while in the other runs an auxiliary low power laser was employed.

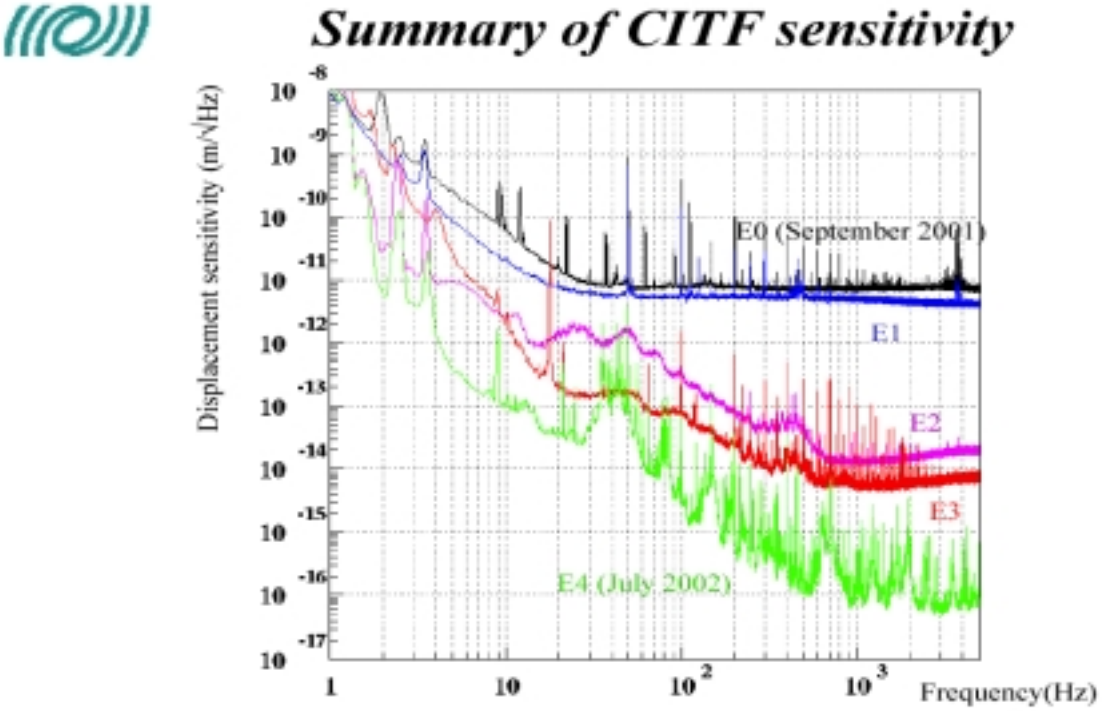

Figure 1: *The CITF sensitivity during the engineering runs.*

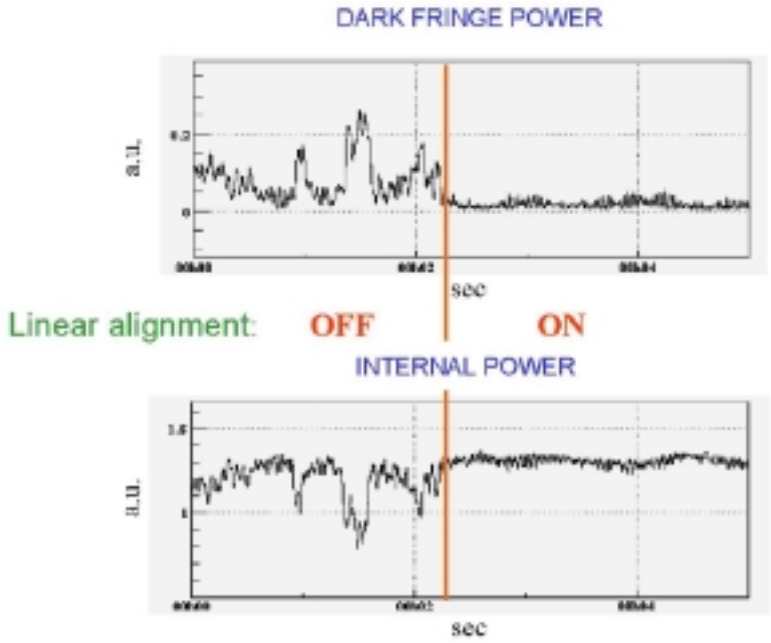

Figure 2: *Improvement of CITF stability with linear alignment feedback.*

Our linear alignment system became operational during E3 allowing the improved sensitivity above 10 Hz clearly visible in the difference between the E2 and E3 curves.

Figure (2) shows the impressive change in the stability of the dark fringe and internal interferometer powers that was caused by the switching on of the angular feedbacks driven by the linear alignment detectors.

4 Activity in 2003

Soon after the end of the CITF commissioning, we started the modifications and upgrades to the electronic components of our system, required for the full Virgo configuration. This task is foreseen to end by March 2003, when we will start to reinstall the system, that will be completed with the addition of remotely controlled laser shutters, whose construction is in progress.

The start of the Virgo commissioning will happen in the second half of 2003 as soon as all the constructions and installations will be over.

5 Publications

1. A. Bozzi *et al.*, Rev. Sci. Instrum. **73**, 2143 (2002).
2. F. Acernese *et al.*, The present status of the Virgo central interferometer in Proc. 4th Edoardo Amaldi Conference on Gravitational Waves (Amaldi 4), Perth, Australia, 8-13 Jul.2001. Published in Class. and Quantum Grav. **19**, 1421 (2002).

WIZARD

S. Bartalucci, G. Basini, F. Bongiorno (Ass.), L. Marino (Ass.),
G. Mazzenga (Tecn.), M. Ricci (Resp.)

Participant Institutions:

ITALY: INFN Bari, LNF, Firenze, Napoli, Roma2, Trieste;
CNR Ist. Fisica Applicata "Nello Carrara" Firenze;
ASI (Italian Space agency);
Electronic Engineering Department, University of Roma 2 "Tor Vergata";
RUSSIA: MePhi Moscow;
FIAN Lebedev Moscow;
IOFFE St Petersburg;
TsSKB-Progress Samara;
SWEDEN: KTH Stockholm;
GERMANY: Siegen University;
USA: NASA Goddard Space Flight Center;
New Mexico State University.

1 Experimental Program and Scientific Objectives

The WIZARD experimental program is devoted to the extensive study of cosmic ray spectra (particles, antiparticles, isotopes, abundances and search for antimatter) in several energy ranges achievable through different apparatus on board stratosferic balloons and long duration satellite missions. WIZARD is an International Collaboration between several Universities and Research Institutions from Russia, Sweden, Germany, USA togheter with the Space Agencies NASA, RSA (Russia), SNSB (Sweden), DLR (Germany) and ASI. The experimental activities are carried out through three main programs:
Balloon flights;
Satellite missions NINA-1 and NINA-2;
Satellite mission PAMELA.
We refer to previous editions of this report for the descrition of the activities related to the balloon flights and to the two NINA missions.

1.1 The satellite mission PAMELA

PAMELA is a cosmic ray space experiment that will be installed on board a Russian satellite (Resurs-DK1) whose launch is foreseen in the first quarter of 2003 from the cosmodrome of Baikonur, Kazakhstan. The satellite will fly for at least 3 years in a low altitude, elliptic orbit (300-600 km) with an inclination of 70.4 degrees. The PAMELA telescope consists of a magnetic spectrometer including a permanent magnet coupled to a silicon tracker, a Transition Radiation Detector, an imaging silicon-tungsten calorimeter and a time-of-flight system including anticoincidence counters [1, 2]. A sketch of the PAMELA instrument is shown in fig.1.

The total height of PAMELA is 120 cm, the mass is 440 kg, the power consumption is 385 W and the geometrical factor is 20.5 cm^2 sr.

The observational objectives of the PAMELA experiment are to measure the spectra of antiprotons, positrons and nuclei in a wide range of energies, to search for antimatter and for

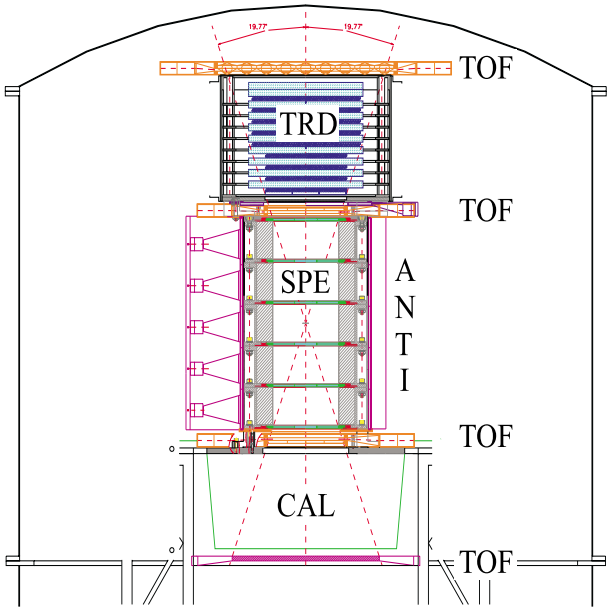

Figure 1: The PAMELA telescope and its main detectors: Transition Radiation Detector (TRD); Permanent Magnet Spectrometer equipped with silicon tracker (SPE); Silicon-Tungsten Calorimeter (CAL). Time Of Flight(TOF) and Anticoincidence (ANTI) systems are also shown.

indirect signatures of dark matter and to study the cosmic ray fluxes over a portion of the solar cycle.

The main scientific goals can be schematically listed as the following:

a) measurement of the antiproton spectrum in the energy range 80 MeV-190 GeV;
b) measurement of the positron spectrum in the energy range 50 MeV-270 GeV;
c) search for antinuclei with a sensitivity of $\sim 3 \times 10^{-8}$ in the $\overline{He}/He$ ratio;
d) measurement of nuclei spectra (He, Be, C) at energies up to 700 GeV/n;
e) measurement of the electron spectrum in the energy range 50 MeV-2 TeV.

Moreover, the PAMELA experiment will be able to address the following additional issues:

a) continuous monitoring of the cosmic rays solar modulation during and after the 23rd maximum of the solar activity;
b) study of the time and energy distributions of the energetic particles emitted in solar flares;
c) measurement of the anomalous component of cosmic rays;
d) study of stationary and disturbed fluxes of high energy particles in the Earth magnetosphere.

Activity in the year 2002 has covered the following items:

- Integration of Mass Dimensional Thermal Model (MDTM).
- Vibration tests of MDTM at IABG facility Munchen (Germany).
- Delivery of MDTM to TsSKBProgress plant (Samara, Russia) and preliminary integration tests and compatibility check with Pressurized Container.

- Delivery to Roma2 and test of Engineering Model (EM) of CPU.
- Test at CERN SPS-H4 beam of Flight Tracker, Flight Calorimeter and Flight Anticounters all integrated with EM of TRD.
- Test at CERN PS-T7 beam of low-energy performance of TRD and Calorimeter.
- Completion and delivery for integration at Roma2 of Tracker, Base Plate and S3/TOF.
- Completion of Flight Model (FM) calorimeter and of FM Anticounters.
- Completion of TRD Gas System and PAMELA general cooling system.
- Delivery to Roma 2 and integration in the PAMELA FM of base plate and spectrometer (FM magnet + FM tracker).
- Completion of the design of the flight CPU.
- Study of the specifications of the PAMELA downlink system.

2 Activity of the LNF group during year 2001

The LNF WIZARD group has been fully involved in all the balloon and satellite programs. During the year 2002 the activity for the PAMELA experiment has been carried on as follows:

- Responsibility of the Mechanical Ground Support Equipment (MGSE) for the assembly and integration of the whole apparatus.
- Organization and coordination of beam test set-up at CERN PS and SPS.
- Responsibility of the counting detectors and trigger for beam tests.
- Preparation and tests of the Mass Dimensional and Thermal Model at TsSKBProgress plant (Samara, Russia).
- Vibrational tests of PAMELA Dummy Model at IABG Company, Munchen (Germany).
- Preparation and assembly of the Technological (Engineering) Model.

3 Programmed activity of the LNF group during year 2003

1. PAMELA
- Completion of Technical/Engineering Model.
- Completion of Flight Model, integration and ground tests.
- Final beam test of Flight Model model at CERN SPS/H4 .
- Delivery of Flight Model to Russia.
- Flight readiness tests and integration with spacecraft Resurs DK1.

2. BALLOON FLIGHT
A new flight of the balloon experiment CAPRICE is programmed for Spring 2004 from New Mexico, USA. The main scientific objective is the measurement of the spectrum of muons at different atmospheric altitudes. The group at LNF shares the responsibility of the silicon-tungsten imaging calorimeter and of the development of the on-board data acquisition system. Work is in progress for the upgrade to VME of the DAQ of the calorimeter (with INFN Roma 2 and Trieste) and for the modification of some mechanical parts which interface with the Payload structure. By fall 2003 the calorimeter will be delivered to the New Mexico State University for the successive phases of the integration in the Payload.

4 List of Publications in 2002

1) S. Avdeev et al.:"Eye light flashes on the Mir Space Station"; Acta Astronautica 50, 511 (2002)

2) V.Bidoli et al.:"Light Isotope Abundances in Solar Energetic Particles measured by the Space Instrument NINA"; Ap.J. 577, 513 (2002)

3) A.Bakaldin et al.:"Geomagnetically trapped light isotopes observed with the detector NINA"; J.Geoph.Res. 107, 8 (2002)

4) O. Adriani et al.:"The PAMELA Experiment on Satellite and its Capability in Cosmic Rays Measurements"; NIM A478, 114 (2002)

5) C.Grimani et al.:"Measurements of the absolute energy spectra of cosmic-ray positrons and electrons above 7 GeV"; Astronomy and Astrophysics 392, 287 (2002)

6) V.Bidoli et al.:"Energy spectrum of secondary protons above the atmosphere measured by the instruments NINA and NINA-2"; Ann. Geophysicae 20, 1693 (2002)

7) M.Casolino et al.:"The Sileye-3/Alteino experiment on board the International Space Station"; Nucl. Phys. 113B, 71 (2002)

8) M.Ambriola et al.:"High-energy deuteron measurement with the CAPRICE98 experiment"; Nucl. Phys. 113B, 88 (2002)

References

1. P. Spillantini for the PAMELA collaboration: "The PAMELA experiment", Proc. XXVII ICRC Hamburg vol. 6 p. 2215 (2001)
2. O. Adriani et al. "the PAMELA experiment on satellite and its capability in cosmic ray measurements", NIM A478, 114 (2002)

AIACE

E. De Sanctis (Resp.), M. Mirazita (Ass.),
A. Orlandi (Tech.), W. Pesci (Tech.), E. Polli, F. Ronchetti (Dott.),
P. Rossi, A. Viticchié (Tech.)

1 Introduction

AIACE stands for Attività Italiana A CEbaf. It is the collaboration of the INFN groups of Frascati and Genova which participate into the physics program carried in the Hall B at the 6 GeV Continuous Electron Beam Accelerator Facility (CEBAF) at the Jefferson Laboratory (JLab), located in Newport News, Virginia (USA). At present, the Hall B collaboration counts about 140 physicists from 35 Institutions from seven Countries.

Hall B is devoted to experiments that require the detection of several loosely correlated particles in the final state, and the CLAS detector [1)], a large acceptance spectrometer, is unique in design to accomodate these requirements and to perform a very broad spectrum of physics measurements.

The themes of the Hall B scientific program are the precision study of the structure of the nucleon and the nature of the strong interaction. Experiments aim to clarify the interplay between hadronic and partonic degrees of freedom and the effectiveness of the traditional nucleon-nucleon theories or QCD inspired models.

This scientific program can be summarized in the following main topics:

- *Baryon Resonances*
- *Spin Structure Functions in the Resonance Region*
- *Nucleon Tomography*
- *Dynamics of the Strong Interactions*

In the period covered by this report the Frascati group has carried out:

- the analysis of data for the determination of the deuteron photodisintegration cross section between 0.5 and 3.0 GeV.
- The calculations of polarization observables in high-energy deuteron photodisintegration within the Quark-Gluon String Model (QGSM).
- The analysis of data for the measurement of the beam-spin asymmetry in the electroproduction of positive pions above the baryon resonance region.
- The drafting of a Letter of Intent submitted to the Jefferson Lab Panel Advisory Committee for the measurement of the transverse polarization effects in hard scattering at CLAS.
- The completion of a new program to monitor the Large Angle Calorimeter High Voltage system, using Java application and a graphical user interface.

In addition, the Frascati group has participated to the various CLAS production runs data taking and to the relative discussions of the analysis work.

2 Deuteron photodisintegration between 0.5 and 3.0 GeV (Experiment E-93-017)

Measurement of the deuteron photodisintegration is well suited for studying the interplay between hadronic and partonic degrees of freedom in the intermediate energy regime where neither the traditional meson exchange models nor pQCD describe the data well.

At high incident photon energy and intermediate angles, conventionally 90°, the $\gamma d \to pn$ differential cross section is well-described by the constituents counting rules (CCR) [2]:

$$\frac{d\sigma}{dt} = \frac{1}{s^{n-2}} f(\theta_{CM})$$

where n is the minimum number of microscopic fields involved in the reaction, s is the square of the total energy, and θ_{CM} is the proton scattering angle. In this case, $n = 13$, and then the CCR predicts $d\sigma/dt \propto s^{-11}$.

Data on the deuteron photodisintegration differential cross section at large angles, $\theta_{CM} = 69°$ and 89° and for $E_\gamma \geq 1$ and at $\theta_{CM} = 37°$ and 53° for 3 GeV and 4 GeV, respectively, seem to follow the scaling prescription. In contradiction, polarization observables measured at 90° and for photon energies up to 2 GeV are not consistently interpreted in a perturbative picture. Therefore, observed scaling in the cross section can not be taken as a stringent test that the perturbative regime as been reached, also because traditional models based on meson exchange current, are able to reproduce the observed behavior of cross section versus energy at all angles [3].

In this context the use of non-perturbative QCD calculations to describe the deuteron photodisintegration process appears more suitable.

This is done by the so-called quark gluon string model (QGSM) [4]. The reaction $\gamma d \to pn$ is described by the exchange of three valence quarks in the t-channel plus any number of gluons. This corresponds to the formation and break-up of a quark-gluon string in the intermediate state, leading to the factorization of the amplitudes. Such a string can also be identified with the nucleon Regge trajectory since the QGSM can be considered as a microscopic model for the Regge phenomenology, and can be used for the calculation of different quantities that have been considered before only at a phenomenological level [5].

Open questions include at what momentum transfer does one reach the perturbative regime, which is the most convenient description in the transition region, and where the conventional picture of the deuteron in terms of nucleons and mesons fail, and partons start to come into play.

The CLAS data on the complete angular distributions for the outgoing proton ($\theta_{LAB} = 10° - 140°$) and for photon energies between 0.5 and 3.0 GeV contribute significantly to answering these questions.

Differential cross sections $d\sigma/d\Omega$ are reported in Fig.1 as a function of the proton angle in the CM frame, for fixed photon energy above 0.9 GeV and up to 2.45 GeV. The present preliminary results [6] are the first complete and accurate data of the cross section in this energy region. They show a persistent forward-backward asymmetry at all energies. These data agree well with the few previous available data from JLab [7] and SLAC [8] in the region of overlap.

Also showed in Fig.1 are the QGSM calculations (solid line). The agreement with the data is very good and the angular dependance of the cross section at fixed photon energy is well reproduced included the observed forward-backward asymmetry.

3 Polarization observables in high-energy deuteron photodisintegration within the Quark-Gluon Strings model

As stated above, the Quark Gluon String Model (QGSM) is a non-perturbative approach, which has been extensively used for the description of hadronic reactions at high energies [5] and due to duality

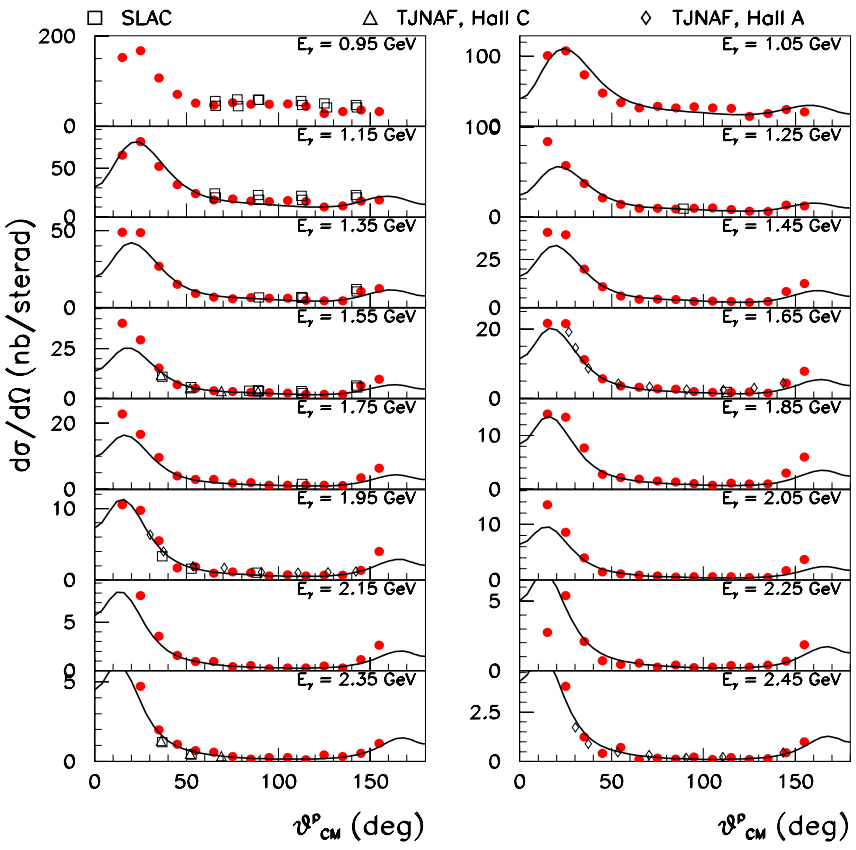

Figure 1: Preliminary results of the $\gamma d \to pn$ differential cross section measured with CLAS (solid dots), compared with the published data from Jlab [7] (open triangles and open diamond) and SLAC [8] (open squares). The curve is the QGSM calculation [4].

property of scattering amplitudes, it can also be applied at intermediate energies for reactions without explicit resonances in the direct channel. This model has been applied for the description of the deuteron photodisintegration reaction, using QCD motivated non linear nucleon Regge trajectories [9], with full inclusion of spin variables and assuming the dominance of the amplitudes that conserve s-channel helicity. The interference between the isoscalar and isovectorial components of the photon has been also taken into account, leading to forward-backward asymmetry in the cross section.

Complementary information to the differential cross sections is provided by polarization observables that should give important tests of nonperturbative calculations in the intermediate energy regime. Data for recoil polarizations have been published recently [10]. Existing Meson-Baryon Models (MBM) fail to describe the data for the induced polarizations, which are surprisingly small for energies above about 1 GeV. Moreover, the polarization transfer data are inconsistent with hadron helicity conservation (HHC), which is generally expected for perturbative QCD.

The polarization observables as calculated within the QGSM are shown in Fig. 2 [11] (for the definitions of these observables in terms of helicity amplitudes see Ref. [12]). It is found that:

i) the induced polarization P_y vanishes at $\theta_{CM} = 90°$, but is different from 0 for $\theta_{CM} \neq 90°$;

ii) the polarization transfers C_x and C_z for circularly polarized photons do not vanish at $\theta_{CM} = 90°$: $C_x \simeq 0.25 \div 0.35$ and $C_z \simeq 0.3 \div 0.4$ and it is almost constant between 1.5 and 6 GeV (Fig. 2 left panel);

iii) the polarized photon asymmetry Σ is about 0.7 at $\theta_{CM} = 90°$ and $E_\gamma = 1.5$ GeV (Fig.2 right panel) and drops smoothly with E_γ reaching the value of 0.3 at 4 GeV.

We observe that for $E_\gamma \geq 1.5$ GeV the calculated values of C_z are in agreement with the new TJNAF data [10].

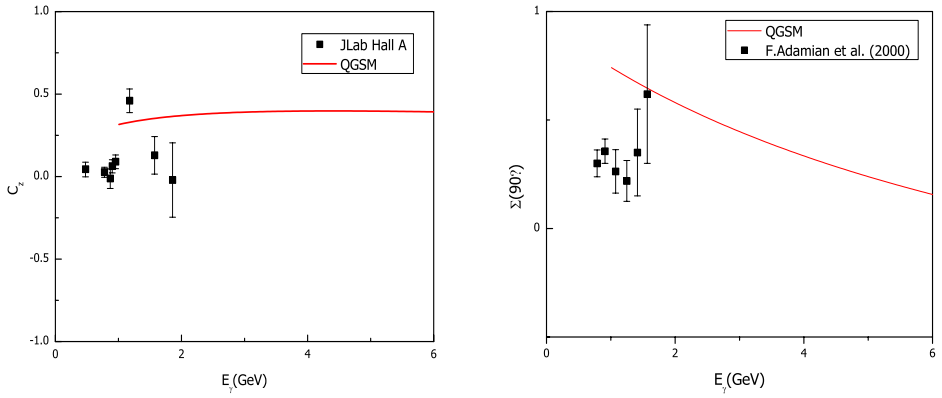

Figure 2: Polarization observables as predicted by the QGSM. Left panel: polarization transfer C_z for circularly polarized photons compared to the experimental data from Ref. [10]. Right panel: the asymmetry $\Sigma(90°)$ for linearly polarized photons as a function of the photon energy. Also shown are the experimental data from Ref. [13].

4 Measurement of Beam-Spin Asymmetries for $\vec{e}p \to e'\pi^+X$ in the Deeply Inelastic Regime

Much of our current knowledge of the nucleon comes from inclusive electron scattering experiments that measure elastic form factors and longitudinal parton densities. However, elastic scattering and deeply inelastic scattering give two orthogonal one-dimensional projections of the proton. The former measures the probability of finding a proton with a transverse size matching the resolution of the probe, while the latter probes the quark's longitudinal momentum distribution, but has no sensitivity to the transverse dimension. The information resulting from these two types of experiments is disconnected, and does not allow one to construct the image of a real 3-dimensional proton.

Semi-exclusive measurements, in which one hadron is observed in addition to the scattered electron, are needed to study the flavour structure of the nucleon and only fully exclusive processes in which all final products are reconstructed can unravel the complete internal dynamics.

The theoretical framework for the interpretation of these new class of experiments is given by the formalism of Generalized Parton Distributions (GPDs) [14, 15, 16] which give information on quark-quark correlations, transverse quark momentum distributions and contributions of correlated quark-antiquark pairs (mesons) to the nucleon wave function.

Presently, one of the major tool for studying Generalized Parton Distributions is the measurement of single spin-asymmetries (SSA) in which the asymmetry depends only on the polarization of the beam or target. SSA give access to subtle distribution and fragmentation functions, such as transversity, Sivers and Collins functions, which can not easily be accessed in other ways.

The first measurement of a significant Beam Single Spin Asymmetry ($A_{LU} sin(\phi)$) in semi-inclusive pion electroproduction above the baryon resonance region has been performed at the Jefferson Lab using a 4.25 GeV longitudinally polarized electron beam and the CLAS detector. In the above notation,"L" stands for the longitudinally polarized beam, "U" (second index) for the unpolarized target and the angle ϕ is the azimuthal angle between the scattering plane defined by the initial and final electron momenta, and the production plane defined by the transverse momenta of the observed hadron and the virtual photon. In Fig. 3 the data are presented as a function of the Bjorken variable x and the fraction of the energy of the virtual photon transfered to the pion, z.

The z dependence of beam SSA in semi-inclusive deep inelastic scattering, analyzed in terms of the fragmentation effect, probes the ratio of polarized (Collins) and unpolarized fragmentation functions, while the x dependence is defined by the ratio of the twist-3 unpolarized distribution function e(x) and the leading twist distribution function $f_1(x)$ [17]. The data from CLAS on SSA allowd the first extraction of e(x) by Efremov et al. [18].

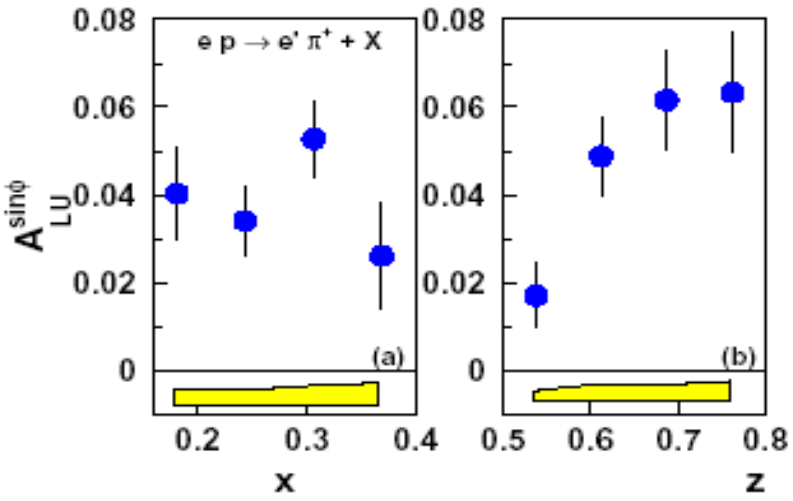

Figure 3: The beam-spin azimuthal asymmetry ($sin(\phi)$ moment in the cross section) extracted from hydrogen data at 4.25 GeV as a function of x and z. The bars show the statistical uncertainty and the band represents the systematic uncertainties.

5 List of Publications

1. First Measurement of the Double Spin Asymmetry in $\vec{e}\vec{p} \to e'\pi^+ n$ in the Resonance Region.
   R. De Vita *et al.* and CLAS Collaboration, Phys. Rev. Lett. 88 (2002) 082001.

2. Q^2 Dependence of Quadrupole Strength in $\gamma^* p \to \Delta^+(1232)$.
   K. Joo *et al.* and CLAS Collaboration, Phys. Rev. Lett. 88 (2002) 122001.

3. η photoproduction on the proton for photon energies from 0.75 to 1.95 GeV.
   M. Dugger *et al.* and CLAS Collaboration, Phys. Rev. Lett. 89 (2002) 222002.

4. Photoproduction of the ω mesons on the proton at large momentum transfers.
   M. Battaglieri *et al.* and CLAS Collaboration, Phys. Rev. Lett. 90 (2002) 022002.

5. Polarization observables in high-energy deuteron photodisintegration within the Quark-Gluon String model.
   V.Yu Grishina *et al.*, Nuc-th/0209076.

6. Quark-Hadron Picture of the Deuteron Photodisintegration.
   M. Mirazita, hep-ph/0206213.

7. The Cebaf Large Acceptance Spectrometer.
   B. Mecking *et al.* and CLAS Collaboration, accepted by Nucl. Instr. and Meth.

8. Measurement of Beam-Spin Asymmetries for Deep Inelastic π^+ Electroproduction.
   H. Avakian *et al.* and CLAS Collaboration, submitted to Phys. Rev. Lett.; hep-ex/0301005.

9. Measurement of Inclusive Spin Structure Functions of the Deuteron with CLAS.
   J. Yun *et al.* and CLAS Collaboration, accepted by Phys. Rev. C; hep-ex/0212044.

10. Measurement of $ep \to e'p\pi^+\pi^-$ and Baryon Resonance Analysis.
    M. Ripani *et al.* and CLAS Collaboration, submitted to Phys. Rev. Lett.; hep-ex/0210054.

11. First Measurement of Transferred Polarization in the Exclusive $\vec{e}p \to e'K^+\vec{\Lambda}$ Reaction.
    D. Carman *et al.* and CLAS Collaboration, accepted by Phys. Rev. Lett.; hep-ex/0212014.

6 Presentation at Conferences

1. *Quark-Hadron Duality in Deuteron Photodisintegration.*
   Marco Mirazita
   Contributed talk at the "XL International Winter Meeting on Nuclear Physics"
   Bormio (Italy), January 21-26, 2002.

2. *Deuteron Two-Body Photodisintegration in the Quark-Hadron Picture.*
   Marco Mirazita
   Contributed talk at the "MESON2002 WORKSHOP"
   Cracow (Poland), May 24-28, 2002.

3. *Deuteron Two-Body Photodisintegration in the Quark-Hadron Picture.*
   Federico Ronchetti
   Contributed talk at the "QNP2002"
   Julich (Germany), June 9-14, 2002.

4. *Deuteron Photodisintegration in the Quark-Hadron Picture.*
   Patrizia Rossi
   Invited talk at the "ELECTRON-NUCLEUS SCATTERING VII"
   Isola d'Elba (Italy), June 24-28, 2002.

5. *Deuteron Two-Body Photodisintegration in the Quark-Hadron Picture.*
   Marco Mirazita
   Contributed talk at the "XVIII EUROPEAN CONFERENCE ON FEW-BODY PROBLEMS"
   Bled (Slovenia), September 8-14, 2002.

6. *Deuteron Two-Body Photodisintegration in the Quark-Hadron Picture.*
   Federico Ronchetti
   Contributed talk at the "5th INTERNATIONAL CONFERENCE ON QUARK CONFINEMENT AND THE HADRON SPECTRUM"
   Gargnano (Italy), September 10-14, 2002.

7. *Fisica della Collaborazione CLAS: Risultati Recenti e Prospettive.*
   Patrizia Rossi
   Invited talk at the "LXXXVIII CONGRESSO SIF"
   Alghero (Italy), September 26-October 1, 2002.

8. *Deuteron Photodisintegration in the Quark-Hadron Picture.*
   Federico Ronchetti
   Contributed talk at the "LXXXVIII CONGRESSO SIF"
   Alghero (Italy), September 26-October 1, 2002.

9. *Deuteron Photodisintegration in the Quark-Hadron Picture.*
   Federico Ronchetti
   Contributed talk at the "AMERICAN PHYSICAL SOCIETY DNP FALL MEETING"
   East Lansing (Michigan-USA), October 9-12, 2002.

References

1. B. Mecking *et al.*, accepted by Nucl. Instr. and Meth.

2. S. L. Brodsky, G. L. Farrar - Phys. Rev. Lett. **31** (1973) 1153.
   V. Matveev *et al.* - Lett. Nuovo Cimento **7** (1973) 719.

3. A. E. L. Dieperink, S. I. Nagorny - Phys. Lett. B **456** (1999) 9.

4. V. Yu. Grishina *et al.* - Eur. Phys. J. A **10** (2001) 355 .

5. A. B. Kaidalov - Z. Phys. C **12** (1982) 63.

6. CLAS Collaboration Meeeting, Newport News February 27- March 1, 2003.

7. C. Bochna *et al.*, Phys. Rev. C **41** (1998) 4576;
   E.C. Shulte *et al.*, Phys. Rev. Lett. **87** (2001) 102302-1;
   E.C. Shulte *et al.*, Phys. Rev. C **66** (2002) 042201(R).

8. S.J. Freedman *et al.*, Phys. Rev. C **48** (1993) 1864;
   J.E. Beltz *et al.*, Phys. Rev. Lett. **74** (1995) 646.

9. M. M. Brisudova *et al.*, Phys. Rev. D **61** (2000) 054013.
10. K. Wijesooria *et al.*, Phys. Rev. Lett **86** (2001) 2975.
11. V. Yu. Grishina *et al.*, Nucl-th/0209076.
12. V.P. Barannik *et al.*, Nucl. Phys. A **451** (1986) 751.
13. F. Adamian *et al.*, Eur. Phys. J. A **8** (2000) 423.
14. D. Muller *et al.*, Fortschr. Phys. **42**, 2101 (1994).
15. X. Ji, Phys. Rev. Lett. **78**, (1997) 610; Phys. Rev. D **55**, (1997) 7114.
16. A. V. Radyushkin, Phys. Lett. B **380**, (1996) 417; Phys. Rev. D **56**, (1997) 5524.
17. J. Levelt and P. J. Mulders, Phys. Lett. B **338**, (1994) 357.
18. A. Efremov *et al.*, hep-ph/0208124.

DEAR

M. Bragadireanu (Ass.), C. Guaraldo (Resp.), M. Iliescu,
V. Lucherini, F. Lucibello (Tech.), C. Petrascu, D. Sirghi (Ass.), F. Sirghi (Ass.)

1 DEAR scientific program

The objective of DEAR (DAΦNE Exotic Atom Research) is the precise determination of the isospin dependent antikaon-nucleon scattering lengths, through a percent level measurement of the K_α line shift and width in kaonic hydrogen, and a similar (the first one) measurement of kaonic deuterium. The shift, with respect to the purely QED calculated value, and the broadening of the line (width) are due to the effect of the strong interaction between antikaon and nucleon, when there is overlap between the two wavefunctions; this effect is present and measurable for the 1s level.

DEAR actually measures the X-ray transitions occuring in the cascade processes of kaonic atoms; a kaonic atom is formed when a negative kaon (coming from the ϕ-decay, produced at DAΦNE) enters a target, looses its kinetic energy through ionization and excitation processes, and is eventually captured, replacing the electron, in an excited orbit ($n \simeq 25$). Via different cascade processes (Auger effect, molecular dissociation, radiative transitions) the kaonic atom deexcites to lower states. When a low-n state with small angular momentum is reached, the strong interaction with the nucleus comes into play. This strong interaction is the reason for the shift in energy of the lowest-lying level from the purely electromagnetic value and the finite lifetime of the state - corresponding to an increase in the observed level width.

For kaonic hydrogen and deuterium the K-series transitions are of main experimental interest, since they are the only ones affected by the strong interaction. The K_α lines are clearly separated from the kigher K transitions. The shift ϵ and the width Γ of the 1s state of kaonic hydrogen are related in a fairly model-independent way (Deser-Trueman formula) to the real and imaginary part of the complex s-wave scattering length, a_{K^-p}:

$$\epsilon + i\Gamma/2 = 412 a_{K^-p}\ eV\ fm^{-1} \tag{1}$$

A similar relation applies to the case of kaonic deuterium and to its corresponding scattering length, a_{K^-d}:

$$\epsilon + i\Gamma/2 = 601 a_{K^-d}\ eV\ fm^{-1} \tag{2}$$

The measured scattering lenghts are then related to the isospin-dependent scattering lengths, a_0 and a_1:

$$a_{K^-p} = (a_0 + a_1)/2, \quad a_{K^-n} = a_1 \tag{3}$$

The extraction of a_{K^-n} from a_{K^-d} requires a more complicated analysis than the simple impulse approximation (K^- scattering from each - free - nucleon): higher order contributions associated with the K^-d three-body interaction have to be taken into account. This means solving the three-body Faddeev equations by the use of potentials, taking into account the coupling among multichanneled interactions.

An accurate determination of the K^-N isospin dependent scattering lengths will place strong constraints on the low-energy K^-N dynamics, which in turn constraints the SU(3) description of chiral symmetry breaking. Crucial information about the nature of chiral symmetry breaking, and to what extent the chiral symmetry must be broken, is provided by the calculation of the meson-nucleon sigma terms.

A meson nucleon sigma-term is defined as the nucleon expectation value of the equal-time double commutator of the chiral symmetry breaking part of the strong-interaction Hamiltonian.

The sigma term is then a quantity which directly gives the degree of chiral symmetry breaking. Consequently, its relation to the scattering amplitude represents the corresponding low-energy theorem in the soft meson limit.

A phenomenological procedure, which implies dispersion relations and suitable extrapolations allows to extract the sigma terms from the measured amplitudes. Presently only estimates, with 70% uncertainties, exist; a measurement of the K^-N scattering lengths at few percent level should allow the determination of these quantities with a precision better than 20%.

The sigma terms are also important inputs for the determination of the strangeness content of the proton. The strangeness fraction depends on both kaon-nucleon and pion-nucleon sigma terms, being more sensitive to the first ones.

2 The DEAR setup used in the 2002 data taking

A schematic drawing of the completely new DEAR setup used in the 2002 runs is shown in Figure 1, where the main components are indicated.

In particular, the new target cell was done in kapton 75μm thick, cylindrically shaped, with a diameter of 11 cm, reinforced with epoxy-fiberglass bars, in order to have as less material as possible in front of the CCDs, in order to avoid all those electronic transitions which could interfere with the kaonic atom measurement.

The new cryogenic setup was equipped with a new control and data acquisition electronics and with a new type of CCDS; 16 CCD-55 were used, in order to increase the efficiency and flexibility. The new electronics together with the use of the new CCDs allowed to obtain the following performances:

- thermal noise about 15 eV FWHM;
- energy resolution at 5.9 keV: 136 eV;
- linearity of the scale from 1 to 16 keV 10^{-4};
- stability: fluctuations below 4 eV/month;
- charge transport inefficiency: 10^{-4}.

The results obtained during the 2002 run periods with the described setup are reported in the next Section.

3 Activity in 2002

3.1 Finalization of the analysis of the experimental results obtained in the 2001 run

A refined analysis was performed for the experimental results obtained in the run on May - June 2001, when for the first time the kaonic nitrogen spectrum was measured with the experimental setup equipped with 8 CCD-22 and 4 CCD-05 and with a target done in aluminium.

The goal of this refined analysis was twofold: to extract very accurately the nitrogen signal for the two lines seen (4.6 and 7.6 keV transitions) from the sea of electronic transitions of different elements (iron, vanadium, chromiun, manganese, copper) present in the target frame, and to determine the position of the lines - as free parameters - being this a test for the possibility to perform in the future a precise measurement of the charged kaon mass, by using the technique of exotic light (nitrogen) kaonic transitions.

The kaonic nitrogen lines were clearly identified and the results were published as *"A new method to obtain a precise value of the mass of the charged kaon"*, in Physics Letters **B**, Vol. 535 (1-4) (2002) 52.

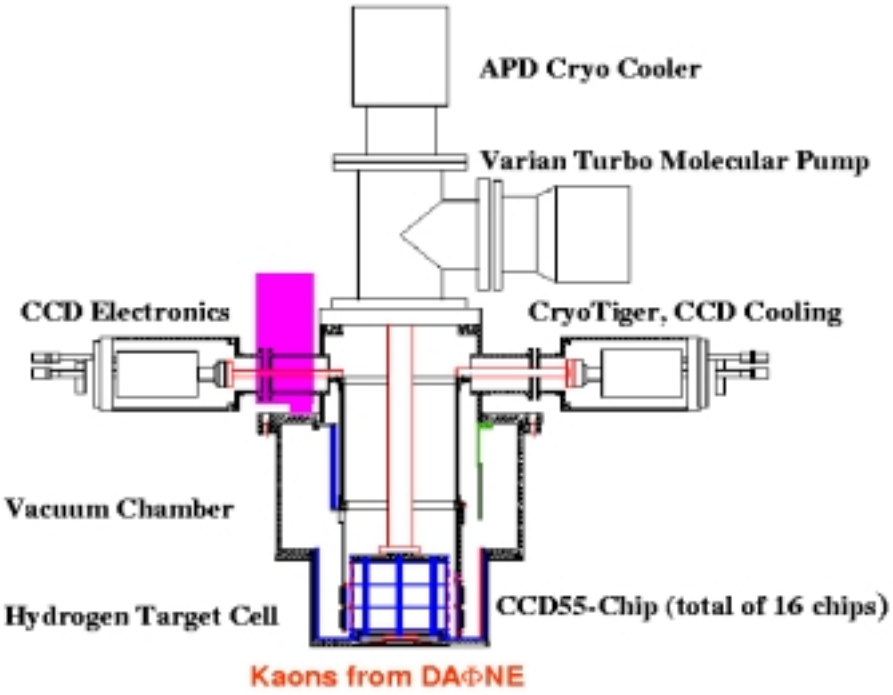

Figure 1: *The DEAR experimental setup*

3.2 New kaonic nitrogen measurement with the new setup used in the 2002 runs

During April 2002 a new run with kaonic nitrogen was performed. The nitrogen measurement was performed to see the lines of nitrogen with a better or equivalent quality with respect to the 2001 run, taking advantage of:

- the new DEAR setup equipped with 16 CCD-55 with additional external and internal shieldings;
- the new machine configuration, after the installation of additional scrapers and octupoles;
- a new low-β optics in both planes for collisions in the DEAR Interaction Point.

Moreover, the scientific aim of this run was the study of different degrader configurations to take into account the effect of the boost in the ϕ-production, and to be able to prepare for the kaonic hydrogen run the "best degrader" compatible with the parameters of produced ϕ's.

After the optimization of the machine optics, working in stable conditions, the kaonic nitrogen corresponding lines were clearly seen, in a region of the spectrum free of electronic excitation peaks, consequence of the use of the new target, kapton made (see Section 2). The overall spectrum is shown in Figure 2. Apart of the kaonic nitrogen transitions there are present:

- calcium line, at about 3.7 keV, due to the presence of the calcium in the fiberglass reinforcement of the kapton target;
- silicon line - silicon being the material of the CCDs;
- aluminium line - from the top cover of the target;
- zirconium line - from the zirconium foil placed inside the setup with calibration purpose.

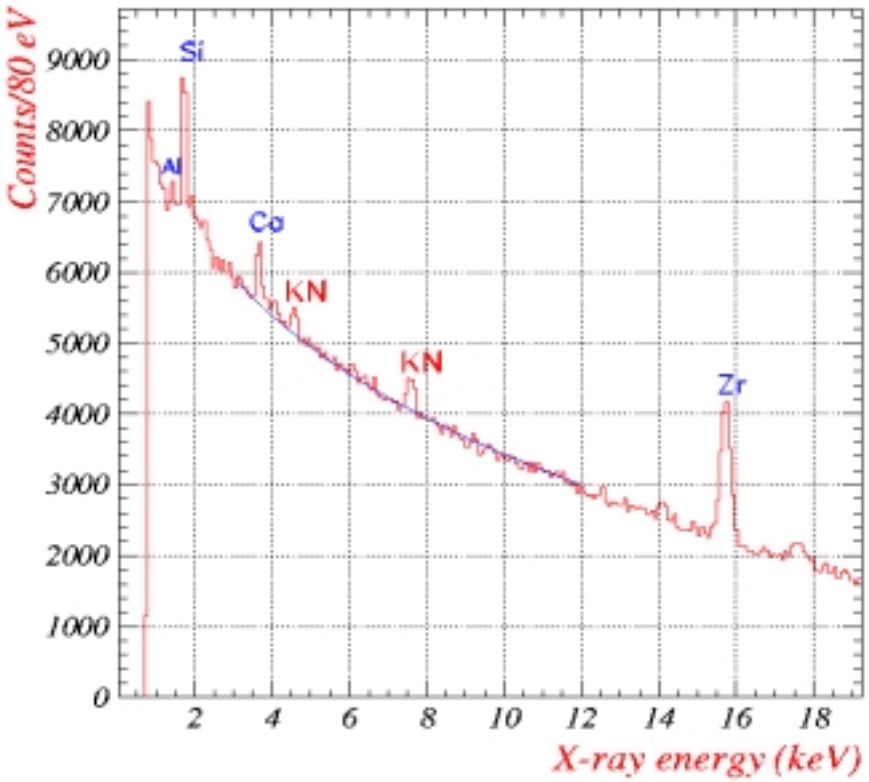

Figure 2: *Energy spectrum obtained for the run of April 2002 with kaonic nitrogen. Kaonic nitrogen transitions are clearly seen, as indicated in the figure*

A pure background run was also performed and no line was present at the energy for which kaonic nitrogen transitions are expected.

The continuous background subtracted spectrum is shown in Figure 3.

All the improvements performed on the setup and the machine optics resulted in a background reduction by a factor ∼8, compared to 2001.

The refined study of the degrader shaping, according with the ϕ-production (mainly the boost) was possible. Monte Carlo simulation results were in very good agreement with the measured data and a new degrader was designed, shaped according to the geometry of the setup and kinematics of ϕ-production - to be used in the run of kaonic hydrogen.

The objective of this run - namely to prove DEAR is ready for the hydrogen measurement - was completely reached, and the collaboration was ready for the kaonic hydrogen measurement - described in the next section.

3.3 Kaonic hydrogen measurement with DEAR at DAΦNE

The last part of 2002 DAΦNE beam (4 October - 22 December) was dedicated to the measurement of the kaonic hydrogen by DEAR.

The measurement of kaonic hydrogen was preceeded by a kaonic nitrogen measurement - with the goal to check in place the new shaped degrader, prepared after the April 2002 run, while the accelerator was still in the optimization phase.

After the machine reached stable conditions, the measurement of kaonic hydrogen followed (30 October - 22 December).

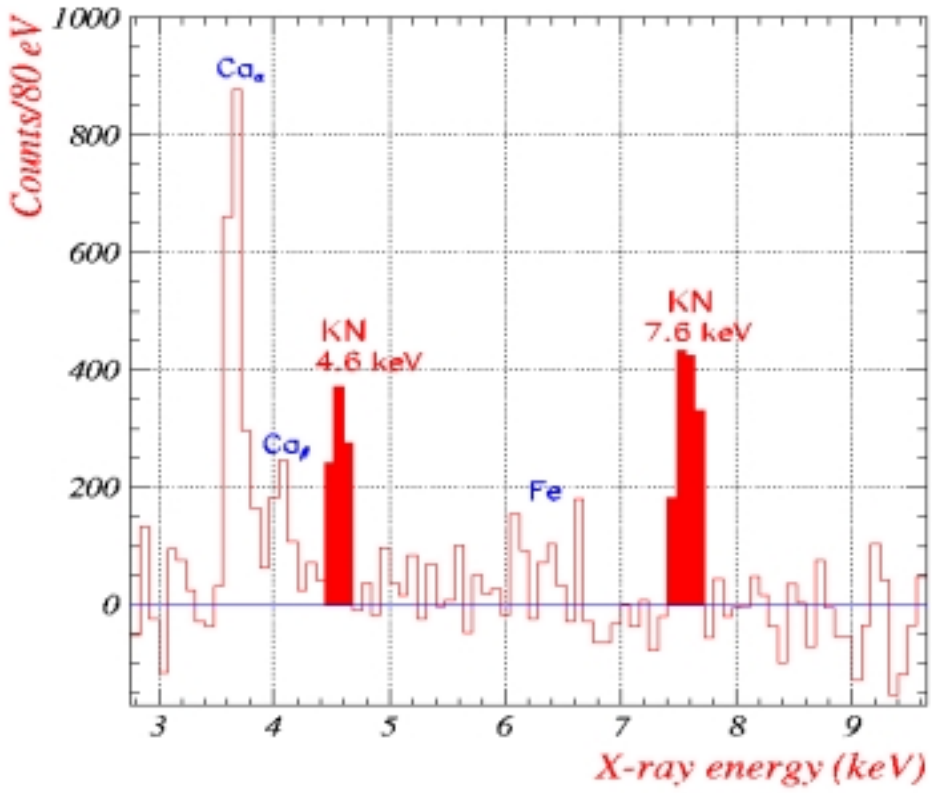

Figure 3: *Continuous background subtracted spectrum obtained for the run of April 2002 with kaonic nitrogen. Kaonic nitrogen transitions are clearly seen, as indicated in the figure*

The results of the nitrogen measurement and of the hydrogen measurement are reported below.

3.3.1 Optimization of machine and DEAR setup by performing kaonic nitrogen measurement, October 2002

The new shaped degrader - going from 280 μm to 1405 μm in 9 steps of 125 μm each - positioned along 9 cm in the ϕ-boost direction was installed and tested for the first time in October 2002. The test was performed with kaonic nitrogen (target was filled with gaseous cryogenic nitrogen, at a temperature of 85 K and a pressure of 1.01 bar), due to the faster response obtainable (higher yield of transitions with respect to the kaonic hydrogen), during the period in which DAΦNE performances were continuously improving (thanks to a new optics).

The signal was seen on all the 16 CCDs with the same weight, in agreement with Monte Carlo predictions. About 2700 events were observed for the $7 \rightarrow 6$ transition (4.6 keV), about 5300 events for the $6 \rightarrow 5$ one (7.6 keV) and 1400 events in the $5 \rightarrow 4$ line (14 keV).

The preliminary background subtracted X-ray spectrum is shown in Figure 4. Note that the titanium transition is present in the spectrum due to the fact that a titanium foil was placed inside the setup for calibration purpose for the kaonic hydrogen measurement.

A more refined analysis is undergoing with the goal of performing for the first time an accurate determination of the yield of the transitions in gaseous nitrogen and to compare it with cascade code predictions.

When the accelerator reached good performances (more than 1 pb^{-1}/day) and the degrader

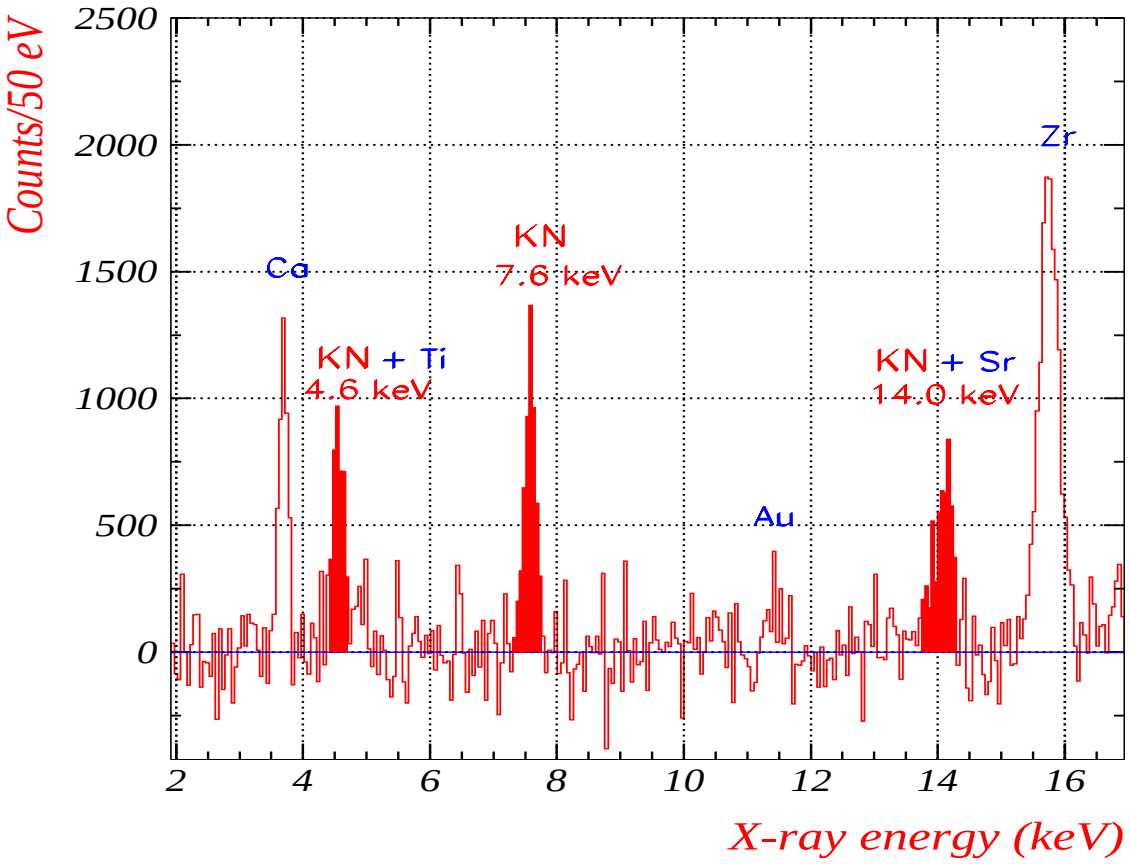

Figure 4: *Continuous background subtracted spectrum obtained for the run of October 2002 with kaonic nitrogen. Kaonic nitrogen transitions are clearly seen, as indicated in the figure*

functionality was completely understood, the kaonic hydrogen measurement started.

3.3.2 Kaonic hydrogen measurement

The target was filled with hydrogen in cryogenic and pressurized conditions: 23 K and 1.82 bar. The kaonic hydrogen measurement lasted from 30 October to 22 December 2002. It was divided into two periods:

- from 30 October to 16 December - continuous run with the kaonic hydrogen; the total integrated luminosity, measured by the DEAR kaon monitor, was about 58 pb^{-1};
- from 16 December to 22 December - background run - with no collisions in the DEAR Interaction Region - with a statistics equivalent to about half of the kaonic hydrogen one - in order to have the pure-background measured.

Preliminary analysis of a partial statistics show the presence of kaonic hydrogen lines (K_α line and the rest of the complex).

More refined data processing and analysis are in progress.

4 Activity in 2003

The complete analysis of kaonic nitrogen data will be completed and results published as the first measurement of kaonic nitrogen transitions obtained in gaseous nitrogen.

Data analysis for the kaonic hydrogen will include:

- study of data selection criteria and their optimization;
- final processing of data selected with the optimized cuts;
- estimate of the experimental background spectrum;
- kaonic hydrogen data analysis, considering the background shape;
- determination of the kaonic hydrogen shift (with a precision about 15%) and width for the 1s level, which is the ultimate goal.

For the future, in order to achieve the percent level measurement of the shift and width for kaonic hydrogen and kaonic deuterium transitions an upgrade of the DEAR setup is previewed. One of the problems to cope with during the kaonic hydrogen measurement performed in 2002 was still the presence of a high background. The CCD devices used to detect the X-ray transitions are non-triggerable devices, due to the fact that data read-out is slow (seconds). In order to further reduce the background, the use of the timing information is a must. Consequently, DEAR is planning to use new fast triggerable devices: Silicon Drift Detectors (SDD) in a new collaboration including the Max Planck Institute of Munich and Politecnico of Milano. The trigger is given by the entrance of the charged kaon in the target volume. The event can be identified and measured with high accuracy and low contamination by the use of a three-scintillator telescope, synchronized with the bunch frequency. The excellent timing performance (1 μs) to be used in trigger together with excellent energy resolution (140 eV at iron position) of the SDD will allow a dramatic decrease of the background and to obtain a signal/background ration of about 1/1 for kaonic hydrogen and 1/3 - 1/10 for kaonic deuterium and to perform the planned precision measurements.

In 2003 the characterization of few SDD chips (energy resolution, time answer capabilities etc.) and the test of preliminary read-out electronics is previewed by using the Beam Test Facility in operation at LNF. In parallel, accurate Monte Carlo simulation will be developed, in order to find the optimal geometry and trigger configuration for the kaonic hydrogen and kaonic deuterium measurements. Production runs of chips are foreseen at Munich starting from the end of 2003.

5 Publications 2002

5.1 List of Conference Talks by LNF Authors in Year 2002

1. M. Iliescu, **Exotic atoms production with DEAR on DAFNE**, "7th International Workshop on Production, Properties and Interaction of Mesons", (MESON)2002, Cracow (Poland), 24-28 May, 2002.
2. C. Guaraldo, **Recent results from DEAR at DAFNE**, Workshop on Hadronic Atoms - HadAtom 02", Switzerland, Bern, 14-15 October 2002.

5.2 Papers

1. M. Iliescu *et. al.* (DEAR Collaboration), **Exotic atoms production with DEAR on DAΦNE**, Proceedings of "MESON 2002 Workshop", Cracow (20020, p.295.

2. G. Beer *et. al.* (DEAR Collaboration), **A new method to obtain a precise value of the mass of the charged kaon**, Physics Letters **B535**, (1-4) (2002) 52.

3. C. Guaraldo *et. al.* (DEAR Collaboration), **Recent results from DEAR at DAΦNE**, Proceedings of the "Workshop on Hadronic Atoms - HadAtom 02", Switzerland, Bern, 14-15 October 2002.

4. J. Zmeskal, *et. al.* (DEAR Collaboration), **The DEAR experiment**, Proceedings of the "EXA 2002 - International Workshop on Exotic Atoms - Future Perspectives", November 28 - November 30, 2002, Vienna, Austria

5.3 Technical Notes

1. C. Curceanu (Petrascu), M. Bragadireanu, M. Cargnelli, L. Curceanu, J. -P. Egger, C. Guaraldo, T. Ishiwatari, K. Itahashi, M. Giersh, M. Iliescu, V. Lucherini, L. Ludhova, L. Shaller, D. Sirghi, F. Sirghi, J. Zmeskal, **Results of the December 2001 "engineering run" - I : Test of the new kapton target cell**, DEAR Note-IR-39, January 11, 2002.

2. C. Curceanu (Petrascu), C. Guaraldo, **Results of the December 2001 "engineering run" - II : Machine performance with a new optics in IP2**, DEAR Note-IR-40, January 14, 2002.

3. M. Bragadireanu, M. Cargnelli, C. Curceanu (Petrascu), L. Curceanu, J. -P. Egger, C. Guaraldo, T. Ishiwatari, K. Itahashi, M. Giersh, M. Iliescu, V. Lucherini, L. Ludhova, L. Shaller, D. Sirghi, F. Sirghi, J. Zmeskal, **Results of the December 2001 "engineering run" - III. Study of shielding configurations**, DEAR Note-IR-41, January 16, 2002.

4. M. Bragadireanu, G. Corradi, C. Curceanu (Petrascu), C. Guaraldo , M. Iliescu, F. Lucibello, R. Petrescu, D. Sirghi, F. Sirghi, J. Zmeskal, **Linearity study of the new detection system for the kaonic hydrogen measurement - Preliminary results -** , DEAR Note-IR-42, February 1, 2002.

5. G. Beer, M. Bragadireanu, M. Cargnelli, C. Curceanu (Petrascu), J. -P. Egger, M. Giersh, C. Guaraldo, M. Iliescu, T. Ishiwatari, V. Lucherini, L. Ludhova, T. Ponta, D. Sirghi, F. Sirghi, J. Zmeskal, **Results of the May - June 2001 runs: measurement of kaonic nitrogen spectrum**, DEAR Note-IR-43, February 18, 2002.

DIRAC

P. Gianotti (Resp.), M. Giardoni, C. Guaraldo, M. Iliescu, A. Lanaro, P. Levisandri,
V. Lucherini, C. Petrascu

1 Introduction

The DIRAC (Dimeson Relativistic Atomic Complex) experiment at CERN will provide a stringent test of Chiral Perturbation Theory (ChPT) by measuring, in a model independent way, the difference between the isoscalar (a_0) and isotensor (a_2) S-wave pion-pion scattering lengths with 5% accuracy. Such determination will be done through a measurement (with 10% accuracy) of the lifetime of Pionic Atoms ($A_{2\pi}$), a weakly bound $\pi^+\pi^-$ system at threshold, produced by proton-nucleus interactions at 24 GeV/c.

The present theoretical estimate of the lifetime of the ground state of the dimeson atom, from calculations performed within the framework of standard ChPT, is $(2.9 \pm 0.1) \cdot 10^{-15} s$ [1].

The DIRAC experimental apparatus is located at the CERN PS East Hall. It is a double arm magnetic spectrometer, consisting of high resolution tracking and particle identification detectors. It is designed to detect with high efficiency charged pion pairs with small relative momentum ($Q < 3$ MeV/c), and small opening angle ($\simeq 0.35$ mrad). The experiment was approved in 1996, the commissioning was done at the end of 1998 and the apparatus became fully operational in the spring of 1999.

The DIRAC Collaboration includes 83 participants from 19 international Institutes. 14% of the participants are from Italian Institutes (INFN-LNF and Trieste University/INFN). About 25% of leadership roles within the collaboration is granted to INFN members. The yearly budget contribution from INFN to the Experiment amounts to ∼20% of the total budget.

The LNF group has contributed to the experiment by providing 2 large threshold Cherenkov counters for e^+e^- identification. The counters use gaseous nitrogen as radiator. Each counter is equipped with 20 mirrors and 10 photomultipliers. The Cherenkov detectors ensure e^+e^- rejection at the trigger level with 99.5% efficiency, and 15 photoelectrons are on average detected in each counter.

2 Activity in 2002

During 2002 the main activities of the DIRAC collaboration were the data taking, and the data analysis. The LNF-DIRAC group contributed to both. The DIRAC data collection tooke place from May to November 2002 and during this period the LNF group kept the responsibility of maintaining and monitoring the performance of the Cherenkov and Preshower detectors. Furthermore, the group coordinated the off-line data quality check. The main results of the data analysis are reported in tab.1.

With the data collected from 2000 to 2002 using nickel and titanium targets about 12000 atomic pairs have been detected. This leads to a statistical accuracy on the $A_{2\pi}$ atom lifetime of about 14% which translates into 7% on $|a_0 - a_2|$. Fig. 1 shows the the atomic pair signal as a function of the F variable. The F variable is defined as:

$$F = \sqrt{\left(\frac{q_L}{\sigma_{q_L}}\right)^2 + \left(\frac{q_x}{\sigma_{q_x}}\right)^2 + \left(\frac{q_y}{\sigma_{q_y}}\right)^2}$$

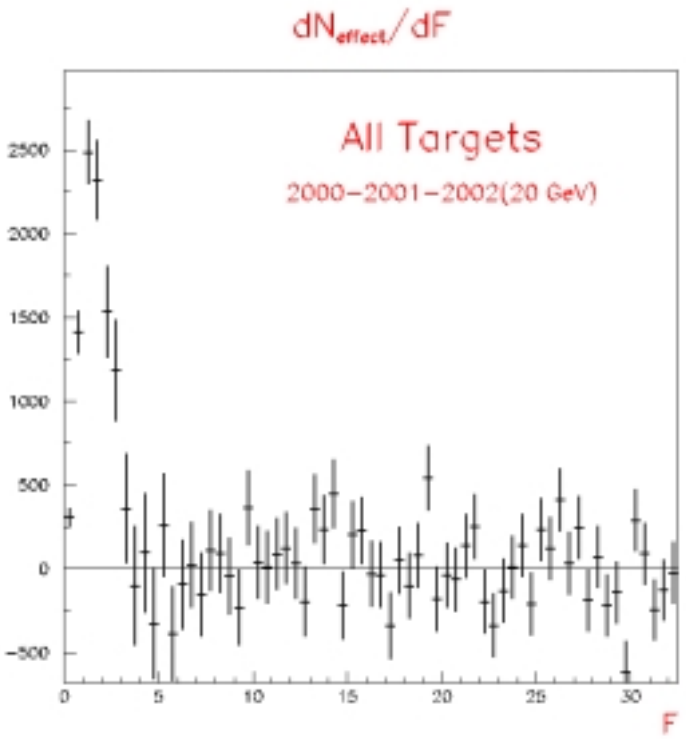

Figure 1: *Atomic pairs distribution as a function of the F variable (see the test for explanations).*

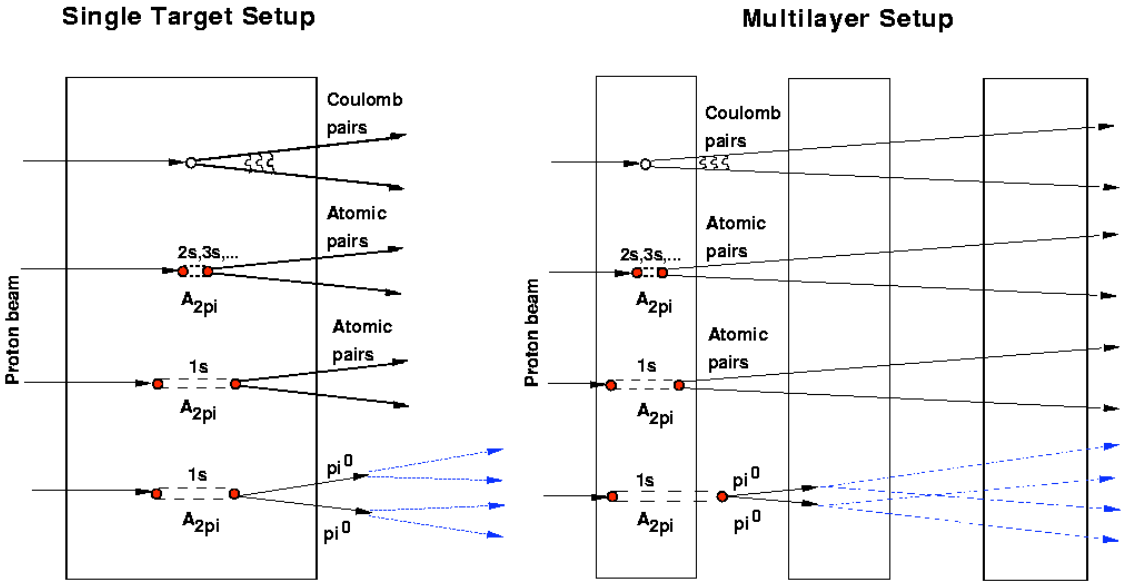

Figure 2: *Layout of the two different target setting - single-layer and multi-layer - used to directly evaluate the background contribution. The different behavior of atomic pairs and background event pairs is shown.*

Table 1: *Summary of DIRAC data analysis.*

Year	Target	Atomic pairs
2000	Ni(65%) + Ti (35%)	1663 ± 321
2001	Ni(80%) + Ti (20%)	5611 ± 482
2002	Ni ($E_p = 20$ GeV)	2020 ± 272
All	Ni + Ti	9294 ± 640
2002	Ni ($E_p = 24$ GeV)	2750 ± 320
All 00-01-02	Ni + Ti ($E_p = 20, 24$ GeV)	12000 ± 710

being q_L, q_x, q_y the three components of the relative momentum, and σ_{q_L}, σ_{q_x}, σ_{q_y} the corresponding uncertainties.

The data analysis of 2002 has been mainly devoted to the accurate study of systematic uncertainties. The major sources of systematic errors have been identified in the correct evaluation of the background as well as in the multiple scattering suffered by the pions. Unfortunately, the data on multiple Coulomb scattering available in literature are not enough accurate to match the present statistical accuracy of the lifetime measurement. Therefore, next year, the collaboration has decided to measure directly the Coulomb multiple scattering on the materials present in the experimental setup. Furthermore, a pilot study has been started to directly evaluate the background contribution using a multi-layer target. Around 0.7×10^9 events have been collected in 2002 using two different nickel targets. Both have almost the same thickness ($98\mu m$), but the second is an array of 12 nickel foils 8 μm thick. During the data collection, the multi-layer target was alternated to the single-layer one to provide a check of the experimental method used to determine the number of atomic pairs. In fact, the break-up probability of the multi-layer target is roughly half of that of the single-layer one. This is because the atomic pairs coming out from one foil can decay in the gap between the next one (see fig 2). Therefore, combining in an appropriate way the two data sets, it is possible to eliminate the signal allowing a direct evaluation of the background. The measurement was successful, but statistically not yet sufficient.

During the summer, LNF-DIRAC group has also checked on a test beam a prototype of a small-size Aerogel Cherenkov counter. This detector was constructed with the idea of studying the possibility of measuring, in parasitic way, the lifetime of the $\pi^- K^+$ atomic system in order to evaluate πK scattering lengths. The test was successful, the detector provide a good capability of detecting kaons.

3 Planned activity in 2003

During 2003 DIRAC has 13 weeks of data taking. The data collection will be performed again alternating the two nickel targets in order to furtherly reduce the systematic error. At the same time, it will be also measured the multiple Coulomb scattering on the different materials present in the DIRAC setup with an accuracy better than 1%.

4 Talks by LNF authors

1. A. Lanaro, Highlight from DIRAC, CERN EP Seminar 17/12/01.

References

1. A. Gall, J. Gasser, V. Lyubovitskij, A. Rusetsky, Phys. Rev. D **64**, 016008 (2001).

FINUDA

L. Benussi(Ass. Ric.), S. Bianco, M. Bertani, M.A. Caponero (Ass.), F.L. Fabbri(Resp.),
P. Gianotti, M. Giardoni, V. Lucherini (Resp.), E. Pace, M. Pallotta,
L. Passamonti(Tecn.), D. Pierluigi(Tecn. Art.15), F. Pompili(Bors.),
A. Russo(Tecn. art.15), S. Tomassini(art.23)

1 Introduction

FINUDA (meaning FIsica NUcleare a DAΦNE) aims to study experimentally hypernuclei formation and decay within the same apparatus. Hypernuclei are nuclei in which a bound nucleon, baryon made of only u (up) and d (down) quarks, is replaced by a hyperon, baryon made also by s(strange) quarks. The added flavour enlarges the basic nucleon-nucleon interactions also to the strange sector: the so changed level scheme of the involved nucleus gives hence information on the modification of the properties of baryon-baryon interaction due to strangeness. High resolution hypernuclear spectroscopy can also, in principle, reveals in a more clearly way a partial deconfinement of quarks in nuclear matter. In case of FINUDA the involved hyperons will be the Λ.

The DAΦNE e^+/e^- collider is optimised in *Luminosity* at the *c.m.* energy corresponding to the $\phi(1020)$ meson. The huge number of ϕs, produced (almost) at rest, decay with a $B.R.$ of 0.49 into back-to-back pairs of slow (127 MeV/c)charged kaons. The K^-s, stopped by a thin target, can hence produce hypernuclei, through the two-body reaction (inside one of the target nuclei):

$$K^- + n \rightarrow \pi^- + \Lambda \tag{1}$$

The levels of the produced hypernucleus can be obtained through an accurate measurement of the momentum of the emitted (*prompt*) π^-. Since the kaons from DAΦNE have a very low and sharp momentum, they can be stopped in very thin targets, allowing high resolution (0.3%) to be reached in hypernuclear spectroscopy. Moreover, the subsequent decay of the hypernucleus, both *mesonic* (p+π^-) and $non-mesonic$ (np or nn) can be detected by FINUDA, allowing the simultaneous study of formation and decay of hypernuclei within the same apparatus, a feature never reached in previous experiments.

FINUDA is a large acceptance magnetic spectrometer based on a medium sized superconducting solenoid (2.7 m long and 2.4 m diameter), operating at a maximum field of 1.1 T. The inner of the solenoid is equipped with tracking detectors, time-of-flight scintillator barrels and vertex detectors, also embedding a system of multiple targets. The volumes between the tracking detectors are filled with He gas in order to reduce the deterioration of resolution due to multiple scattering effects. A special and complex system of thin windows bags (He bag) is used for this purpose. A sketch of FINUDA spectrometer is shown in fig.1), which also reports the name and type of the different detectors.

The FINUDA Collaboration is formed by almost 50 physicists from LNF, several INFN sections and Universities (Torino, Bari, Trieste, Pavia, Brescia) and with the participation of rearchers from TRIUMF Laboratory of Vancouver, Canada.

An extensive description of the FINUDA experiment can be found in [1], [2], and [3].

2 Activity up to December 2002

During the year 2002, the activity of FINUDA has again been devoted to installation, debugging and test of detectors and subsystems of the apparatus. These activities, requiring the presence

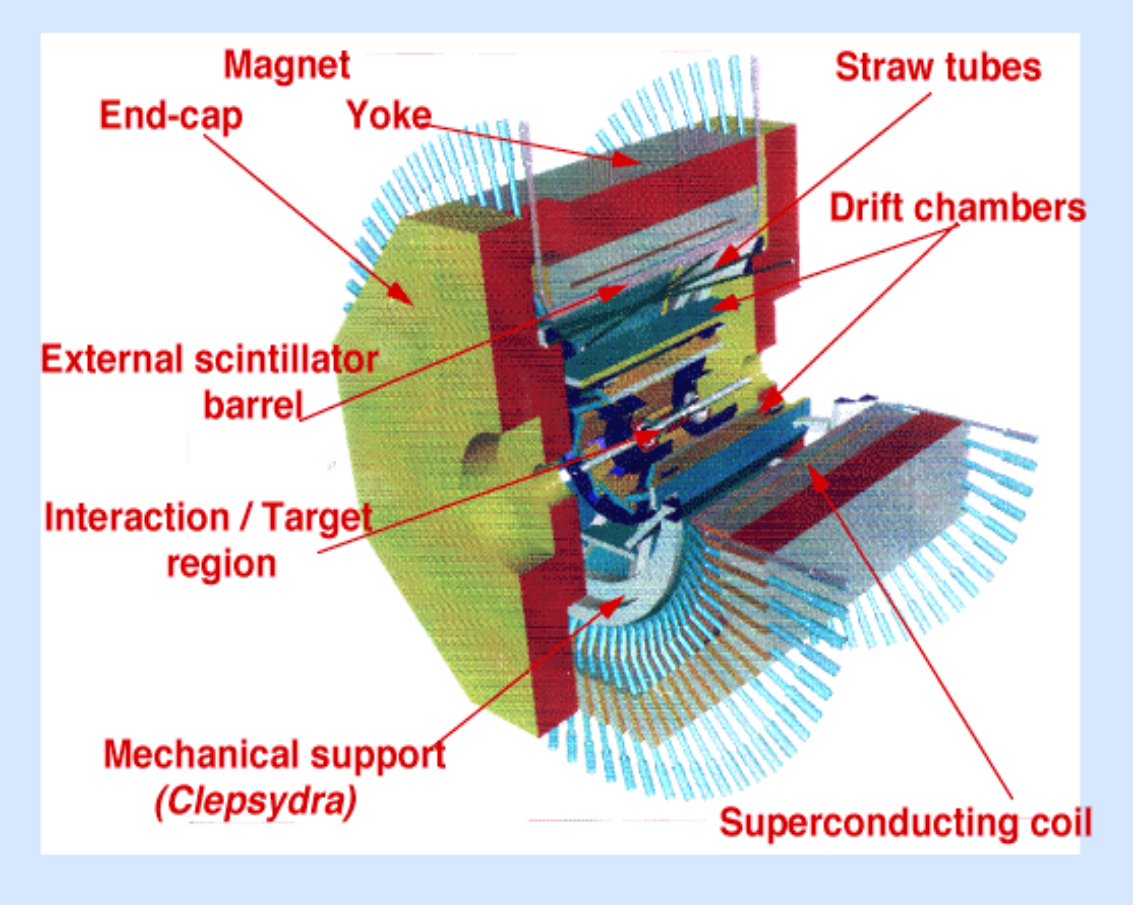

Figure 1: *Three dimensional layout of the FINUDA apparatus.*

inside the machine hall, had to be fitted in between the DAΦNE operation periods, that have been particularly long due to the intense data taking activity of both the experiments already mounted.

In the following we summarise the main tasks performed.

2.1 Activity from Juanuary 2002 up to February 2002

This period was used to:

a) cool the magnet and take it energetized at its nominal field for several days, in order to check for long periods the reliability of all the system, in particular the new software used for the controls;

b) Continue the debugging of mounted detectors and associated electronics.

2.2 Activity in May 2002

FINUDA detectors had never worked inside a megnetic field. It was therefore crucial an operative test in such conditions. This was true in particular for the drift chambers whose drift wire voltage dividers were previously displaced to take into account the effect of the Lorentz angle. This problem was addressed in May 2002, when FINUDA was energetised and data daking of all mounted detectors was performed using cosmic rays. In spite of the short period allocated (for fear to perturb with stray fields machine operation during data taking of mounted experiments), it resulted that all detectors performed smootly and the modification on the drift chambers was correct.

2.3 Activity during August 2002

This period was devoted to debug the straw tube Patch Panels that were previously non accessible since the magnet end caps were left open to provide the access to the inner detectors and subsystems.

2.4 Other activities during 2002

During the second half of 2002 it was also removed the tofino detector (inner scintilator barrel), that was mounted in the vertex region in order to perform the global test with field on. The reason was that it resulted necessary to change all HPDs due to aging problems. In any case the removal of such detector was foreseen in order to prepare the Clepsydra for the insertion of the beam pipe. Also one Drift Chamber resulting not properly working during data taking was removed and changed.

While during the time of machine shut down the FINUDA Collaboration activity was mainly devoted to operations in the pit, only in those periods accessible, during all other periods of the year other activities proceeded. One was a continuous refining of the software tools for both the on-line and off-line, and the final installation of the slow controls of all detectors. Moreover, in ASTRA laboratory, the removed tofino detector was equipped with the new HPD and througoughly tested (fig.2).

3 Conclusions

At the end of 2002, FINUDA was ready for the shut down period starting at begginning of Juanuary 2003, devoted to the final operations in view of the roll-in of the experiment.

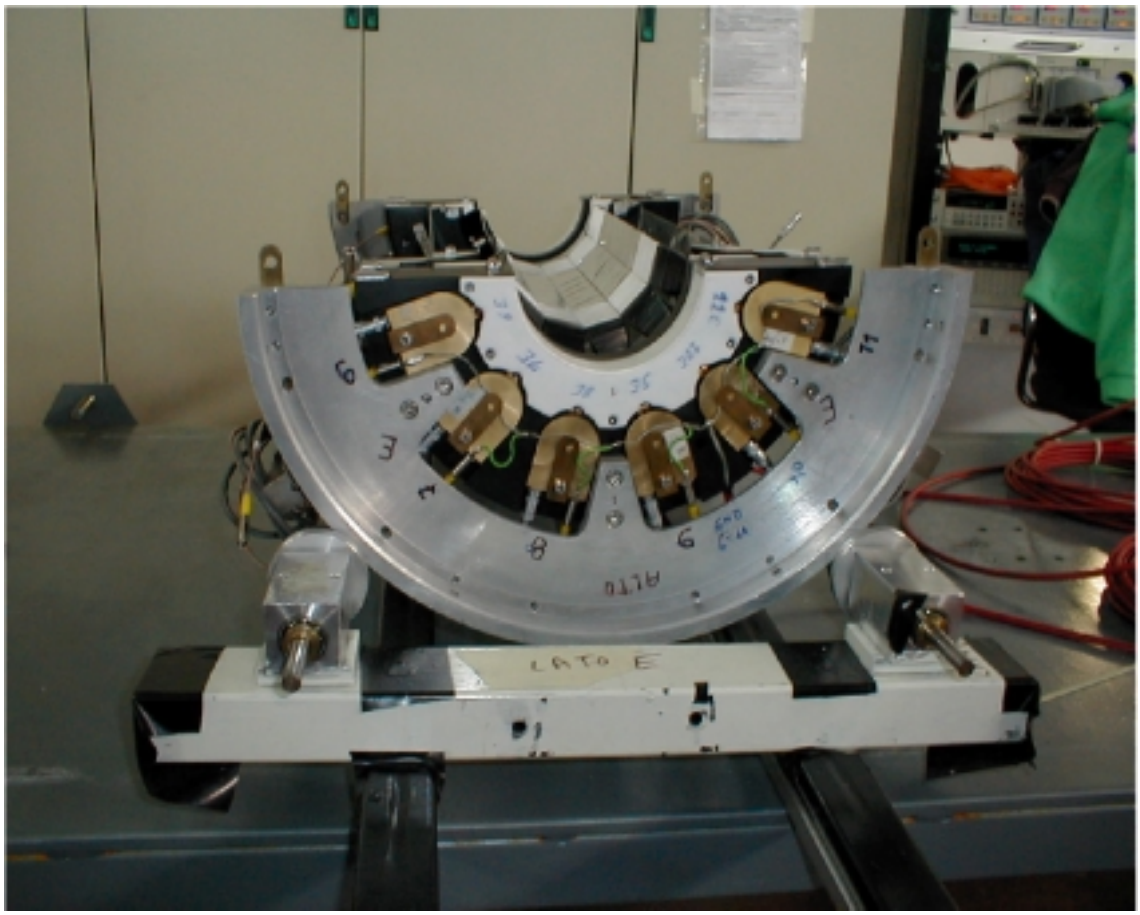

Figure 2: *The tofino detector: equipping with the new HPDs.*

References

1. P. Gianotti *et al*, The FINUDA experiment at DAΦNE, in: Proc. HYP2000 VII International Conference on Hypernuclear and Strange Particle Physics (Torino, October 23-27, 2000).

2. A.Zia *et al*, Nucl. Instr. and Meth. **A461**, 60 (2001).

3. L.Benussi *et al*, Nucl. Instr. and Meth. **A461**, 98 (2001).

GRAAL

O. Bartalini (Dott.) P. Levi Sandri (Resp.)

1 Introduction

The Graal experiment aims at a more detailed knowledge of the baryon spectrum via the precise measurement of polarisation observables in photo induced reaction on the nucleon.

The use of the electromagnetic probe and of it's polarisation, coupled to large acceptance detectors with cylindrical symmetry and high efficiency in the detection of all final state particles, is the technique chosen in many laboratories to perform the ambitious program of a full determination of the scattering amplitude of a given photonuclear reaction. Such determination requires the measurement of the cross section, of the three single polarisation observables and of four appropriately chosen double polarisation observables.

The Graal esperiment is performed in collaboration between 6 INFN Sections (Roma2, LNF, Catania-LNS, Roma1, Genova and Torino), IPN-Orsay, ISN-Grenogle and INR-Moscow) The Frascati group is responsible of running and maintaining the $\Delta E/\Delta x$ scintillator barrel detector, the Montecarlo simulation program LAGGEN, the off-line reconstruction of events in the BGO calorimeter and the data analysis for coherent η photoproduction off the deuteron.

2 The Graal Beam and the Lagrange apparatus

The Graal facility provides a polarised and tagged photon beam by the backward Compton scattering of laser light on the high energy electrons circulating in the ESRF storage ring [1]. Using the UV line (350 nm) of an Ar-Ion laser we have produced a gamma-ray beam with an energy from 550 to 1470 MeV. Its polarisation is 0.98 at the maximum photon energy and the energy resolution has been measured to be 16 MeV (FWHM).

The Lagrange detector is formed by a central part surrounding the target and a forward part. Particles leaving the target at angles from 25^o to 155^o are detected by two cylindrical wire chambers with cathode readout, a barrel made of 32 strips of plastic scintillator parallel to the beam axis, used to determine the $\Delta E/\Delta x$ of charged particles, and the BGO rugby-ball made of 480 crystals of BGO scintillator.

The BGO ball is made of crystals of pyramidal shape with trapezoidal basis which are 21 radiation lengths long (24 cm). This calorimeter has an excellent energy resolution for photons [2], a good response to protons [3] and is very stable in time due to a continuous monitoring and calibration slow control system [4].

Particles moving at angles smaller than 25^o encounter two plane wire chambers, (xy and uv) two walls of plastic scintillator bars 3 cm thin located at 3 m from the target point, that provide a measurement of the time-of-flight for charged particles (700 ps FWHM resolution) followed by a shower wall made by a sandwich of four layers of Lead and plastic scintillators 4 cm thick that provides a full coverage of the solid angle for photon detection (with 95 percent efficiency) and a 20 percent efficiency for neutron detection.

Finally, two disks of plastic scintillator separated by a disk of Lead complete the solid angle coverage in the backward direction.

The beam intensity is continuously monitored by a flux monitor, composed by three thin plastic scintillators and by a lead/scintillating fibre detector that measures energy and flux [5].

3 2002 activity

During the year 2002 the Graal experiment has almost completed the data acquisition for a proton target and 60 percent of the necessary deuteron statistics was collected. Data analysis for high energy η and π^0 photoproduction is being performed while for the reaction with π^+ photoproduction the final data were produced. Also the cross section and beam asymmetry data for the photoproduction of two π^0 and ω were obtained and the corresponding paper are being submitted.

4 Activity in 2003 and conclusions

The Graal experiment started data taking in 1997. It was run both with the green laser line giving rise to a photon beam of maximum energy of 1100 MeV and with UV multi-line with the corresponding gamma-ray beam of 1470 Mev maximum energy. The typical intensity was $2 \cdot 10^6 s^{-1}$ in both cases, very close to the design intensity. The detector was found very stable during the six years of operation, with only minor maintenance problems.

Proton and deuteron targets of different lenghts were used and asymmetry data and cross sections have been produced for η, π^0, π^+, $2\pi^0$ and and ω photoproduction channels providing, for these reactions, the most extended and coherent data base available until now. The analysis of the Compton process on the proton, and of all the mentioned photoreactions on the quasi-free neutron of the deuteron target are underway.

During the year 2003 a new polarised target, made of HD molecules in frozen state will be installed replacing the present cryogenic target. Data taking will restart soon after the installation with the aim of measuring for the first time double polarisation observables in π^0 an η photoproduction, and the contribution from 500 to 1500 Mev to the GDH integral for both protons and neutrons.

5 Main publications in 2002

Phys. Lett. B 544 (2002) 113
Nucl. Phys. A 699 (2002) 218c
Phys. Lett. B 528 (2002) 215

References

1. Graal Collaboration, Nucl. Phys. A622, (1997) 110c.
2. P. Levi Sandri *et al.* Nucl. Inst. and Meth. in Phys. Research A370, (1996), 396.
3. A. Zucchiatti *et al.*, Nucl. Inst. and Meth. in Phys. Research A321, (1992), 219.
4. F. Ghio *et al.*, Nucl. Inst. and Meth. in Phys. Research A404, (1998), 71.
5. V. Bellini *et al.*, Nucl. Inst. and Meth. in Phys. Research A386, (1997), 254.

HERMES

M. Albicocco, E. Avetisyan (Ass.), N. Bianchi (Resp. Naz.),
A. Borysenko (Ass.), G.P. Capitani (Resp. Loc.), E. De Sanctis, P. Di Nezza (Ass.),
A. Fantoni, D. Hasch (Ass.), V. Muccifora, K.A. Oganessyan (Ass.),
A. Orlandi (Tecn.), W. Pesci (Tecn.), E. Polli, A.R. Reolon, C. Schill (Ass.), A. Viticchié (Tecn.).

1 Introduction

HERMES (HERa MEasurement of Spin) is an experiment at DESY mainly dedicated to study the spin structure of the nucleon. Nucleons (protons and neutrons) are the basic ingredients of the matter of the known universe and their most important quantum number is the spin 1/2. The nucleon is a composite object which can be described in terms of moving quarks of different flavors (up, down and strange) in different configurations (valence and sea) and gluons. Up to year 2000, HERMES collected data with a longitudinally polarized electron/positron beam of 27.5 GeV on longitudinally polarized H, D and ^{3}He internal gas targets. From these runs HERMES provided the most accurate and complete data set for the polarized struture function g_1 and allowed a direct flavor decomposition of the nucleon spin [1)]. Runs on several unpolarized nuclear gas targets have been also collected while from year 2000 a transversely polarized H target is fully operational on HERA ring.
HERMES is an International Collaboration of about 180 physicists from 33 Institutions from 12 Countries. Italy participates with 4 groups and more than 30 physicists from Bari, Ferrara, Frascati and Rome. The Frascati group is responsible for the electromagnetic calorimeter and have participated in the project and in the construction of two RICH detectors (Pub 9). It is currently involved in the project of a new recoil detector to be installed in 2004. The Frascati group has the responsibility of the analysis working groups of single spin azimuthal asymmetries in semi-inclusive processes and of the pseusoscalar meson exclusive production. LNF members are leading in the analysis of many physics processes and are playing a major role in in the physics paper draftings and in the editorial process.

2 Experimental activity of the LNF group in 2002

2.1 Calorimeter

The HERMES calorimeter consists in a wall of 840 Lead-Glass blocks [2)]. The calorimeter is the basic detector for the main trigger and for the electron-hadron separation. It is used to reconstruct energy and angle of photons, π^0 and η. The responsibility of the calorimeter required the online monitoring and check of the status of detector for the whole period of data taking. During 2002 there were in total 5 reproductions of existing data with the re-calibration of all detectors, including the calorimeter. All the calibration and monitoring software was ported from the HERMES SGI/IRIX platform to a PCfarm with Linux. In addition, new codes for a more precise position reconstruction of the shower, for a better comparison of the energy reconstruction with the momentum and for accounting for the photon showering in the preshower detector were implemented into the production program. During data taking there were some cases of calorimeter malfunction, mostly due to cabling and to shortcuts in the photomultiplier voltage divider which were recovered with the deposition of an insulator film on the socket.

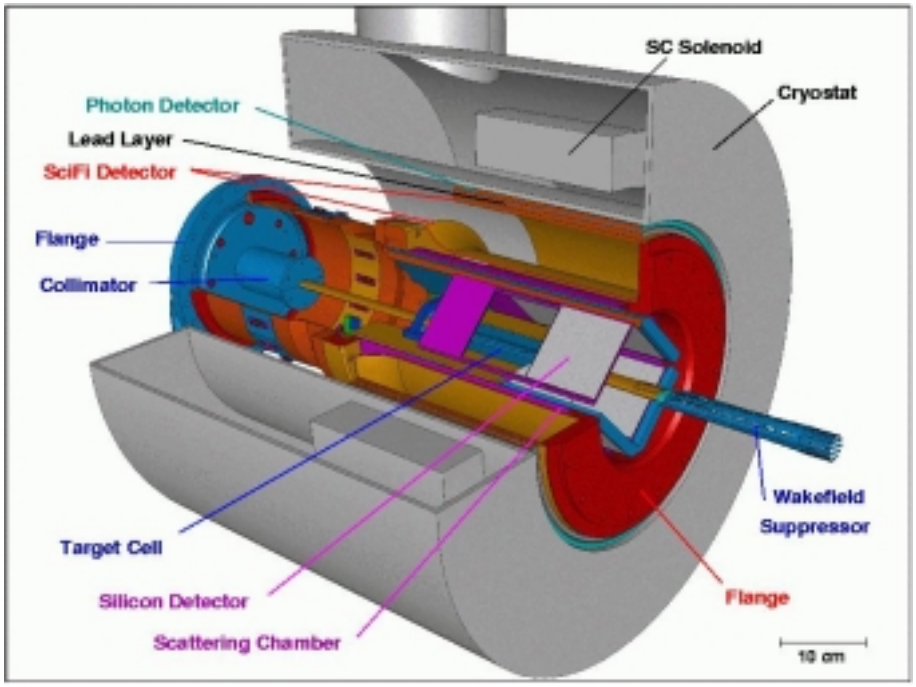

Figure 1: 3-D view of the Recoil Detector project.

2.2 Recoil detector

The recent proof of factorization for exclusive processes and their interpretation in terms of Generalized Parton Distributions to describe the nucleon structure, suggested the detailed investigation of these processes in which a fast meson or a photon is emitted in the forward direction while the slow nucleon is recoiling intact at large angle. Several exclusive processes have been already investigated by HERMES with the missing mass technique [3]. To better identify these processes, a compact Recoil Detector is under construction to be installed around the target. Basically, it will consist of silicon detectors located under vacuum inside the beam pipe, a SciFi tracking system and a Lead-Scintillator barrel. The Frascati group is involved in the latter detector which will be used to detect photons from the π^0 decay. It will also provide an energy loss measurement to separate p and π^+. Simulations and cosmic ray and radiactive source tests have been performed to optimize the efficiency for the photon detector and for the π^0 reconstruction and to define the final design of the barrel. It will consist of three layers of scintillating strips with a WLS fiber system readout. Multi-anode photomultipliers will be used with specially designed fan-in/preamplifiers to ensure capable transmittance of the signal.

2.3 Technical software

The Particle Identification (PID) is crucial for any analysis of HERMES data. To separate hadrons and leptons a Bayesian algorithm has been applied. The necessary probability distributions are extracted from the responses of four particle identification detectors: the lead glass calorimeter, a preshower detector, a transistion radiation detector and a threshold Cerenkov detector. The latter was replaced by a ring imaging Cerenkov detector (RICH) in 1998. Studies where performed and

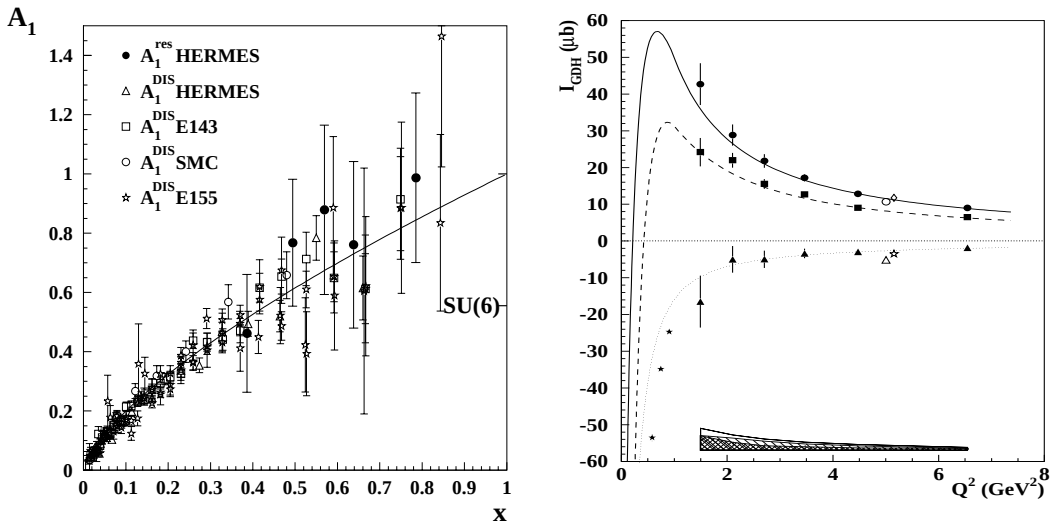

Figure 2: Left : Spin asymmetry A_1 measured in the nucleon resonance region compared with A_1 measured in the Deep-Inelastic region. Right : Generalized GDH integral for proton (upper), deuteron (middle) and neutron (lower) as a function of Q^2. HERMES data are the filled circles, squares and triangles.

a software code structure proposed to include the new RICH detector in standard PID libraries. LNF member were main responsible for the maintenance and code development of the PID library function and for the PID calibration. At low momenta, the PID was obtained with the Time of Fligth technique (Pub 8).
During 2002 the LNF group acted also as HERMES Linux administrator and represented HERMES on DESY Linux user meeting, where user requirements and future strategy for Linux support were discussed. There were 31 desktops installed with DESY Linux (AFS) versions 3 and 4, 12 upgraded from version 3 to 4 and 14 notebooks have been installed with SuSE Linux versions 7.3-8.1.

3 Data analysis and physics results of the LNF group in 2002

3.1 Quark-hadron duality in spin structure function

The quark-hadron duality concept was introduced by Bloom and Gilman to describe the relationship between phenomena in the nucleon resonance region and the deep-inelastic region. The duality was observed from long time in the case of unpolarized structure functions [4]. In HERMES the validity of duality, i.e. the successful description of the nucleon resonance region in terms of the partonic variable x and of quark degrees of freedom instead of the usual nucleonic excitation variable W, has been shown for the first time in the case of spin structure functions. The study of the integral of the spin dependent photon-nucleon cross section, that enters in the generalized Gerasimov-Drell-Hearn sum rule, has been extended to the polarized deuteron target in addition to the already published ones on the Helium-3 and hydrogen targets [5]. Two papers on duality and GDH have been written and are currently in print (Pubs 3 and 4).

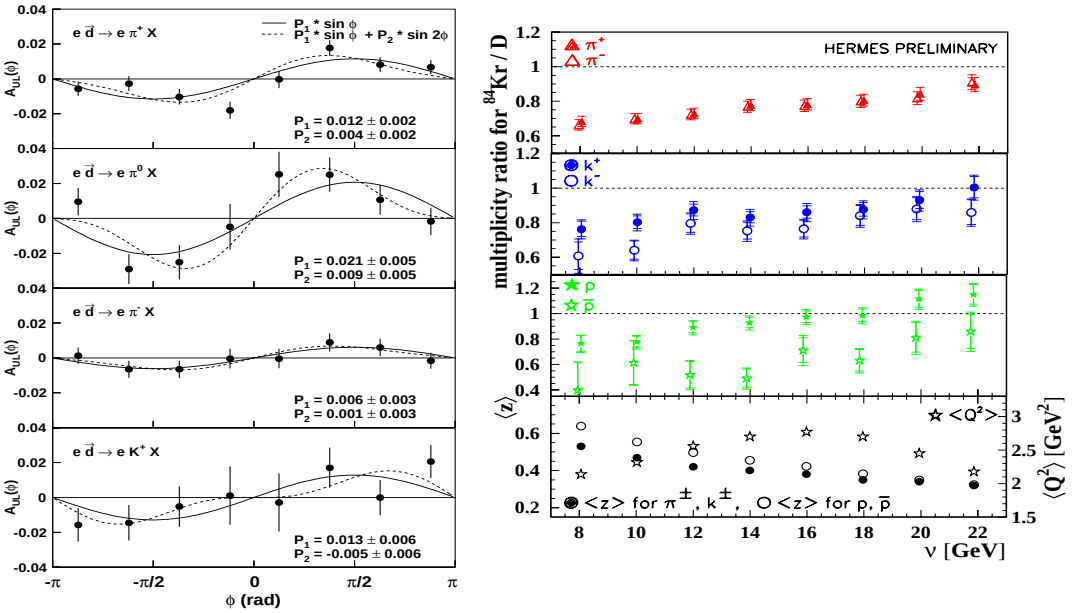

Figure 3: Left : azimuthal distribution (around the leptonic scattering plane) of semi-inclusive production of mesons on a longitudinally polarized deuteron target. Right : preliminary multiplicity ratio of different hadrons in krypton with respect to deuteron as a function of the virtual photon energy ν.

3.2 Single-spin azimuthal asymmetries on the Deuteron

Single-spin azimuthal asymmetries have been recently recognized as a powerful source of information on the structure of the nucleon complementary to the inclusive deep-inelastic scattering. In particular, it has been suggested that target spin asymmetries may provide information on the still unmeasured transversity distribution, which describes the probability to find a quark with its spin parallel or antiparallel to the spin of the nucleon. The transversity function $h_1(x)$ enters at the same leading order level of the well known $f_1(x)$ and $g_1(x)$ functions in the description of the nucleon structure, but its chiral-odd nature does not allow to be measured in inclusive DIS [6]. First measurements on a longitudinally polarized hydrogen target have been proposed, analyzed and published in the recent years by the LNF group [7]. In 2002 a similar analysis has been completed on a longitudinally polarized deuterium target. The results for the $sin\phi$ azimuthal distribution of charged and neutral pions have been found consistent with the ones on the hydrogen target and have been submitted for publication (Pub 7) together with the new asymmetries in the distribution of kaons. A new analysis has been started by investigating beam spin asymmetries, i.e with polarized beam and unpolarized target, as a possible tool to investigate the twist-3 unpolarized distribution $e(x)$ [8].

3.3 Unpolarized and double-polarized azimuthal asymmetries

Inclusive unpolarized and double-polarized scatterings provide measurements of structure functions f_1 and g_1, respectively. The analysis of these data when considering the azimuthal distribution of pions in addition to the scattered lepton, revealed small but not negligible asymmetries. In

the unpolarized case, a $cos\phi$ and a $cos2\phi$ distribution was measured. In this case, a precise determination of the false asymmetries induced by the detector acceptance has been performed. In the double-polarized case, an unexpected asymmetry has been found at large-x and it is still under investigation. Both these asymmetries may result from a combination of transversity related effects and QCD effects.

3.4 Exclusive production of neutral and charged pions

The exclusive production of mesons and photons (DVCS) on the nucleon gives access the new Generalised Parton Distribution (GPD). GPDs are able to provide a 3-D view of the nucleon with the determination of the full correlation of the partonic variables (position and momentum) and to investigate the orbital motion of partons [9]. In the case of exclusive pseudoscalar meson production, a measurement of an azimuthal asymmetry has been published in 2002 (Pub 2) and the subsequent analysis has been addressed to the determination of the cross sections and of the relative production yields for different mesons and targets. In particular, the measurement of exclusive π^+ cross section is related to the largely unknown space-like pion form factor, while exclusive production of π^0 and η on the neutron is expected to be largely suppressed with respect to the proton case in relation with the QCD axial anomaly [10]. The intriguing aspect of these studies relies in the fact that the exclusive *unpolarized* production of pseudoscalar mesons can be described by the *polarized* GPDs which in the forward limit coincide with the ordinary polarized parton distribution.

3.5 Interference effects in the scalar-vector-tensor meson production

The study of the angular distribution of $\pi^+\pi^-$ pairs has been proposed to study the interference in the exclusive production of the dominant p-wave channel (ρ meson) with the much weaker s- and d-wave channels (f_0 and f_2 mesons) [11]. At large-x, the quark-exchange production mechanism is expected to dominate, while at low-x the gluon exchange it is important. In particular at low-x the interference between 2-gluon and 3-gluon exchanges may reveal the effect of the still elusive Odderon (the C=-1 partner of the Pomeron) [12]. The analysis performed so far at large-x has shown a possible signature of the ρ^0 - $\pi\pi_{s-wave}$ and ρ^0 - f_2 interferences. The analysis at low-x is still ongoing. Monte Carlo codes to generate exclusive single pion and double pion events were developed and implemented into the general HERMES MC for data production.

3.6 Medium modification of parton fragmentation function

It is well known that the parton *distribution* functions are modified by the nuclear medium. HERMES has measured the medium modification of the parton *fragmentation* function on a ^{14}N target [13]. In 2002, the analysis of new data taken on a Krypton target have revealed for the first time, different effects for parton fragmentation into different hadrons. In contrast to the similarity between π^+, π^- and π^0, a significant difference was found between K^+ and K^- and between p and $\overline{p}$. In addition, the so called Cronin effect has been observed in the p_T-broadening of the hadron distribution in nuclei. These results provide information on the partonic energy loss and scattering probability and on the hadron formation time, which are necessary ingredients to understand the heavy-ion interactions at high energy which are performed to study the Quark Gluon Plasma [14]. Hadron multiplicites on a proton target were also studied and compared with the fragmentation functions derived from e^+e^- data [15].

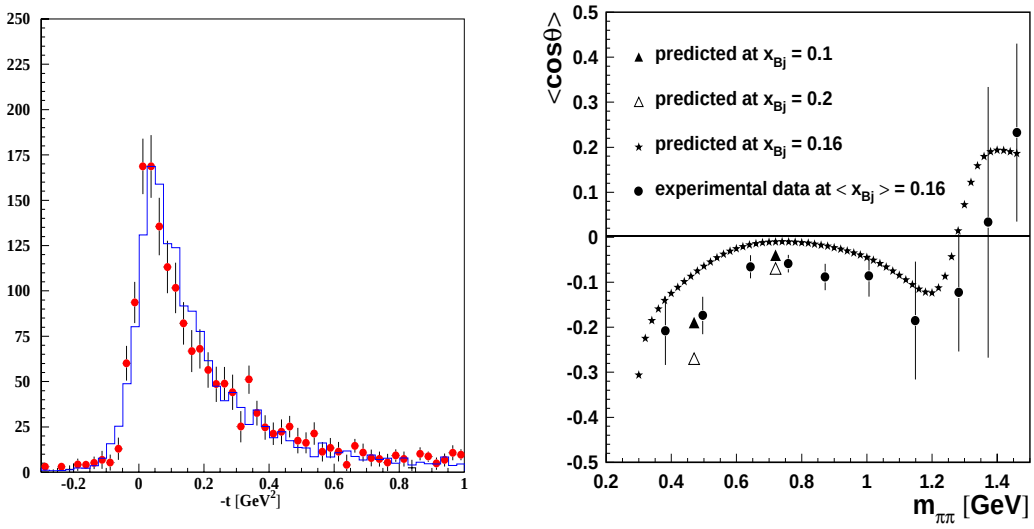

Figure 4: Left : Preliminary t-distribution of exclusive π^+ production compared with a Monte-Carlo distribution based on a GPD event generator which includes the pion-pole term. Right : Preliminary distribution for the exclusive $\pi\pi$ intensity density as a function of the $\pi^+\pi^-$ invariant mass and compared with theoretical prediction which includes the interference between the ρ^0 - $\pi\pi_{s-wave}$ and ρ^0 - $f_2(1270)$.

4 Phenomenology on HERMES physics of the LNF group in 2002

4.1 Spin dependent cross section and GDH sum rule

The long-standing crisis of the fundamental GDH integral was suggested to be solved by considering the spin-dependent cross section for real photon at high energy [16]. A multiple Regge approach was used to connect the electroproduction region, where plenty of data exist, with the unmeasured photoproduction region. In 2002, this phenomenological framework was started to be implemented by considering the most recent and precise data from HERMES and from SLAC-E155 experiments.

4.2 Quark-hadron duality

The quark-hadron duality has been investigated by comparing resonance region data for both unpolarized structure function (from JLab) and polarized structure function (from HERMES) with different parameterizations of world data in the DIS region. It appeared that LO and NLO QCD fits to DIS data are unable to describe the resonance data at large Q^2. On the contrary, phenomenological parameterizations, like NMC, ALLM or GRVmod which implicitly include higher order and high twist partonic effects, can be used to reproduce the hadronic resonance excitation.

4.3 New distribution functions

Different leading and sub-leading distribution functions are accessible by measuring unpolarized, single-polarized and double-polarized azimuthal distribution of hadrons in semi-inclusive DIS [17]. In this context, the role of the intrinsic transverse momentum of partons in the nucleon has been

studied and new distribution functions appear to be dependent on this fundamental quantity. The observation of these new distribution functions often requires the existence of new time-odd fragmentation functions.

4.4 Nuclear medium effects in fragmentation

Predictions for semi-inclusive deep inelastic lepton-nucleus scattering have been calculated by taking into account the rescaling of fragmentation functions in the nuclear medium (Pub 1), in analogy of what introduced for nuclear structure functions [18] . Both the effects of gluon radiation by the struck quark and the absorption of the produced hadron were considered. In this framework, the gluon radiation covers a larger window in virtuality Q^2 because of the increased deconfinement of quarks inside nuclei.

5 Outlook

In 2003, the data taking with a transversely polarized hydrogen target, which started in 2002 will continue. The photon detector of the Recoil Detector will be constructed. The ongoing physics analysis (see 3.2, 3.3, 3.4, 3.5 and 3.6) and phenomenological investigation (see 4.1, 4.2 and 4.3) will be completed. New analysis will be performed on data with the polarized transverse target where a large azimuthal asymmetries for the exclusive pion production is expected to arise from the interference of pseudoscalar and pseudovector amplitudes of GDPs

6 Conferences by LNF Authors in Year 2002

6.1 Conference Talks

1. N. Bianchi, Spin structure of the nucleons from HERMES, MESON 2002. Krakow, Poland.
2. N. Bianchi, Nuclear attenuation in SIDIS, High-Energy Spin Physics, Nor Amberd, Armenia.
3. N. Bianchi, Nuclear medium effect in hadron leptoproduction, Nuclear Dynamics: from quark to nuclei. Lisbon, Portugal.
4. A. Borysenko, The HERMES recoil detector, Innovative Particle and Radiation Detectors, Siena, Italy.
5. P. Di Nezza, Hadron Formation in DIS in a Nuclear Environment, Winter Meeting on Nuclear Physics, Bormio, Italy.
6. P. Di Nezza, Structure of Hadrons and Nuclei on the Light Cone, Los Alamos, USA
7. P. Di Nezza, The Spin of the Nucleon at HERMES, Frontier Science, Frascati, Italy.
8. A. Fantoni, Experimental Evidence for Quark-Hadron Duality in Spin Structure Function, Winter Meeting on Nuclear Physics, Bormio, Italy.
9. A. Fantoni, Quark-Hadron Duality in Spin Structure, DIS 2002, Kracow, Poland.
10. A. Fantoni, Quark-Hadron Duality and Q2-evolution of the GDH Integral in the HERMES Experiment, Electron-Nucleus Scattering, Marciana Marina, Italy.
11. A. Fantoni, Spin Physics at HERMES, GDH2002, Genova, Italy.
12. D. Hasch, Azimuthal asymmetries in pion electroproduction, Winter Meeting on Nuclear Physics, Bormio, Italy.
13. D. Hasch, Hermes results ad future on DVCS and DVES, QCD Structure of the Nucleon, Ferrara, Italy.
14. D. Hasch, Azimuthal asymmetries in meson electroproduction at HERMES; and The physics programme of HERMES Run II, Spin 2002, BNL, USA.

15. V. Muccifora, Hadron Formation in DIS from Nuclear Target and Nuclear Transparency, QCD Structure of the Nucleon, Ferrara, Italy.
16. V. Muccifora, Transversity at HERMES, GDH2002, Genova, Italy.
17. V. Muccifora, Hadron Formation in nuclei at HERMES, Quark Matter 2002, Nantes, France.
18. V. Muccifora, Hadronization Process in DIS on nuclei, Coherent effects at RHIC and LHC: initial conditions and hard probes, Trento, Italy.
19. K.A. Oganessyan, Perturbative and nonperturbative aspects of azimuthal asymmetries in polarized ep, Summer program: Current and future directions at RHIC, BNL, USA.
20. K.A. Oganessyan, Access to Novel Structure Functions and Perturbative; and Nonperturbative aspects of azimuthal asymmetries in polarized ep, Spin 2002, BNL.
21. K.A. Oganessyan, Azimuthal asymmetries in SIDIS: are they interrelated, Testing QCD through Spin Observables, University of Virginia, USA.
22. K.A. Oganessyan, Azimuthal asymmetries in SIDIS, QCD'02, Montpellier, France.
23. K.A. Oganessyan, Kinematical contributions to the transverse asymmetry in semi-inclusive DIS, QCD Structure of the Nucleon, Ferrara, Italy.
24. C. Schill, Exclusive electroproduction of Vector and Pseudoscalar mesons at HERMES, SPIN2002, BNL, USA.

6.2 Conference organization and advisoring

1. N. Bianchi, (Convener) BARYONS 2002, Newport News, USA.
2. N. Bianchi, (International Organizer) QCD Structure of the Nucleon, Ferrara, Italy.
3. N. Bianchi, (International Advisor) Testing QCD through Spin Obs., Charlottesville, USA.
4. N. Bianchi, (International Advisor) GDH 2002, Genova, Italy.
5. E. De Sanctis, (Co-Chair and Proc. Ed.) QCD Structure of the Nucleon, Ferrara, Italy.
6. E. De Sanctis, (International Advisor) BARYONS 2002, Newport News, USA.
7. E. De Sanctis, (Organizer) LNF Spring School, Frascati, Italy.
8. V. Muccifora, (Proc. Ed.) QCD Structure of the Nucleon, Ferrara, Italy.

6.3 Lectures and seminars

1. N. Bianchi (Lectures), Lecture week on Complex systems, Rauisch. Castle, Germany.
2. N. Bianchi (Lectures), International School of Physics, Varenna, Italy.
3. P. Di Nezza (Seminar), Berkeley, USA.
4. P. Di Nezza (Seminar), Brookhaven National Laboratory, USA.
5. P. Di Nezza (Seminar), Bari, Italy.
6. D. Hasch (Seminar), Frascati, Italy.
7. K.A. Oganessyan (Seminar), University of Rochester, USA.
8. K.A. Oganessyan (Seminar), University of Wuppertal, Germany.
9. K.A. Oganessyan (Seminar), Brookhaven National Laboratory, USA.
10. K.A. Oganessyan (Seminar), University of Maryland, USA.

6.4 Presentations at HERMES Collaboration Meetings (CM) and Analysis Weeks (AW)

1. E. Avetisyan, Status of beam-SSA from proton data, AW February.
2. E. Avetisyan, A_{LU} from proton data, CM April.
3. E. Avetisyan, Status of new calorimeter calibration, AW May.
4. N. Bianchi, Exclusive π^+, CM April.
5. N. Bianchi, Report from the editorial board, CM July.
6. N. Bianchi, Overview of hadron attenuation, CM July.
7. G.P. Capitani, Photon Detector Status, CM November.
8. P. Di Nezza, Hadron attenuation on Krypton, AW February.
9. P. Di Nezza, Status of the photon energy reconstruction studies, AW May.
10. P. Di Nezza, Update of pseudoscalar production from semi-inclusive to exclusive, AW May.
11. P. Di Nezza, SIDIS gamma-effect, CM July.
12. A. Fantoni, Duality in the spin sector, AW February.
13. A. Fantoni, Update on duality, CM April.
14. D. Hasch, Exclusive π^+ cross section, AW February.
15. D. Hasch, Summary of exclusive/SSA Working Group, AW February.
16. D. Hasch, Summary of exclusive/SSA Working Group, AW May.
17. D. Hasch, π^+ cross section, CM July.
18. D. Hasch, Overview of ongoing analysis, CM November.
19. V. Muccifora, Hadron Formation in DIS from Heavy Nuclei, CM April.
20. V. Muccifora, Status of attenuation ratios at 27 GeV, AW September.
21. V. Muccifora, Status of the analysis for Kr and extension for N at lower x, CM November
22. C. Schill, Measurement of SSA on Deuteron, AW February.
23. C. Schill, Deuteron SSA, CM July.
24. C. Schill, A_{UL}: 00b1/ 00c1 comparison and sys. error from RICH, CM November.

7 Publications of LNF Authors in Year 2002

1. A. Accardi, V. Muccifora, H.J. Pirner, Hadron production in deep inelastic lepton-nucleus scattering, Nucl. Phys. A in print (nucl-th/0211011)
2. A. Airapetian et al., Single-spin azimuthal asymmetry in exclusive electroproduction of π^+ mesons, Phys. Lett. B 535 (2002), 85
3. A. Airapetian et al., The Q^2 Dependence of the Generalized Gerasimov-Drell-Hearn Sum Rule for the Deuteron, Proton and Neutron, Eur. Phys. Jour. C in print (hep-ex/0210047)
4. A. Airapetian et al., Evidence for Quark-Hadron Duality in the Proton Spin Asymmetry A_1, Phys. Rev. Lett. in print (hep-ex/0209018)
5. A. Airapetian et al., Q^2 Dependence of Nuclear Transparency for (In)coherent ρ^0 production, Phys. Rev. Lett. in print (hep-ex/0209072)
6. A. Airapetian et al., Deep-inelastic Scattering on Nuclei, submitted to Phys. Lett. B (hep-ex/0210068)
7. A. Airapetian et al., Measurement of single-spin azimuthal asymmetries in semi-inclusive electroproduction of pions and kaons on a longitudinally polarized deuterium target, submitted to Phys. Lett. B (hep-ex/0212039)

8. A. Airapetian et al., The time-of-flight technique for the HERMES experiment, submitted to Nucl. Instr. and Meth.
9. N. Akopov et al., The HERMES dual-radiator Ring Imaging Cherenkov detector, Nucl. Instr. and Meth. A 479 (2002), 511
10. N. Bianchi and R. Jakob, Nucleon insight: Echoes from QCD-N '02, CERN Courier 42 (2002) 17
11. N. Bianchi, Single-spin azimuthal asymmetries at HERMES, J. Phys. G 28 (2002), 791
12. E. De Sanctis and W.D. Nowak, Preface to QCD-N '02, Nucl. Phys. A 711 (2002), xi
13. A. Fantoni, Results from the HERMES experiment, Nucl. Phys. B 105 (2002), 28
14. D. Hasch, HERMES results and future on DVCS and DVES, Nucl. Phys. A 711 (2002), 148
15. V. Muccifora, Hadron formation in DIS from nuclear target and nuclear transparency, Nucl. Phys. A 711 (2002), 254
16. V. Muccifora, Hadron formation in a nuclear environment at HERMES, Nucl. Phys. B 105 (2002), 66
17. V. Muccifora, Physics at HERMES, Nucl. Phys. A 699 (2002), 286
18. K.A. Oganessyan, P.J. Mulders and E. De Sanctis, Double-spin $\cos\phi$ Asymmetry in semi-inclusive electroproduction, Phys. Lett. B 532 (2002) 87
19. K.A. Oganessyan, P.J. Mulders, E. De Sanctis and L.S. Asilyan, Kinematical contributions to the transverse asymmetry in semi-inclusive DIS, Nucl. Phys. A 711 (2002), 89
20. K.A. Oganessyan, L.S. Asilyan, M. Anselmino and E. De Sanctis, Spin-independent and double-spin cos(phi) asymmetries in semi-inclusive pion electroproduction, submitted to Phys. Lett. B. (hep-ph/0208208).

References

1. HERMES Coll.: Phys. Lett. **B 404**, 383 (1997); Phys. Lett. **B 442**, 484 (1998); Phys. Rev. Lett. **81**, 5519 (1998); Phys. Lett. **B 464**, 123 (1999); Phys. Rev. Lett. **84**, 2584 (2000) and hep-ex/0210049.
2. H. Avakian et el., Nucl. Instrum. Meth. **A 417**, 69 (1998).
3. HERMES Coll.: Phys. Rev. Lett. **87**, 182001 (2001) and Eur. Phys. J. **C 17**, 389 (2000).
4. F.E. Close and N. Isgur, Phys. Lett. **B 509**, 81 (2001) and refs therein.
5. HERMES Coll.: Phys. Rev. Lett. **82**, 3025 (1999) and Phys. Lett. **B 494**, 1 (2000).
6. V. Barone, A. Drago and P.G. Ratcliffe, Phys. Rept. **359**, 1 (2002) and refs therein.
7. HERMES Coll.: Phys. Rev. Lett. **84**, 4047 (2000) and Phys. Rev. **D64** 097101 (2001).
8. R.L.Jaffe and X. Ji, Nucl. Phys. **B 375**, 527 (1992).
9. X. Ji, Phys. Rev. **D 62**, 7114 (1997) and M. Burkardt, Phys. Rev. **D 62**, 071503 (2000).
10. M.I. Eides, L.L. Frankfurt and M.I. Strikman, Phys. Rev. **D 59**, 114025 (1999).
11. J.C. Collins, L. Frankfurt and M. Strikman, Phys. Rev. **D 56**, 2982 (1997) and B. Lehmann-Dronke et al., Phys. Rev. **D 63**, 114001 (2001).
12. Ph. Haegler, B. Pire, L. Szymanowski and O.V. Teryaev, Phys. Lett. **B 535**, 177 (2002).
13. HERMES Coll.: Eur. Phys. J. **C 20**, 479 (2001).
14. E. Wang and X.-N. Wang , Phys. Rev. Lett. **89**, 162301 (2002).
15. HERMES Coll.: Eur. Phys. J. **C21**, 599 (2001).
16. N. Bianchi and E. Thomas, Phys. Lett. **B450**,439 (1999).
17. K.A. Oganessyan, H.R. Avakian, N. Bianchi and P. Di Nezza, Eur. Phys. J. **C5**, 681 (1998); K.A. Oganessyan, N. Bianchi, E. De Sanctis and W.-D. Nowak, Nucl. Phys. **A 689**, 784 (2001).

18. R.L. Jaffe, F.E. Close, R.G. Roberts and G.G. Ross, Phys. Lett. **B 134**, 449 (1984).

FA-51

E. Nardi

1 Summary of the project

This research project covers two main areas:

1. study of the neutrino signal from a future Galactic core-collapse supernova;
2. study of the electromagnetic properties of the neutrinos.

1) A future supernova explosion within our Galaxy, triggered by the gravitational collapse of the star iron core (type II supernova) will result in several thousands of neutrino events in a large detector as SuperKamiokande, and in hundreds of events in SNO, LVD, KamLAND etc. We are proposing a new strategy to study the effect of a non-vanishing neutrino mass on the measured signal, and to analyze in detail the achievable sensitivity. 2) Experimental evidences for non-vanishing neutrino masses imply that neutrinos are the first particles whose properties cannot be fully accounted for within the Standard Model (SM). It is therefore interesting to study to what extent other neutrino properties, as for example their electromagnetic interactions, might deviate from the SM predictions, and what could be the impact on neutrino astrophysics and cosmology.

2 Study of the neutrino signal from a future Galactic core-collapse supernova

Informations on the neutrino masses can be derived from the study of the time of flight of the neutrinos emitted from the collapsing core of a supernova. Most of the methods proposed in the literature analyze only a limited number of neutrinos with arrival times close to a particular "timing" event (e.g. the deleptonization burst, the abrupt interruption of the neutrino signal due to the formation of a black hole, etc...). Typically, these methods show a sensitivity of the order $m_\nu \gtrsim 3$ eV for distances $\sim$10 Mpc.

We are proposing a new approach that uses the full statistics of the signal. To study the sensitivity of the method we started from an idealized situation assuming that the neutrino energy spectrum and the time evolution of the neutrino luminosity are both known. By means of a maximum likelihood method applied to a Monte Carlo generated neutrino signal we verified that the effects of a mass of 1 eV can be easily detected. However, the characteristics of the neutrino signal are not known in detail. Therefore we formulated the working hypothesis that the effects of a neutrino mass are largely uncorrelated with the details of the neutrino light curve and energy spectrum. This hypothesis can be motivated on physical grounds and eventually proved to be correct. In our procedure, the high energy neutrinos (for which the mass effects are largely suppressed) are used to reconstruct the spectrum by fitting a non-thermal Fermi-Dirac like distribution distorted by a "pinching" factor η. Next we observe that while the details of the luminosity curve are not known, its gross features are predicted with some reliability: an initial fast rise is expected, followed by a power law decay with a time scale of 10-20 sec. Accordingly, we assumed a shape $L(d, f, t) \sim t^{-d} e^{(-f/t)}$. Using $L(d, f, t)$ together with the fitted energy spectrum, we carried out a maximum likelihood analysis of several neutrino samples, generated according to different models of the supernova explosion published by different groups. We minimize the Log-Likelihood with respect to the neutrino mass m_ν, to the time of emission of the first neutrino $t_{\rm ini}$ and to the luminosity parameters d and f.

Our results indicate that the effects of $m_\nu \approx 1\,\mathrm{eV}$ can be in most cases identified, and distinguished from the case of a massless neutrino. Moreover, when $m_\nu = 0$ the upper limits obtained are in general below 1 eV. The method appears to be reasonably stable with respect to the different models used, and it is reliable in the sense that a bad guess for the shape of the luminosity curve will only result in larger errors in the fitted neutrino mass, but it will not have the effect of faking a mass if the neutrino is massless, or producing other misleading results.

This project has been quite demanding in terms of computational time, affecting heavily the rate of production of the results. We expect to publish our final results within about one or two months, once a reasonably large statistics of different neutrino samples will be fully analyzed.

3 Study of the electromagnetic interactions of the neutrinos

Neutrinos can interact with photons through electromagnetic form factors generated at the loop level. A well known example is the neutrino magnetic moment. The neutrino charge radius and the anapole moment (also denoted as axial vector charge radius) are other two less studied form factors. Unlike the magnetic moment, they couple neutrinos only to off-shell photons. In particular, the anapole moment is the only non-vanishing electromagnetic form factor for Majorana neutrinos. Due to intrinsic problems with gauge invariance and with the apparent dependence of their definition from specific physical processes, for a long time the neutrino vector and axial vector charge radius were considered as unphysical quantities. Only recently a consistent definition that proved to yield well defined physical observables was proposed. A brief account of the development of this topic was presented in. [1)]

The possible astrophysical and cosmological effects of a large anapole moment for Majorana neutrinos were analyzed in. [2)] Unlike the Dirac case, and differently from the case of the magnetic moment, it was argued that essentially no observable effects would arise even when the assumed values are unusually large. The rate of star cooling, the duration of the supernova neutrino burst, as well as Big Bang nucleosynthesis are insensitive to a new interaction of this kind. Therefore, informations on this quantity can be derived essentially only from laboratory experiments. We have used a large set of experimental data to constrain the anapole moment for different neutrino flavors. From TRISTAN and LEP data on the process $e^+e^- \to \nu\bar{\nu}\gamma$ we have derived the first limit on the ν_τ anapole moment, while from an analysis of the CHARM-II, E734, CCFR and NuTeV neutrino scattering data we improved existing limits on the ν_μ charge radius.

4 Work Program for the year 2003

The first line of research will be continued by including neutrino oscillations in the analysis. Concerning the second one, we will use the data on off Z-resonance neutrino counting, collected and analyzed in [2)] to derive global constraints on graviton production in theories with large extra dimensions.

References

1. *On the neutrino vector and axial vector charge radius.*
   E. Nardi. E-Print Archive: hep-ph/0212266
2. *Bounds on the τ and μ neutrino vector and axial vector charge radius.*
   M. Hirsch, E. Nardi and D. Restrepo. Phys. Rev. **D 67:033005**, 2003.

LF-11

S. Belluci, M. Benfatto, S. Di Matteo (Ass.), R. Gunnella (Ass.), K. Hatada (Visit.)
C.R. Natoli (Resp.), P. Onorato (Ass.), N. Perkins (Ass.), A. Tenore, Wu Ziyu (Visit.),

1 The Project

The aim of this project is the theoretical analysis of strongly correlated electron systems, like the manganites, the cuprates and the transition metal oxides, on one side, and the low-dimensional systems, like Nanotubes and Nanostructures, on the other. When appropriate, methods borrowed from field theory and statistical mechanics are used to bear on the description of the essential physics of such systems. At the same time in-depth studies of significant synchrotron radiation spectroscopies that can shed light on their charge and magnetic correlations are carried out and others are suggested to detect them. Finally the theory underlying the multiple scattering programs used to analyse such spectroscopies is improved and applications are made to obtain structural and electronic information in systems of biological relevance.

2 Nanotubes and Nanostructures

This research activity is devoted to the investigation of the transport properties of carbon nanotubes (CN). In particular we focused on the role of electron-electron correlations, in order to explain various phenomena recently observed in CN (electron transport, superconductive behaviour), and, sometimes, to predict some experimental observations. Our research intends to investigate how the electron transport is influenced by the temperature growth and we tried to formulate one coherent theory for several thermal regimes.

A first result of our research was to show that the Coulomb interaction in single wall CN (SWCN) produces interesting effects not yet experimentally observed. In particular it regards CN with a large radius, that can have the same electronic proprieties of a single graphene sheet, when the energy decreases. The temperature dependent measurements of small bias conductance (M. Bockrath *et al*, Nature 397 (1999) 598 and Z. Yao *et al*, Nature 402 (1999) 273) showed an anomalous dimension of the electron that grows when the energy scale goes to zero. Therefore, a second field of our research was the investigation, from the theoretical point of view, of the transverse dimension and of the critical exponents dependence on the scale. In fact experimental investigations of the Luttinger Liquid (LL) behavior in SWCN ropes, show some deviations of the conductance from the power law (typical of this behavior) in the low temperature regime. The experimental measurements are in agreement with the quasiparticle weight suppression and with the density of states at low energies that we calculated.

When the temperature is less than a critical value ($KT << h^2/(2L^2 m_e)$) the transport regime is totally different and corresponds to the one known as Coulomb Blockade regime, where the single electron transport (tunneling) plays a central role. In recent letters Cobden *et al* (Phys. Rev. Lett. 89, 046803 2002) and Liang *et al* (Phys. Rev. Lett. 88, 126801 2002) have shown "Coulomb oscillations" in SWCNT with some details (a first observation is due to Bockrath in 1997) and has allowed a better analysis of the electronic transport of SWNT at low temperatures. Our research has evidenced the role that the long range electron-electron interaction can play in the attenuation of the oscillations of the addition energy in analogy with what happens in Quantum Dots. From the analysis of the SWCNT excitations, obtained with a numerical implementation of the problem we can characterize the transition to Luttinger Liquid behavior when the temperature increases up to the critical value.

A second topic is connected to the Multi Walled Carbon Nanotubes (MWCNT) phenomenology: we have theoretically investigated the the critical exponents and the tunneling conductance of these systems. [1] MWCN are coaxial systems of Nanotubes that can also have a very large radius, so their transport proprieties are intermediate between the closely unidimensional systems (as SWNTs) and the bidimensional ones (as graphene sheet). The experiments about the tunneling conductance in MWCNT also showed power law behaviors [C. Schoenenberger *et al*, Appl. Phys. A69, (1999) 283; To Bachtold *et al*, report cond-mat/0101306] and confirmed our hypothesis that the Coulomb interaction (with its singular long range character) breaks the Fermi Liquid behavior in all dimensions between D=1 and D=2. The critical exponent experiments for tunneling in the bulk of MWCNT give a value of approximately 0.3, near to the one measured in the SWCNT by Bockrath *et al* and Yao *et al*. This unexpected value of the measuredcritical exponent confirms the strong effects of the unscreened long range Coulomb interaction in these systems. We used a Renormalization Group theory combined with a dimensional crossover in order to investigate the breakdown of the Fermi-Liquid behaviour in MWNT. So we can carry out a comparison with the experiments MNCT: near the fixed point D=1, the density of the states exhibits an effective power law behavior with a gradually increasing exponent while on the other side of the dimensional crossover the behaviour is quite similar to the one of a graphite sheet. We can conclude that an appropriate description of the dimensional crossover shows that a representation of a MWNT as sum of 1-dimensional channels does not allow us to obtain the correct values of the critical exponents.

The most recent research concerns the physics of MWNT in the presence of doping. The recent measurements of Bachtold (PRL 87, 166801 2001) show that, because of the doping, in MWCNT a number N of subbands between 10 and 20 are occupied instead of the 4 that characterize the ideal SWCNT. Also in this case we developed a dimensional regularization approach to deal with the low-energy effects of the long-range Coulomb interaction in 1D electron systems. The method allowed us to avoid the infrared singularities arising from the long-range Coulomb interaction at D = 1, providing at the same time insight about the fixed-points of the theory. We showed that the effect of increasing the number N of subbands at the Fermi level is opposite to that of approaching the bare Coulomb interaction in the limit D -¿ 1. Then, we devised a double scaling limit, in which the large N effects are able to tame the singularities due to the long-range interaction. Thus, regular expressions can be obtained for all observables right at D = 1, bearing also a dependence on the doping level of the system. Our results imply a variation with N in the value of the exponent for the tunneling density of states, which is in fair agreement with that observed in different transport experiments involving carbon nanotubes. As the doping level is increased in nanotubes of large radius and multi-walled nanotubes, we predicted a significant reduction of order $N^{-1/2}$ in the critical exponent of the tunneling density of states.

A different topic of our research is the quantum mechanics in the non commutative plane, in the presence of a magnetic field B. This type of model appears in several systems that describe spinning particles and can be applied to Quantum Hall Effect [Laughlin 1983, G.V. Dunne, R. Jackiw, C.A. Trugenberger, Phys. Rev. D41 (1990) 661] and to the description of pointlike vortices in thin films of superfluid He^4 II [Onsager 1949]. We showed that the model has two phases that differ in an essential way and are separated by a definite critical value of B. The spinning proprieties of non commutative particles can be drastically changed by a change in the orientation of the magnetic field. [2, 3]

Finally channeling of particle beam in straight and bent single-wall nanotubes has been studied in computer simulations. We have found that the nanotubes should be sufficiently narrow in order to steer efficiently the particle beams, with preferred diameter of the order of 0.5-2 nm. Wider nanotubes, e.g. 10-50 nm, appear rather useless for channeling purpose because of high sensitivity of channeling to nanotube curvature. We have compared bent nanotubes with bent crystals as elements of beam steering technique, and found that narrow nanotubes have an efficiency

of beam bending similar to that of crystals, and we studied also X-ray channeling. [4, 6]

3 Physics of strongly correlated electron systems.

The research in this field has developed along three main directions:

- Analysis of synchrotron radiation experiments (resonant x-ray scattering, absorption and dichroism) in strongly correlated electron systems.
- Analysis of the space magnetic symmetries of magnetoelectric materials by means of x-ray dichroism and resonant scattering.
- Investigation of the physics of the complex magnetic oxides (V_2O_3, $LaSr_2Mn_2O_7$, LiV_2O_4, Sr_2FeWO_6 and $Nd_{1-x}Sr_xMn_{1-x}Ru_xO_3$).

Concerning item 1) we have completed the description of electronic correlations of the low-temperature, antiferromagnetic insulating phase in V_2O_3, started in 2001. We have drawn the phase diagram of this system in terms of the hopping parameters and the interelectronic coulomb repulsion. [7, 8, 9, 10] The analysis performed in the first two articles shows that the phases found for the system admit a different magnetic space group than suggested by a recent dichroic experiment at vanadium K edge (Goulon *et al*, PRL 85, 4385 (2000)), where it is found that the system allows non reciprocal effects, implying that time-reversal and inversion symmetries are broken and only their product is conserved. This situation led to a further experiment to remove the stalemate so as to choose between two possible magnetic space groups [11]: however no magnetoelectric effect was found in the system, and this fact is not compatible with the presence of a non-reciprocal gyrotropic linear dichroism. This result solved a problem but raised another question: the correct interpretation of the dichroic experiment at vanadium K edge. We then analysed this experiment in order to give a coherent interpretation of all the recent x-ray resonant scattering and dichroic experiments on V_2O_3. [12] Here we performed numerical simulations based on the multiple scattering theory for both the dichroic spectra and the resonant scattering , analysing the experimental implications related to the different magnetic space symmetries. We showed in this way the paradoxical consequences of the accepted interpretation on the physics of this system and suggested how to perform correctly the dichroic experiment in order to dissipate any doubt about the behavior of the system.

Following this line of research and using the general multiple-scattering theory for circular and linear dichroism in photoemission and photoabsorption, [13] an in-depth analysis has been carried out in the case of the magneto-chiral dichroism in Cr_2O_3 [14] and, as already mentioned, the linear dichroism (non-reciprocal gyrotropic effect) in V_2O_3. [12] The adaptation of the MS program CONTINUUM for the calculation of magnetic and non-magnetic resonant diffraction has been completed, in view of an extensive analysis of the scattering data and their implications for the physics of transition metal oxides. In particular, in the case of Cr_2O_3 we have developed a theory on the effects of a medium-intensity magnetic field on the symmetries of the system: the magnetic space symmetry cahnges as a function of the applied magnetic field. These effects can be observed by means of linear dichroism, as proposed in the article [14] and can be theoretically tested quantitatively by such numerical simulations. Another subject of research of extreme interest concerns the application of x-ray experiments to superconducting cuprates in the light of the previous symmetry considerations. In fact quite recently a possible magnetoelectric phase for high-temperature superconducting cuprtaes has been proposed. Following these predictions, dichroic and anomalous scattering experiments using synchrotron radiation have been suggested to verify them. [15]

The third direction of research concerned the investigation of the physics of complex magnetic oxides such as V_2O_3, LiV_2O_4, Sr_2FeWO_6, $Nd_{1-x}Sr_xMn_{1-x}Ru_xO_3$ and the manganites which exhibit a whole variety of interrelated phenomena such as metal-insulator transitions, orbital and magnetic ordering, double exchange, geometrical frustration, heavy fermion distortion and colossal magnetoresistance. We already dealt with the most intersesting case of V_2O_3. The study of the pyrochlore LiV_2O_4 was motivated by the recently observed heavy fermion features at low temperatures (for the first time in a d-electron system). We derived a description of the system including the geometrically frustrated lattice structure and the strong electronic correlations. By solving this model exactly on a small cluster (one tetrahedron) we studied how the interplay of the lattice frustration, spin interactions and multiband electronic structure give rise to such an unusual behavior. This work is not completed yet but the preliminary results show already that the geometrically frustrated lattice structure plays a very important role in the formation of the heavy fermion behaviour in this compound. Another field in growing interest is that of the so-called double perovskite, that are becoming more and more important after the discovery of the colossal magnetoresistance. The material we described is an insulating double perovskite, Sr_2FeWO_6, for which we derived the phase diagram on the bases of an effective spin-orbital Hamiltonian and suggested a possible experiment to detect the predicted antiferromagnetic and orbital ordering. [16] In collaboration with the neutron diffraction group in Dubna, we also studied $Nd_{1-x}Sr_xMn_{1-x}Ru_xO_3$. In this case, the correlated doping of A- and B-sites with Sr and Ru ions in $Nd_{1-x}Sr_xMn_{1-x}Ru_xO_3$ leads to long-range ferrimagnetic ordering but leaves the system insulating. Such an experimental fact has been observed for the first time and, in order to explain it, the role of Ru-doping has been analyzed under several aspects. One is the understanding of what is the electronic configuration of Ru ion, if it changes or remains the same upon doping. Also, it is important to realize what kind of virtual processes determines the exchange interaction between Ru and its nearest-neighbors. However the main question is why the insulating behavior sets in while a metallic behaviour is expected, via the double-exchange mechanism, on the basis of the ferrimagnetic long-range order ($x = 0.25$ and $x = 0.5$). This work is in preparation. Finally, the role of the orbital degrees of freedom has been investigated in the doping dependance of the exchange energies in bilayer manganites [17] and the origin of Resonant x-ray scattering in $LaSr_2Mn_2O_7$ at the Mn K edge has been studied. [18]

4 Improving the analysis of synchrotron radiation spectroscopies

4.1 Fitting of the XANES spectra by a full multiple scattering procedure

In year 2001 M. Benfatto and co-workers have proposed in the literature a new method, called MXAN, for performing a complete fit of the XANES energy range (from the edge to about 200 eV) in terms of selected structural parameters. The novelty of the method is in the use of the full multiple scattering approach for the calculation of the photoabsorption cross-section, i.e. this quantity is calculated without any series expansion. In this way the whole XANES energy region can be used for a quantitative analysis. This is very relevant for biological systems where the low S/N ration and the weak scattering power of the light elements surrounding the metal site limit normally the k-range of the experimental absorption data. Using this method a complete quantitative analysis of the MbCO and Mb*CO polarized XANES spectra at the iron K-edge has been performed in terms of local geometry of the heme site. During year 2002 the program has been tested in details and in particular a systematic analysis of K-edges of transition metals in aqueous solution has been performed to compare the geometry derived by the MXAN procedure with the one obtained by standard EXAFS type of analysis. The structural geometry around the absorber is well recovered, and the values of both metal-oxygen distance and the angles between bonds are in good agreement with those derived by standard methods. The use of a combined

quantitative XANES and EXAFS investigation based on fitting procedure has allowed an accurate determination of the coordination geometry of the Cu2+ ion in aqueous solution. It has been shown that, at variance with the generally accepted Jahn-Teller octahedral model, the Cu2+ hydration complex is fivefold coordinated.

4.2 Implementation of the GW approximation for the photoelectron optical potential.

As already anticipated in the previous report, the GW approximation has been implemented in the CONTINUUM code along the lines illustrated in Fujikawa, Hatada & Hedin (Phys. Rev. (2001). B 62, 5387), extending the method to low photoelectron energies. Simulations of XANES spectra have been done on selected compounds to test the validity of this new optical potential. In the course of these simulations problems were found in some cases with the convergence of the self-consistent solution of the coupled, nonlinear equations that provide the GW optical potential. A modified Broyden's method to accelarete the convergence procedure (D.D. Johnson, Phys. Rev. 38, 12807, (1988)) is under test to ensure convergence in a large variety of cases. A communication on the performance of the GW optical potential will be presented at the XAFSXII Conference (June 2003, Lund, Sweden).

4.3 Beyond the muffin-tin approximation in Multiple Scattering (MS) programs

A third method for solving the Schrodinger-Dyson equation for non spherically symmetric potentials has been devised, beside the two described in the previous report, respectively based on the discretization of the Laplacian in polar coordinates (method 1) and the transformation of the 3-d problem in a set of coupled radial Schrodinger equations (SE) obtained by projecting the wave function and the potential onto the complete set of spherical harmonics (method 2). The new method avoids the inaccuracy of the solution near the poles of the quantization axis present in method (1) and is computationally faster than method (2) by at least a factor of five. It has therefore been implemented in the MS non-muffin-tin (NMT) program. Numerical routines for performing surface integrals on the surface of polyhedral cells have also been written and comparison between this version of the NMT program and the FDM program by Y. Joly are under way. This new NMT program combines the advantage of the MS method (partitioning of space in non overlapping cells) with the relative ease for generating local (ie within cells) NMT solutions of the SE, in such a way that large cluster calculations not affordable with the FDM program become feasible with reasonable requirement of CPU time and computer memory.

4.4 Multichannel Multiple Scattering Theory.

In collaboration with P. Krueger (ESRF, Grenoble) progress has been made in the development of a new computational method for X-ray absorption spectroscopy of d- and f- electron systems. The method combines eigenchannel R-matrix and multiple scattering formalisms to take account of atomic multiplet-like electron correlation effects in condensed systems, on the basis of ab initio electron structure calculations. First results have been obtained on the X-ray absorption at the $L_{2,3}$ edge of Ca metal, where the spectral shape, and in particular the branching ratio, deviates strongly from that obtained in single-particle theory.

References

1. S. Bellucci, "An explanation for the puzzling tunneling conductance measurements in multiwalled carbon nanotubes", - Proc. of the School and Workshop on Nanotubes & Nanostructures 2001, Frascati (RM), Ed. S. Bellucci, (Compositori, Bologna 2002, in print).

2. S. Bellucci, A Nersessian, "Phases in noncommutative quantum mechanics on (pseudo)sphere", - Phys .Lett. B **542** (2002) 295.

3. S. Bellucci, A Nersessian, "(Super)Oscillator on CP(N) and Constant Magnetic Field", - hep-th/0211070, to be published on Phys. Lett. B.

4. S. Bellucci, V.M. Biryukov, "Nanotube diameter optimal for channeling of high-energy particle beam", - Phys. Lett. B **542** (2002) 111 [PHYSICS 0205023].

5. S. Bellucci, Z. Wu, J. Zhang, K.Ibrahim, D.C. Xian, *et al*, "Structural determination of titanium-oxide nanoparticles by x-ray absorption spectroscopy", - Appl. Phys. Lett. **80** (2002) 2973.

6. S. Bellucci, S.B. Dabagov, "On X-Ray Channeling in mu- and n-capillaries", - J. Phys. Cond. Mat. (submitted), physics/0209011.

7. S. Di Matteo, N.B. Perkins, C.R. Natoli, "Spin-1 effective Hamiltonian with three degenerate orbitals: An application to the case of V_2O_3" - Phys. Rev. B **65**, (2002), 054413-1 to 36

8. S. Di Matteo, N.B. Perkins, C.R. Natoli, "Ground state electronic properties of V_2O_3" - J. Phys.: Condens. Matter, **14**, (2002), L37-L41

9. S. Di Matteo, N.B. Perkins, C.R. Natoli "Open points on the nature of the antiferromagnetic ground state of V_2O_3" - Acta Physica Polonica B, **34** (2003), 775

10. S. Di Matteo, "Ground state symmetry of the antiferromagnetic phase of V2O3" - Physica B **318** (2002), 321-327

11. S. Di Matteo, A.G.M. Jansen, "Magnetoelectricity in V_2O_3" - Phys. Rev. B **66** (2002) 100402-1 to 4(R)

12. S. Di Matteo, Y. Joly, C.R. Natoli "A critical re-examination of the non-reciprocal x-ray gyrotropy in V_2O_3" - Phys. Rev. B **67**, xxxxxx (2003)

13. S. Di Matteo, C.R. Natoli "A multiple scattering theory of circular and linear dichroism for photoemission and photoabsorption" - - J. Synchrotron Rad. **9**, (2002), 9-16

14. S. Di Matteo, C.R. Natoli, "Magnetochiral dichroism in Cr_2O_3" - Phys. Rev.B **66** (2002) 212413-1 to 4

15. S. Di Matteo, C.M. Varma, "Symmetry considerations for detection of time-reversal breaking phases in cuprates by x-ray diffraction and absorption" - Phys. Rev. B **67**, 1345xx (2003)

16. S. Di Matteo, G. Jackeli, N.B. Perkins, "An effective spin-orbital Hamiltonian for the double perovskite Sr2FeWO6: Derivation of the phase diagram" - sumbitted to Phys. Rev B

17. N.B. Perkins, G. Jackeli, "Doping dependance of the exchange energies in bilayer manganites: Role of orbital degrees of freedom." - Phys. Rev. B **65**, 212402 (2002)

18. S. Di Matteo, T. Chatterjee et al. "Resonant x-ray scattering from $LaSr_2Mn_2O_7$ at the Mn K edge" - sumbitted to Phys. Rev B

19. M. Benfatto P. D'Angelo, S. Della Longa *et al*, "Evidence of distorted fivefold coordination of the Cu^{2+} aqua ion from an x-ray-absorption spectroscopy quantitative analysis" - Phys. Rev B**65**: 174205 (2002)

20. P. D'Angelo, M. Benfatto S. Della Longa *et al*, "Combined XANES and EXAFS analysis of Co^{2+}, Ni^{2+}, and Zn^{2+} aqueous solutions" - Phys. Rev B **66**: 064209 (2002)

21. M. Benfatto, J.A.Solera, J.G. Ruiz *et al*, "Combined XANES and EXAFS analysis of Co^{2+}, Ni^{2+}, and Zn^{2+} aqueous solutions" - Chem. Phys. **282**, 441 (2002)

22. M. Pedio, Z.Y. Wu, M. Benfatto *et al*, "NEXAFS experiment and multiple scattering calculations on KO_2: Effects on the π resonance in the solid phase" - Phys. Rev B **66** : 144109 (2002)

23. C.R. Natoli, M. Benfatto, S. Della Longa and K. Hatada "X-ray absorption spectroscopy: state-of-the-art analysis" - J. Synchrotron Rad. **10**, 26-42, (2003)

24. M. Benfatto, S. Della Longa and C.R. Natoli "The MXAN procedure: a new method for analysing the XANES spectra of metalloproteins to obtain structural quantitative information" - J. Synchrotron Rad. **10**, 51-57, (2003)

LF-21

G. Isidori, G. Pancheri (Resp.)

1 Summary of the project

The research topics investigated by this project can be divided into three main areas:

- Flavour physics;
- Precision physics in hadronic processes at DAPHNE;
- Potential models and quarkonium radiative decays
- Quantum Chromodynamics and the rise of total cross-sections.

The first area, discussed in Section 2, concerns the possibility to perform new precision tests about the mechanism of quark-flavor mixing, within and beyond the Standard Model (SM). Other studies concerning precision physics in hadronic processes at DAPHNE and quarkonium bound states will then follow in Sects. 3 and 4.

An altogether different field of investigation, dedicated to reach into a much higher energy range, is the project related to the QCD description of hadronic and photonic total cross-section, which will be described in detail in Sect. 5.

2 Flavour Physics

Despite the Standard Model (SM) provides a successful description of particle interactions, it is natural to consider it only as the low-energy limit of a more general theory, or as the renormalizable part of an effective field theory valid up to some still undetermined cut-off scale Λ. Since the SM is renormalizable, we have no direct indications about the value of Λ. However, theoretical arguments based on a natural solution of the hierarchy problem suggest that Λ should not exceed a few TeV.

One of the strategies to obtain additional clues about the value of Λ is to constrain (or find evidences) of the effective non-renormalizable interactions, suppressed by inverse powers of Λ, which encode the presence of new degrees of freedom at high energies. These operators should naturally induce large effects in processes which are not mediated by tree-level SM amplitudes, such as $\Delta F = 1$ and $\Delta F = 2$ flavour-changing neutral current (FCNC) transitions. Up to now there is no evidence of these effects and this implies severe bounds on the effective scale of dimension-six FCNC operators. For instance the good agreement between SM expectations and experimental determinations of K^0–$\bar{K}^0$ mixing leads to bounds above 10^3 TeV for the effective scale of $\Delta S = 2$ operators, i.e. well above the few TeV range suggested by the Higgs sector.

The apparent contradiction between these two determinations of Λ is a manifestation of what in many specific frameworks (supersymmetry, techincolour, etc.) goes under the name of *flavour problem*: if we insist with the theoretical prejudice that new physics has to emerge in the TeV region, we have to conclude that the new theory possesses a highly non-generic flavour structure.

Interestingly enough, this structure has not been clearly identified yet, mainly because the SM, *i.e.* the low-energy limit of the new theory, doesn't possess an exact flavour symmetry. The attempt to clarify this structure, both at the phenomenological level (with the help of precision data on rare decays) and at a more fundamental level (with the help of new symmetry principles), is one of the main activity of our group.

Recently, the flavour problem has been considerably exacerbated by the new precise data of B-factories, which show no sizable deviations from SM expectations also in B_d–$\bar{B}_d$ mixing and in a clean $\Delta B = 1$ FCNC processes such as $B \to X_s\gamma$. One could therefore doubt about the need for new tests of the SM in the sector of (quark) flavour physics. However, there are at least two arguments why the present status cannot be considered conclusive: [1, 2]

- The information used at present to test the CKM mechanism and, in particular, to constrain the unitary triangle, is obtained only from charged currents (i.e. from tree-level amplitudes) and $\Delta F = 2$ loop-induced processes. In principle, rare K and B decays mediated by $\Delta F = 1$ FCNCs could also be used to extract indirect information on the unitary triangle, or to constrain new-physics effects. However, with the exception of the $B \to X_s\gamma$ rate, the quality of this information is very poor at present, either because of experimental difficulties or because of theoretical problems. [3] As shown by specific examples, such as supersymmetric models with large $\tan\beta$, [4] new physics could affect in a very different way $\Delta F = 2$ and $\Delta F = 1$ loop-induced amplitudes, even with order-of-magnitude enhacements in the former and $\mathcal{O}(10\%)$ corrections in the latter. It is then mandatory to improve the quality of the $\Delta F = 1$ information. [3]

- The most reasonable (but also most *pessimistic*) solution to the flavour problem is the so-called *Minimal Flavour Violation* (MFV) hypothesis. Within this framework, which has been recently formulated in a model-independent way, [5] all flavour- and CP-violating interactions are linked to the known structure of Yukawa couplings also beyond the SM. This implies that deviations from the SM in FCNC amplitudes rarely exceed the $\mathcal{O}(10\%)$ level, or the level of irreducible theoretical errors in most of the presently available observables. Moreover, theoretically clean quantities such as $a_{\rm CP}(B \to J/\Psi K_S)$ and $\Delta M_{B_d}/\Delta M_{B_s}$, which measure only ratios of FCNC amplitudes, turn out to be insensitive to new-physics effects. Within this framework the need for additional clean and precise information on FCNC transitions is therefore even more important. As we have explicitely shown, the measurements of a few rare processes, such as $\Gamma(K \to \pi\nu\bar{\nu})$ or the *Forward-backward asymmetry* in $B \to X_s\ell^+\ell^-$ – evaluated for the first time at the NNLL accuracy [6] – would offer a unique opportunity in this respect (see Figure 1,2).

3 Precision physics in hadronic processes at DAPHNE

3.1 *QCD and meson interactions below 1 GeV*

The radiative $\phi \to \pi^0\eta\gamma$ decay is discussed emphasizing the effects of the $a_0(980)$ scalar resonance which dominates the high values of the $\pi^0\eta$ invariant mass spectrum. In its lowest part, the proposed amplitude coincides with the reliable and ChPT-inspired contribution coming from chiral

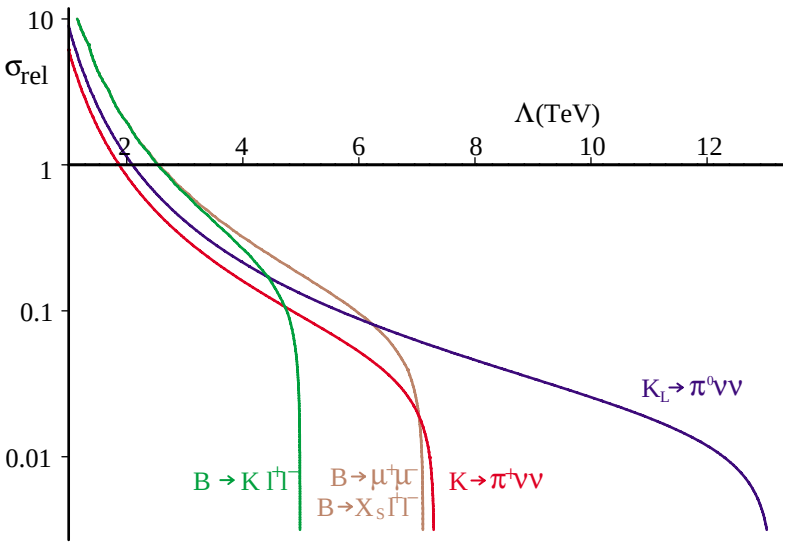

Figure 1:

loops. The $a_0(980)$ resonance is then incorporated exploiting the complementarity between ChPT and the LσM for this channel. The recently reported experimental invariant mass distribution and branching ratio can be satisfactorily accommodated in our framework. For the latter, a value of $B(\phi \to \pi^0\eta\gamma)$ in the range $(0.75\text{–}0.95) \times 10^{-4}$ is predicted [7].

3.2 Radiative corrections to the hadronic cross-section at DAPHNE

Other work has focussed on applying NLO radiative corrections to the measurement of the hadronic cross-section at DAPHNE, to be obtained through the method of the radiative return, in and around the ρ resonance region [8].

4 Potential models and charmonium decays

Using various potential models, studies have continued towards the calculation of the radiative decays of charmonium pseudoscalar states, like η_c and η_b [9, 10].

5 Quantum Chromodynamics and the rise of total cross-sections

This project [11, 12, 13] is developed through collaborations between G. Pancheri and Rohini Godbole, for what concerns strictly the Eikonal Minijet Model, Martin Block for the factorization picture, Godbole, A. Grau and Y.N. Srivastava for the studies of the effect of Soft Gluon Resummation on the taming of the rise of total cross-section.

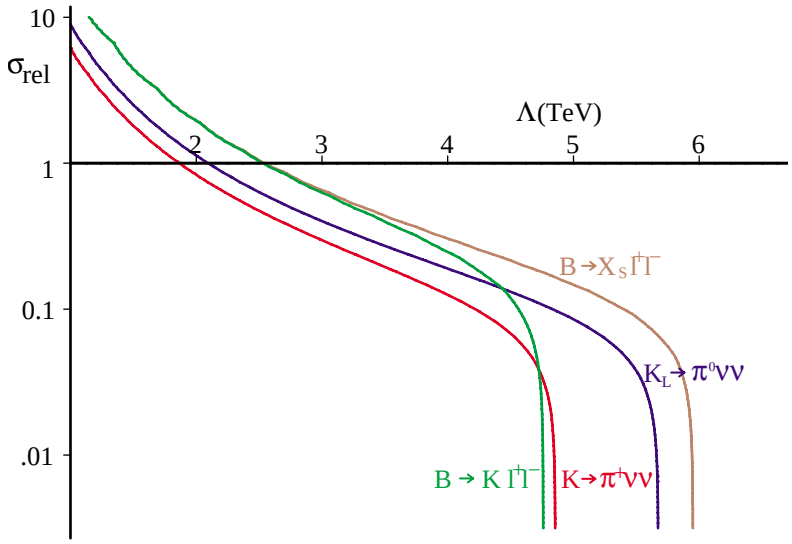

Figure 2: *Comparison of the effectiveness of different rare modes in setting future bounds on the effective scale of new physics within MFV models.* [5] *The vertical axis indicates the relative precision of an hypothetic measurement of the rate, with central value equal to the SM expectation. The curves in the two panels are obtained assuming an uncertainty of 10% (left) or 1% (right) on the corresponding overall CKM factor.*

The goal of this project is to obtain a QCD description of the initial decrease and the final increase of total cross-sections through soft gluon summation (via Bloch-Nordsieck Model) and QCD calculable jet x-sections, also known as mini-jets in this context. Thus, the physical picture includes multiple parton collisions and soft gluons dressing each collision.

5.1 *The Eikonal Minijet Model for protons and photons*

In the Eikonal Minijet Model (EMM) the rise can be obtained using the QCD calculable contribution from the parton-parton cross-section, whose total yield increases with energy. For a unitary description, the jet cross-sections are embedded into the eikonal formalism, where the eikonal function contains both the energy and the impact parameter distribution in b-space. The simplest formulation with minijets to drive the rise, and hadronic form factors for the impact parameter distribution, can be applied to all the available x-sections. One finds that proton-antiproton high energy data can be reproduced by this model. However it is not possible to describe both the early rise, which in proton-antiproton scattering takes place around $10 \div 50\, GeV$, and the Tevatron data, with a single set of parameters.

Photo-production data can be described through the same simple eikonal minijet model, with the relevant parton densities for the jet cross-sections, scaling the non perturbative part with VMD and quark counting factors. However, just like in the proton-proton case and in the gamma gamma

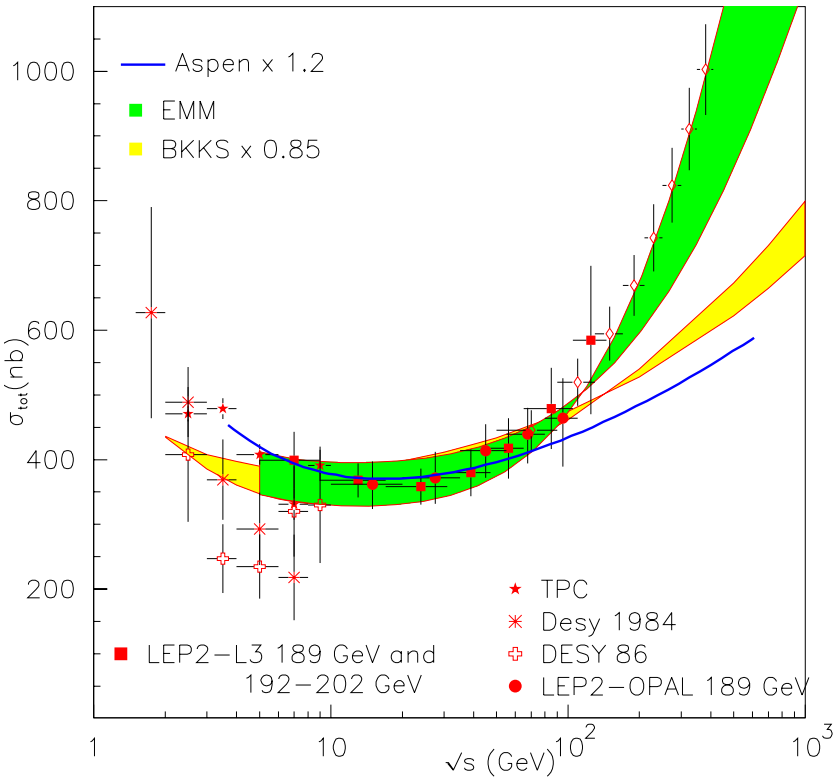

Figure 3: *Prediction for $\gamma\gamma$ total hadronic cross-section for the future Linear Collider measurement and comparison with existing models.*

case, the case for extrapolation of the EMM to higher energies is not convincing. A compilation of $\gamma\gamma$ data, including present LEP data, done for future Linear Collider, Fig. (3), has indicated that the EMM describes quite well the rise at present energies, but the extrapolation to even higher energies appears unrealistic and may need to be modified, as found in the proton case. In the figure the predictions of this model for photon-photon collisions are shown in comparison with predictions from different models A possible way to circumvent this problem is pursued through resummation of soft gluon emission from the initial state partons, a feature absent from most simple EMM.

5.2 *Soft Gluon Summation and the impact parameter distribution of partons*

A model for the impact parameter space distribution of parton in the hadrons has been developed and applied to the proton cross-sections in order to obtain a better description of total cross-section. The physical picture underlying this model is that the fast rise due to mini-jets and the increasing number of gluon-gluon collisions as the energy increases, can be reduced if one takes into account that soft gluons, emitted mostly by the initial state valence quarks, determine an acollinearity between the partons which reduces the overall parton-parton luminosity. This model can describe very well all available data for proton collisions.

6 Work Program for the year 2003

Most of the activity previously described in hadronic physics will be continued into the year 2003. The work on QCD and total cross-sections, a long term project, will focus mainly on discussing the

normalization of total cross-sections and the impact parameter distribution of partons in both in protons and photons. Work to extend the model for the infrared behaviour of the strong coupling constant to the calculation of meson decay constants is under progress.

References

1. G. Isidori,

   Int. J. Mod. Phys. A **17** (2002) 3078.

2. G. Isidori, *Kaon decays and the flavour problem,* invited talk at TH-2002 (Unesco, Parigi, August 2002), to appear in the proceedings [hep-ph/0301159].

3. G. D'Ambrosio and G. Isidori, Phys. Lett. B **530** (2002) 108.

4. G. Isidori and A. Retico, JHEP **0209** (2002) 063.

5. G. D'Ambrosio, G. F. Giudice, G. Isidori and A. Strumia, Nucl. Phys. B **645** (2002) 155.

6. A. Ghinculov, T. Hurth, G. Isidori and Y. P. Yao, Nucl. Phys. B **648** (2003) 254.

7. A.Bramon, R. Escribano, J.L. Lucio M, M. Napsuciale, G. Pancheri, Eur.Phys.J.C26:253-260,2002 e-Print Archive: hep-ph/0204339

8. V.A. Khoze, M.I. Konchatnij, N.P. Merenkov, G. Pancheri, L. Trentadue, O.N. Shekhovtzova, Eur.Phys.J.C25:199-213,2002 e-Print Archive: hep-ph/0202021

9. N. Fabiano, G. Pancheri, To appear in the proceedings of 1st International Workshop on Frontier Science: Charm, Beauty, and CP, Frascati, Rome, Italy, 6-11 Oct 2002. e-Print Archive: hep-ph/0210279

10. N. Fabiano, G. Pancheri, Eur.Phys.J.C25:421-425,2002 e-Print Archive: hep-ph/0204214

11. R.M. Godbole, A. Grau, G. Pancheri, *Total Cross-sections*, IISC-CTS-04-02, May 2002. 5pp. Presented at International Conference on the Structure and Interactions of the Photon and 14th International Workshop on Photon-Photon Collisions (Photon 2001), Ascona, Switzerland, 2-7 Sep 2001. e-Print Archive: hep-ph/0205197

12. R.M. Godbole, A. Grau, G. Pancheri, Y.N. Srivastava, *Soft gluons and the energy dependence of total cross-sections*, Presented at QCD@Work: International Conference on QCD: Theory and Experiment, Martina Franca, Italy, 16-20 Jun 2001. Published in *Martina Franca 2001, QCD@WORK* 127-138 e-Print Archive: hep-ph/0205196

13. M. Block, G. Pancheri, Eur.Phys.J.C25:287-289,2002 e-Print Archive: hep-ph/0206166

MI-12

S. Bellucci (Resp.), P.-Y. Casteill, S. Ferrara (Ass.), A. Galajinsky,
E. Latini (Laur.), F. Morales, C. Sochichiu

1 Research Activity

We showed that any conformal field theory in d-dimensional Minkowski space, in a phase with spontaneously broken conformal symmetry and with the dilaton among its fields, can be rewritten in terms of the static gauge (d-1)-brane on $AdS_(d+1)$ by means of an invertible change of variables. Some possible implications of this transformation, in particular, for the study of the quantum effective action of N=4 super Yang-Mills theory in the context of AdS/CFT correspondence, have been discussed. We studied also quantum mechanics of a massive superparticle in d=4 which preserves 1/4 of the target space supersymmetry with eight supercharges and so corresponds to the partial breaking N=8 down to N=2.

We looked at the issue of the violation of the weak and null energy conditions and the second law of thermodynamics in wormhole solutions of Einstein's theory with classical, nonminimally coupled, scalar fields as material source. We showed that the discussion is only meaningful when ambiguities in the definitions of stress-energy tensor and energy density of a nonminimally coupled scalar are resolved. We traced the root of the ambiguities to the energy localization problem for the gravitational field.

We considered quantum N=2 string embedded into the N=4 topological framework from the perspective of covariant quantisation. Making use of the causality and cyclic symmetry of tree amplitudes we argued that no Lorentz covariant boson emission vertex can be constructed within the N=4 topological formalism. We also found a Lagrangian and displayed all local symmetries for N=4 topological string by Berkovits, Vafa and Siegel, the latter previously known in the superconformal gauge. Leading to a small N=4 superconformal algebra and exhibiting the manifest Lorentz invariance the model is proposed to be a framework for restoring the manifest Lorentz invariance in N=2 string scattering amplitudes. We also compared N=2 string and N=4 topological string within the framework of the sigma model approach. Being classically equivalent on a flat background, the theories are shown to lead to different geometries when put in a curved space. In contrast to the well studied Kaehler geometry characterising the former case, in the latter case a manifold has to admit a covariantly constant holomorphic two-form in order to support an N=4 twisted supersymmetry. This restricts the holonomy group to be a subgroup of SU(1,1) and leads to a Ricci–flat manifold.

Noncommutative dualities in gauge models and in Matrix theory were also studied. The research activity has focused, as well, on the study of various aspects of the holographic gauge/gravity correspondences and non-perturbative effects in gauge theories.

2 List of Conference Talks by LNF Authors in Year 2002

1. S. Bellucci, Frascati, Congresso di Fisica Teorica "Cortona 2002", Cortona, Italy
2. S. Bellucci, Frascati, Conferenza "Problemi Attuali di Fisica Teorica", Vietri sul Mare (Italy)

References

1. "ADS / CFT EQUIVALENCE TRANSFORMATION", S. Bellucci, E. Ivanov e S. Krivonos, hep-th/0206126, Phys. Rev. D 66 (2002) 086001.

2. "QUANTUM MECHANICS OF SUPERPARTICLE WITH 1 / 4 SUPERSYMMETRY BREAKING", HEP-TH 0112075, S. Bellucci, A. Galajinsky, E. Ivanov e S. Krivonos, Physical Review D 65 (2002) 104023.

3. "ENERGY CONDITIONS AND CLASSICAL SCALAR FIELDS", S. Bellucci, V. Faraoni, hep-th/0106168, Nucl. Phys. B640 (2002) 453.

4. "CAN ONE RESTORE LORENTZ INVARIANCE IN QUANTUM N=2 STRING?", HEP-TH 0112024, S. Bellucci, A. Galajinsky, Nuclear Physics B630 (2002) 151.

5. "COMPLETE LAGRANGIAN FORMULATION FOR N=4 TOPOLOGICAL STRING", S. Bellucci, A. Galajinsky, Physical Review D65 (2002) 044013.

6. "THE GEOMETRY OF N=4 TWISTED STRING", S. Bellucci, A. Deriglazov e A. Galajinsky, [HEP-TH 0110287], Physical Review D65 (2002) 104026.

7. Continuum limit(s) of BMN matrix model: Where is the (nonabelian) gauge group? By Corneliu Sochichiu. [hep-th/0206239] Submitted to Phys. Lett. B (Jun 2002) 10p.

8. Gauge invariance and noncommutativity. By Corneliu Sochichiu. (lecture notes) [hep-th/0202014] (Feb 2002) 46p.

9. Duality in noncommutative gauge theories as a nonperturbative Seiberg-Witten map. By Elias Kiritsis and Corneliu Sochichiu. [hep-th/0202065] (Feb 2002) Submitted to Phys.Rev.D 24p.

10. J.F. Morales and M. Trigiante, *"Walls from fluxes: An analytic RG-flow"*, JHEP **02** (2002)018, hep-th/0112059.

11. J.F. Morales and H. Samtleben, *"Supergravity duals of matrix string theory"*, JHEP(2002)042, hep-th/0206247.

12. J. F. Morales, *"String theory on Dp-plane waves"*, JHEP **0301** (2003) 008, hep-th/0210229.

13. E. Gava, A.B. Hammou, J.F. Morales and K.S. Narain, *"D1D5 systems and AdS / CFT correspondences with sixteen supercharges"*, hep-th/0201265, Fortschritte der Physik, Vol. 50, No 8-9 (2002) 890.

14. RENORMALISABILITY OF T DUALISED NONHOMOGENEOUS SIGMA MODELS. By Pierre-Yves Casteill. Published in Phys.Lett. **B543**,241 (2002), e-Print Archive: hep-th/0202181.

15. U(1) X U(1) QUATERNIONIC METRICS FROM HARMONIC SUPERSPACE. By Pierre-Yves Casteill, Evgeny Ivanov, Galliano Valent. Published in Nucl.Phys. **B627**, 403 (2002), e-Print Archive: hep-th/0110280.

16. Ferrara S, Sokatchev E Conformally coupled supermultiplets in four and five dimensions J HIGH ENERGY PHYS (8): (2002)art. no. 051 AUG 2002

17. Andrianopoli L, D'Auria R, Ferrara S, et al. Gauging of flat groups in four dimensional supergravity J HIGH ENERGY PHYS (7): (2002) art. no. 010 JUL 2002

18. Ferrara S, Porrati M Observations on the holographic duals of 4-d extremal black holes PHYS LETT B 545 (3-4): (2002) 384-388 OCT 10

19. Ferrara S, Porrati M N=1 no-scale supergravity from IIB orientifolds PHYS LETT B 545 (3-4): (2002) 411-415 OCT 10 2002

20. D'Auria R, Ferrara S, Vaula S N=4 gauged supergravity and a IIB orientifold with fluxes NEW J PHYS 4: (2002) art. no. 71 OCT 4 2002

21. Andrianopoli L, D'Auria R, Ferrara S, et al. On the super-Higgs effect in extended supergravity NUCL PHYS B 640 (1-2): (2002) 46-62 SEP 23 2002

22. Andrianopoli L, D'Auria R, Ferrara S, et al. Duality and spontaneously broken supergravity in flat backgrounds NUCL PHYS B 640 (1-2): (2002) 63-77 SEP 23 2002

23. Ferrara S, Lledo MA Considerations on super Poincare algebras and their extensions to simple superalgebras REV MATH PHYS 14 (6): (2002) 519-530 JUN 2002

24. Andrianopoli L, D'Auria R, Ferrara S Supersymmetry reduction of N-extended supergravities in four dimensions J HIGH ENERGY PHYS (3): (2002) art. no. 025 MAR 2002

25. Andrianopoli L, D'Auria R, Ferrara S Consistent reduction of N=2 -¿ N=1 four-dimensional supergravity coupled to matter NUCL PHYS B 628 (1-2): (2002) 387-403 APR 29 2002

26. Eden B, Sokatchev E, Ferrara S (2,0) superconformal OPEs in D=6, selection rules and non-renormalization theorems J HIGH ENERGY PHYS (11): (2002) art. no. 020 NOV 2001

27. Ferrara S, Sokatchev E Universal properties of superconformal OPEs for 1/2 BPS operators, NEW J PHYS 4: (2002) art. no. 2 JAN 18 2002).

PI-11

F. Palumbo (Resp.), S. Caracciolo (Ass.)

Motivated by the severe difficulties met in numerical simulations of QCD on a lattice at finite baryon density, we have investigated some features of the coupling of the chemical potential in the path integral. The form of this coupling generally adopted was in fact proposed only on euristic grounds. We have therefore constructed an ab initio derivation of the path integral from the trace of the transfer matrix. In this way we have found the coupling of the chemical potential is not unique: in addition to the standard one we have given an alternative expression which is closer to the continuum. We have also constructed an expansion of the quark determinant in a series in the number of quark-antiquark pairs.

References

1. Noncompact gauge fields on a lattice: SU(N) theories F. Palumbo and R.Scimia, Phys. Rev. D65:074509, 2002
2. Transfer matrix with Kogut-Susskind fermions F.Palumbo, Phys. Rev. D66, 075503, 2002
3. Series expansion of the quark determinant in the number of quark-antiquark pairs F.Palumbo, Nucl.Phys. B 643: 391, 2002
4. The chemical potential in the transfer matrix and in the path integral formulation of gauge theories on a lattice F.Palumbo, Nucl.Phys. B 645: 309, 2002
5. Larger physical volume with a noncompact lattice regularization of SU(N) theories G. DiCarlo, F.Palumbo and r. Scimia, Nucl. Phys. Proc. Suppl. 106, 2002
6. Different definitions of the chemical potential with identical partition function in QCD on a lattice F.Palumbo, hep-lat/0210045

PI-31

F. Palumbo (Resp.), A. Barbaro (Ass.), A. Molinari (Ass.), M. Quaglia (Ass.)

We continued our project of deriving the Interacting Boson Model from a fundamental nuclear hamiltonian. We started from the pairing model, introduced in the path integral for this model auxiliary fields and derived a saddle point expansion. This reproduces with good accuracy the energy spctrum and elucidates the connection with the BCS model of superconductivity.

References

1. Noncompact gauge fields on a lattice: SU(N) theories F. Palumbo and R.Scimia, Phys. Rev. D65:074509, 2002
2. Transfer matrix with Kogut-Susskind fermions F.Palumbo, Phys. Rev. D66, 075503, 2002
3. Series expansion of the quark determinant in the number of quark-antiquark pairs F.Palumbo, Nucl.Phys. B 643: 391, 2002
4. The chemical potential in the transfer matrix and in the path integral formulation of gauge theories on a lattice F.Palumbo, Nucl.Phys. B 645: 309, 2002
5. Larger physical volume with a noncompact lattice regularization of SU(N) theories G. DiCarlo, F.Palumbo and r. Scimia, Nucl. Phys. Proc. Suppl. 106, 2002
6. Different definitions of the chemical potential with identical partition function in QCD on a lattice F.Palumbo, hep-lat/0210045

ALFAP

A. La Monaca (Resp.), G. Cappuccio (Ass.), E Costa, G. Di Persio,
L. Pacciani, G. Patria, A. Rubini, P. Soffitta, N. Zema

1 Introduction

ALFAP is an experiment in X-ray Astronomy with the aim to achieve an Advanced Large Field and wide Area Polarimeter for detecting polarized X-rays emitted from extreme compact astronomical sources, like black holes and gamma-ray bursts (GRB). The pertinent physics ranges from the X-ray afterglow sources to the cosmic rays ($>10^{19}$ eV) and neutrinos of very high energy ($\sim 10^{14}$ eV).

ALFAP project differs from the traditional polarimeters. It is based on X-ray gas photoelectric effect and can get a three order of magnitude increase in sensibility. The polarimeter measures the photoelectron direction by multiple ionizations yields by the photoelectron that, drifting inside a couple of scintillation GEMs (Gas Electron Multipliers), produces UV light trace along its path. The instrument does not utilize focussing optics and scans a sky angle of 1.8 steradiants measuring about 4 GRBs/month. However, because of high cost of the project (which should include 25 backside illuminated CCD matrixes), a minimal configuration, using two CCD matrixes was funded by INFN Gruppo 5 (G5).

ALFAP activity has been carried out at LNF in collaboration with CNR-IASF that also contributes to a partial funding, and CNR-ISM (Roma - Tor Vergata) and CNR-ISMN (Montelibretti). Unfortunately during 2002, ALFAP has suffered a dramatic cut-off in the assigned funding by G5, for this reason it was impossible to provide the second CCD matrix necessary to the project.

2 Activities 2002

In spite of the serious above mentioned financial problems during the 2002 year our group worked quite according to the scheduled plans. First of all a new electronic chain and a CCD read-out system were realized. As the first prototype BAL-ALF-010 read-out CCD control system resulted too slow (270 nsec/pixel), a second fast enough BAL-ALF-020 system was realized (40 nsec/pixel). It was able to drive and support our optical images and set-up the GEM output trigger. Furthermore in order to improve the overall reliability the TH79KA95 Thomson optical head was upgraded by interfacing a new Pentium-IV PC via the hosted digital frame grabber.

A couple of 110x110mm^2 large GEM devices, to be used as scintillation chamber and trigger of physical events, were installed on the ALFAP polarimeter (Fig.1). In order to synchronize the data acquisition of the events detected at the GEM output, a suitable synchronization control circuit was realized and connected to the BAL-ALF-020 system.

Finally the mechanic designs and the commissioning were done to external firms for: 1) a rotating table using an aluminium crystal at 45° to realize a polarized X-ray source for laboratory tests, 2) a small GEM (ϕ=38 mm) characterized by a more fine subdivision of photoelectron track and therefore able to provide a more precise definition of polarization direction.

Preliminary measurements and tests with Fe55 were done using an optical camera annexed to the GEM and connected to the CCD, operating in a sub-second frame readout with low noise and a 14-bit A/D converter. A suggestive picture of the pinhole structure of GEM at the focal plane of ALFAP polarimeters CCD is shown in Figure2. A sample of photoelectron track as view by the CCD is also reported in Figure3. The head of the track less bright but clearly visible, provides the

polarization information. It is followed by a large and bright tail, due to a higher energy loss of the photoelectron at the end of the path.

Upgrade of instrumentation, measurements and report notes are in progress.

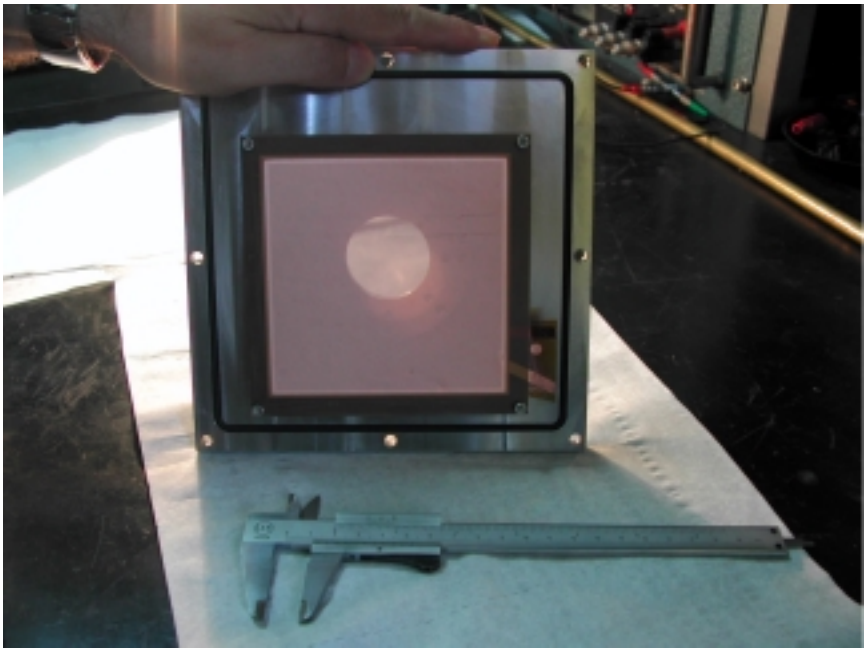

Figure 1: *The GEM devices mounted inside the entry flange of the chamber*

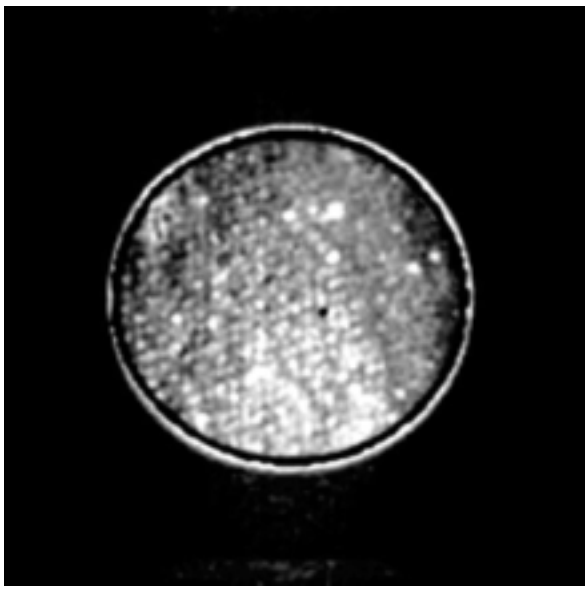

Figure 2: *The picture shows in detail the GEM pinhole structure with diameter ∼50μm, resolved by the CCD matrix, whose pixel size is ∼20μm.*

Figure 3: *Image of photoelectron track at the focal plane of CCD. It is evident the head of the track less bright carrying the polarization information, followed by a large and bright tail due to a higher energy loss of the photoelectron at the end of the path.*

ARCO

F. Tazzioli (Resp.), R. Sorchetti (Tech.)
LNF INFN

Participant Institutions: Universita' Roma2 and INFN, IPJ Swierk

1 Apparatus

From mid 2001 to mid 2002 the planar arc apparatus installed in Roma2 has been considerably improved regarding both the layout and the vacuum system. The new system features two separate deposition chambers, newly designed, sharing the same ultra clean vacuum pumping system. The double chamber system has the advantage of allowing the deposition of different materials. A magnetic filter to remove the macroparticles present in the arc has been installed and commissioned. New sample holders have been built, electrically insulated from the apparatus and controllable in temperature, that allow to make different depositions during the same run.

In collaboration with the Polish IPJ Institute, a linear arc system has been built and set working in the Swierk laboratory . It has been used to make the first deposition tests on Tesla type cavity half-cells, obtaining a proof of principle of the possibility of depositing on such a geometry. In the autumn of 2002 the system has been transported to Roma2, reassembled and commissioned.

2 Results

The production and measurement of various series of samples has allowed to identify and implement several modifications to the apparatus to improve the arc stability and the reproducibility of the sample quality. Measured samples did show film properties quite comparable to those of the bulk material (Tc = 9:26 K, DTc $\leq$ 0.02 K, Jc = A/cm2, RRR from 10 to 50 for thicknesses up to a few tenths of mm). Some samples have been sent to Cornell University for RF properties evaluation.

Detailed information can be found on the web site :
http://ares.roma2.infn.it/ARCO/arcoHome.html

References

1. R. Russo, L.Catani, M. Cirillo, J. Langner, F.Tazzioli, S. Tazzari, "Formation of thin superconducting films by means of ultra-high vacuum arc", Czechoslovak Journ. of Phys., Suppl. D(2002), D829-835

2. R. Russo, L.Catani, J. Langner, F.Tazzioli, S. Tazzari, "Deposition of superconducting films for RF accelerating cavities", Invited paper at the International Conference on Modification of Materials with Particle Beams and Plasma Flows (2002), Tomsk (Ru).

CORA

D. Alesini, R. Boni, M. Ferrario (Resp.), A. Gallo, F. Marcellini, M. Vescovi

1 Activity

The object of the CORA experiment is the study and fabrication of RF accelerating structure prototypes aimed to the particle bunch length reduction by means of the "RF compression" technique. In particular, the LNF group inside the CORA collaboration is studying the application of such a technique to the S-band electron Linac beams to be used for SASE-FEL radiation production.

The velocity buncher concept is based on the longitudinal focussing properties of the slow waves, and allows compressing the bunch length up to a factor 20. The obtainable rms longitudinal dimensions of the bunches are of the order of few hundreds of μm with a controllable effect on the bunch emittance being the compression process completely integrated in emittance correction process which is accomplished in the first 150 MeV of acceleration. The velocity buncher is a modified accelerating structure to allow the inside propagation of a wave whose phase velocity v_{ph} is close to, but slightly less than, the light velocity c (slow wave, $v_{ph}/\mathrm{c} = 0.999 \div 1$). The required gradients are similar to that of the standard S-band structures (about 20-25 MV/m).

During year 2002 the LNF group has completed a preliminary study and defined the approach strategy to the problem. In principle a standard accelerating section (SLAC type, for instance) made of cells whose length is reduced by a factor $\approx 0.1\%$ would have the required characteristics. In this case, at a fixed frequency, the structure would show the nominal cell-to-cell phase advance (equal to $2\pi/3$ in the SLAC case). However, this corresponds to a variation of the nominal cell length of few hundreds of μm. It is mandatory in this case that the new nominal dimensions are strictly respected in the construction phase, and that they do not vary during the operation. On the other hand if a uniform variation of all the RF structure dimensions is considered instead of the longitudinal one only (i.e. a linear scaling of the structure) it turns out that the relative phase velocity variation is proportional to the scaling factor Δf/f through a constant equal to the ratio between the phase and the group velocity of the structure:

$$\Delta v_{ph}/v_{ph} = \Delta f/f(1 - v_{ph}/v_g) \approx -\Delta f/f \;\; v_{ph}/v_g$$

In a SLAC type section the value of the ratio is $v_{ph}/v_g \approx 100$, which means that deformations of the order of 10^{-5} are sufficient to produce phase velocity variation of the order of 10^{-3}. Since the Copper linear thermal expansion coefficient is $\approx 1.6 \times 10^{-5}/^{\circ}$C, a variation of 1°C of the operating temperature of the structure produces a variation of the structure phase velocity larger than desired. This means that a special accelerating section whose length is reduced by $\approx 1\%$ to be used as velocity buncher requires a thermal regulation system capable to stabilize the section temperature at a small fraction of 1°C to maintain the slow wave phase velocity at his correct value. Because of that, there is no reason to use a reduced length structure as velocity buncher. A standard accelerating structure can be used for this task if a sophisticated thermal regulation system is implemented, and the phase velocity can be controlled by changing the temperature set-point. In this case at a fixed frequency the cell-to-cell phase advance will not be exactly $2\pi/3$ anymore. But, being the structure of TW type, any cell-to-cell phase advance is allowed, and this does not affect the accelerating structure operation at all. The experimental activity will be mainly orientated to the demonstration of the feasibility and reliability of such a temperature regulation system to precisely control the accelerating structure phase velocity.

Another important point related to the use of standard SLAC accelerating sections as velocity buncher is that they are "constant gradient" structures, which means that the iris diameter decreases along the section to compensate the wave attenuation and keep the accelerating E-field constant. As a consequence, the group velocity has a significant variation along the structure and, in the thermal deformation regime, the phase velocity will not be perfectly uniform. The impact of such effect on the longitudinal dynamics and on the compression process has to be evaluated by means of numerical simulations. In case this study will show unacceptable beam dynamics effects, the constant gradient structures will be discarded and only "constant impedance" ones considered. The constant impedance structures are those having constant iris diameter along the structure, with no modulation of the group velocity and uniform phase velocity.

In conclusion, to get a stable and reliable slow wave structure we will work on:

- sophisticated and precise temperature regulation systems;
- study on high group velocity accelerating structures to decrease the phase velocity sensitivity to temperature;
- studying the adoption of materials with linear thermal expansion coefficient lower than that of pure Copper.

Constant gradient SLAC type sections will be considered as a first choice and will be studied both experimentally (dispersion curve monitoring at various temperature) and theoretically (effect of the phase velocity variation along the structure on the beam dynamics). As a possible alternative we will design a high group velocity, constant impedance structure to facilitate the phase velocity control through the temperature regulation.

Finally, a numerical evaluation of the effect of the mechanical supporting system on the real thermal deformation has to be worked out, since the mechanical constraints are likely to produce a different final profile with respect to a free linear thermal expansion.

2 Publications

1. M. Boscolo *et al.*,"Beam Dynamics Study of an RF Bunch Compressor for High Brightness Beam Injectors", Proc. of EPAC 2002, Paris.
2. M. Ferrario *et al.* "Recent Advances and novel ideas for high brightness electron beam production based on photo-injectors", Proc. of ICFA Workshop , "The physics & Application of High Brightness Electron Beam", July 1-6 2003, Torre Chia (Cagliari) Italy.

FLUKA

M. Pelliccioni (LNF) (Resp.), S. Villari (Specializ.)

1 Report year 2002

In the past years the Fluka code has been used for the evaluation of the doses due to the galactic component of cosmic rays at aviation altitudes. During year 2002 work was in progress in order to determine the influence of aircraft structures on the calculated doses in atmosphere. To this aim a simplified geometry of Airbus-340 is proposed. This kind of aircraft is operated by many airlines companies and it flies usually on intercontinental routes. Great efforts have been made for the implementation of the model in the geometry of the Fluka code. More than one hundred regions are nedeed in order to obtain a reasonable reproduction. The aircraft geometry is arranged in order to allow the modification of various parameters (fuel and cargo loads, number of passengers, etc.).

2 Program for 2003

During 2003, the geometry of the aircraft model will be completed. Then simulations of the irradiation of the aircraft in the cosmic ray environment will be performed. Effective dose and ambient dose equivalent within the aircraft will be obtained by folding the calculated fluences with appropriate sets of conversion coefficients.

3 Conference Talks in 2001

1. M. Pelliccioni, Flight Dosimetry with FLUKA, DOSMAX Meeting, Vienna 18/03/02.

4 List of Publications 2001

1. P.Beck, D.T. Bartlett, J-F. Bottollier-Depois, L. Lindborg, D. O'Sullivan, L. Tommasino, F. Wissmann, F. d'Errico, W. Heinrich, M. Pelliccioni, H. Roos, H. Schraube, M. Silari and F. Spurny, Space Weather and Radiation Exposure Analysis at Aircraft Altitudes, paper presented at the Space Weather Conference at ESA, Netherlands.

2. D.T. Bartlett, P. Beck, J-F. Bottollier-Depois, L. Lindborg, D. O'Sullivan, L. Tommasino, F. Wissmann, F. d'Errico, W. Heinrich, M. Pelliccioni, H. Roos, H. Schraube, M. Silari and F. Spurny, Investigation of Radiation Doses at Aircraft Altitudes During a Complete Solar Cycle, Proc. "SOLSPA: The Second Solar Cycle and Space Weather Euroconference" , Vico Equense, 24-29 Sept. 2001, European Space Agency Report ESA SP-477 (ESA Publications Division: Noordwijk) (ESA SP-477, February 2002).

3. A. Ferrari, M. Pelliccioni and T. Rancati, Study of the Dosimetric Characteristics of Cosmic Radiation at Civil Aviation Altitudes, Rad. Prot. Dosim. 102, 305-314, 2002.

4. A. Ferrari, M. Pelliccioni and T. Rancati, Cosmic Ray Dosimetry at Aircraft Altitudes, Proceedings of the Workshop on Radiation Dosimetry: Basic Technologies, Medical Applications, Environmental Applications, Roma, February 5-6, 2002, 175-194.

FREEDOM

F. Celani (Resp.), A. Spallone (Ass. Res.), E. Righi (Ass. Res.),
G. Trenta (Ass. Res.), C. Catena (Ass. Res.), G. D'Agostaro (Ass.),
P. Quercia (Guest Res.), V. Andreassi

1 Introduction

The experimental task of FREEDOM (Fusion Research by Electrolytic Experiments of Deuterium On Metals) is to develop [1] highly innovative and reproducible $> 60\%$ success rate) techniques to maximise the value of Hydrogen (H), and later Deuterium (D), concentration into Palladium (Pd), the so-called "overloading", through light water (H) electrolysis (H/Pd > 0.95) with short waiting time for overloading (< 50 hours) and long stability (> 4 hours). Obviously, the final target is to transfer the "method" to heavy water (D_2O) system in order to study, in a more reliable way, some (excess heat, tritium production) of the unusual phenomena related to the so-called "Cold Fusion" phenomena.

During the overloading studies we moved from water-based electrolyte to hydro-alcoholic solution, see details in followings.

In parallel, as spin-off of results obtained with FREEDOM, we were also involved in:

- better understanding of the behavior of a specific bacteria that that we discovered in 1999 inside heavy water (we also studied several other bacteria); we focused on bio-remediation properties using the safe Ralstonia genere;
- new studies and methodologies in order to take full advantage of the anti-cancer property of heavy water at high concentration ($> 60\%$). This property which was known since 1938, although with controversial results. Over 1500 papers have been published up to now on this subject (according to Pub. Med. data bank) and the italian scientists were pioneers in this field. We made the effort to keep such property stable over time and active even at low concentration ($< 20\%$, which are not really dangerous for humans), hopefully down to $< 10\%$, where there are "not–at–all adverse side effects").

We tried to achieve the above by means of:

b1 massive sterilisation of (D_2O) (against the dangerous Stenotrophomonas genera, the other bacteria usually found in (D_2O)), using a ^{60}Co gamma ray source);

b2 purification of (D_2O) (by an innovative, home-made, procedure: 40°C vacuum-distillation and a PTFE-based 100nm ultra-filtration on line). The main distillation system is a "rotavapor" by BUCHI;

b3 promotion of some new and strong synergetic effect, due to our specific physical-chemical treatments.

Task b) is the main interest of the INTRABIO experiment, performed at INFN-LNF, in which several members of FREEDOM experiment are involved. Some preliminary results, with "stabilised" normal and tumour cells in vitro look quite promising (see details in this Activity Report).

[1] Collaboration with ENEA-Frascati and Companies: EURESYS, ORIM, Pirelli Labs, Centre for Materials Development.

2 Experimental activity

The experimental activity performed during year 2002 is summarised in the following.

(a) Further development (Ref. 1), of the new electrolytic procedures (from us introduced since 1999) to maximise H(D) loading into Palladium thin wires (diameter only 50μm) at NTP: alcohol + water (5-10% concentration) solution, alkaline-earth and Hg salts (both at an as-low-as micromolar concentration), pH value (4.0-5.0) optimisation and stabilisation over time (Ref. 2).

We recall again that the "best" procedure found at LNF, with "light" solutions, was fully reproduced, and for some aspects even improved, at Pirelli Labs in Milan ("Advanced Research" department, group leaded from Flavio Fontana). In short, it was obtained a resistance ratio (in Pd wire) as low as 1.05 in a time shorter than 30 minutes from the beginning of electrolysis, made by a solution of both light ethyl alcohol and water (relative concentration close to azeotropic one). We recall that the resistance ratio of Pd is the parameter generally adopted to evaluate the H/Pd and D/Pd ratio. In our peculiar experimental conditions, i.e. long and thin wires of Pd (typical resistance, at the beginning of the experiment, of 15 Ohm for a 30 cm long wire) and electrolytic solution of quite high values of impedance (over several thousand of Ohm), because salts and acid added at only micromolar concentrations, it is quite easy to measure the loading value with an accuracy as good as 0.5%. Moreover, we recall that beyond the maximum relative value of resistivity due to loading, in the "right side" of the loading curve, such value is lower the higher the loading. Up to now, the best value reported in the literature is 1.43 for Hydrogen and 1.6 for Deuterium, at room temperature and at an applied pressure as high as 50000 bar. At present time, we are able to get at NTP, with a success rate of the order of 60%, a resistance ratio of 1.3 with Hydrogen. The results obtained, at least with light water-alcohol, is an experimental proof that the key problem of the overloading process can be kept under control.

(b) Minimization of the input power of electrolysis in order to measure excess heat, if any, with high accuracy, by the reliable "flow calorimeter" method (used since 1992 in our measurements and continuously improved). Results are satisfactory with D. In an experiment, where we get a large enough value of overloading (average D/Pd > 0.95) for > 150 minutes, we get an excess heat of 150mW over an input power of 400mW (Ref. 2 and Ref. 5).

(c) Minimization of the amount of Tritium (T, half life 12.3 yr, β^- 100% emission with end point at 18.6keV) and measurement of some anomalous excess of it, if any. The T is intrinsically present inside the solution because of the use of the heavy water. Its typical concentration, in a reactor grade ((D_2O) isotopic purity 99.97%) "low Tritium content heavy water", is of the order of 200dpm/ml. The amount of T anomalously produced in some "lucky" experiments, as reported in the literature, is of the order of only 10^4-10^6atom/s. Our results were positive (i.e. excess T detected out of experimental statistical or systematic errors) just because we used a heavy ethyl alcohol-heavy water mixture (C_2H_5OD 93%, (D_2O) 7%): that mixture had an overall low value of T, in comparison with usual experiments were only concentrated D_2O is used. According to our measurements, the C2H5OD (from Aldrich), had a T content (20.3dpm/ml) over 10 times lower then that of D_2O (from Ontario Hydro, 219.6dpm/ml) used. We detected Tritium in excess with good (over 6 standard deviations) statistical significance (Ref. 3 and Ref. 6). Measurements about T were performed in a joint collaboration with ENEA Frascati (group leaded from Sandro Sandri) using a high sensitivity instrument: Wallac 1414, WinSpectral vl.20 (EG&G Company). It is based on the well-known and reliable liquid scintillation counting method. Because of the large amount of alcohol, the Liquid Scintillation Cocktail (LSC) was based on "Ultima Gold" from Packard.

Moreover, the amounts of liquid to be analysed was quite large (4ml added to 16ml of LSC, in spite of usual 1ml to 4ml) in order to reduce both statistical and systematic errors at low level counting, as in our experiment. In short, we expected at the end of the experiment, in the final solution (i.e. after addition of small amounts of deuterated salts and acids, in respect to the initial solution), 37.6(± 2%)dpm/ml and found 51.8(± 2%)dpm/ml. For the measurements we adopted the "double blind" procedure.

We stress that we get excess Tritium only in the experiment, quoted in Ref. 2, that get large D overloading and some excess heat. In other words, at least two anomalies look related each other.

(d) Analysis, by ICP-MS (Inductively Coupled Plasma, Mass Spectroscopy) and, for some elements, also ICP-OES (Optical Emission Spectroscopy) of new elements, if any, coming out after prolonged electrolysis. The elements were found on: Pd cathode surface, solution (dissolved in the electrolyte), mixed in the "powder" collected at the bottom of electrolytic cell.

The reason of such specific analysis come out from the experiments performed at Mitsubishi Heavy Industries (Yokohama, Japan) by Dr. Y. Iwamura and collaborators. They found, and published on Japanese Journal of Applied Physics (July 2002), the apparent "transmutation" of Strontium into Molybdenum and Caesium into Praseodymium when a proper x(like a diode structure) multiple layer of Pd-CaO-Pd is subjected to prolonged (1-2 weeks) flow of deuterium gas. Because of our specific method of electrolysis and salt used (Sr, Hg at micromolar concentration with Ca always present both in Pd wire and Sr salt as impurities; promotion of a multi-layer coating of Pd surface due to several loading-deloading cyles) there are several aspects similar to that used (but in a gaseous environment) from Mitsubishi group. The measurement where made using a high resolution ICP-MS (made by HP-Yokogawa) located at Centro Sviluppo Materiali Laboratories (Castel Romano). The numbers of calibration and blank were especially high, and repeated over time, in order to rule out interference problem or malfunctioning of the measurement system. We stress that, in our analysis, the amount of main elements (Pd, Sr, Hg) are several order of magnitude larger with respect to the "new elements", if any, to be detected: some "matrix effect" can affect the results. Moreover, we adopted the "double blind" protocol in order to rule out any "interference" due to the human operator. We have found a measurable amount of Molybdenum, not explainable with any kind of contamination, and with an isotopic composition different from the natural one (Ref. 4).

3 Reasons to use acidic water solution, with micromoles of Sr and Hg, and even alcohol-water, in electrolytic overloading of Pd with H(D)

The lack of reproducibility observed in "Cold Fusion" experiments is mainly connected with the difficulty of obtaining loading atomic ratios (D/Pd) close to one. It has been shown in fact that such a high D/Pd ratio, which is considered a necessary condition for the production of the so called "anomalous heat", is very difficult to be obtained and, in particular, to be maintained for a reasonably long time. In order to solve such a serious problem our group has performed a systematic campaign of experiments, starting with a simpler and more economic Pd-H system, with the goal of finding a protocol capable to ensure a fast and reproducible loading with thin Pd wires, up to a H/Pd ratio close to one. The protocol, tested successfully in three different Laboratories (Pirelli-Labs, Milan-Italy; Stanford Research Institute International-USA; our Laboratory, in two completely different arrangements of the electrolytic cells), is based (in an acidic environment, pH about 4.5), on the addition of a very small amount (typically 10-5M) of alkaline-heart ions

(Strontium seems to be the most effective) to the re-distilled water used for the preparation of the electrolyte. The use of re-distilled water was found to be a mandatory requirement: it was found that the impurities normally still present in the distilled and/or de-ionised water can negatively affect the loading process. The following explanations are due in large part to the very close collaboration (since 1989) with electrochemistry at EURESYS company (Paolo Marini, Vittorio di Stefano; Missa Nakamura since 1994) and support, mainly for chemical and metallurgical analysis, at ORIM company (led by Alfredo Mancini). The protocol is based on the following physics-chemical principle: Strontium ions (as $SrCl_2$) are added to the re-distilled water in such an amount that no precipitation as $SrCO_3$ can occur in the bulk of the electrolyte with the carbonic ions (as H_2CO_3) dissolved in the water at NTP. Strontium carbonate is allowed to precipitate only on the cathode surface, because of the local alkalinization produced by the flowing of the electrolytic current: it is well known that the solubility of carbonates decreases strongly following the increase of the pH. In the cathodic process:

$$2H_2O + 2e \rightarrow 2H(ads) + 2OH^-$$

the OH^- ions formed on the cathode promote the precipitation of $SrCO_3$. The atomic Hydrogen adsorbed on the cathodic surface can either be absorbed into the Pd bulk

$$a) \quad H(ads) \rightarrow (H)Pd(loading\ \ reaction)$$

or bubbled out as H_2 gas

$$b) \quad 2H(ads) \rightarrow H_2(parasitic\ \ reaction).$$

The intrinsically catalytic surface of Pd, used as cathode, promotes generally the b reaction, deleterious to (H,D) overloading. By using our procedure, viceversa, because of the precipitation on the cathodic surface of a thin layer of $SrCO_3$ the catalytic properties are consistently reduced and the loading reaction a) turns to be predominant, thus allowing a fast achievement of H/Pd ratio =1. We have found that the addition of very small amounts of mercuric ions are also effective in maintaining the loading level over a large period of time. Hg, because of its ability to form amalgamas, is supposed to act as "anti-cracking agent" against Pd damage due to H,D absorption. When we tried to apply our protocol for D-Pd loading and H_2 was replaced by D_2 the results in terms of D/Pd were consistently lower, and/or unstable, than those obtained with light water. The reasons of such an evident failure were essentially:

- The amount of the impurities generally contained in the "as received" heavy water is too large. Foreign inorganic ions, galvanically deposited on the cathode, were found to hinder the formation of the proper $SrCO_3$ layer. Double distillation of D_2O which is very difficult to be accomplished because of its hygroscopicity (no contact with the atmosphere is required), is a necessary but not sufficient pre-treatment.
- Heavy water contains bacteria that were identified by us in a joint collaboration with ENEA-Casaccia (group leaded from Giacomo DAgostaro). These bacteria belong to two new species, which were also found to form colonies on the Pd cathodhic surface disturbing, in such a way, the Deuterium absorption.

Therefore, several long treatments of the D_2O are needed, like the addition of KMnO4 (1g/l) at a pH adjusted in sequence at $1 \rightarrow 7 \rightarrow 13 \rightarrow 7$ (i.e. addition of D_2SO_4 to get pH=1, LiOD to get pH=13). The multiple distillations have to be performed under nitrogen at 90°C and at 40°C under

vacuum: final conductivity, at NTP, has to be lower than 3μmS/cm). The most critical parameter of the D-Pd loading seemed to be the ratio between the amount of the impurities present in the electrolyte and the surface of the cathode. In trying to minimize time-consuming and troublesome pre-treatments needed to "kill" the bacteria and purify the heavy water from inorganic and organic pollutants, we realized that the problem could be tackled with two different approaches:

1. build up a very thin cell, just around the electrodes (Pd surface about $1cm^2$), thus containing a very small amount of electrolyte (i.e.50cc $\Rightarrow$ negligible amount of impurities);

2. fill the cell recently used in our experiments, whose volume is about 750cc, with a new electrolyte prepared by mixing a large quantity of suitable organic solvent (i.e.700cc) with a smaller quantity (i.e.50cc) of heavy water.

In both cases, with respect to the 750cc of D_2O normally used in our tests, the reduction to 50cc is equivalent to a 15 times reduction of the impurities, arising from D_2O, which could be deposited on the cathodic surface. The #2 seemed to be much more attractive because of its simplicity (no need to build a new and very delicate cell) and its flexibility (the ratio between the organic solvent and the heavy water can be varied to a large extent). As far as the choice of the organic solvent is concerned, the following requirements should be satisfied:

* large miscibility with water;

* very small amount of H_2 present as residual impurity (isotopic contamination of H in the D-Pd loading);

* no (or negligible) acid properties (isotopic contamination for partial dissociation and production of H^+ ions);

* boiling point not too far from 100°C.

Alcohol, keton, esther seem to be the solvents which meet the above requirements. If the hydro-organic electrolyte could be considered an elegant solution for the problem of the impurities, the proper precipitation of $SrCO_3$ on the surface of the cathode seemed difficult to accomplish in the new ambient. Key problem: how to control the concentration of carbonic ions ? Taking into account that the actual concentration, the "activity", of the ions in the hydro-organic electrolyte could be remarkably higher than their nominal concentration (referred to both the components of the liquid phase), we realised that Strontium ions could be precipitated as $SrCO_4$ even though the solubility product of this compound is about 50 times higher than that of $SrCO_3$. In this case, the $SrCO_4$ precipitation in the hydro-organic ambient could be accomplished simply by controlling the amounts of Sr^{++} and $SO_4^{=}$ ions added to the electrolyte. After several tests we found that a suitable electrolyte could be prepared just by using 700cc of ethyl alcohol (95% concentration, i.e. 50cc is water) and by adding to the hydro-alcoholic solution 20mg of $SrCl_2$, 1-2cc of H_2SO_4 (0.01M) and 0.5-2cc of $HgCl_2$ (0.01M). The electrolysis was started with the following conditions: anode: Pt (wire, length 60cm, diameter 200μm); cathode: Pd (wire, total length 60cm with 2 portions of 30cm, diameter 50μm); electrodes parallel (inter-distance 4cm); current:10mA.; voltage:20-100V; T=24°C.

In conclusions, the loading of the cathode, in some "lucky" experiments, was high enough to get some anomalous effects (heat, Tritium, "new elements") as reported in Ref.: 2, 3, 4, 5, 6.

Further studies are in progress in order to increase the number of experiments that give the "anomalous effects" of our interest.

4 Publications

1. A. Spallone, F. Celani *et al.*, "Experimental studies to achieve H/Pd loading ratio close to 1 in thin wires, using different electrolytic solutions". LNF-02/015 (P), 2 Luglio 2002. Contributed Paper at the ICCF9, Beijing (China), 19-25 May 2002; to be published as Conference Proceedings by Springer und Verlag.

2. F. Celani, A. Spallone *et al.*,"Electrochemical D loading of palladium wires by heavy ethyl-alcohol and water electrolyte, related to Ralstonia bacteria problematics". LNF-02/014 (P), 2 Luglio 2002. Invited Paper at the ICCF9, Beijing (China), 19-25 May 2002; to be published as Conference Proceedings by Springer und Verlag.

3. F. Celani, A. Spallone *et al.*,"Evidence of anomalous tritium excess in D/Pd overloading experiments". LNF-02/013 (P), 2 Luglio 2002. Invited Paper at the ICCF9, Beijing (China), 19-25 May 2002; to be published as Conference Proceedings by Springer und Verlag.

4. F. Celani, A. Spallone *et al.*,"Unexpected detection of new elements in electrolytic experiments with deuterated ethyl-alcohol, Pd wire, Sr and Hg salts". LNF-02/031 (P), 18 Dicembre 2002. Invited Paper at the "4th Meeting of Japan CF-Research Society", Morioka, October 17-18, 2002. Submitted to "Japan CF-Research Society" for publication.

5. F. Celani, A. Spallone et al. *et al.*, Evidenze di Trizio e calore anomali in esperimenti elettrolitici di alcool etilico ed acqua pesante con catodi filiformi di Palladio". Contibuted Paper at "LXXXVIII Congresso della Società Italiana di Fisica". Alghero, 26 Settembre-1 Ottobre 2002

6. Francesco Celani, "Novità significative presentate al IX Congresso Internazionale sulla Fusione Fredda (ICCF9)". Relazione su Invito at "LXXXVIII Congresso della Società Italiana di Fisica". Alghero, 26 Settembre-1 Ottobre 2002

INTRABIO

E. Righi (Resp. Naz.), C. Catena (Ass.), F. Celani, D. Pomponi, G. Trenta (Ass.)

1 Experiment purpose

The INTRABIO project is essentially oriented to investigate biophysical, particularly oncological responses of living matter under the action of physical stressors with the use of physical resources, mainly ionising and non ionising radiations. At this aim we programmed the study, employing infrared DAFNE radiation, of particular proteins structure and abundance in living cells after a chemical, biological or physical mutagenic damage. This particular object of our experiment would firstly allow qualitative and quantitative analysis of p53 protein which has an oncological interest.

Jointly with the FREEDOM Group we would investigate the properties of the Ralstonia detusculanense as far as its bioremediations ability, its eventual activity in oncological processes and his feature as hydrogen producer is concerned. Namely the preliminary results we obtained in a unscheduled study curried out in the previous year was very promising.

Nevertheless with the aim of investigate on oncological problems we intended to verify if the Ralstonia or at the contrary the heavy water was responsible of the effects the historical literature indicates on some tumours regression in animals. So our program was also to investigate the response of some oncological cell lineages to the irradiated and to non irradiated heavy water. A LNF report has already edited on this subject in 2001 year.

At the same time we had to settle the tails of the research work we conducted in the previous years on validation of our methodology in micronucleous technique trough the international HUMN project and of the evaluation of the individual radiation sensitivity in irradiated oncological patients.

2 2002 results

The international intercomparison of the HUMN Project reached its object with the final recent publication of results collected in 24 world-wide laboratories. Whereas the publication of the results on the evaluation of the radiosensitivity in irradiated oncological patients is still in progress as a manuscript no. JRB/2002/73 submitted to International Journal of Radiation Biology.

The unavailability for a long time of the infrared beam from DAΦNE prevented us from initiate the research on numerical and conformational protein alterations following the action of a physical stressor; but we intend to undertake this objective in the near future.

Also the research on the investigations of the distinctive features of the Ralstonia detusculanense are at moment deferred awaiting the response of the Istituto Superiore di Sanit on the environmental biocompatibility of the bacterium.

The research on the effects of heavy water in three stabilized cell lineages: RPMI 1788 (normal leucocytes), CCRF-CEM (lymphoblastic leukaemia) and DAUDI (Burkitt lymphoma), bear evidence of a very high sensitivity to the treatment with heavy water irradiated at high dose compared with to the treatment with the heavy non-irradiate water. The scientific literature looked up dont include experiments curried out with a similar methodology. The following Figures 1, 2 (where "D2OR" and "D2O" mean respectively: treatment with irradiated and with non-irradiated heavy water) indicates the surviving fraction (SF) or the apoptosis percentage of RPMI, CEM and DAUDI stabilized cell lineages as a function of deuterated water concentration. Those outcomes, that are a fortuitous result of an interesting serendipity process, incite us to enlarge the research

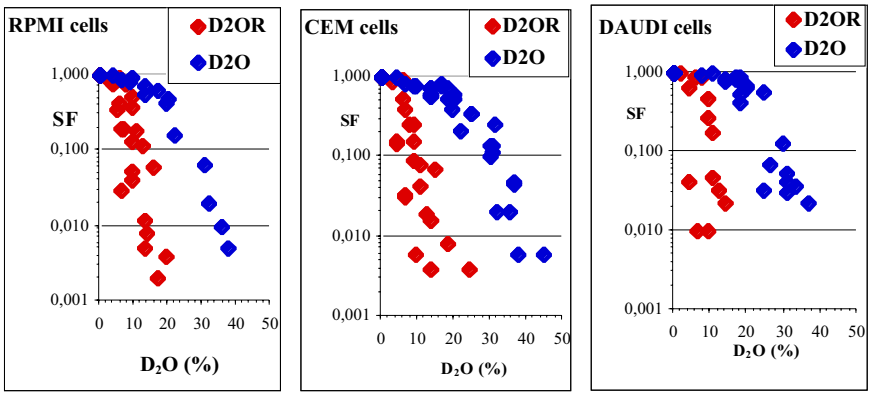

Figure 1: *Lethal effect induced by D_2O (irradiated and non irradiated) in the three lines considered.*

to some both normal and pathological primary cell lineages to reach a more realistic results usable, we hope, in a practical application.

The collaboration with the FREEDOM group is in progres as far as the bacteriological component and related consequences in the heavy water is concerned. A particular attention was devoted to the uncontrolled pH variations and to the captation of a specific metal (Hg) fed in solution to stabilize the system. For this topic you can see the FREEDOM report.

3 Publications

1. Fenech M. et al. (Trenta G. for DOSIME Group/LNF-INFN) Intra- and inter-laboratory variation in the scoring of micronuclei and nucleoplasmatic bridges in binucleated human lymphocytes: Results of an international slide-scoring exercise by HUMN project. Mutation Research (2003) **534**: 45-64.

2. Righi E. Interventi nellirradiazione esterna. Corso su gestione degli interventi nelle emergenze complesse a seguito di contaminazione nucleare, biologica e chimica Giornate di studio su: "Emergenze sanitarie per eventi accidentali e ostili", Padova 20-21/9/2002 e Fiano Romano 25/9/2002.

3. Trenta G. Interventi nella contaminazione radioattiva. Corso su gestione degli interventi nelle emergenze complesse a seguito di contaminazione nucleare, biologica e chimica Fiano Romano 25/9/2002.

4. Righi E. Rivelazione di mine antipersona: aspetti di olfattometria comparativa - Convegno su "Limpegno delle Nazioni Unite contro le mine antipersona" Bracciano 12/12/2002.

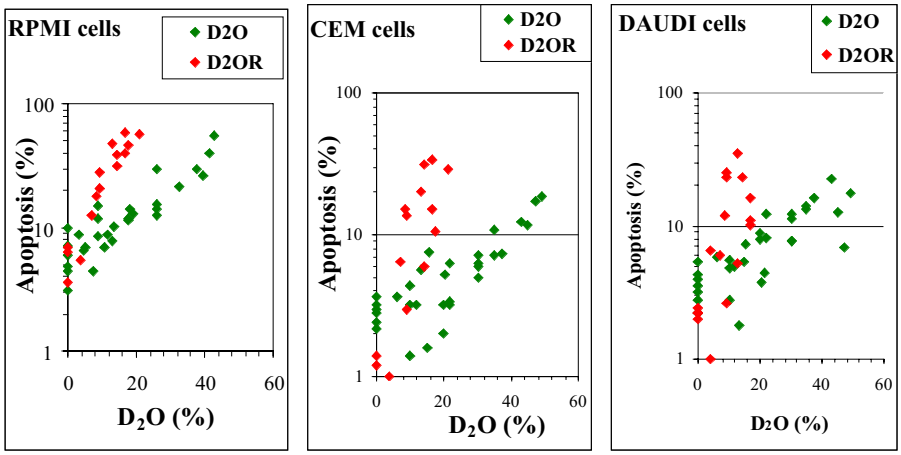

Figure 2: *Apoptosis induced by D_2O (irradiated and non irradiated) in the three lines considered.*

5. Trenta G. Interventi per contaminazione da sostanze radioattive. Giornate di studio su: "Emergenze sanitarie per eventi accidentali e ostili", Padova 20-21/9/2002.

6. Trenta G. Aspetti sanitari del rischio lavorativo Giornate di studio in materia di sicurezza negli ambienti di lavoro dellINFN 20-21 febbraio 2002 LNGS ; 10-11 aprile 2002 Sez. Trieste.

7. Trenta G. Session Chairmanship on "Radiation health effects and Radiobiology" in European IRPA Congress "Towards harmonisation of radiation Protection in Europe". Florence 8-11 October 2002.

8. Trenta G. Rischio, informazione, aspetti medico-legali. 16 Corso avanzato di Radioprotezione Medica, Bressanone 26-30 agosto 2002.

9. Righi E. Le linee guida per la sorveglianza medica: commenti e aggiornamenti. 16 Corso avanzato di Radioprotezione Medica, Bressanone 26-30 agosto 2002.

10. Malesani F, Righi E. Il giudizio didoneit in Radioprotezione medica: unarte difficile. 16 Corso avanzato di Radioprotezione Medica, Bressanone 26-30 agosto 2002.

11. Trenta G. Malattie genetiche e radiazioni (UNSCEAR 2001). 16 Corso avanzato di Radioprotezione Medica, Bressanone 26-30 Agosto 2002.

12. Righi E. Biodosimetria: il Manuale IAEA n. **405** del 2001. 16 Corso avanzato di Radioprotezione Medica, Bressanone 26-30 Agosto 2002.

13. Righi E. Presupposti clinico-epidemiologici della sorveglianza sanitaria dei lavoratori esposti a radiazioni ionizzanti, con particolare riferimento alle basse dosi. DBA 2002 Modena, 26 settembre 2002.

14. Trenta G. PC nellesposizione a radiazioni e ad altri cancerogeni. 16 Corso avanzato di Radioprotezione Medica, Bressanone 26-30 agosto 2002.

15. Trenta G., Righi E. La probabilit di causa e la medicina legale. In: Barni M. "Consulenza medico-legale e responsabilità medica" . Giuffrè Editore, Milano (2002).

16. Trenta G. Radon e rischio sanitario. Convegno AIRM su "Esposizione al radon e sorveglianza medica". Acireale, 6-7 Giugno 2002.

17. Catena C. *et al.* Radiobiological aspects of lymphocytes before and during radiotherapy: micronuclei, 3AB index, apoptosis and cell survival. Submitted 2002 to International Journal of Radiation Biology.

18. Trenta G. *et al.* Radioprotezione delloperatore e del paziente: evoluzione della normativa. Congresso nazionale AIRB, Torino 24-26 ottobre 2002.

19. Trenta G. *et al.* Epidemiologia: il rischio, le serie epidemiologiche, gli strumenti valutativi. Corso di formazione su "Le emergenze radiologiche: aspetti clinici e di igiene pubblica" San Marino, 4-6 novembre 2002.

20. Righi E. Effetti deterministici: caratteristiche cliniche ed esperienze operative. Corso di formazione su "Le emergenze radiologiche: aspetti clinici e di igiene pubblica" San Marino, 4-6 Novembre 2002.

LCCAL

S. Bertolucci, S. Miscetti (Resp.)

1 Introduction

An excellent jet energy reconstruction is one of the most important requirements for a Linear Collider Detector[1]. This can be achieved by separating in a jet the contribution due to charged and neutral particles by combining the information from the tracking and calorimeter systems. This request translates in designing a calorimeter able to distinguish electromagnetic from hadronic showers with the highest possible granularity while keeping in mind costs and a *still* reasonable number of channels. The LCCAL collaboration proposes an hybrid technique[2] for the electromagnetic compartment consisting on a sampling calorimeter made by 45 absorber and scintillator layers and 3 planes of Si pads.

2 Status of prototyping

A prototype has been built alternating layers of lead absorber $(25 \times 25 \times 0.3)\text{cm}^3$ with scintillator layers subdivided in 25 x-y cells of $(5 \times 5 \times 0.3)\text{cm}^3$. Each cell is readout via a green WLS fiber inserted in the scintillator with the "sigma-tail" scheme[2]. The calorimeter is constituted by a total of 45 layers (corresponding to $45 \times 0.6/1.1\ \text{X}_0 \sim 25\ \text{X}_0$) grouped in four longitudinal z-sectors S1÷S4 integrating 4,7,11,23 layers respectively. The WLS fibers are then optically connected to clean fibers and are grouped in 25×4 bundles (one bundle for each x-y cell and longitudinal subdivision). The prototype has been built in Padova by the INFN group of LCCAL while the final assembly has been done at LNF (Fig.1) where the central (3×3) x-y cells of each longitudinal sector have been optically coupled to traditional photomultipliers (PM). The external (4×4) x-y cells have been summed in a less clear fashion after integrating also along z to reduce the number of used PMs. During 2003, we plan to install multianode Hamamatsu PMs (H6568) to readout all 100 cells.

Three planes of 252 silicon diode pads ($0.9 \times 0.9\ \text{cm}^2$) have also been built and are to be inserted at $\sim$ 2,6 and 12 X_0 from the calorimeter front face (i.e. at the end of longitudinal sectors S1,S2,S3). Each plane consists of 3×2 detectors of 6×7 pads connected trough a conductive glue to a PCB where the front-end chip VA Hdr9c from IDEas is mounted.

A preliminar test has been carried out at CERN SPS H4 beam exposing the S1 sector and a prototype for the Si pad detector to electrons of 40, 50 GeV and pions of 50,150 GeV. This allowed us to measure the light yield for the scintillator layers, to control the uniformity on response along the cell ($< 10\%$) and to measure the position resolution for the Si pads. A first test on the response to MIPs and electromagnetic showers was also done. At the moment of writing, we are carrying out tests at the Frascati Beam Test Facility (BTF) and planning to have more extensive studies at the CERN SPS beam during summer 2003 with the detector fully assembled.

3 First test at BTF

A preliminar succesfull test has been carried out at BTF during November 2002 with the prototype equipped with 48 PMs and no silicon pads. We exposed the detector to electron beams of 480 MeV working in single electron mode to check the response of all scintillator layers and to make the first round of gain equalization.

Figure 1: *LCCAL prototype during the final assembly at LNF.*

P_B(MeV)	E(Cnt)	E/P_B(Cnt/MeV)	σ_E(Cnt)	σ_E/E (%)	$\sigma_E/E \times \sqrt{E/GeV}$ (%)
486	1302.0 ± 2.2	2.68	229 ± 2	17.6	12.3 ± 0.1
400	1092.0 ± 3.5	2.73	198 ± 4	18.1	11.4 ± 0.2
300	816.8 ± 2.2	2.72	173 ± 2	21.2	11.6 ± 0.1

Table 1: *Results on energy response and resolution for cell 13 at BTF.*

The beam was crossing the cell almost orthogonally with a beam spot of ~ 1 cm^2. In Fig. 2.top the total energy distribution of cell 12 is shown (black solid line) before any HV adjustment. The relative gains of all cells, with respect to the ones of sector S2, were adjusted by miniminizing the observed total energy resolution. In Fig.2.top the red line shows the energy distribution after applying such a minimization procedure. A much better separation between one and two electron spectra can be observed. In Fig.3 a comparison of the energy distribution for the longitudinal sectors between cells 12 and 14 is reported to show the uniform behaviour of the prototype after calibration.

We have also taken data at 3 different energy values with beam impinging at calorimeter center (cell 13). A reasonable linearity in response and an energy resolution better than $\sim 12\%/\sqrt{E/GeV}$ are achieved (see Tab.1).

References

1. TESLA Technical Design Report DESY 2001-011 ECFA 2001-209, Part IV.
2. S. Bertolucci et al. "Construction and test of an Electromagnetic Calorimeter Prototype" DESY PRC R&D 00/02.

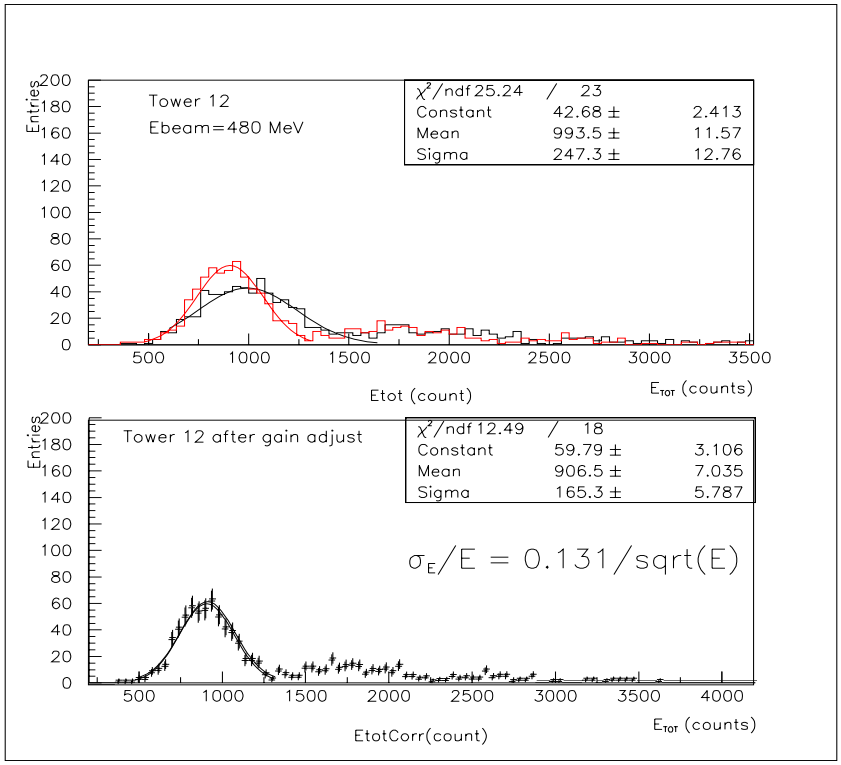

Figure 2: *(Top) Total energy distribution before (black line) and after (red line) gain adjustment. (Bottom) Gaussian fit to total energy distribution.*

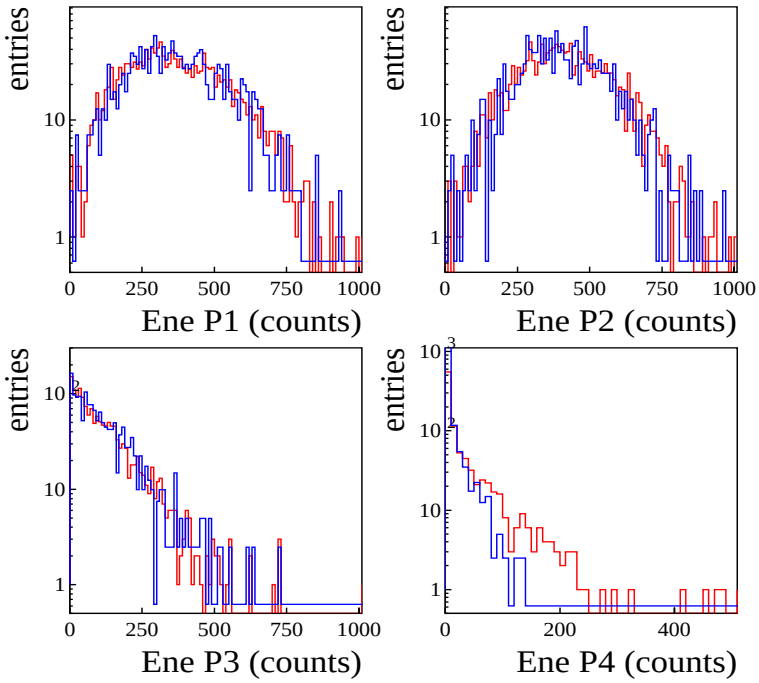

Figure 3: *Energy distributions for longitudinal sectors S1÷S4 for cell 12 (blue) and cell 14(red).*

Ma - Bo

D. Di Gioacchino, U. Gambardella (Resp.)
G. Celentano, A. Mancini, P. Tripodi
S. Pace

1 Purposes of the project

The *Ma-Bo* experiment is devoted to analyze the use of the magnesium diboride MgB_2 compound. As it becomes superconducting at temperatures below 39 K, its potentiality either in wire applications (magnets) or in thin films applications (RF applications or electronics) will be investigated. Six sections of INFN are involved: Genova (group leader), Milano, Torino, LNL, LNF, and Napoli, in collaboration with INFM Genova, CNR Genova, and ENEA Frascati.

2 The Frascati group activity

The Frascati group takes care of studying the technology of thin film deposition as well as to analyze the MgB_2 superconducting properties by means of current transport and *ac* susceptibility measurements in high magnetic fields.

2.1 Thin film sinthesis

The activity carried out in this field is focused to set up a suitable process to realize MgB_2 superconducting thin films [1)]. In order to analyze the process parameters which can give rise to crystallize the correct phase, small samples have been grown on [111] MgO, or Al_2O_3 *r*-cut substrates. We use *dc* magnetron sputtering deposition technique from stoichiometric MgB_2 targets, followed by a simple annealing at moderate temperatures, in the range of 500 C. The deposition route also included sputtering processes assisted by pure Mg co-evaporation, alternate layer depositions MgB_2/Mg, with different heat treatments. The aim of the work is to achieve the optimized Mg phase diagram pressure to promote MgB_2 phase sinthesis. XRD, SEM and critical temperature measurements are routinely performed on samples. The present highest critical temperature is 27 K. Some samples have been analyzed in Genova by means of XPS, while others have been used in Torino for testing photolitography and wet etching processes.

2.2 AC susceptibility measurements

During this year we studied the vortex dynamics of the MgB_2 bulk samples. We have computed the irreversibility line using the onset of the measured third harmonic amplitude of *ac* susceptibility in *dc* magnetic field [2)]. The analysis of magnetic behavior of the MgB_2 bulk samples has also included magnetization cycles measured in an high field vibrating sample magnetometer, to gather further information on the fluxon dynamics at lower frequencies. Magnetization cycles at different temperatures have been compared to the 3rd harmonic amplitude of the *ac* susceptibility measurements at comparable fields. ¿ From these analyses, with the support of numerical simulations, a 3D glass collective pinning behaviour was derived [3)].

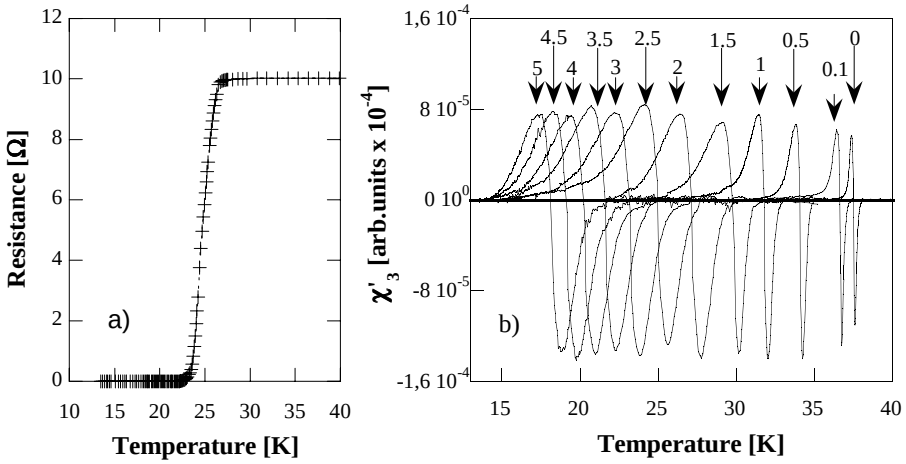

Figure 1: *a) superconducting resistive transition in our MgB_2 film; b) real amplitude 3rd harmonic of the ac susceptibility for a bulk MgB_2 sample under different applied dc magnetic fields.*

3 List of Conference Talks by LNF Authors in Year 2002

1. U. Gambardella [1], "Growth of superconducting thin films", 5th Symposium of European Vacuum Coaters, Sep 29th-Oct 2nd, 2002, Anzio, Italy

References

1. A. Mancini, V. Galluzzi, U. Besi Vetrella, V. Boffa, G. Celentano, L. Ciontea, U. Gambardella, G. Grassano, T. Petrisor, A. Rufoloni, S. Sprio, M. Vadrucci, "Properties of MgB_2 films grown by means of different vapour phase techniques", IEEE Applied Superconductivity (2003), to be published

2. D. Di Gioacchino, P. Tripodi, U. Gambardella, "Third harmonic ac susceptibility measurements on MgB2 bulk: irreversibility line and frequency dynamic behaviour", Physica C: Superconductivity (2003), to be published

3. D. Di Gioacchino, U. Gambardella, P. Tripodi, G. Grimaldi, "Irreversibility line and magnetic field dependence of the critical current in superconducting MgB2 bulk samples", Superconducting Science and Technology **16** (2003), to be published

[1] On behalf of the Ma-Bo collaboration

MUST

S. Dabagov, A. Marcelli (Resp.), M. Matzuritsky (Ass.), A. Soldatov (Ass.), A. Raco (Tecn.)

1 Activity

This project is based on an European, American and Japanese INFN Patent concerning a the novel idea to manufacture more efficient curved x-ray diffractors using the Bragg geometry (see Fig. 1, top drawing). Because the standard x-ray diffractors exploit cylindrical geometries (e.g., Johann and Johansson curved crystals), these devices are really new systems based on a pseudospherical geometry. These multi-crystals diffractors have a novel layout capable of focussing an x-ray beam with high resolution and large throughput and of providing, at constant resolution, a gain up to one order of magnitude larger than a spherical or cylindrical crystal of comparable size. In 2002 we completed tests and analysis of the prototypes with a cylindrical shape and assembled a system based on perfect crystals (quartz) for a commercial micro-analyzer. We also completed the manufacturing and tested two large devices with three large spherical crystals devoted to synchrotron radiation applications. Fig. 1b shows a photograph of the first three-step spherical diffractors devoted to synchrotron radiation experiments. These devices have been assembled with three quartz crystals and with silicon spherically bent crystals respectively, that were set on a spherical holder using the optical contact method (Fig. 1, bottom photo).

With this experiment funded by the Vth Scientific Committee of INFN we demonstrated the feasibility of this novel layout and that significant gain can be achieved by these compact systems, in a wide range of photon energies. To clarify the potential gain of these prototype systems we show in Fig. 2 (top plot) the diffracted intensity by a multistepped device manufactured with quartz (10-11) crystals at the energy of the Sn La x-ray emission. This comparison demonstrates that the resolution is excellent and does not degradate when only the central step (black curve) or the whole system (4 steps) (red curve) is illuminated by x-ray radiation. In Fig. 2 (bottom) we show also the diffracted intensities by the same device at the energy of the Mo La x-ray emission.

The results achieved by MUST indicate that the multi-stepped pseudo-spherical design offers all the expected advantages in term of resolution and transmitted photon intensity. Moreover, it also demonstrated that these devices may replace with success curved crystals with Johann or Johansson mountings, installed in commercial spectrometers working with photons or using electron beams. MUST closed the activity within the 2002 with success. To conclude the experiment it is necessary to test the large spherical devices using synchrotron radiation beams. Experiments are planned in the next months at the DAΦNE Light laboratory. (Additional information are available at the URL: http://www.projectx.aaanet.ru).

2 References

1. E.M. Latush and M.I. Mazuritsky, Dependence of the Resolution of an X-Ray Diffractor on the Shape and Curvature of the Reflecting Surface, Tech. Phys. Lett., V 28 (2002) 21.

2. E.M. Latush and M.I. Mazuritsky, A Focusing X-Ray Diffractor: Effect of the Crystal Bending Parameters on the Spectral Resolution, Tech. Phys. Lett., **V28** (2002) 142.

3. E.M. Latush *et al.*, A Large-Aperture X-Ray Monochromator with stepped surface, Instruments and Experimental Techniques **45** (2002) 819.

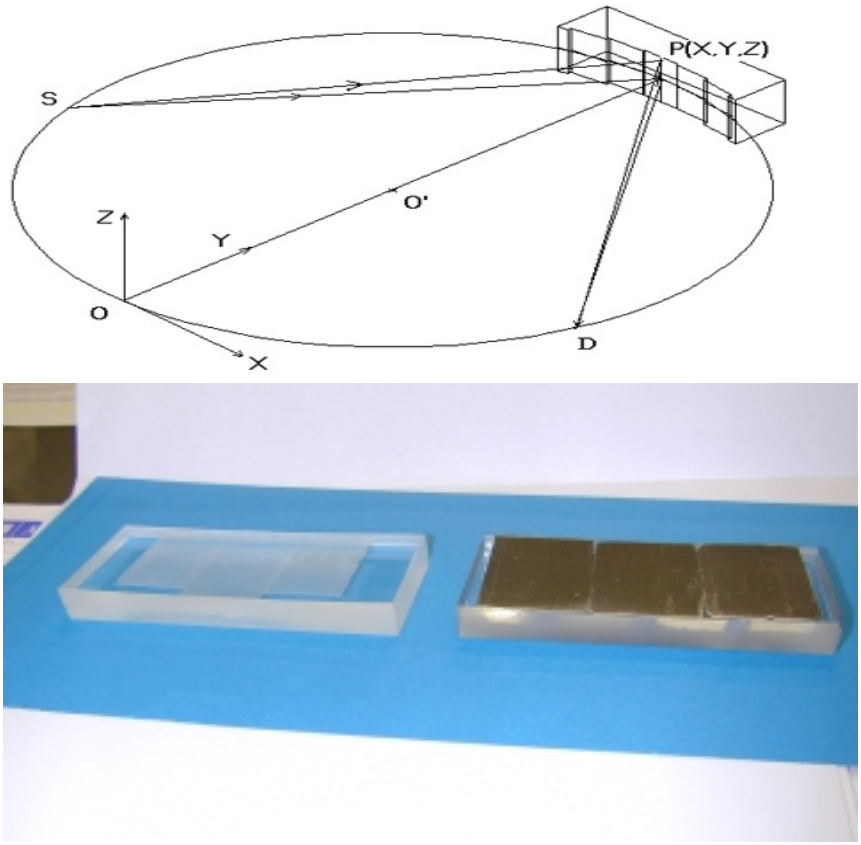

Figure 1: *The top drawing shows the optical layout of the diffractor geometry of a multistepped device. The bottom photo shows the two large diffractors for synchrotron radiation application assembled with both quartz and silicon spherically bent crystals.*

4. E.M. Latush *et al.*, High resolution compact multi-stepped x-ray diffractors, NIM **A491** (2002) 512.

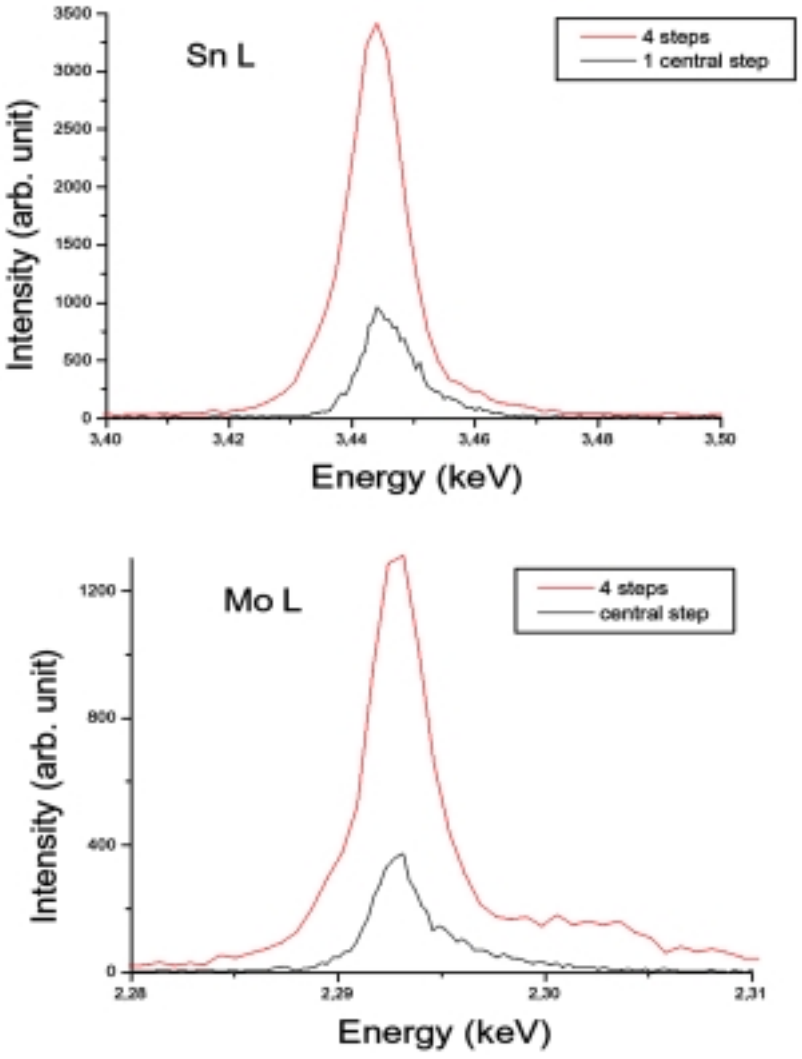

Figure 2: *Diffracted intensity by a multistepped device manufactured with quartz (10-11) crystals at the energy of the Sn La x-ray emission line (top) and at the Mo La x-ray emission line (bottom). In both panels the black curve refers to the central crystal only, while the behaviour of the entire system, e.g., 4 illuminated crystals, is represented by the red curve.*

NANO

S. Bellucci (Resp.), S. Bini, G. Giannini, A. Marcelli,
F. Tombolini (Dott.), Z. Wu (Ass.), G. Cappuccio (Ass.)

1 Experimental task and activity

1) Manufacture of C Single Walled Nanotubes (SWNT) (ropes and isolated) by arc discharge. 2) Use of C nanotube films for the study of field emission properties, in order to determine their efficiency for the realization of coldcathods and analyse the dependence of the efficiency on the nanotubes alignment. 3) Use of ordered C nanotube films for applications of the channeling mechanism to steering of accelerated particle beams. Synthesis and characterization by SEM, TEM and STM of C SWNT and setting up of a Chemical Vapor Deposition equipment for producing patterned C Multi Walled Nanotubes (MWNT) and SWNT. Setting up of a chamber for field emission measurements. Theoretical study of the effect of doping in transport properties for C MWNT and simulations for channeling through SWNT.

2 Main results

Good quality samples of aligned ropes of SWNT, with the average tube diameter of 1.3 nm and a bundle diameter of 40 nm. Good field emission properties of the samples, with activation fields of 6 V/micron and a current emission of 1 micro A/ mm2. Our results may be checked against future measurements carried out in MWNT and nanotubes of very large radius. Such features may be of interest when developing carbon-based devices made of graphene and nanotube structures with different shapes. Precise determination of the optimal experimental conditions for channeling of accelerated particles (protons, positrons, photons, neutrons) through micro- and nano-structured crystals and films of aligned nanotubes, as promising candidates for producing highly focused beams.

3 International leadership and benchmarking

In SWNT synthesis and field emission studies, we confirmed that our experimental parameters are in line with the best achievements in the international community active on this topic. In channeling the group has a clear worldwide leadership, especially from the point of view of theory and simulations. Our good results attracted interest for collaboration from industrial sponsors, such as VARIAN, MICOS, HITESYS. Our group is coordinating a proposal for a FP6 European Network of Excellence called PROMS with 31 research groups, 165 reserachers and 35 PhD students. Our group organizes since 2000 a series of international meetings in the area of nanotechnology www.lnf.infn.it/conference/nn2003. Part of the yearly event consists in a school dedicated to training of Ph.D. students and young postdocs in the basics of nanoscience. Also, our group in Frascati has been selected as the host of the 2004 international conference on relativistic channeling and coherent phenomena in strong fields.

4 Spinoff: interdisciplinary relevance and industrial impact

The enhancement in the efficiency and stability of directional electron emission in cold cathods, for the production of laser-like collimated electron beams, at low cost and with a long lifetime.

Our results based on field effects from C nanotubes can be useful for benchmarking with other techniques developed at INFN, based on high temperature diamond emission. Development of new radiation sources and steering of accelerated particle beams through channeling mechanism. Production of micro and nanostructured films and crystals, as promising candidates for producing highly focused beams, aimed at improving tumor diagnostic and therapy, as well as for biological and space research applications (e.g. interactions of protons with DNA, molecules, living cells). Theoretical study and simulations for providing a fundamental understanding of nanoscience, aimed at improving basic knowledge in material science and condensed matter systems. Our activity drags interest from collaborating enterprises, including large companies (VARIAN, MICOS) which are world leaders in their fields (vacuum technology, sensors, robotics and mechanical devices), as well as SME (HITESYS) with an eminent position in the market of electro-medical devices. Nanostructured materials can be used for applications, such as sensors, filtering, vacuum, electronic and mechanical devices, radiotherapy, sterilization, beam control for medical and environmental uses, sensing nanoparticles and layered mineral structures for catalytic reactions in industrial and environmental applications.

5 Talks at conferences in 2002

1. S. Bellucci, Frascati, 19th International Conference on X-Ray and Inner-Shell Processes, Rome, Italy
2. Z.Y. Wu, 19th International Conference on X-Ray and Inner-Shell Processes, Rome, Italy
3. F. Tombolini, Frascati, 19th International Conference on X-Ray and Inner-Shell Processes, Rome, Italy

References

1. S. Bellucci, S. Bini, V.M. Biryukov, Yu.A. Chesnokov, S. Dabagov, *et al*, "Experimental Study For The Feasibility Of A Crystalline Undulator", physics/0208028, Phys. Rev. Lett. (in press).
2. S. Bellucci, V.M. Biryukov, Yu.A. Chesnokov, V. Guidi and W. Scandale, "Channeling of high energy beams in nanotubes", presented at COSIRES 2002 (Dresden, 24-27 June 2002), physics/0208081, Nucl. Instr. Meth. B (in press).
3. S. Bellucci, V.M. Biryukov, Yu.A. Chesnokov, V. Guidi and W. Scandale, "Making Micro- and Nano-beams by Channeling in Micro- and Nano-structures", physics/0209057, Phys. Rev. Special Topics AB (in press).
4. S. Bellucci and V.M. Biryukov, "Nanotube diameter optimal for channeling of high-energy particle beam" con V.M. Biryukov, Phys. Lett. **B542**, 111 (2002).
5. Z. Wu, J. Zhang, K. Ibrahim, D.C. Xian, S. Bellucci, *et al*, "Structural determination of titanium-oxide nanoparticles by x-ray absorption spectroscopy", Appl. Phys. Lett. **80**, 2973 (2002).

OBD

M. Pelliccioni (Resp. naz.)

1 Report year 2002

The dosimetric characteristics of galactic cosmic radiation have been studied using the Monte Carlo transport code Fluka. In particular, the depth dose curves in the ICRU sphere have been determined with the aim to make clear the relationship between effective dose and ambient dose equivalent. The effective quality factor at 10 mm depth in the ICRU sphere has been evaluated. At civil aviation altitudes, a value of 2 seems to be appropriate, independently of altitudes, latitude and solar activity. The equivalence of ICRU tissue and A-150 plastic has been investigated. The A-150 plastic can be considered a good substitute of ICRU tissue for photon, proton, electron and muon spectra, while some differences occur in the case of neutrons. The response of a tissue equivalent ionization chamber in the cosmic ray environment has been simulated. It is demonstrated that a crude approximation of the ambient dose equivalent could be obtained multiplying by 2 the absorbed dose measured by a such type of device with walls 10 mm thick.

Work is in progress is order to determine the influence of the aircraft structures on the calculated doses in atmosphere. Since the OBD experiment has been closed by 2002, the work will be completed in the frame of Fluka program.

2 Conference Talks in 2002

1. M. Pelliccioni, Dosimetria dei raggi cosmici ad alta quota, INFN - Commissione Scientifica Nazionale V, Dosimetria: Tecnologie di base, Applicazioni mediche, Applicazioni ambientali, Workshop 5-6 Febbraio 2002.
2. M. Pelliccioni, Flight Dosimetry with FLUKA, DOSMAX Meeting, Vienna 18/03/02.

3 List of Publications 2002

1. P.Beck, D.T. Bartlett, J-F. Bottollier-Depois, L. Lindborg, D. O'Sullivan, L. Tommasino, F. Wissmann, F. d'Errico, W. Heinrich, M. Pelliccioni, H. Roos, H. Schraube, M. Silari and F. Spurny, Space Weather and Radiation Exposure Analysis at Aircraft Altitudes, paper presented at the Space Weather Conference at ESA, Netherlands.
2. D.T. Bartlett, P. Beck, J-F. Bottollier-Depois, L. Lindborg, D. O'Sullivan, L. Tommasino, F. Wissmann, F. d'Errico, W. Heinrich, M. Pelliccioni, H. Roos, H. Schraube, M. Silari and F. Spurny, Investigation of Radiation Doses at Aircraft Altitudes During a Complete Solar Cycle, Proc. "SOLSPA: The Second Solar Cycle and Space Weather Euroconference" , Vico Equense, 24-29 Sept. 2001, European Space Agency Report ESA SP-477 (ESA Publications Division: Noordwijk) (ESA SP-477, February 2002).
3. A. Ferrari, M. Pelliccioni and T. Rancati, Study of the Dosimetric Characteristics of Cosmic Radiation at Civil Aviation Altitudes, Rad. Prot. Dosim. 102, 305-314, 2002.
4. A. Ferrari, M. Pelliccioni and T. Rancati, Cosmic Ray Dosimetry at Aircraft Altitudes, Proceedings of the Workshop on Radiation Dosimetry: Basic Technologies, Medical Applications, Environmental Applications, Roma, February 5-6, 2002, 175-194.

POLYX

G. Cappuccio (Resp., Ass.), S. Dabagov, A. Marcelli, V. Sessa,
C. Veroli (Tecn.), M. Kumakhov, R. Fedorchuk

1 Experiment aims

The main aim of this project, funded by INFN - Gruppo V, is to study and to utilize polycapillary optics (PO) in x-ray applications using both conventional sources (x-ray tubes) and synchrotron radiation (SR). With polycapillary lenses (PL) it is possible to increase the radiation density in the focal spot position; with polycapillary semi-lenses, parallel x-ray beams can be obtained from divergent sources or convergent beams from parallel sources (SR). Straight polycapillaries (pillars) allow parallel beams to be matched with x-ray detectors, monochromators, etc. One of the purposes of the POLYX project is to insert PO on the x-ray diffractometer now operative at the Dafne Light Laboratory. The advantage in using PL for diffraction measurements will be a net increase in the spot density on the samples, and a decrease in the peak profile width, which corresponds to an increase in spectral resolution.

2 2002 Activities

During 2002 the research activity was slowed down for three reasons. Firstly, the setting-up, alignment and adjustment operations of the x-ray beam-line at the Dafne Light Laboratory were partly limited by the few Dafne machine runs available for such activities. Secondly, use of the x-ray diffraction station, which had been operating with a Cu x-ray tube since the beginning of the year, was limited by the radiation protection rules, i.e., when the diffraction station is in use the x-ray beam-line hutch cannot be accessed and viceversa. These facts, plus the prevalent role of the alignment operations, strongly affected the use of the diffraction station. Finally, the delivery of two polycapillary lenses by a company from Saratov (Russia) was considerably delayed due to Russian administrative-bureaucratic problems. Therefore the main activity in 2002 was the design and construction of special holders for the polycapillary lenses and two mechanical statives to support the Gimbal mounts in front of the x-ray tube and scintillation detector (Fig.1). Software programs were also developed for positioning the lens through the remote control of the Gimbal mounts. A preliminary test was done using the programming statement set supplied with the positioning actuators. Afterwards, in order to improve the reliability it was decided to develop a control program using the LabView package, which is more powerful both in the mechanical control operation and in the visual presentation of the results.

3 2003 Program

The main activity in 2003 will be to prove the experimental advantage of inserting polycapillary optics on the high-resolution x-ray diffraction station. For thin solid films analysis we would like to put a polycapillary half lens in front of the x-ray tube and a cylindrical capillary lens ("pillar")

as a collimator in front of the scintillation detector. Such a configuration will produce a quasi-parallel x-ray beam that will reduce the defocusing effect due to the flat-sample, displacement, and transparency errors that are typical of Bragg-Brentano geometry. For micro-diffraction measurements we would like to utilize a focusing lens, which allows the beam to be concentrated in a sub-millimeter spot size. Finally it would be possible to increase the synchrotron radiation spot density at the entrance of the diffractometer by using tapered polycapillary optics.

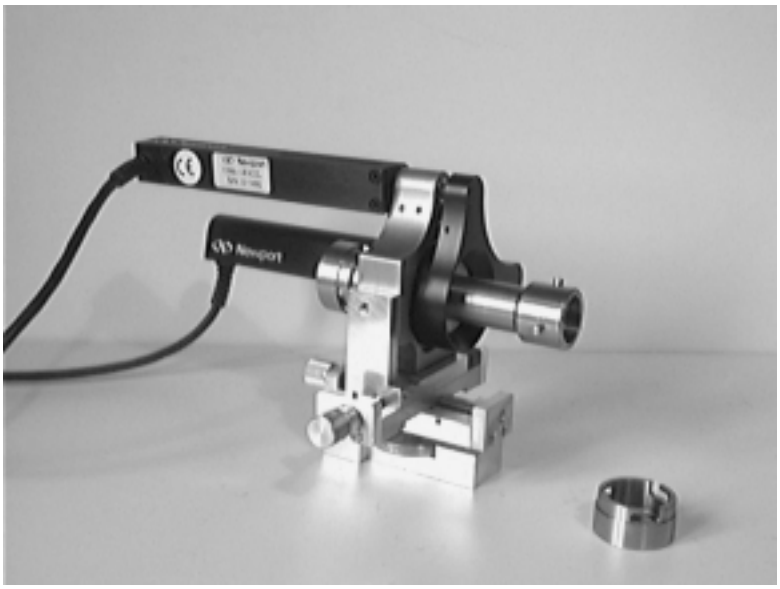

Figure 1: *Cylindrical holder for polycapillary lens installed on the Gimbal mount*

4 Publications

1. S. B. Dabagov, A. Marcelli, G. Cappuccio, E. Burattini, "On propagation of X-rays in capillary channels", Nucl. Instr. and Meth. B 187, 169-177, (2002).

2. S. B. Dabagov, "Quantum theory of x-ray channeling in capillary systems", Proceedings of SPIE 4765, 87-98(2002).

3. G. Cappuccio, S. B. Dabagov, "Alignment procedure and divergence behaviour in capillary optics: first results with X-ray tubes and synchrotron radiation", Proceedings of SPIE 4765, 99-103 (2002).

4. S. B. Dabagov, "Wave theory of X-ray scattering in capillary structures", X-ray spectrometry 31, 333-341, (2002).

5 Conferences

1. S. B. Dabagov, "Status of capillary Optics" Workshop "Applications of Carbon Nanotubes and Fullerites in High Energy Physics, X-ray and Neutron optics" Athens, May (2002)

2. S. B. Dabagov, "On features of X-ray channeling in capillaries" European Conference on Energy Dispersive X-ray Spectrometry Berlin, June (2002)

SAFTA

D. Alesini (Art. 23), V. Fusco (Dott.), M. Migliorati (Ass.), C. D'Alessio (Laur.),
L. Palumbo (Ass.), B. Spataro

1 Aim of the experiment

The aim of SAFTA group is mainly related to the study of the electromagnetic interaction between a particle beam and the accelerator pipe wall, the generation of the parasitic fields, the corresponding energy loss and the instability effects. The main investigated subjects are: the coupling impedance of the LHC and SPS machines and a parasitic diagnostic device for bunch length-position monitoring. The first activity, done in collaboration with SL/AP group at CERN, consists to estimate the longitudinal and transverse impedance budget of the LHC and SPS rings in order to evaluate the instability thresholds. Results obtained from simulations have been cross-checked with analytical estimations and whenever possible with experimental results. The second activity has been focused to completely characterize a new promising bunch-length position monitor for ultra-short bunches in term of theoretical analysis, numerical simulations and measurements.

2 Main results of 2002

The energy losses, the parasitic resonances and the longitudinal and transverse impedances of several beam pipe components have been studied with the MAFIA3D, HFSS and ABCI codes:

- a) pumping port cavity of the SPS machine;
- b) kicker magnets for the SPS machines;
- c) hybrid beam position monitor for LHC.

In all cases the analysis of the results have suggested an optimization of the design in order to obtain acceptable values of the coupling impedance and energy loss. Particularly interesting has been the investigation of the special type beam position monitor, which will be installed in some dedicated positions of the LHC straight sections. It is referred to as "hybrid monitor" in the sense that the BPM's body is equipped with both the conventional button electrodes, and, in addition to it, also contains strip lines.

The bunch length-position monitor consists of a small coaxial cavity coupled to the beam pipe through four slots (see Fig. 1).

If the length of the cavity is properly chosen, the beam power spectrum lines can excite the resonant longitudinal or transverse modes in the cavity resonator. Probing the field by a small antenna it is possible to measure the amplitudes of the beam power spectrum lines and to calculate the bunch length and the position. The theoretical and numerical study was carried out by using the Bethes theory and by performing electromagnetic simulations with MAFIA3D and HFSS.

Wire measurements have been made on the aluminum prototype shown on Figgs. 2 and 3. In particular to excite the dipolar modes the wire inside the beam pipe has been properly displaced from the axis of the beam pipe with a thin nylon wire connected to the central wire and displaced from the beam pipe axis in a controlled way.

The comparison between the theoretical and the experimental results confirm the potential application of this device as a bunch-length position monitor. The very low coupling impedance of the device and the possibility of a calibration by simply wire measurements make the device hopefully usable in the accelerators machines.

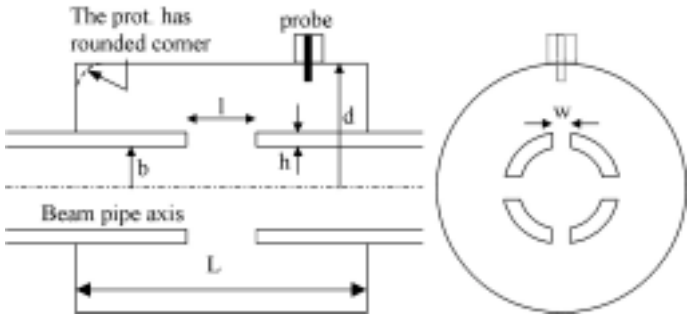

Figure 1:

3 Activity 2003

It is foreseen the continuation of the successful with the SL/AP of CERN in order to study other components to be installed on LHC and SPS machine. In particular it will be investigated the cold-warm transitions with different geometries for the SPS and the collimator for the LHC superconducting magnets. For the microwave monitor we intend to investigate the possibility to modify the slot sizes in order to use the monitor in different operating conditions and we intend to find possible applications of the device in modern accelerator projects.

4 Publications

1. L. Palumbo*et al.*, "On trapped modes in the LHC recombination chambers: numerical and experimental results", submitted for publication on NIM.

2. B. Spataro *et al.*, "Impedance of the LHC hybrid Beam Position Monitor BPMC", submitted for publication on LHC Project Note.

3. B. Spataro *et al.*, "Electromagnetic simulations and RF Mesurements Results of an ultra-short Bunch length monitor", Proc. of the 2002 European Part. Acc. Conf., 1834, Paris 2002.

4. L. Palumbo *et al.*, "Wakefields due to surface waves in a beam pipe with a periodic rough surface", Physical Review Special Topics - Accelerators and Beams, **5** - 044401 (2002).

5. M. Migliorati *et al.*, "Interplay between electron beam instabilities and storage ring FEL dynamics", Nuclear Instruments and Methods in Physics Research, A**491** (2002), pp. 507-511.

6. M. Migliorati *et al.*, "An analytical solution for the Haissinski equation with purely inductive wake fields", Europhysics Letters, **60** (1), pp. 66-71, (2002).

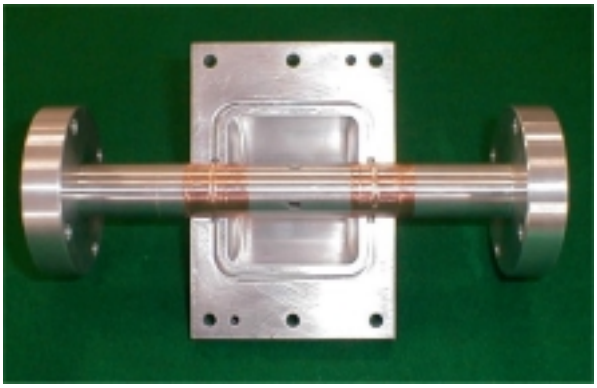

Figure 2:

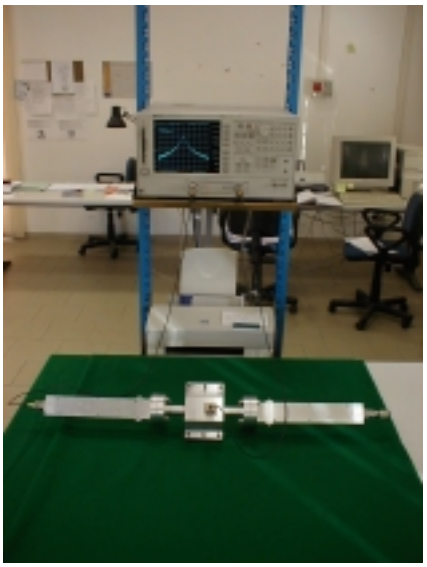

Figure 3:

SFERA-2

F.Tazzioli (Resp.), C.Vicario(Dott.)

Participant Institutions:

Univ. Roma1-Dip. Energetica and INFM; Univ. Roma2-Dip. Scienze e Tecnologie Chimiche; Univ. Milano-Dip. Fisica e INFN

1 Introduction

Year 2002 was a concluding one for the SFERA experiment . It was launched in Frascati Laboratories in 1999 with the aim of studying robust electron photo-cathodes for the use in advanced particle accelerators. Two main classes of wide band gap insulators have been investigated: ferroelectric ceramics and synthetic diamond CVD films. The cathodes were illuminated by intense Nd:Yag laser harmonics with 25 ps pulse duration. The Milan and Roma1 collaborators have supplied the ceramic samples. The Roma1 and Roma2 collaborators have produced and characterized the synthetic diamond CVD films. All the participants have contributed to the acquisition and elaboration of the data. The experiments on ferroelectrics as photoemitters were abandoned after a thorough study because the value of the quantum efficiency (Q.E.)resulted too low for the envisioned application. The CVD films instead have given interesting results that have spurred the participants to propose for year 2003 a new experiment (CAERES) dedicated to the study of diamond films .

2 Activity

In 2002 we have pursued improvements of the Q.E. of diamond films by varying the deposition parameters, by adding various impurities (Nd, N) and by terminating the surface with Hydrogen. Emission efficiencies up to 5x 10^{-6} at 266 nm laser wavelenth (4.7 eV photon energy), that is below the diamond band gap, have been obtained. A strategy to improve the efficiency has been devised, supported by theory. A special device, the RF streak camera [1], has been set up to analyze the temporal distribution of the emitted electrons.

3 References

References

1. M.Castellano et al, Measurement of the temporal response of photocathodes, LINAC 2000 Conference,169.

2. I. Boscolo *et al*, Photo-emission from diamond films illuminated by intense Nd:Yag laser harmonics, submitted to Applied Physics, A.

3. S.Orlanducci et al, Structural features of diamond layers photo-emitting at sub-band gap energies, Submitted to Diamond and rel. mat.

SIEYE2

L.Marino (Ass.), G.Mazzenga (Tecn.), M.Ricci (Resp.)

Participant Institutions:

ITALY: INFN LNF, Firenze, Roma2, Trieste;
RUSSIA: MePhi, IBMP, RKK"Energia" (Moscow)
SWEDEN: KTH (Stockholm)

1 Introduction

The SIEYE2 experiment has been carried out on the MIR Space Station to study, using a silicon strip segmented detector, the biophysical effects related to the radiation environment inside the Station (altitude 400 Km , inclination 51.5°) with particular attention to the phenomenon of "Light Flashes" (LF) [1]. A prototype of the detector (SIEYE1) was placed on the Station MIR in October 1995 obtaining, during its two years in operation, 25 measurement sessions with 6 different astronauts, and recording more than 50 LF's. Following the success of this mission, a new detector (SIEYE2) has been developed and built in order to have a more accurate analysis of the radiaton flux (in particular for high Z particles) in the zone of the South Atlantic Anomaly (SAA) and in the subpolar zones. The equipment of SIEYE2 provides the opportunity for a simultaneous definition of the particle trajectory and its arrival time, an estimation of its energy and the recognition of its charge. A complete description of the experiment is given in [2], [3] and [4]. SIEYE2 was delivered on board of the Space Station MIR in October 1997, and several acquisition sessions (since February 1998) have taken place with different astronauts until the reentry of MIR in March 2001 and its subsequent destruction in the Earth atmosphere.

The SIEYE2 experiment makes use of silicon strip detectors to measure the coincidence between the passage of a ionizing particle and the occurrence of a LF. The astronaut wears a helmet which holds on its side the detector box; a joystick, connected to the same detector box, and controlled by the acquisition PC, is used for LF acquisition. The system can be seen as a completely software controlled solid state instrument. Its main characteristics are: small dimensions, portability, low power consumption, user friendly interface, real time data analysis.

The detector is compact (max dim. 264 mm) and with a low mass (less than 5.5 Kg); it measures particle energy losses from 0.25 to more than 250 MeV and determines the particle trajectory with an angular accuracy of 3 degrees.

Analysis of SIEYE2 data is completed [5], [6], [7], [8], [9], while a new project, called ALTEA [10] is under development to install on board the International Space Station a larger telescope with the concomitant use of electroencephalography and visual stimulation, to directly correlate LF and particle crossing the head with brain activity. A preliminary version, called SIEYE3-ALTEINO [11], has been carried on board the International Space Station by italian astronaut R. Vittori in April 2002 and is foreseen to take data for about two years.

2 Activity of the LNF group

The LNF group has taken the responsibility of the design, test and construction of all the mechanical structures and interfaces of both SIEYE1 and SIEYE2 detectors contributing also to the

integration of the mechanical support for the DAQ. It participates in the beam test activity (performed at GSI-Darmstadt and TSL-Uppsala). In view of the new ALTEA experiment, the LNF group, with the support of the local Service of Development and Construction of Detectors, has taken the responsibility of the design, test and construction of the complete structure and assembly of the qualification and flight models of SIEYE3-ALTEINO for ground testing and calibrations.

References

1. G. Horneck: "Radiobiological experiments in space: a review", Nucl. Tracks Radiat. Meas., 20, 185 (1992).
2. A. Galper et al.: "Sileye on MIR – First active detector for the study of light flashes in space", Proceeding of the Sixth European Symposium on Life Sciences Research in Space 17-21 June, Trondheim, Norway, (1996).
3. A. Morselli, et al.: "Cosmic ray studies on the MIR space station", Proc. XXIV ICRC, Durban 1997 Vol.5, (1997).
4. G.Furano et al.: "Measurement of Nuclear Mass Distribution of Primary and Recoil Heavy Ions inside MIR Space Station with SilEye Silicon Detector", Proc. XXVI ICRC, Salt Lake City vol.5 p128 (1999).
5. S.Avdeev et al.:"The SilEye nuclei cosmic ray and eye light flash experiment onboard the Mir Space Station", Proc. XXVII ICRC, Hamburg (2001) p.1745.
6. M.Casolino et al.:"Cosmic ray measurements on board space station MIR with SILEYE-2 experiment", Proc. XXVII ICRC, Hamburg (2001) p.4011.
7. V.Bidoli et al.:"In-flight performances of SilEye-2 Experiment and cosmic ray abundances inside space station MIR"; Journal of Physics G: Nuclear and Particle Physics 27, 2051 (2001).
8. S.Avdeev et al.:"Eye light flashes on the Mir Space Station"; Acta Astronautica, 50, 511 (2002).
9. P.Maponi et al.:"A syncitium model for the interpretation of the phenomenon of anomalous light flashes occurring in the human eye during space missions"; Nuovo Cim., 116B, 1173 (2001).
10. L.Narici et al.:" The ALTEA facility on the International Space Station"; Physica Medica Suppl. 1 17, 255 (2001).
11. M.Casolino et al.:"The Sileye/3-Alteino experiment on board the International Space Station"; Nucl.Phys. 113B, 88 (2002).

SUE

F. Belloni (Ass.), D. Bettega (Ass.), E. Burattini (Resp.), P. Calzolari (Ass.), A. Grilli (Tecn.), F. Monti (Ass.), A. Raco (Tecn.), L. Tallone (Ass.)

1 Activity

The increase in the amount of UVB radiation (280 320 nm, 4.5 3.9 eV) reaching the earth surface due to the reduction of the stratospheric ozone layer has potentially significant impact on the incidence of skin cancer in humans. Goal of the SUE (Solar Ultraviolet Effects) experiment is a systematic investigation, as a function of the wavelength, of various biological effects (cell death, micronucleus induction and oncogenic transformation) induced in cultures of human cells and their progenies by the UV radiation B band.

The experiment is carried out by means of a dedicated beamline (the UV beamline at the DAΦNE-Light facility), using monochromatic photon beams obtained from Synchrotron Radiation (SR) emitted at the DAFNE storage ring, in operation at the Frascati INFN National Laboratories. The possibility to work with SR monochromatic beams in the wavelength range of 280 320 nm, with higher resolution and intensity as compared to conventional sources, offers a unique experimental technique in the study of UVB biological effects. An apparatus devoted to photobiology has been set up in order to perform the irradiation and the first treatments of the cell cultures.

The SR photon beam, extracted from a wiggler (six pole equivalent, critical energy ϵ_c= 311 eV for 0.51 GeV electron beams) under a horizontal collection angle of 15 mrad, is splitted into two beams by a grazing incidence ($\theta_i = 40$ mrad) Au coated mirror, resulting in two separate beamlines, the X-ray beamline (straight line) and the UV beamline (deflected of about 80 mrad). The UV beamline collects radiation at energies below 800 eV (corresponding to the grazing incidence gold mirror cut-off) and carries it down to the experimental hutch dedicated to the irradiation of cell cultures. At the end of the beamline, a sapphire window (26 mm diameter and 2.7 mm thick) separates the irradiation apparatus working in air from the vacuum of the SR beamline. The experimental hutch is equipped with a Jobin-Yvon monochromator able to select photons in the spectral range between 2 and 6 eV with a resolution of about 0.3%. After the sapphire window, the beam outgoing the pipe is suitably deflected and focussed at the entrance slits of the monochromator by means of a spherical and a plane Al coated mirrors. Since photons of wavelengths below 180 nm are not transmitted through the sapphire window, second order light contamination is avoided. The monochromatized output beam travels inside a special sample holder mounted for irradiation.

Since uniform exposure (within 10%) of the sample is required, a careful analysis of the light intensity distribution at the sample position has been carried out using suitable radiographic plates placed at the sample position. The scanning of the developed film by means of a microdensitometer shows that the optical density is reasonably uniform inside the spot, with small stochastic fluctuations (within 10% of the mean value) over a sharp plateau (Fig. 1).

Dosimetry is accomplished by previously determining the radiant power on the sample per unit of electron beam current by means of a pre-calibrated Hamamatsu Photonics silicon photodiode. Exposure time that gives the dose required is then obtained by monitoring the beam current in the DAΦNE electron ring during irradiation. Linearity of the ratio of the radiant power to the electron beam current versus electron beam current has been checked in a range of currents from 0.1 A to 1 A. Typical values of the radiant power on the sample per unit of electron beam current for monochromatic (2.5 3 nm bandwidth) beams in the UVB band from 280 to 300 nm range from 3 to 5 μW/A. The value of the total radiant power per electron beam current in the whole

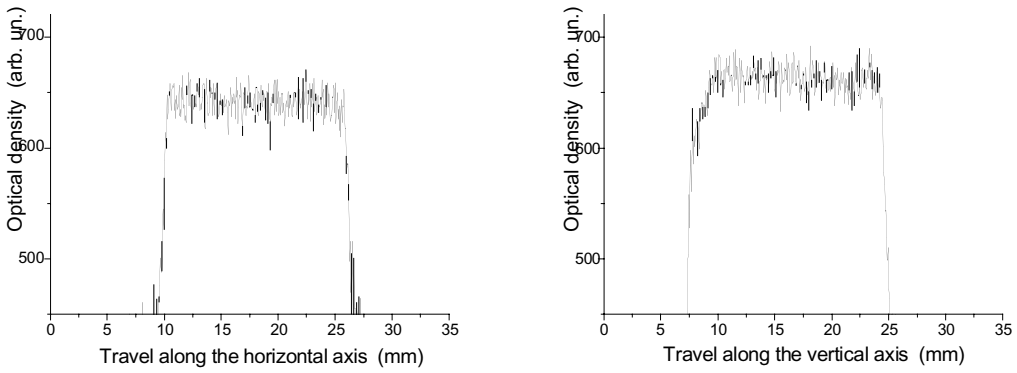

Figure 1: *Analysis of a spot of monochromatic radiation at 280 nm, recorded on a radiographic film placed at the sample position. The film optical density along two orthogonal diameters of the spot is shown.*

spectral band from 200 nm to 1200 nm (range of sensitivity of the photodiode) was also measured both at the entrance (1.5 mW/A, in good agreement with the SR flux estimated from theoretical calculations) and at the exit slits of the monochromator (zero order diffraction), where it reduces to 0.42 mW/A, due to the losses in the optical system inside the monochromator. In the last months of 2002, two irradiation sessions were performed aimed to study various early and delayed biological effects on human cells (survival, delayed reproductive death, micronucleus induction and neoplastic transformation): cultures of human hybrid cells, CGL1 (HeLa x human skin fibroblast) were exposed to monochromatic beams of three different wavelenghts (285, 292 and 295 nm) in the dose range between 5 and 55 J/m2. Analysis of the obtained results is still in progress at the Radiobiology Laboratory of the Department of Physics of the University of Milan. Preliminary results obtained in 2002 are shown in Fig. 2: they concern the cell surviving fraction as function of both released dose and SR wavelength. The wavelength dependence of the cell survival and delayed effects in the narrow energy range investigated has to be clarified with a wider data acquisition coming from data under analysis and further irradiation sessions planned in next dedicated runs.

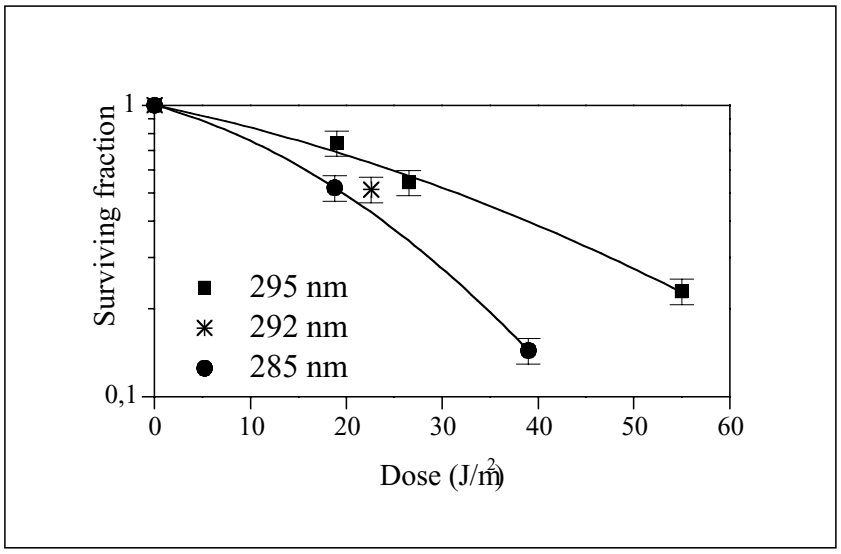

Figure 2: *SUE preliminary results: irradiated cell surviving fraction versus exposure dose of monochromatic UVB radiation at three different wavelengths.*

BTF

D. Alesini, G. Benedetti, M.E. Biagini, C. Biscari R. Boni, M. Boscolo, A. Clozza,
G. Delle Monache, G. Di Pirro, A. Drago, A. Gallo, A. Ghigo, S. Guiducci, M. Incurvati,
C. Ligi, F. Marcellini, G. Mazzitelli (Resp.), C. Milardi, L. Pellegrino, M. Preger, P. Raimondi,
R. Ricci, C. Sanelli, M. Serio, F. Sgamma, A. Stecchi, A. Stella, C. Vaccarezza,
P. Valente, M. Vescovi, M. Zobov

1 Description of the DAΦNE BTF

The Beam Test Facility (BTF) is a beam line optimized for the production of a defined number of electrons or positrons, in a wide range of energy (up to 800 MeV) and multiplicities, but mainly intended for the single electron operation mode. The facility is aimed mainly for detector calibration purposes.

The BTF is part of the DAΦNE accelerator complex, consisting of a double ring electron-positron collider, a high current linear accelerator (LINAC), an intermediate damping ring (Accumulator) and a system of 180 m transfer lines connecting the various machines. The LINAC delivers electrons with energy up to 800 MeV, with a maximum current of 500 mA/pulse, or positrons with energy up to 550 MeV, with a maximum current of 100 mA/pulse; the typical pulse duration is 10 ns with a maximum repetition rate of 50 Hz. When injecting for the operation of the main rings at the ϕ resonance, the beam energy is 510 MeV.

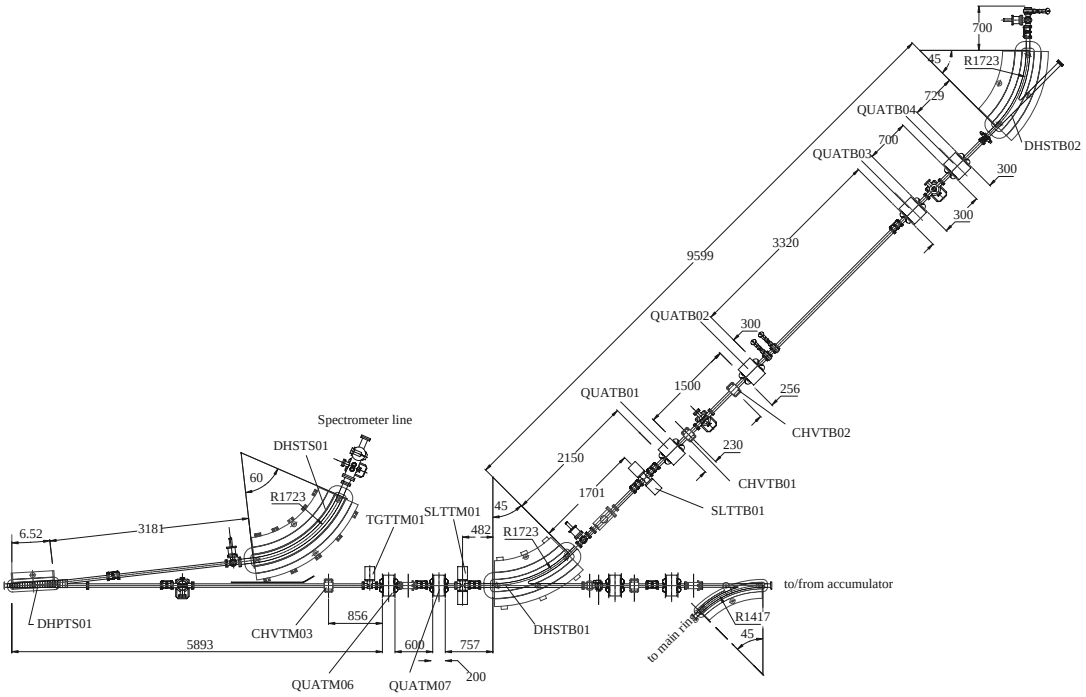

Figure 1: *Plan of the transfer line from the LINAC exit to the BTF hall, showing all the relevant elements.*

Almost half-way of the DAΦNE transfer line, a tungsten target (`TGTTM01`) allows to strongly attenuate the LINAC beam, that is then deviated to a separated line by means of a 45° bending

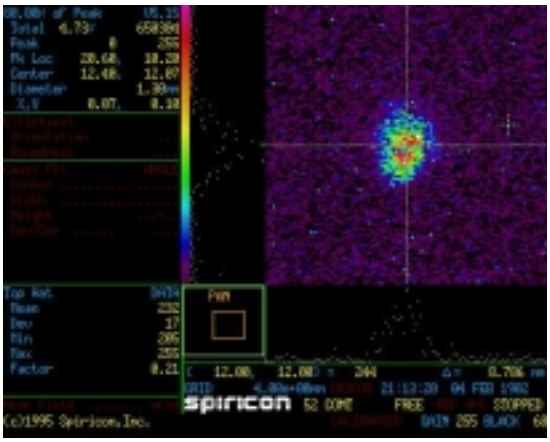

Figure 2: *High-fluorescence target image of the first beam injected in the BTF hall, on Feb. 4, 2002.*

magnet (DHSTB01); the attenuated beam is transported by a ≈ 12 m transfer line to the BTF hall, where the experimental set-ups can be installed. The dipole magnet, together with a downstream collimator, selects the momentum of the particles. At the end of the BTF line a second bending magnet (DHSTB02) allows to use two separate test lines: one directly from the straight section (dipole off), one coming out from the magnet at 45° (dipole on). The layout of the BTF and of the relevant part of the transfer line – from the LINAC to the test area and the beam line exits – together with their main elements, is shown in Fig. 1.

Since the minimum LINAC beam current that can be conveniently measured by the DAΦNE current monitors is $I \approx 1$ mA, the corresponding number of electrons (positrons) for a 10 ns pulse is 6.24×10^7. It is thus necessary to strongly reduce the number of particles to reach the few particles range. The reduction of the particle multiplicity can be achieved with different methods, the one chosen for the BTF operation is the following [1)]: first the LINAC beam is intercepted by a (variable depth) target in order to highly increase the energy spread of the primary beam; then the outcoming particles are energy selected by means of a bending magnet and slit system. The energy selector only accepts a small fraction of the resulting energy distribution, thus giving a reduction of the number of electrons by a large and tunable factor. The target is shaped in such a way that three different radiation lengths can be selected, $1.7, 2.0, 2.3\ X_0$, by inserting it at different depths into the beam-pipe.

Due to the momentum dispersion introduced by the bending magnet, the relative energy spread $\Delta E/E$ is essentialy determined by the magnet/collimators configuration [2)]; in the BTF configuration for a wide range of slit apertures a resolution better than 1% can be obtained.

2 2002 Activities

In the year 2002 the BTF has been successfully commissioned and started operation, delivering beam to the first user experiments. A first phase of the BTF commissioning was carried on in February: a first optimization of the transport has ben performed by monitoring the beam position and size by means of a high-fluorescence target (flag FL1TB01). The very first beam injected in the BTF line – on Feb. 4, 2002 – is shown in Fig. 2 (the beam was dumped onto a lead Faraday cup). In this phase we have also checked that the beam orbit was centered with respect to the beam-pipe, since this is important in order to correctly set the energy out of the selector system. For

radiation safety reasons, no beam was allowed into the BTF hall without inserting the attenuating target. No beam diagnostics at all is then available during BTF operation, and we could rely only on particle detectors. A second phase of the commissioning and the first users access started in November. Both the single electron production and the high multiplicity operation of the facility have been extensively tested.

Two different calorimeters have been used as main diagnostic devices, positioned at the two exits of the BTF line. Both detectors are lead/scintillating fibers calorimeters of the KLOE type, with single side photomultiplier readout. The main features are a sampling fraction of $\approx 15\%$, a good energy resolution, $\sigma_E/E = 4.7\%/\sqrt{E(\mathrm{GeV})}$, and excellent timing resolution, $\sigma_\mathrm{t}/\mathrm{t} = 54\mathrm{ps}/\sqrt{E(\mathrm{GeV})}$.

The LINAC setting has been optimized to provide a 510 MeV energy, $4 \div 5$ mA intensity beam. The repetition rate of the LINAC was 24 Hz (+1 shot to the spectrometer line for LINAC energy measurement), and the pulse duration was the same as for injection in the accumulator, ≈ 10 ns. The typical collimator settings used were 2 mm of total aperture, both for the upstream and downstream slits; in this configuration only a few electrons reach the diagnostic detectors.

Due to the good energy resolution of the calorimeters, $\approx 7\%$ at 500 MeV, the number of produced electrons can be counted simply by measuring the total deposited energy E: $n = E/E_1$, where E_1 is the energy deposited by a single electron. In the left plot of Fig. 3 an example of ADC spectrum for the Calorimeter 2 (pedestal subtracted) is shown, for a selected energy of $E_\mathrm{sel} = 471$ MeV: the individual peaks corresponding to $0, 1, \ldots, n$ electrons can be easily identified. The total number of events in each peak should represent the probability of producing n particles: in the right plot of the same Fig. 3, the distribution of the number of events in each peak is shown, with a fit to the Poisson function (average number of particles $\overline{n} = 2.3$).

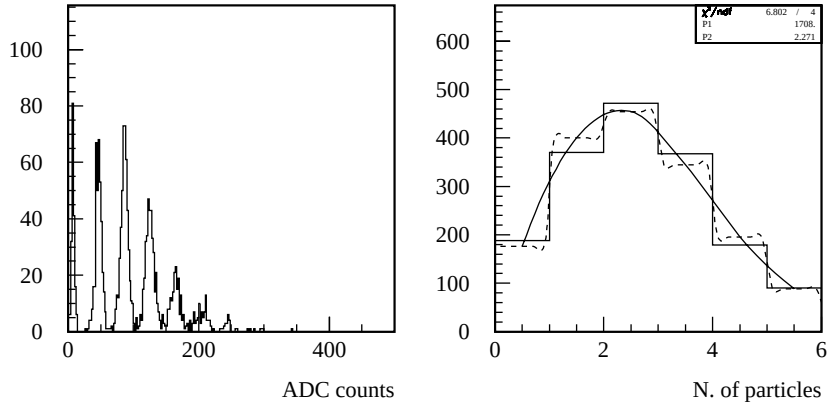

Figure 3: *Counting electrons in Calorimeter 2 ($E_\mathrm{sel} = 471$ MeV): charge spectrum (left), and Poisson fit of the average number of particles in each peak (right).*

The most effective way to change the average number of particles in the beam is to change the selected energy E_sel; in particular, at the **same** LINAC energy and intensity and with the **same** collimator settings, the multiplicity increases by lowering the chosen E_sel. In addition, the multiplicity can be tuned by changing the aperture of the upstream and/or downstream collimators. In this case the energy resolution of the selector will be also affected, but by a relatively small amount, in any case well below the intrinsic resolution of our calorimeters. In particular, the measured multiplicity increases by increasing the slits aperture until the intrinsic beam spot size is exceeded.

There are two intrinsic limitations to the particle counting with calorimeters. Since the absolute width of the peaks increases as $\sqrt{n}$, increasing the average multiplicity the peaked structure in the energy distribution gradually disappears, approching a Gaussian shape. In this case the number of particles in the beam cannot be measured *event by event*, but only the average multiplicity $\overline{n}$ can be statistically estimated. Another intrinsic limitation to the particle counting performed by means of the total energy measurement in a calorimeter is the detector saturation, *i.e.* when the signal begins to be no longer proportional to the number of particles. This is in general due to one or more of the following factors: saturation of the ADC scale, of the photomultiplier gain or the scintillation light yield.

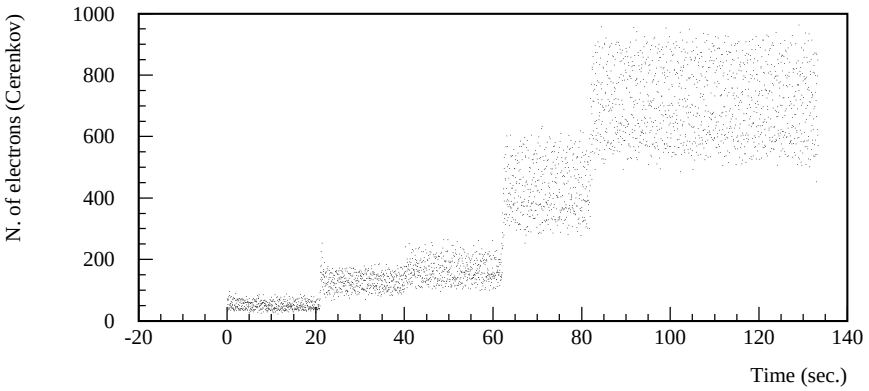

Figure 4: *Number of estimated particles in the Cerenkov counter (after normalization with Calorimeter 2 yield) as a function of time: the average multiplicity during the run has been increased by opening the collimators.*

Above ≈ 20 particles the calorimeters are no longer effective due to saturation effects. In order to have a diagnostic device in the $\overline{n} = 100$-1000 range (and higher), a different detector has been developed and tested in collaboration with the AIRFLY group [3]. It is essentially a counter based on the Cerenkov light emission in a PLEXIGLAS radiator when transversed by relativistic electrons (which in the BTF energy range is always the case). The light is then extracted thanks to the appropriate shaping of the end part of the radiator itself and collected by a photomultiplier, without optical connection: this gives the possilibity of interposing a calibrated optical filter between the radiator and the PMT, in order to attenuate the Cerenkov light by a known factor thus extending the dynamical range of the counter. The Cerenkov light yield, and in turn the phototube analog signal, should be proportional to the number of electrons traversing the radiator; this phenomenon should be linear up to a very high number of electrons. The Cerenkov counter signal shows a good correlation with the energy deposited in the calorimeter, with a suitable low multiplicity beam; using the cross-calibration between the two detectors, the Cerenkov counter has been used to monitor the beam multiplicity up to ≈ 1000, as shown in Fig. 4.

Another important parameter is the beam energy, that can be changed by changing the current of the energy selector dipole magnet. The average measured energy of the single electron signal in the calorimeter is fairly proportional to the incoming beam energy $E_{\rm sel}$, as shown in Fig. 5, where the average value and the width of the single electron peak is shown as a function of $E_{\rm sel}$.

The BTF commissiong has been performed during the run of the DEAR experiment (at the second interaction point of the DAΦNE main rings). This allowed to use the LINAC for BTF operation only between two injection cycles, the so-called parasitic mode. Another possibility is a

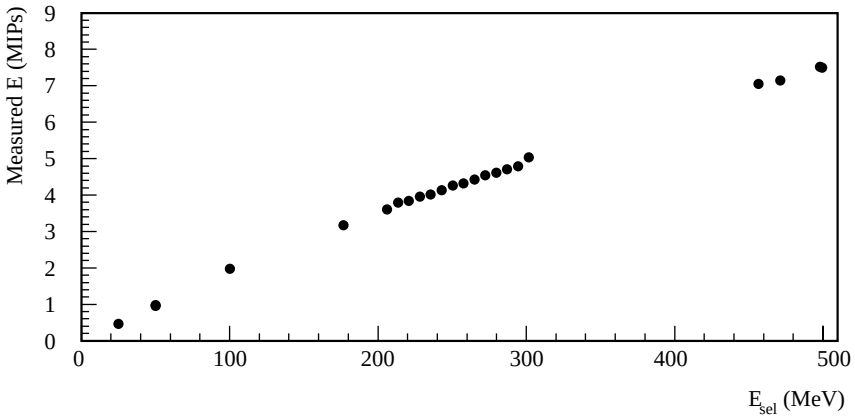

Figure 5: *Energy deposited in calorimeter 1: average of the Gaussian fit to the first electron peak as a function of* $E_{\rm sel}$ *(calculated on the basis of the bending magnet setting).*

dedicated mode, when the BTF runs with no collisions at all in the main rings, and the facility can be used 24h/day; however this is restricted to the maintenance/shutdown periods of the main experiments at the collider.

The typical bunch configuration in 2002 DEAR runs was $100 + 100$ bunches; an injection cycle during the DEAR runs is the following: electrons are injected into the accumulator and from there into the e^- main ring at 1 Hz repetition rate, requiring 2-4 min (100 bunches $\times$ 1 sec. $\times$ n. of fillings), then the LINAC and transfer lines are switched to positron mode (typically 3.5 min are needed for the magnets ramping). A similar procedure is followed for the injection of positrons in the accumulator and e^+ ring at 1 Hz (again 2-4 min are required). When the DEAR run starts, the LINAC is switched to BTF mode: the target and collimator slits are inserted, magnets are cycled and ramped on (1-2 min.). The BTF beam can be delivered until 3.5 min before the following DEAR injection, so that the typical BTF run duration was 20-25 min. A complete cycle in this configuration lasts 40-45 min, so that the duty-cycle for the BTF operation is about 50%.

During the KLOE experiment operation, data taking does not stop during injections, so that DAΦNE is operated in topping-up mode: the injection cycles lasts only 15-20 min. to optimize the average luminosity. This leaves essentially no time for the BTF parasitic operation.

Two user tests were carried on during Nov.-Dec. 2002 in parasitic mode (see photograph in Fig. 6): the AIRFLY experiment (air fluorescence yield measurement) [3], and the LCCAL [4] electromagnetic calorimeter test. This two first users represented two extreme operation mode of the BTF facility:

- AIRFLY: high multiplicity in a wide range of energies (the widest accessible for the BTF beam), detector in a fixed position;
- LCCAL: single electron for a few energy points, full coverage of the detector by moving it across the beam;

In this period the BTF demonstrated to be easily tuneable both from the point of view of the desired particle multiplicity (from single electron mode to $\approx$ 1000) and energy setting. In order to overcome the present limitations imposed by KLOE operation, where practically no time is now left for beam delivery in the BTF test area, but also to largely improve the duty-cycle during FINUDA operation, we plan to upgrade the facility in January 2004 during the DAΦNE cryogenic system maintenance. A complete separation between the DAΦNE transfer lines to the

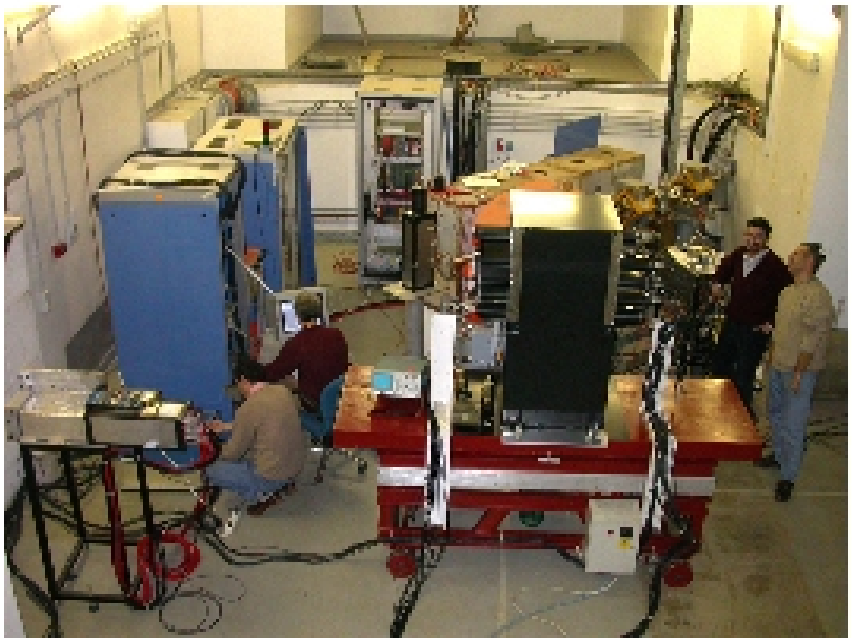

Figure 6: *Photograph of the BTF hall during the LCCAL installation.*

Main Rings and the BTF channel will allow to operate in the BTF mode with the only limitations of the LINAC switching time and the time spent for filling the Main Rings. A duty-cycle of order of 80% during KLOE, and around 90% in FINUDA operation, is expected.

More diagnostic systems, especially devoted to beam profiling, as well as high multiplicity measurement, are under development in order to improve the characterization of the beam quality.

3 List of Conference Talks by LNF Authors in Year 2002

1. G. Mazzitelli, DAΦNE-KEK Workshop, Feb. 19, 2002, Frascati, Italy
2. G. Mazzitelli, Rapporto Attivita' Consiglio dei Laboratori, Nov. 7, 2002, Frascati, Italy
3. P. Valente, AIRFLY Collaboration Meeting, Sep. 23, 2002, INFN Sez. Roma II, Italy

References

1. L. Rinolfi *et al.*, *Single electron beams from the LEP pre-injector*, in Proceedings of PAC 89, Chicago (1989) 298.
2. F. Sannibale, G. Vignola, DAΦNE Techical Note **LC-2** (1991).
3. P. Privitera *et al.*, *AIRFLY Letter of Intent*, INFN Gr. V, unpublished.
4. S. Bertolucci *et al.*, *Construction and test of an Electromagnetic calorimeter prototype*, DESY PRC R&D 00/02.

CTF3

D. Alesini, C. Biscari, G. Benedetti (Dott.), R. Boni, A. Clozza, G. Delle Monache,
A. Drago, A. Gallo, A. Ghigo (Resp.), M. Incurvati (Ass.), F. Marcellini, C. Milardi, L. Pellegrino,
M.A. Preger, R. Ricci, C. Sanelli, M. Serio, F. Sgamma, A. Stecchi, A. Stella, M. Zobov

1 Introduction

The Compact Linear Collider (CLIC) collaboration explores the technical feasibility of beam acceleration by travelling wave structures at room temperature and high frequency (30 GHz), powered from a drive beam: the so-called Two Beam Acceleration scheme. CLIC has the potential to achieve a center-of-mass energy range for electron-positron collisions of 0.5 to 5 TeV.

The CLIC RF power source is based on a new scheme of electron pulse compression and bunch frequency multiplication, in which the drive beam time structure is obtained by the combination of electron bunch trains in isochronous rings.

The next CLIC Test Facility (CTF3) will be built at CERN in order to demonstrate the generation of the drive beam with the proper time structure, the extraction of 30GHz RF power from this beam and the acceleration of a probe beam with 30GHz RF cavities.

The facility will be built in the existing infrastructure of the CERN LPI complex and makes maximum use of equipment which became available after the end of LEP operation. The project started within the framework of a world-wide collaboration between CERN, INFN - LNF (Italy), LAL (France), SLAC (USA) and Uppsala University (Sweden).

2 Activity of the LNF group in year 2002

Activities of the INFN-LNF group have been focused on the design of the CTF3 compressor system. It consists of two rings connected together by a 60 meter long transfer line: the first (Delay Loop) multiplies the Linac bunch frequency by a factor 2, the secon d (Combiner Ring) by another factor 5.

During year 2002 the final Design Report has been completed, gone through a comprehensive project review of the CERN Editorial Board committee and a supervision of LNF Accelerator Division Editorial board and is now published.

The optics of the CTF3 compressor system has been designed with great care for first and second order beam dynamics. The delay loop, in the frequency multiplication scheme of CTF3, doubles the peak current of the drive beam. The preservation of the transverse and longitudinal beam structures asks for isochronicity, path length tuning, and large energy acceptance in the device. A new design of the delay loop ring has been proposed to achieve achromaticity and isochronicity fulfilled in each half of the ring. This condition, still assuring the preservation of the longitudinal phase plane, is less critical from the point of view of transverse beam dynamics, moreover the total number of quadrupoles and their fields h ave been strongly reduced.

Mechanical drawings and prototypes of the main parts of the vacuum chamber have been designed with the constraint of maintaining the beam coupling impedance as low as possible. Vacuum gaskets with special profile have been developed in order to avoid RF contacts in the junction. A bellows prototype with RF shielding has been developed with sliding contacts with the same inner shape of the rest of the vacuum chamber. In correspondence of the connection with the ion pumps, the vacuum chamber has been realized with shielded pumping slots.

The beam instrumentation for CTF3 requires special developments due to the peculiar beam characteristics. Beam dynamics requires a measurement of beam transverse position with a precision of 0.1 m. The short bunch spacing ranging from 20 cm in the linac to 2 cm at Combiner Ring

extraction makes use of strip line or button type beam position monitors (BPM) inefficient. For this reason pickups resembling the ones form erly installed in the CERN LEP pre-injector have been re-designed for the combiner ring and delay loop needs to provide the measurement of the average position of the whole bunch train at each turn. BPM design has been completed during this year and has been followed by the realization of a final prototype which allowed to carry out a set of bench measurements to fully characterize the device, in order to estimate dynamic range, accuracy, resolution and sensitivity. The proposed pickup works in the 400 KHz-200 MHz frequency range and offers an appropriate response to the CTF3 beam.

The bunch interlacing scheme of CTF3 is based on the operation of RF deflectors. Further studies to analyse the wake generated by the interaction between the beam and the deflecting mode in the RF deflector (beam loading) have been carried out to investigate the impact they have on the final quality of the beam extracted. It has been demonstrated that the beam loading of a couple of 10-cell separ ators does not affect significantly the beam quality, provided the betatron phase advance between the two device is properly chosen. Following these results, two deflectors to be used in CTF3 preliminary and nominal phases have been built in collaboration with the Soltan Institute for Nuclear Studies (Poland).

The INFN-LNF CTF3 group collaborated to the CTF3 preliminary phase (which started in autumn 2001 and has been completed during year 2002) whose goal was to demonstrate, in the EPA damping ring formerly used for LEP injection, the "funnelling" injection scheme and bunch train compression in an isochronous lattice. The main difference between these preliminary experiments and the nominal CTF3 is the limited beam current available from CERN LEP Injector Linac. During this studies the major result of demonstrating of the concept of bunch train combination by RF deflectors in an isochronous ring (combination factors 3 to 5) was achieved with the expected peak current inc rements.

All the presented work has been strongly supported by the DAFNE Technical Staff.

3 Foreseen activity of the LNF group during year 2003

- Completion of the final layout of the Delay Loop and Transfer Line, including the bunch stretcher chicane, where the rms bunch length is increased in order to minimise energy spread and losses in the ring
- Beam instrumentation: construction of the BPMs. Design of the hardware for detection of signals from diagnostic devices and data acquisition system for beam position and beam charge measurements.
- Realization of the Transfer Line stretcher vacuum chamber
- Study and design of Delay Loop RF deflector. The dynamics implications of the RF deflector for the Delay Loop are less demanding with respect to the Combiner Ring ones. Besides scaling the Lengeler structure used for the CTF3 preliminary phase to 1.5 GHz, other options such as standing wave cavities can be considered.

References

1. CTF3 Design report, edited by G. Geschonke, A.Ghigo in CERN/PS 2002-008 (RF) and LNF-02/008 (IR), 9 maggio 2002.
2. CTF3 Preliminary Phase Commissioning Report; PS/AE/Note 2002-026; P. Baldini, R. Corsini, B. Dupuy, A. Ferrari, A. Gallo, M. Preger, L. Rinolfi, P. Royer (Editor), F. Tecker

3. CTF3 Preliminary Phase Commissioning Report; PS/AE/Note 2002-045; D. Alesini, C. Biscari, R. Corsini, A. Drago, B. Dupuy, A. Ferrari, A. Ghigo, M. Masciarelli, L. Rinolfi, P. Royer (Ed.), M. Scampati, M. Serio, F. Tecker

4. CTF3 Compressor System; C. Milardi, D. Alesini, C. Biscari, R. Boni, A. Clozza, G. Di Pirro, A. Drago, A. Gallo, A. Ghigo, F. Marcellini, M.A. Preger, C. Sanelli, F. Sannibale, M. Serio, F. Sgamma, A. Stecchi, A. Stella, M. Zobov, INFN-LNF, Frascati (Roma); R. Corsini, CERN, Geneva; Proceedings of the European Particle Accelerator Conference, Paris (2002)

5. Desig n of a Beam Position Monitor for the CTF3 Combiner Ring; A. Stella, A. Ghigo, F. Marcellini, A. Zolla, CTF3 Technical Note, INFN-LNF, CTF3-008 (2002).

6. RF Beam Deflectors for CTF3 Combiner Ring; D.Alesini, A. Kucharczyk, S. Kulinski, M. Pachan, E. Plawski, R. Boni, A. Gallo, F. Marcellini, Proceedings of the European Particle Accelerator Conference, Paris (2002)

7. New Design for the Delay Loop in CTF3; C.Biscari, INFN-LNF Acc.Div CTFF3 Technical Note CTF3-006 (2002)

8. The Theory of Beam Loading in RF Deflectors for CTF3; D.Alesini, INFN-LNF Acc.Div CTF3 Technical Note CTF3-007 (2002)

DAΦNE

The DAΦNE Team: D. Alesini, G. Benedetti, M.E. Biagini, C. Biscari, R. Boni,
M. Boscolo,A. Clozza, G. Delle Monache, G. Di Pirro, A. Drago, A. Gallo, A Ghigo,
S. Guiducci, M. Incurvati,C. Ligi,F. Marcellini, G. Mazzitelli, C. Milardi, L Pellegrino,
M. Preger, P. Raimondi (Resp), A. Reali, R. Ricci, C. Sanelli, M. Serio,
F. Sgamma, A. Stecchi, A. Stella, C. Vaccarezza, M. Vescovi, M. Zobov

The DAΦNE Technical Staff: G. Baccarelli, G. Baldini, P. Baldini, A. Battisti,
A. Beatrici, M. Belli, B. Bolli, G. Ceccarelli, R. Ceccarelli, A. Cecchinelli, S. Ceravolo,
R.Clementi, O.Coiro, S.De Biase, M.De Giorgi, N.De Sanctis, R.Di Raddo, M.Di Virgilio,
G.Ermini, G.Fontana, U.Frasacco, C.Fusco, F.Galletti, O.Giacinti, E.Grossi, F.Iungo,
R.Lanzi, V.Lollo, V.Luppino, C.Marchetti, M.Marchetti, C.Marini, M.Martinelli, M.Masciarelli,
A.Mazzenga, M.Monteduro, A.Palleschi, M.Paris, E.Passarelli, V.Pavan, S.Pella,
D.Pellegrini, R.Pieri, G.Piermarini, S.Quaglia, F.Ronci, M.Rondinelli,
F.Rubeo, M.Sardone, M.Scampati, G.Sensolini, A.Sorgi, M.Sperati, A.Sprecacenere,
P.Tiseo, R.Tonus, T.Tranquilli, M.Troiani, V.Valtriani, R.Zarlenga, A.Zolla

1 Introduction

The electron-positron collider DAΦNE has been the first "factory" in operation at the Φ energy. The accelerator complex consists of a double ring collider, a linear accelerator (LINAC) an intermediate damping ring to make injection easier and faster and 180 m of transfer lines connecting these machines. The geometry of this complex has been designed to reuse the buildings hosting ADONE (the 3 GeV center of mass electron-positron collider in operation at LNF from 1969 to 1993) and its injector, a LINAC used both to refill the collider and to perform nuclear physics experiments. The complex is shown schematically in Fig.1.

The structure of the collider consists of two rings, laying in the same horizontal plane and crossing in two Interaction Points (IP) at a small horizontal angle of 1.5 degrees. Each ring consists of a long external arc and a short internal one. Starting from the IP the two beams travel together inside a common vacuum chamber and their distance increases until it becomes ≈12 cm at the level of the magnetic separators called "splitters" (SPL). These are special magnets with two regions of opposite field which deflect the two beams in opposite directions, allowing them to reach the separate vacuum chambers of the long and short arcs. Each arc consists of two "almost achromatic" bends (deflecting the beam by 81 degrees in the short arc and 99 degrees in the long one) similar to those frequently used in synchrotron radiation sources, with a long straight section in between. Each bend consists of two dipoles, three quadrupoles, two sextupoles and a wiggler: the amount of synchrotron radiation power emitted in the wigglers is the same as in the bending magnets and the wigglers can be used to change the transverse size of the beams. The increase of emitted power doubles the damping rates for betatron and synchrotron oscillations, thus making the beam dynamics more stable, while the possibility of changing the beam sizes makes the beam-beam interaction parameters more flexible.

The double ring scheme with many bunches, as in DAΦNE, has been chosen in order to increase the number of colliding bunches, and therefore the achievable luminosity. However it has also some drawbacks: the total current in the ring can reach extremely high values (5 A in the DAΦNE design) and the high power emitted as synchrotron radiation (≈50 KW) needs to be absorbed by a complicated structure of vacuum chambers and pumping systems in order to reach the very low residual gas pressure levels necessary to avoid beam loss. In addition, the number of possible oscillation modes of the beam increases with the number of bunches, calling for

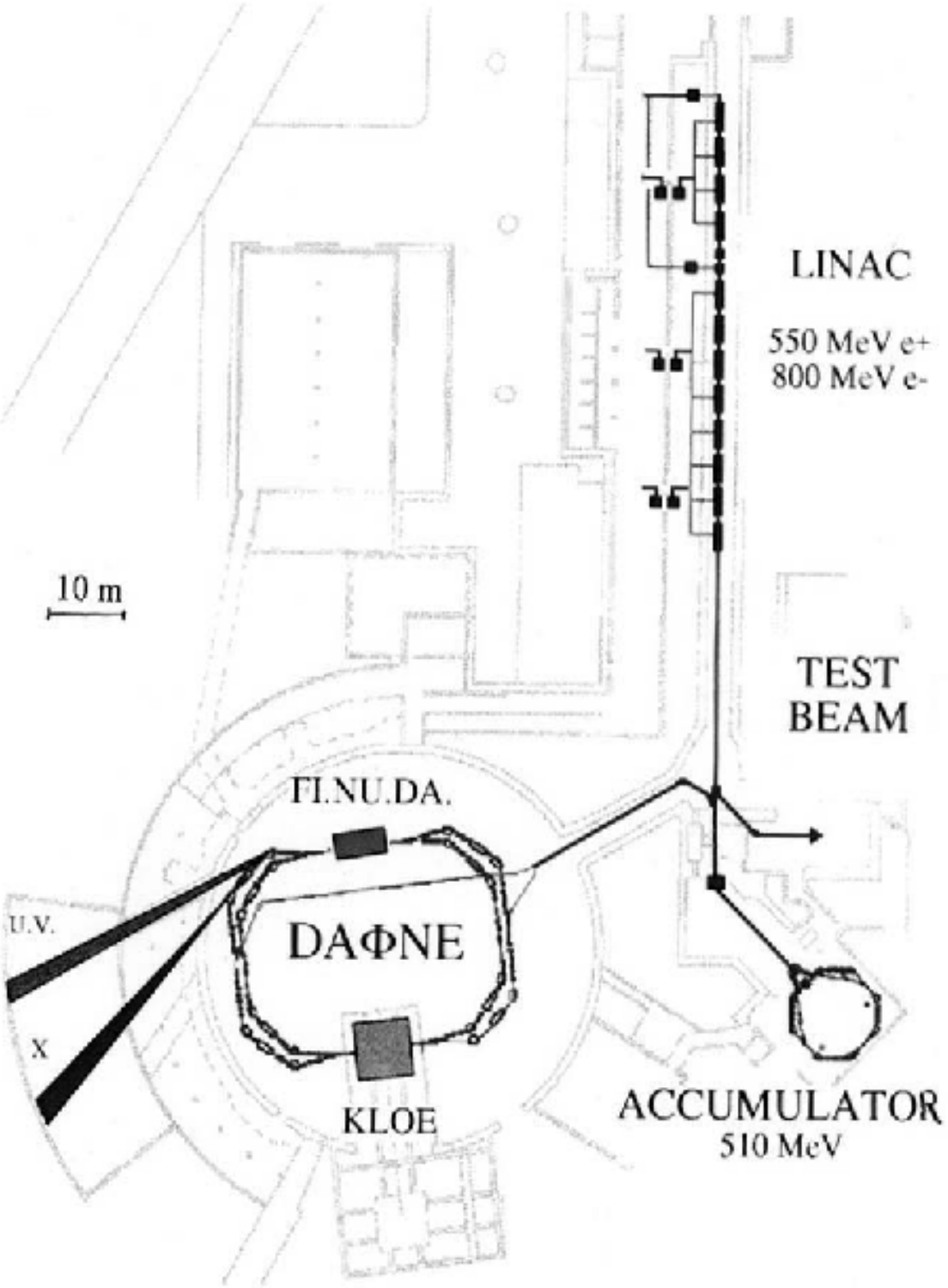

Figure 1: *The layout of the DAΦNE accelerator complex inside its buildings.*

sophisticated bunch-to-bunch feed-back systems. A sophisticated longitudinal feedback has been then built to maintain a reasonable safety margin on the threshold of multibunch instabilities. The system is based on a digital signal processing technique and acts on each single bunch individually. Additional feedback systems on the vertical betatron motion have been also realized following the observation of coherent instabilities during the collider operation.

The collider can host two experiments in the two Interaction Regions (IR). Three detectors have been realized, KLOE, DEAR and FINUDA. The first two have been installed in the two IP's, since May 1999, while the third is being assembled in its pit inside the DAΦNE hall and will be installed in Spring 2003 in the IR occupied by DEAR until December 2002. The detectors of KLOE and FINUDA are surrounded by large superconducting solenoid magnets for the momentum analysis of the decay particles and their magnetic fields represent a strong perturbation on the beam dynamics. This perturbation tends to induce an effect called "beam coupling", consisting in the transfer of the betatron oscillations from the horizontal plane to the vertical one. If the coupling is not properly corrected, it would give a significant increase of the vertical beam size and a corresponding reduction of luminosity. For this reason a superconducting solenoid magnet with half the field integral of the detector one and of opposite direction is placed near each splitter in such a way that the overall field integral in the IRs vanishes.

In the KLOE IR the low-β_y at the IP has been realized by means of two quadrupole triplets. Due to the flat shape of the beam at the IP, the low-β is realized only in the vertical plane. The quadrupole cannot be of the conventional electromagnetic type for two reasons: the first is that the iron of the joke would degrade the flatness of the magnetic field in the detector and the second is that the overall transverse size of a conventional quadrupole is at least twice its useful aperture. Therefore quadrupoles realized with permanent magnets (PM) have been built, which exhibit an excellent field quality, very small transverse size and are fully transparent to external fields. The region of space around the IP occupied by machine elements, which is unavailable for the detection of decay particles by the experiment consists in two cones with the vertex at the IP and a half aperture of only 9 degrees. In order to obtain a good compensation of the above mentioned coupling effects induced by the solenoids, these quadrupoles are rotated around their longitudinal axis by angles between 10 and 20 degrees and are provided with actuators to finely adjust their position and rotation. The whole structure is completely embedded inside the KLOE detector. The KLOE IR has been redesigned in 2002 and will be modified in the Winter shutdown 2003.

The structure of the second IR, where the FINUDA detector will be installed, is quite similar. Since its superconducting solenoid magnet has half the length (but twice the field) of the KLOE one, the low-β focusing at the IP is obtained by means of two permanent magnet quadrupole doublets inside the detector and completed with two other conventional doublets outside. The DEAR experiment, which has been installed in IR2, did not need magnetic field and therefore only conventional quadrupoles were used. Moreover, two synchrotron radiation lines, one from a bending dipole and the other from the wiggler have also been realized by the DAΦNE-LIGHT group.

2 Year 2002 activity

During the first two months of the year a machine shutdown allowed to pursue several activities, such as:

- installation of octupole magnets;
- installation of new, modified scrapers;
- mechanical alignement measurements in the KLOE IR;

- installation of the new Beam Test Facility, to be used for detector tests with the Linac beam (single electron mode);
- repairs and general maintenance of all the machine subsystems.

In order to fight the effect of the nonlinearities found in the wiggler magnets, limiting the dynamic aperture of the machine, with serious consequences on the beam lifetimes, two sets of four lumped octupoles were built, to be inserted into proper locations of the ring lattices. In this way it is possible to compensate the overall nonlinearity seen by the stored particles at each revolution in the rings. Each octupole has its own power supply, so that the whole system has a wide range of tunability. The eight octupoles have been designed at LNF and built by a magnet factory in France. Magnetic measurements have been performed on the octupole magnets before their installation. Two sextupoles and two correctors have been removed to leave space for the octupoles. The picture of one octupole, the blue magnet, mounted on the machine, is shown in Fig. 2.

A new set of ten scrapers was installed in the DAΦNE vacuum chamber, in order to lower the background rates in the experiment detectors. The location of these new scrapers, near to the wigglers, was previously occupied by the OFHC Copper synchrotron light absorbers. It was then necessary to design a special scraper with a double function: scraper and synchrotron light absorber. This difficulty was solved with of a brand new design: a motorized water cooled OFHC Copper synchrotron light absorber with a Tungsten end. The scrapers have a 35 mm stroke each. In the "out" position they act like absorbers, when they are moved towards the beam the Tungsten end intercepts the off-orbit particles. The movement is done by means of a precision screw driven by a stepping motor. The mechanical precision for the positioning is about 0.01 mm. Water cooling is necessary to take away the power of the synchrotron radiation that hits the scraper. A sketch of the new scraper is shown in Fig. 3. The new scrapers have also been equipped with new absolute encoders and interfaced with the DAΦNE Control System.

The vacuum conditioning of both rings was completed at the beginning of March, and the machine started up with operation of the DEAR experiment. Two months were dedicated to collider tuning and data taking by the DEAR experiment.

2.1 Operation with DEAR. Phase I

In a low energy electron-positron collider, such as DAΦNE, the lifetime of the stored current is mainly limited by the Touschek effect, namely the particle loss due to the scattering of the particles inside the bunches. A low beam lifetime is not only a limitation to the integrated luminosity delivered, since injection of fresh beams is more frequent, but also a source of backgrounds for the detectors. For this reason, besides the optimization of the machine parameters aimed at increasing the peak luminosity, the main effort during 2002 operation has been also the optimization of the beam lifetimes, togheter with the decrease of the detector backgrounds. With this goal, the first DEAR runs were devoted to machine optimization, in particular:

- backgound rates were reduced thanks to the installation of the new scrapers, the beam orbit optimization and sextupole and octupoles optimisation. The levels were reduced by a factor 10 with respect to 2001;
- the value of β_x at the DEAR IP was lowered from 4.4 m to 1.7 m;
- non linearities were cured both by optimizing the sextupoles (with a resulting 15% improvement) and the octupoles configuration (15% improvement as well). The octupoles have been

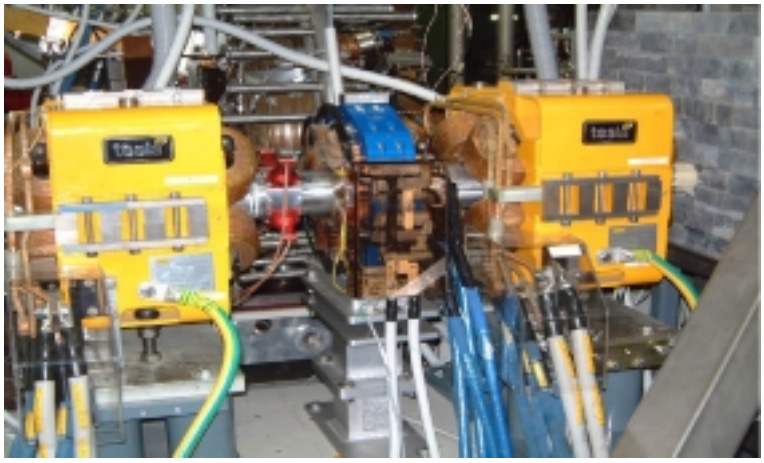

Figure 2: *Octupole magnet (blue) installed in DAΦNE.*

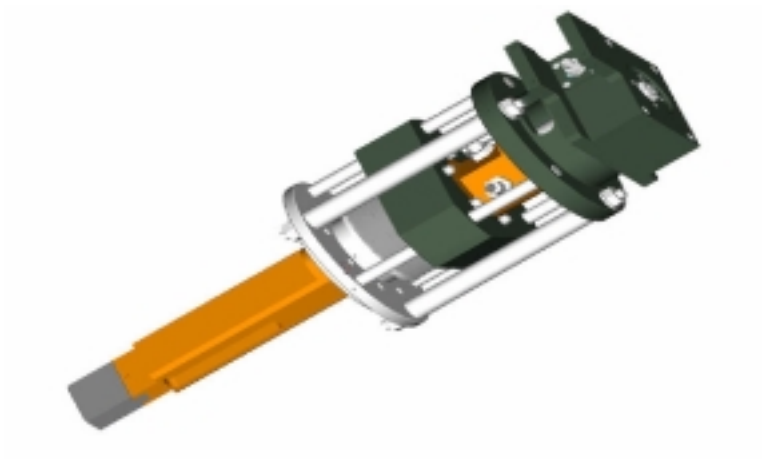

Figure 3: *Scraper sketch.*

also found useful to improve the lifetime in collision ($\approx$ 10% improvement), compensating the strong beam-beam nonlinearities.

During the two months of data taking the DEAR experiment was able to collect $\approx 20 pb^{-1}$, working with 45+45 bunches, with a peak luminosity of $4.6\,10^{31}\mathrm{cm}^{-2}\mathrm{s}^{-1}$, significantly higher than in 2001, and a current per beam of 0.7 A. Due to both machine and detector improvements, the signal-to-noise ratio was also enhanced by a factor 40 with respect to the DEAR shifts in May 2001. An important contribution to the background reduction, that was of crucial importance for the experiment, came from the decrease of the horizontal beta function at the IP. With the collected data DEAR was able to clearly observe the capture of kaons in Nitrogen atoms.

2.2 Operation with KLOE

The runs of the KLOE experiment resumed in May and lasted until the end of September, with a short summer break. The same optimization procedure applied to the DEAR configuration was performed for KLOE. Particular care was dedicated to the optimisation of the background rates, that were decreased by a factor 4. In summary, the background reduction came from:

- orbit optimization;
- old and new scrapers optimization;
- sextupoles optimization;
- octupoles optimization;
- improved linear and non-linear knowledge of the machine;
- increased dynamic aperture with optimised β functions at the sextupoles and wigglers;
- increased lifetimes from all of the above.

In the Fall runs for KLOE a peak luminosity of $\approx$ 0.8 x $10^{32}\mathrm{cm}^{-2}\mathrm{s}^{-1}$ was measured, with a record integrated luminosity per day of $\approx 5 pb^{-1}$.

In total KLOE acquired in the 2002 runs 304 pb^{-1} out of the 317 pb^{-1} delivered. The progress in peak luminosity was achieved mainly with a "step-by-step" gradual reduction of the IP β functions, and also by:

- adiabatic machine tuning;
- different working point for the electron beam;
- smaller IP β_y (from 3.0 cm to 2.6 cm);
- smaller IP β_x (from 5.6 m to 2.7 m);
- decreased horizontal emittance (from 0.96 mm mrad to 0.76 mm mrad).

At present the positron current is limited to $\approx$ 1.1 A in normal running condition, since at higher currents the background rates are still too high, and the beam lifetime too short.

The operation with 100 bunches in KLOE was also tested. The results were good in terms of beam stability, but the peak luminosity was not improved with respect to the standard bunch

pattern (49+49) operation. The IP β_x is still too high, and does not allow to increase beam currents with reasonable background. A further decrease of the IP β_x was very difficult without the upgrade of the IR, that will take place in the 2003 Winter shutdown.

In summary, the performance obtained by DAΦNE during the KLOE runs are:

- number of bunches per beam: 49 + 49;
- total current per beam e-/e+: 0.8/1.1 A;
- peak luminosity $\approx$ 0.8 x 10^{32}cm^{-2}s^{-1} ;
- average luminosity $\approx$ 0.5 x 10^{32}cm^{-2}s^{-1};
- maximum integrated luminosity per day $\approx 5. pb^{-1}$;
- luminosity lifetime: 0.6 h;
- number of fillings per hour: 3 to 4;
- injection frequency e-/e+: 2/1 Hz;
- data acquisition during injection: ON.

2.3 Operation with DEAR. Phase II

The last three months of the year were again dedicated to data taking by DEAR. With the experience acquired with KLOE it was possible, by decreasing the horizontal emittance, and with a lower β_x, to successfully collide with 95+95 bunches, with an increment of 40% in the peak luminosity (the record being $\approx$ 0.7 x 10^{32}cm^{-2}s^{-1}). The reduction of the IP β functions was done not only in order to increase the luminosity in single bunch collisions, but also to relax the influence of the parasitic crossings (PC) to allow doubling the number of colliding bunches. This bunch pattern was routinely used in collision for the DEAR experiment. It was possible to store up to 1.3 A of stable positrons and 1.8 A of electrons in this bunch pattern. As a consequence, there has been a large improvement on the integrated luminosity, since the DEAR detector is kept OFF during the beams injection. Due to the lower bunch currents both beam lifetimes and backgrounds were also improved in this configuration.

During 2002 DEAR has acquired $\approx 107 pb^{-1}$ in total, with very promising physics results. In summary, here are the obtained machine performances with DEAR:

- number of bunches per beam: 95 + 95;
- total current per beam e-/e+: 1.3/1. A;
- peak luminosity $\approx$ 0.7 x 10^{32}cm^{-2}s^{-1} ;
- average luminosity during runs $\approx$ 0.2 x 10^{32}cm^{-2}s^{-1};
- maximum integrated luminosity per day $\approx 2.2\, pb^{-1}$;
- luminosity lifetime: 0.6 h;
- number of fillings per hour: 1.7;
- injection frequency e-/e+: 2/1 Hz;
- data acquisition during injection: OFF.

2.4 DAΦNE achievements

The peak luminosity was increased by more than a factor 10 during the past three years (from November 1999 to October 2002), reaching a maximum value of ≈ 0.8 x 10^{32}cm^{-2}s^{-1}. As shown in Fig. 4, during last year the peak luminosity was steadily increasing, while the integrated luminosity per day grows faster, indicating an improvement of the overall efficiency. The peak luminosity for the two experiments (blue for Kloe, green for DEAR) is shown in the top picture, the daily integrated luminosity (red for Kloe, gray for DEAR) is reported in the middle plot, and in the bottom one is the total 2002 DAΦNE (green), KLOE (red), DEAR (gray) integrated luminosity.

In summary, the DAΦNE achievements during 2002 have been the following:

- 317 pb^{-1} delivered to KLOE in less than 5 months;
- ≈ 0.8 x 10^{32}cm^{-2}s^{-1} peak luminosity for KLOE in less than 5 months;
- 5. pb^{-1}/day, 30 pb^{-1}/week, 100 pb^{-1}/month integrated luminosity for KLOE;
- 107 pb^{-1} delivered to DEAR in less than 5 months;
- 95 bunches operation "routine" for DEAR;
- ≈ 0.7 x 10^{32}cm^{-2}s^{-1} peak luminosity for DEAR;
- 2.2 pb^{-1}/day, 12 pb^{-1}/week integrated luminosity for DEAR;
- strong reduction of backgrounds levels in both detectors.

3 Accelerator physics

The above described significant luminosity progress was realized by means of continuous machine physics study. The major items leading to the luminosity performance improvement can be summarised as follows:

- linear optics improvements;
- working point choice;
- coupling correction;
- nonlinear beam dynamics study;
- single and multibunch instability cures;
- collider parameters fine tuning during data taking.

As a result, lifetimes, background rates and luminosity were greatly improved. In the following a description of the main accelerator physics items addressed during 2002 is presented.

3.1 Linear optics study

During the 2002 Winter shutdown the accelerator physics group improved the machine theoretical model, to have a better agreement between model and measurements of betatron functions and tunes. This is a crucial point for a better understanding of the machine behaviour. Moreover a realistic lattice model allows for a realistic prediction of the machine parameters. The theoretical description of the DEAR IR quadrupoles was changed, and several online procedures were installed in the Control System to calculate the Twiss parameters describing the machine optics, used to characterize the lattice. With this new model it has been possible to design a new optics to decrease both the horizontal and vertical β functions at the DEAR IP, a useful knob to increase luminosity. A 50% reduction on β_x and a 30% reduction on β_y at the IP were performed by changing the focusing configuration in the IR from a triplet to a doublet of quadrupoles. The most important effect was the consequent reduction of β_x at the location of the first PC. This allowed to change the bunch pattern from the "by 2" configuration (every second bucket filled) to the "by 1" configuration (every bucket filled), with a beneficial effect on the luminosity. The good results obtained by the optics changes in the DEAR IR suggested similar modifications to the KLOE IR during the KLOE runs. The procedure to lower the β functions at the KLOE IP is more difficult, due to the presence of PM quadrupoles. Nevertheless, using the quadrupoles outside the IR it was possible to lower the IP β_x from 5.7 m to 2.7 m, and the IP β_y from 3 cm to 2.7 cm. The latter is only a 10% change, however it is the maximum possible at the moment without loss of luminosity due to the hourglass effect, that occurs when the IP β_y function is equal to or smaller than the bunch length. The optics was also successfully modified to lower the horizontal emittance, with the result of a decreased background rate. With further improvements to the model and with a description of the bending magnets closer to the magnetic measurements performed before the installation, it was finally possible to describe the positron and electron rings by the same model, both for the DEAR and for the KLOE operation modes, the only difference being the quadrupoles in the DEAR IR that work in different excitation regimes for the two different configurations (close to saturation for DEAR). An improved steering algorithm was also implemented, to simultaneously minimize the beam orbit and the corrector strengths, allowing the rings to reach optimal orbit correction. Consequently the measured vertical dispersion, much less than 1 cm, is one of the smallest ever reached in a storage ring.

An important step leading to luminosity increase was obtained for KLOE in 2001 by means of a new "detuned" lattice without low-β insertion at the second IP, where the beams are separated during the KLOE runs, not to perturb the luminosity. The main advantages of this lattice can be summarised as following:

- the separation of the beams at IP2 is larger, therefore spurious collisions at IP2 have no influence on the luminosity;
- the low-β insertion at IP2 has been eliminated thus reducing the chromaticity. This allowed to reduce the IP β_y, from 6 cm to 3 cm, at the KLOE IP by keeping the same sextupole strengths;
- the β functions in the wigglers are lower. As a consequence, the lattice is less sensitive to the cubic nonlinearity in comparison with the previous KLOE lattice.

In 2002 the same modification was studied for the DEAR lattice. Although in this configuration the situation was not so favorable, since the KLOE PM quadrupoles do not allow to eliminate the low-β at the KLOE IP, however a vertical β of 7 cm has been realized, while at the DEAR IP2 its value was 3 cm. Switching off the couple of quadrupoles nearest to IP2 allowed to decrease also the horizontal β from 4 to 1.5 m, with a significant reduction of chromaticity and backgrounds in the experiment, and a consequent luminosity improvement.

Analytical estimates and numerical simulations have shown that the only working point on the tune diagram above integers, where the project luminosity parameters can be met, is a small area around (Q_x=5.09, Q_y=5.07). However, during collider commissioning the working point (5.15, 5.21) was chosen for collisions. Despite some expected reduction in luminosity, this point has a number of advantages of particular importance during machine tuning: the dynamic aperture is larger, the second order chromaticity terms are smaller, coupling correction is easier, the closed orbit is less sensitive to magnetic element errors. An intensive numerical study has been carried out for this working point, considering different factors affecting the luminosity performances such as the separation at IP2, vertical crossing angle, parasitic crossings. At present the positron ring is tuned at this working point. However, during operation the electron ring working point was shifted from (5.15, 5.21), mainly because at high currents a strong vertical instability in the positron ring is transmitted to the electron ring if the tunes are equal. Separating the tunes the instability is eliminated by the Landau damping due to the nonlinear beam-beam interaction. Empirically, after gradual optimisation of collision parameters, the working point of the electron ring was set to (5.11, 5.14). Actually, according to numerical simulations this is yet another "safe" working point in the tune area above integers where the beam blow up is relatively small and tails induced by the beam-beam interaction are well confined within the dynamic aperture.

In a storage ring different sources can excite coupling between vertical and horizontal betatron oscillations: skew magnets, vertical dispersion, solenoids, off-axis sextupoles etc. Depending on the coupling sources and their distribution along the ring, the normal betatron modes can propagate in a different way down to the IP. As a consequence, the two beams can have different sizes and rotations at the IP resulting in different core blow up and tail growth. Numerical simulations have shown that for the nominal coupling of 1% the beam core blow up in DAΦNE may vary in a wide range. This was a clear indication of the necessity of deeper coupling study and correction below the design value. Here is a list of the main steps that led to coupling reduction:

- KLOE detector solenoid and compensator magnet current variation;
- global coupling correction with skew quadrupoles;
- residual vertical dispersion correction;
- nonlinear terms minimization;
- working point fine tuning.

As a result, coupling was reduced down to 0.2% for both rings and the luminosity in single bunch collisions increased by, at least, a factor of 2.

3.2 Nonlinear optics study

Nonlinear dynamics study was considered as a crucial task for luminosity increase. Three main techniques were adopted for this study: tune scans, localized orbit bumps inside critical magnetic elements and beam decoherence measurements. The tune scan was used to define safe areas for beam-beam collisions on the tune diagram not affected by nonlinear lattice resonances. By changing the tunes and observing the lifetime and blow up of a single bunch at the synchrotron light monitor, it was found that for some tunes the lifetime was strongly reduced or the beam size increased. By analyzing the results it was found that nonlinear resonances up to 6th order were responsible for these effects. Since such resonances can be driven only by strong nonlinear magnetic elements, a campaign of measurements was performed in 2001, when it was found that the DAΦNE wigglers are a strong source of octupole-like terms providing a cubic nonlinearity. The high order multipole terms in the magnetic field of the wigglers mostly account for the measured

betatron tune shift dependence on the particle oscillation amplitude and residual second order chromaticity. These nonlinear magnetic fields affect the dynamic aperture, the beam lifetime (strictly connected with backgrounds and noise rates of the experiments), and the beam-beam performance. The consequences of this multipolar effect on the machine model have been simulated adding in each wiggler an octupolar term that fits the nonlinear coefficient of the chromaticity. Numerical simulations carried out taking into account the measured cubic nonlinearity have shown that they have indeed a dramatic impact on the collider luminosity performance.

In order to provide a knob to control unwanted cubic nonlinearities, three octupole magnets have been installed in both rings in January 2002, in the most feasible and less perturbative configuration for the original machine layout. The first measurements of the nonlinear behaviour of the machine came out to be in agreement with the analytical and numerical predictions. For both KLOE and DEAR experiment configurations the tuning of the strength of the octupoles performed in collision led to an improvement of the beam lifetime due to a compensation of the strong beam-beam non linearities and to an increase of the energy acceptance of the machine.

3.3 Beam-beam interactions study

Luminosity optimization in storage rings is a long, difficult process, involving a wide spectrum of parameters, such as working points, linear and nonlinear optics, coupling between particle oscillations in the 6D phase space. Practically, the only way to cope with such a large number of parameters is to numerically simulate the process of beam-beam interactions. Besides, a single simulation for a given set of parameters requires huge amounts of CPU time, since it is necessary to simulate at each step an electromagnetic interaction of millions charged particles and to track this process over many beam revolution turns.

The beam-beam interactions in DAΦNE have been successfully simulated by using the code LIFETRAC, which allows also to estimate the colliding beam lifetimes. This code has proven to reproduce well and to predict operating conditions in DAΦNE. With this purpose the code has also been modified to run on the parallel computer cluster of the E. Fermi Center for Physics in Rome. This has allowed to increase the computing power in terms of CPU time by almost two order of magnitude. As a result, a parametric study of the beam-beam collisions has started, taking into account nonlinear effects present in the collider, parasitic crossings and the influence of a residual horizontal dispersion at the IP's. This work is still in progress.

3.4 Backgrounds study

Dedicated simulations and measurements have been devoted to the study of beam backgrounds to optimize the background rates in the KLOE and DEAR experiments. A set of movable collimators (scrapers) is used at DAΦNE to reduce the background in the detectors. These collimators are placed upstream each IR in the two rings. To obtain a further background reduction a set of 3 new scrapers have been installed in dispersive regions of the rings in January 2002, on the basis of simulation studies.

Measurements have been performed to investigate the new collimators performance, showing an overall decrease of the induced background rates. A qualitative agreement has been found with simulation. The new scrapers also increase the efficiency of the scraper upstream the experiments. In fact, the new collimators stop particles that would be just deviated by the IR scraper and eventually lost in the detector.

In addition to a direct background reduction the new collimators help in making the scrapers upstream the experiments more effective. In fact, since they are very close to the detectors, their insertion can indeed increase the background. A factor of 1.6 was gained due to the fact that the scraper can be inserted closer to the center of the pipe.

3.4.1 Background Reduction at DEAR

A detailed study of the distribution of the particles hitting the pipe at the two IRs has been very useful to find the proper tools to control the background rates. In particular, the DEAR background has been reduced by a factor larger than 10. The trajectories of the Touschek particles and their hit position along the beam pipe have been studied in the two IRs with the simulation. The background has been reduced both by properly shielding the detectors and by reducing the beam envelope where the particles are expected to be lost, i.e. by reducing β_x at the focusing quadrupole closest to IP2. With this change the particles get lost at QF2 farther from IP2, and have been easily shielded.

3.4.2 Background Reduction at KLOE

During the KLOE run, a background reduction by about a factor 4 has been obtained quite immediately with respect to the 2001 runs. In the KLOE IR most of the particles are lost at the focusing quad far from IP1 (QF2) and only a small fraction at the first one close to IP1 (QF1). The distribution of this latter background component has been measured with the KLOE detector showing a good agreement with the simulation. Simulations indicate that the background component coming from QF2 could be reduced by a mask inserted just below the quadrupole, that will be mounted in the new IR, to be installed during the 2003 shutdown. In summary, the background improvements in the Kloe run came for a 70% from better orbits in the rings, for a 70% from the new scrapers installed, for a 80% from sextupoles and octupoles optimization, for a 70% from lattice changes.

3.5 Beam dynamics study

In DAΦNE strong, coupled bunch synchrotron oscillations make active damping systems necessary in multibunch operation. In each ring, a broadband bunch-by-bunch Longitudinal Feedback (LFB) is operating since 1998. The systems have been developed in collaboration with PEP-II/SLAC and ALS/Berkeley. The LFB works fairly well, but in 2002 an unexpected longitudinal quadrupole instability was limiting the total storable current to $\approx$ 700 to 800 mA in the electron ring, even with the LFB on, with a significant luminosity reduction. Fig. 5 shows the beam spectrum as observed by the spectrum analyzer.

The current limit means that new injections can produce loss of bunches and/or loss of LFB control with successive large decrease of the total beam current. In order to overcome this limit, a strong effort, both theoretical and experimental, was focused on this problem by the Beam Dynamics group. The quadrupole instability threshold was measured as a function of the following machine parameters:

- radiofrequency voltage;
- momentum compaction;
- orbit (considering the eventuality of a trapped mode);
- injection patterns and number of bunches;
- bunch length and LFB backend setup.

A clear variation of the quadrupole threshold was observed as a function of the RF voltage: storing 47 bunches, the threshold was $\approx$ 550 mA with a cavity voltage of 120 kV and $\approx$ 750 mA with 170 kV. The dependence on the momentum compaction was also evaluated. A $\approx$ 10%

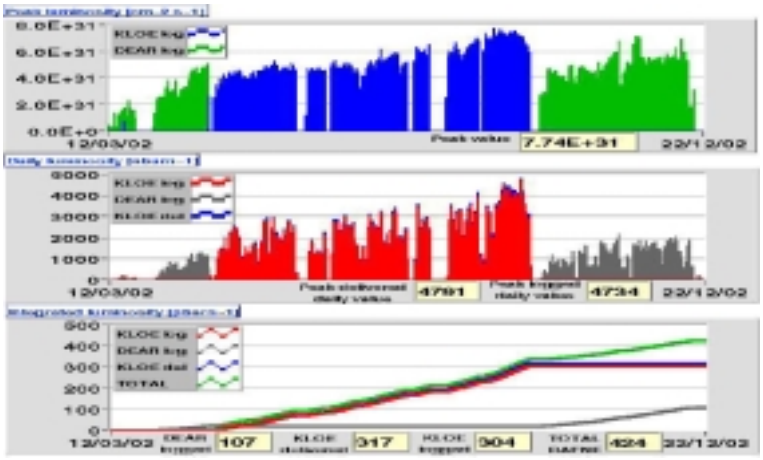

Figure 4: *The DAΦNE luminosity during 2002.*

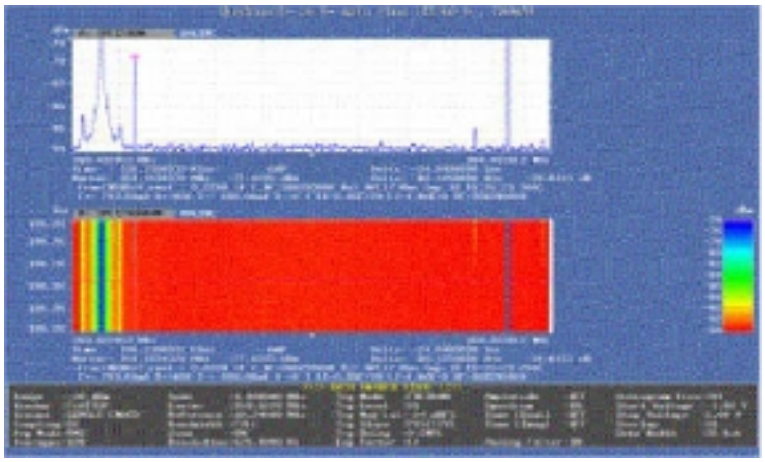

Figure 5: *Quadrupole instability (with the cursor) in e- ring at ≈ 700 mA with LFB on. The largest peak on the left is the revolution harmonic, the small peak in the middle is the synchrotron oscillation (under feedback control).*

increase of the momentum compaction value has allowed to increase the quadrupole threshold by $\approx 17\%$. However, variations of this parameter have not given a definitive solution for the instability damping. Afterwards, the quadrupole threshold was measured by varying the number of bunches and the fill patterns. It has been found that the threshold increases with the number of bunches, but this is neither conclusive nor sufficient to cancel the current limit.

Finally, the measurement of the single bunch quadrupole threshold as a function of the RF cavity voltage, with LFB OFF and ON, has allowed to identify the problem. In fact, by observing the single bunch longitudinal back-end (BE) response as a function of the timing in the cavity kicker of the LFB system, it is clear that the bunch passage should be synchronized with the centre of the highest lobe to exploit most of the power. The useful period is 418 ps, and contiguous lobes are in LFB opposite phases. By measuring the FWHM electron bunch length versus the RF cavity voltage, it was found that it decreases as the voltage increases, being less than 144 ps at 1 mA and growing up to 300 ps at 39 mA, for a cavity voltage of 120 kV. It was clear that a bunch length comparable to the BE period could drive an interaction between the LFB and the quadrupole instability threshold.

By measuring the quadrupole threshold versus the LFB BE delay, it was found that increasing conveniently the BE timing (i.e. kicking the bunch tail) produces higher or no thresholds, while decreasing delay (i.e. kicking the bunch head) lowers the quadrupole threshold. This cure has turned out to be very reliable if used together with a feedback front-end setup giving an offset of the same sign for all the bunches. This study has allowed to adjust the LFB BE delay to avoid the quadrupole instability for all the typical collision patterns, and to store more than 1850 mA of stable electron beam. Further tests have shown that in multibunch operation, and with a stored beam current above the threshold, the quadrupole oscillation exists independently of the dipole (synchrotron), and it is not generated by the LFB. Besides, another test on the beam has demonstrated that kicking the bunch tail can be equivalent to kick the bunch head, if the overall feedback phase response keeps the same sign. A similar LFB setup has given better control of the beam at very high currents also for the positron beam.

3.6 Third harmonic cavity study

The installation of a passive 3rd harmonic cavity in each DAΦNE ring has been proposed to increase the Touschek lifetime and to weaken the coherent instabilities by increasing the Landau damping due to the non-linearity of the longitudinal potential well. Due to the peculiarity of the DAΦNE parameters (low RF voltage, high beam current), powering the cavity in a passive way is the simplest and the most effective choice. The required harmonic voltage can be obtained with a modest cavity shunt impedance and over a wide range of beam currents. The choice of the harmonic number 3 is a compromise between beam dynamics requirements and constraints related to the space available for the cavity installation. The implications of the harmonic voltage on the beam dynamics have been carefully considered. The most relevant issues are the shift of the frequency of the coupled bunch (CB) coherent motion and the effects of a non uniform filling pattern in the multi-bunch configuration (bunch train with gap in the filling pattern). The harmonic voltage can be almost completely "switched-off" by tuning the cavity as far as possible from the harmonic 3h. In order to minimize the coherent effects, it is worth tuning the cavity at (3h+n+1/2)frev, with the integer n as high as the tuning system allows. This is the so-called "parking option" that can be used to approximately recover the operating conditions obtained before the harmonic cavity installation. A picture of the actual cavity is shown in Fig. 6.

The damping of the cavity HOM has been obtained by means of a special ferrite ring developed for the superconducting cavities installed on the High Energy Ring (HER) of the collider KEK-B in Japan. The cavity has been designed by an extensive use of the e.m. code MAFIA and HFSS. The measurements performed on the real cavities are in good agreement with the results obtained

by the e.m. simulations.

Two harmonic cavities have been fully tested on bench, and are now ready for installation on the machine, together with their tuning system with all the low-level control electronics. All the equipment will be mounted during the 2003 machine shutdown and will be ready for operation by May 2003.

3.7 Control system upgrades

The DAΦNE Control System is based on a three level architecture, where the third level consists of a large number of CPU's placed along the rings and the power supply halls. These CPU's perform all kinds of control tasks on the corresponding devices and are linked by means of a mailbox system (the second level) to the computers in the Control Room, where high-level procedures allow to control and tune all machine and beam parameters.

The Control System has been recently improved with a new operating system, a new third level processor and several supported items such as the streak camera on the synchrotron light monitor, which allows to measure the bunch length, the new power supplies for the octupoles, and the Wall Current Monitors in the Transfer Lines.

During year 2002 the DAΦNE Control System has performed regularly, with an uptime larger than 99% of the machine operation time. This result confirms the high stability of the system, due also to the use of VME embedded processors, for the user's applications, instead of the personal computers used before. At present the System consists of:

- 13 consoles in the Control Room;
- 4 remote consoles;
- 5 processors dedicated to user's applications;
- 43 distributed processors dedicated to the control of machine devices;
- 3 servers for the consoles management, the diskless boot of the processors, the execution of off-line codes, the manteinance of the file system and all the service operations.

With the aim to power the system interconnections, and to extend them to the new BTF experimental hall, both the distributed acquisition bus links and the private Ethernet network, that will be upgraded to Gigabit-Ethernet, have been completely redesigned.

The networks will have a star topology, and will use multimodal 50/125 optical fibers for a total length of 10 km. The installation is foreseen for March 2003. At the beginning of 2003 final tests of the new distributed processors will be performed. The new processors will smoothly substitute the present ones.

4 Year 2003 foreseen activity

During the shutdown (from January 2003 to May 2003) a new IR will be installed for KLOE and the new magnetic detector FINUDA, aimed at the study of hypernuclear physics, will roll-in in IR2. Two compensating solenoids, similar to those installed in IR1, will cancel the field integral due to the FINUDA detector solenoid.

Moreover, besides the main work on the two IRs, the following items will be addressed:

- the two 3rd harmonic cavities will be installed;
- several ion clearing electrodes will be dismounted and repaired, the vacuum chamber modified and the electrodes reinstalled;

- magnetic measurements on the new spare wiggler will be performed.

The latter item is very important for a better understanding of the performance of the machine. In fact, to correct the nonlinearity in the wiggler locally, by eliminating the perturbation to the ideal flat field inside the poles, the shape of the poles can be changed properly, by means of shims directly applied on the pole surface. Of course, it is not reasonable to find the optimum shape of the shims on the wigglers installed on the machine, since this would mean stopping the collider for a very long time, because this shape comes out from a converging procedure using magnetic calculations, realization of the shims on a milling machine, and magnetic measurements. Therefore a spare wiggler, exactly equal to those installed on the rings, has been realized by the same factory which has built the other ones, and will be measured during the Winter 2003 shutdown. This offline analysis will help in obtainingan "almost flat field" wiggler, and the modification to all wigglers in DAΦNE will be undertaken subsequently in 2004.

The biggest challenge in 2003 though will be the operation with the FINUDA detector solenoid switched on. Modifications of the KLOE and FINUDA IR's were designed with the aim to make the operation, with just one or none detector on, easier. The main advantage of the new IRs is a great flexibility due to the fact that it will possible to operate the machine with any field value for each of the two solenoids, with a great improvement in the operational efficiency. In the following the characteristics of the new IRs will be summarized.

4.1 KLOE IR

Major modifications to the KLOE IR will take place. The KLOE IR will be extracted from the detector and reassembled according to a new design, with a modified optic and supports in order to decrease the IP β functions, optimise background rejection and provide variable quadrupole rotation to operate at different magnetic fields (from 0 to maximum) in the solenoids. This will allow to obtain a better correction of coupling in the machine for any value of the KLOE solenoid field. It will make possible also to run the machine with the KLOE solenoid off, in order to guarantee the maximum flexibility to the collider operation. Therefore, the mechanics will be modified, in order to allow the PM quadrupoles to rotate by any angle between the horizontal symmetry plane of the ring and that corresponding to the full field of the solenoid. This rotation will be performed by stepping motors and remotely controlled. Since measurements of the IP β functions were never possible in the KLOE IR, because of the presence of PM quadrupoles, Printed Circuit Board (PCB) quadrupoles will be inserted inside them, in order to allow for a small change in their focusing strength, thus making possible IP β measurements in the future.

The vacuum chamber will be modified with a new structure in beryllium alloy (AlBeMet) similar to the existing one but shorter, in order to allow the insertion of two new beam position monitors. Tungsten masks will also be installed to better shield the detector from machine background.

The lattice will also be modified. The first quadrupole (QF i.e. focusing in the horizontal plane) will been removed and the third will been reinforced with another quadrupole to get a factor 1.5 higher integrated gradient. In such a way the old FDF triplet will be converted into a DF doublet. The DF scheme allows to obtain the same IP β_y with a lower chromaticity, leading to longer beam lifetimes and better beam-beam performances. Moreover it will allow to reduce the IP β_x from 2.7 m down to 1.5 m. This is needed to double the number of colliding bunches (from 50 to 100) in the KLOE configuration without losing luminosity by the parasitic crossings. The FDF scheme was adopted in the DAΦNE design in order to allow for good beam separation at the splitters with a low value of the horizontal crossing angle ($\approx$25 mrad), while the DF solution needs an angle of the order of 30 mrad. However, during recent runs, it has been shown that a crossing angle as large as 30 mrad can be used without performance limitations. A better coupling

correction within the IR and the possibility of colliding at the second IP with the KLOE solenoid off is expected. Fig. 7 shows a sketch of the new KLOE IR.

4.2 FINUDA IR

A new interaction region with four permanent magnet quadrupoles and a thin berillium chamber will be inserted in the detector FINUDA. The original design has been improved by adopting some of the solutions used for KLOE. The mechanics will be modified in order to allow the four PM quadrupoles around the IP to rotate by 135 degrees, so that it will be possible to run the collider also with the FINUDA solenoid off. With this range of rotation it will be also possible to change the sign of the quadrupole focusing, thus allowing to realize a detuned lattice, similar to that used for the 2001-2002 operation, when running with a single IP. The four conventional quadrupoles between the solenoid and the compensators will be also equipped with rotating supports, allowing rotation in a range of 23 degrees, corresponding to the difference between the solenoidal field on and off. Four PCB trim quadrupoles, similar to the KLOE ones, will also be installed inside the PM quadrupoles closest to the IP. Fig. 8 shows a sketch of half FINUDA IR. Fig. 9 is a picture of the actual IR before its insertion in the apparatus.

4.3 Year 2003 schedule and goals

The 2003 DAΦNE upgrades, that hopefully will increase the machine performances, are listed below:

- new KLOE interaction region;
- smaller IP β_x (from 2.7 m to 1.7 m);
- better detector shieldings;
- reduced chromaticity;
- 100 bunches operation;
- reduced wiggler nonlinearities;
- additional quadrupoles for better machine tunability;
- smaller beam emittances.

After the shutdown, sometime will be devoted to the machine commissioning with the new IRs and the FINUDA solenoid on. A machine coupling correction as good as the one performed in the past for KLOE will be then studied and performed. The 2003 operation goal is to run with the experiment KLOE for about 5 months and with FINUDA for about 2 months, with the aim to reach a peak luminosity in the $\approx$ 1 to 2 x $10^{32}\mathrm{cm}^{-2}\mathrm{s}^{-1}$ range.

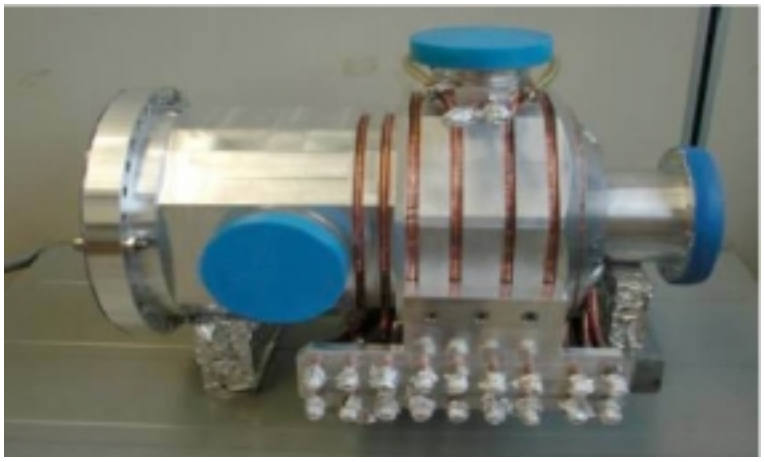

Figure 6: *The DAΦNE 3rd harmonic cavity.*

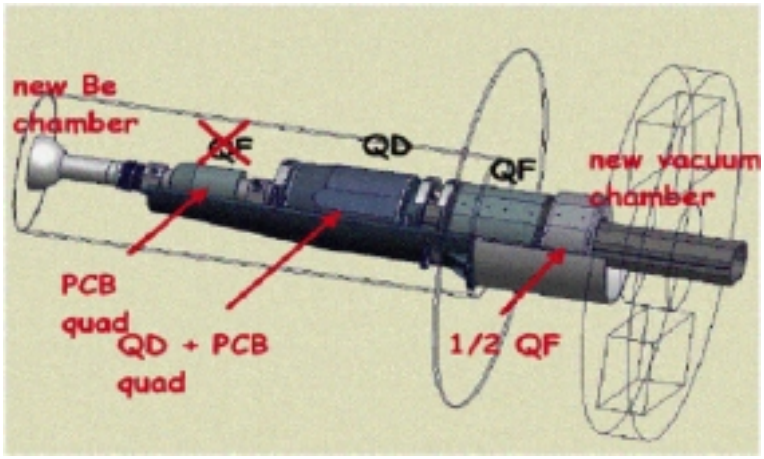

Figure 7: *A sketch of the new KLOE IR.*

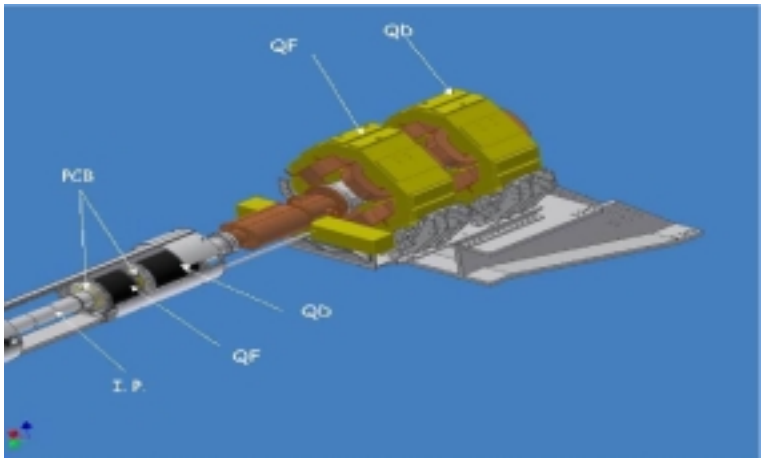

Figure 8: *A sketch of half FINUDA IR.*

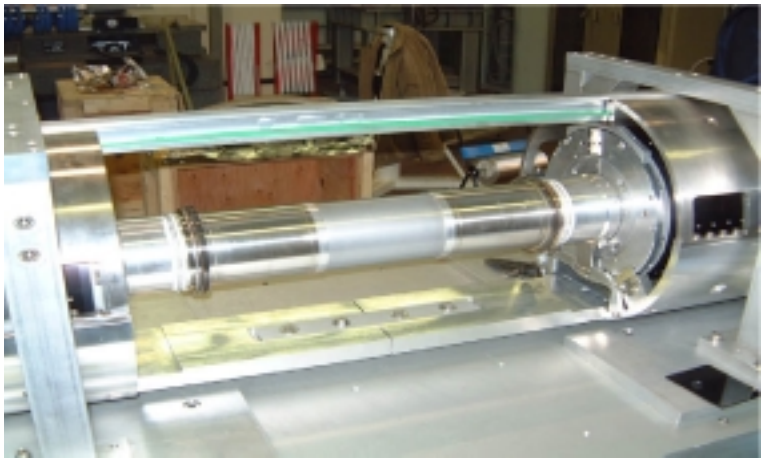

Figure 9: *The new FINUDA IR before its installation.*

5 Publications

1. M. Incurvati, R. Ricci, C. Sanelli: "DAΦNE Power Supply System: 5 Years of Experience and Statistics", presented at EPAC2002, 3-7 June 2002, Paris, France.

2. C. Ligi, G. Delle Monache, R. Ricci, C. Sanelli: "DAΦNE Cryogenic Cooling System: Status and Perspectives", presented at EPAC2002, 3-7 June 2002, Paris, France.

3. A. Ghigo, D. Alesini, C. Biscari, A. Drago, A. Gallo, F. Marcellini, C. Milardi, M. Serio, M. Zobov: "DAΦNE Broadband Impedance", presented at EPAC2002, 3-7 June 2002, Paris, France.

4. A. Drago, A. Gallo, A. Ghigo, M. Zobov: "Longitudinal Quadrupole Instability in DAΦNE Electron Ring", presented at EPAC2002, 3-7 June 2002, Paris, France.

5. M. Boscolo, M. Antonelli, S. Guiducci: "Simulations and Measurements of the Touschek Background at DAΦNE", presented at EPAC2002, 3-7 June 2002, Paris, France.

6. M. Zobov, D. Alesini, G. Benedetti, S. Bertolucci, M.E. Biagini, C. Biscari, R. Boni, M. Boscolo, A. Clozza, G. Delle Monache, G. Di Pirro, A. Drago, A. Gallo, A. Ghigo, S. Guiducci, F. Marcellini, G. Mazzitelli, C. Milardi, L. Pellegrino, M. Preger, P. Raimondi, R. Ricci, C. Sanelli, F. Sannibale, M. Serio, F. Sgamma, A. Stecchi, A. Stella, C. Vaccarezza, M. Vescovi: "Luminosity Performance of DAΦNE ", presented at EPAC2002, 3-7 June 2002, Paris, France.

7. S. Guiducci: "Beam Lifetime Studies in DAΦNE ", presented at EPAC2002, 3-7 June 2002, Paris, France.

8. C. Vaccarezza, M.E. Biagini, A. Drago, C. Sanelli, F. Sgamma, M. Zobov: "Preliminary Results on DAΦNE Operation with Octupoles", presented at EPAC2002, 3-7 June 2002, Paris, France.

DAΦNE-L

F. Belloni (Bors.), E. Burattini (Resp.), P. Calvani (Ass.),
G. Cappuccio (Ass.), G. Cavallo (Ass.), G. Cinque, S. Dabagov,
M. Guidi Cestelli (Ass.), A. Grilli (Tec.), A. Marcelli, F. Monti (Ass.),
A. Nucara (Ass.), E. Pace, M. Piccinini (Bors.), A. Raco (Tec.)

1 Activity

In 2002, the DAΦNE-Light Synchrotron Radiation Laboratory operated with all its three beamlines: due to the characteristics of the DAΦNE storage ring, an intense photon emission spectrally peaked in the low energy domain is provided. From November 2001, the Synchrotron INfrared Beamline At DAΦNE (SINBAD) worked in full parasitic mode in the whole IR domain and, by October 2002, also as SR facility to european users within the TARI (Transnational Access to Research Infrastructure) LNF program (see Table1). In late 2002, the soft X-ray beamline started its tests of beam characterization: in the energy region around 2-4 KeV the DAΦNE wiggler supplied a high flux and horizontally wide SR emission: a niche of research and technological applications are therefore possible and competitive with other SR facilities. During 2002, the Ultra-Violet beamline was successfully carried on SUE, the Solar Ultraviolet Effects experiment, which is devoted to the investigation of the effects induced by irradiations of biological specimens with UV radiation. These studies were performed during a few dedicated shifts.

Table 1: *Experiments at SINBAD within the TARI program of the EU.*

Exp.	Project	Group leader	Institution	Status
n.2	Magnons on diluted antiferromagnetic materials	Prof. A. Kuzmin	University Latvia	active
n.11	Far Infrared studies of multinary compounds	Prof. E. Sheregii	Jagellonian	active
n.12	Effects of IRSR on anchoring process of liquid crystals	Prof. E. Barna	Bucharest University	completed
n.18	Infrared properties of Ladders	Prof. P. Roy	L.U.R.E.	active
n.27	Infrared spectroscopy of macromolecules	Prof. E. Barna	Bucharest University	active

The Infra Red source is one of the eight bending magnets on the electron ring: the critical wavelength ($\sim$60 $\AA$) does not affect the IR intensity since the asymptotic spectral emission is at low energies; furthermore, the moderate electron beam emittance is dominated by the intrinsic IR SR divergence. The front end, 3 m far from the source, collects a SR solid angle of about 45x18 mrad^2 (vxh) through a set of four remotely controlled slits defining the SR beam size. By changing the accepted angle over the vertical coordinate, either linear (in the orbit plane) or circular (out of the orbit plane) IR polarization can be selected. The IR optical line, under UHV to minimize absorption by residual gas, consists of six gold-plated mirrors (one ellipsoidal, two toroidal and three plane mirrors), all remotely controlled in angle and monitored by CCD cameras. The SR beam is thus refocused into a final spot of about 1x2 mm^2 at CVD diamond wedged window 25 m located afterwards. This is the effective source of a Michelson interferometer, modified to work under vacuum, which allows both transmission and reflectivity experiments. The wavenumber

range of the instruments is 10-10000 cm^{-1} (1-1000 μm), covered with different detectors and beam splitters for a maximum resolution of 0.5 cm^{-1}. In cascade, an IR microscope is connected to an output port of the instrument, (see Figure 1).

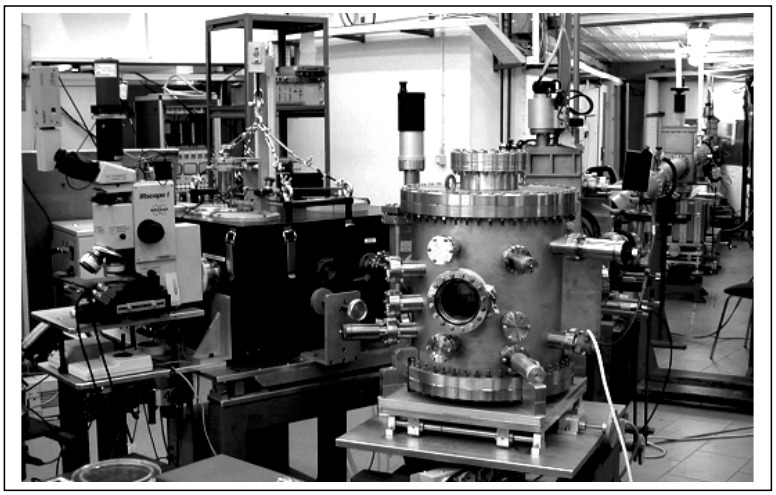

Figure 1: *SINBAD beamline experimental area: the last mirror chamber is visible with the Bruker FTIR interferometer, working under vacuum, and the IR microscope in cascade.*

The IR beamline performances have been measured in terms of ratio between SR intensity and black body (BB), $I_{SR}(\omega)/I_{BB}(\omega)$, versus the pupil diameter, d, at the sample position: the plot of Figure 2 compares calculations and measurements of Actual Brilliance Ratio for SINBAD. All data are normalized to a beam current of 1 A under the assumption of a linear dependence

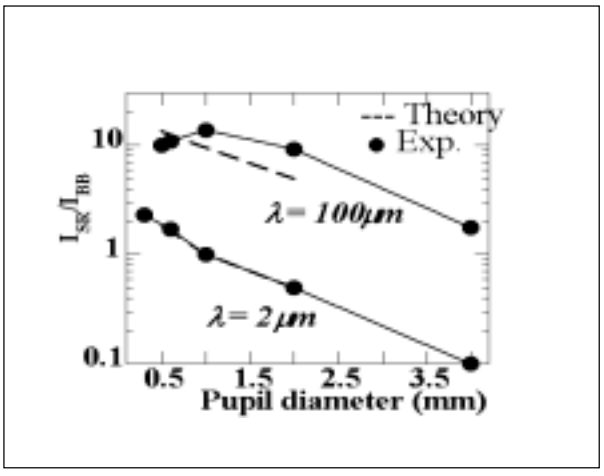

Figure 2: *Ratio between SR and black-body (BB) intensities versus aperture diameter at sample position in the far- (100 μm) and mid-IR (2μm). The solid lines are guides to the eye, while the dashed lines give the Actual Brilliance Ratio between SR (normalized to 1 A of current) and BB.*

between intensity and circulating current. The BB was an Hg lamp for $\lambda \geq$100 μm and a glowbar for $\lambda \geq$2 μm. At 100 μm $I_{SR}(\omega)/I_{BB}(\omega)$ was circa 2 for full aperture ($\sim$ 4 mm), but approached

a maximum value of 20 for d = 1 mm. The agreement with theory is excellent, and the deviations observed in the far-IR for the smallest apertures were attributed to diffraction effects not considered in the calculation. Taking advantage of this significant gain, first experimental results have been obtained on a solid system inside a Diamond Anvil Cell (DAC) in the far-IR domain. These preliminary observations showed that SINBAD performances fulfil its original design expectations. The linear polarization degree was also measured to be 80% in the mid-IR with full open slits. The light observed at a different angle over the orbit is circularly polarized: in the case of SINBAD, the first observations indicated that >80% circularly polarized light was collected by the slits selecting 50% of the total flux available.

One of the 4 multi-pole wigglers installed on the electron ring for vertical beam compaction is utilized as X-ray source. The ∼2 m long 5-pole equivalent planar insertion device emits a wide fan of electromagnetic radiation mostly polarized in the horizontal plane. Thus, two families of non-coherent poles contribute to a typical SR continuous spectral distribution with critical wavelength of circa 40 $\mathring{A}$. The over 1 A circulating current (record value of 1.8 A in 2002) allowed an intense flux of soft X-rays over more than one decade beyond the critical energy. Apporoximately, at the collimation slits of nominal size 15 x 2 mm^2 (h x v) 18 m far from the wiggler (at the monochromator entrance) a maximum SR flux density of $1.5 \cdot 10^{13}$ ph/($smrad^2$) was expected. After the front-end, 4 m downstream the wiggler, the X-Ray beamline design accepts all the vertical SR divergence and more than 12 mrad of the photon fan in the orbit plane. The first horizontal slits, about 1 m far from the front-end, select the beam entering the vacuum pipe through two concrete shielding walls separating the DAΦNE Hall from the rest of the SR laboratory. The X-Ray optics develops afterwards in a tunnel, accessible from the experimental area, with a second set of both horizontal-vertical slits about 10 m aside the wiggler. This collimation system selects the two radiation lobes overlap from the wiggler structured source and define the SR beam size entering into the next mirror chamber. Here, the beam cross section of 20 mm x 50 mm (v x h) corresponds approximately to 5 mrad in horizontal and the full SR vertical divergence. An Au-coated silicon mirror, 80 cm long and 10 cm wide, is used for deflecting in the horizontal plane about one half of the SR fan inward the UV branch line (see below). The actual X-Ray beamline proceeds in the straight section where an 1100 $\mathring{A}$ thick polymide window (70 lines/inch Ni mesh support) guarantees the machine UHV environment with high transmittance of the soft X-rays (>80% at the oxygen K-edge). A last set of precision slits with submillimetric resolution defines the beam entering the monochromator, at most 15 mm x 24 mm (v x h). The monochromator installed on the beamline was a double-crystal system (by Toyama) with the "boomerang" geometry to ensure a fixed beam exit at all energies. Working with Bragg's angles from 15° to 75°, the present equipment of Si (111) and α-Quartz (10-10) crystals couples the spectrum of energies above 2 KeV (and <7.6 KeV) with a resolution $\Delta E/E$ better than 10^{-4} (and 10^{-3}, respectively). The new KTP (011) crystals will extend the working region in the softer X-ray range down to about 1 KeV. The device allows, on demand, the white beam crossing directly from the wiggler source. The experimental set-up immediately after the monochromator (Figure3) includes a multipurpose cylindrical experimental HV chamber for X-Ray Spectroscopy, and two ion chambers (IC) to detect in- and out-ward photon flux in the instance of X-ray Absorption Spectroscopy (XAS) on thin samples. The 26 mm thick kapton windows allowed transmission measures down to the P K-edge, but polymeric films are going to be used in the 1 KeV energy domain. In cascade, an already existing Clean Room (class A 100) have to be equipped with the upgraded remotely controlled stepper device to apply lithographic and micro-engineering techniques on soft X-ray photoresists.

The X-Ray beamline characterization was obtained on performing XAS on material standards. Both EXAFS (Extended X-ray Absorption Fine Structure) and XANES (X-ray Absorption Near-Edge Structure) spectroscopy techniques were applied from 2 KeV up to 4 KeV, which is more than 10 times the critical energy of the wiggler, using the monochromator and Si(111) crystals.

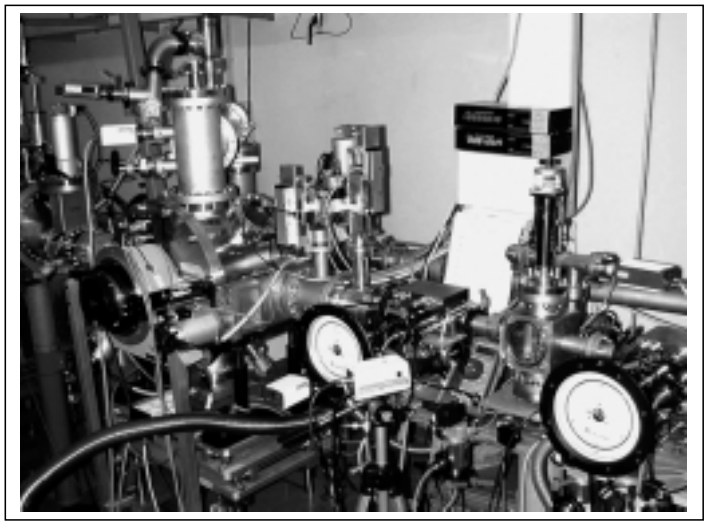

Figure 3: *X-ray beamline experimental set-up: after the double-crystal monochromator, the experimental vacuum chamber is connected in between IC detectors for XAS measurements in transmission mode.*

Data acquisitions were performed in runs of circa 20 minutes in parasitic mode, thus constraining the actual acquisition time to 1 - 3 sec per point. All spectra were acquired by 19 cm long ICs (Oken) in planar geometry filled with Ar or He. Energy calibration was achieved at high resolution using as reference the energy of the Rydberg-like peak of Ar K-edge. Pure Cd and Ag metal foils of thickness, respectively, 2 mm and 1 mm, were analysed and their three L-edges spectral region measured in a single scan (over 2 KeV): low resolution EXAFS spectra were acquired to test both monochromator and IC sensitivity (e.g. the L1-edge "white line" detection). XANES spectra were measured on thin samples in the low energy side of the available spectral range: for example, the perfectly detected potassium K-edge of a thin mica layer is reported in Figure 4, but Cl in a KCl solution deposited on paper filter was also measured. Further XANES acquisition were successfully carried on standard materials of lighter elements like S and P. Planned up-grade on both the detection equipment and experimental set-up can extend the spectral range toward lower energy side of soft X-rays (e.g., down to sodium K-edge), while improvements on the monochromator control system should reach the 6 KeV upper limit.

The SR fan from the wiggler source is splitted by a grazing incidence mirror and originates the Ultra-Violet beamline horizontally deflected at about 80 mrad (cut-off energy ∼800 eV); it collects about 2 mrad^2 of SR radiation down to an experimental hutch dedicated to the SUE experiment. Supported by the INFN 5^{th} Committee, it is devoted to investigate biological effects like cell death, micronucleus induction and oncogenic transformation induced on cultures of human cells and progenies by the B band of the UV radiation (280 - 320 nm). The interesting threshold effect in the narrow energy range investigated has to be clarified with both longer data acquisitions (data under analysis) and finest wavelength scanning planned in next dedicated runs.

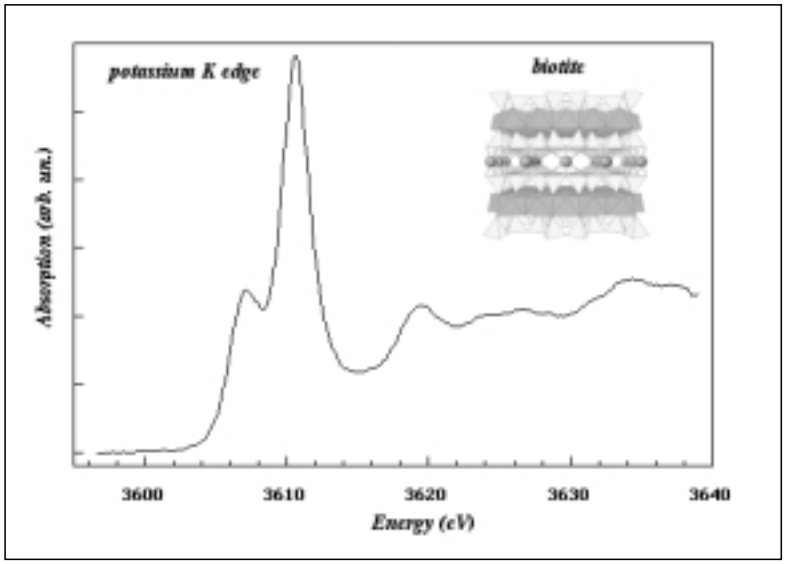

Figure 4: *K-edge normalized XANES spectra in transmission of potassium in a 40 μm thick biotite (mica) foil: the single scan was acquired in a parasitic run of 20 minutes (average current 800 mA). In the inset a 3-D structure of mica crystals is shown.*

2 Conference Proceedings 2002

1. E. Burattini, G. Cinque, G. Bellisola, G. Fracasso, F. Monti, and M. Colombatti, in "X-ray and Inner-shell Processes", Eds. A. Marcelli, A. Bianconi, and N.L. Saini, AIP Conference Proceedings 652 (1) 515I.

2. Z.Y. Wu, C.R. Natoli, A. Marcelli, E. Paris, A. Bianconi and N.L. Saini, in "X-ray and Inner-shell Processes", Eds. A. Marcelli, A. Bianconi, and N.L. Saini, AIP Conference Proceedings 652, 497.

3. S. Bellucci, S. Botti, A. Marcelli, K. Ibrahim and Z.Y. Wu, in "X-ray and Inner-shell Processes", Eds. A. Marcelli, A. Bianconi, and N.L. Saini, AIP Conference Proceedings 652, 355.

4. S.B. Dabagov, in "X-ray and Inner-shell Processes", Eds. A. Marcelli, A. Bianconi, and N.L. Saini, AIP Conference Proceedings 652, 89.

5. G. Cappuccio, S.B. Dabagov, A. Pifferi, Riassunti dei lavori Associazione Italiana di Cristallografia, XXXI Congresso, 44 (2002),

6. S.B. Dabagov, Proc. SPIE 4765, 87 (2002).

7. G. Cappuccio, S.B. Dabagov, Proc. SPIE 4765; 99 (2002).

8. R.V. Fedorchuk, S.B. Dabagov, V.A. Murashova, M.N. Yakimenko, Proc. SPIE 4765, 104 (2002).

9. G. Cappuccio, S.B. Dabagov, Proceedings SPIE 4765, 99 (2002).

10. R.M. Montereali, G.C. Righini, S. Pelli, E. Burattini, A. Grilli, M. Piccinini, Proc. SPIE 4829, 683 (2002).

11. R.M. Montereali, F. Bonfigli, A. Pace, M. Montecchi, E. Nichelatti, A. Grilli, M. Piccinini, S. Bigotta, Quaderni di ottica e fotonica SIOF9, 89 (2002).

3 Publications

1. A.N. Mansour *et al.*, Phys. Rev. B **65**, 134207 (2002);

2. E.M. Latush *et al.*,Nuclear Instr. & Meth. A **491**, 512 (2002);

3. Z. Wu *et al.*, Appl. Phys. Lett. **80**, 2973 (2002);

4. S.B. Dabagov *et al.*, Nucl Instr. & Meth. B **187**, 169 (2002);

5. A. Mottana *et al.*, Rev. Miner. & Geochem. **46**, 371 (2002);

6. F. Tombolini *et al.*, Inter. J. Mod. Phys. B**16**, 1673 (2002);

7. E.M. Latush *et al.*, Instr. Exp. Tech.**45**, 819 (2002);

8. T. Polivka *et al.*, Biochemistry **41**, 439 (2002);

9. G. Zucchelli *et al.*, Biophysical Journal **8**2, 378 (2002);

10. F. Belloni *et al.*, Radiat. Prot. Dosim., **99** (1-4), 199 (2002);

11. G.F. Grossi *et al.*, LNL INFN Annual Report 2001, LNLINFN rep 182, 87 (2002);

12. F. Belloni *et al.*, LNF INFN Annual Report 2001, LNF-02/024 (IR), 142-144 (2002);

13. Z.Y. Wu *et al.*, Chen, Appl. Phys. Lett. **80**, 2973 (2002);

14. N.L. Saini *et al.*, Superconductor Science and Technology **15**, 439 (2002);

15. G. Giuli *et al.*, Eur. J. Mineral. **14**, 429 (2002);

16. Z.Y. Wu *et al.*, Intern. J. Modern Physics **B16**, 1605 (2002);

17. S. Qin *et al.*, Eur. J. Mineral. **14**, 1049 (2002);

18. Z.Y. Wu *et al.*, J. Synchrotron Rad.**9**, 394 (2002);

19. M. Pedio *et al.*, Phys. Rev. **B6**6, 144109 (2002);

20. J. Zhang *et al.*, Optical Materials **21**, 573 (2003);

21. N.L. Saini *et al.*, J. Phys.: Condens. Matter **14**, 13543 (2002);

22. Y.L. Ji *et al.*, J. Am. Chem. Society **124**, 14864 (2002);

23. E. Burattini *et al.*, Nuovo Cimento **117**(7), 769 (2002);

24. S.B. Dabagov *et al.*, Nucl. Instr. Meth. **B187** (2) 169 (2002);

25. A.G. Revenko *et al.*, Zavodskaya Laboratoriya **68** (5) 3 (2002);

26. C. Ercole *et al.*, Int. J. Speleol. **30A** (I/4) 69 (2002);
27. S. B. Dabagov*et al.*, Nucl. Instr. and Meth. **B187**, 169 (2002);
28. R.M. Montereali *et al.*, Optics Communications **209**, 201(2002);
29. R.M. Montereali *et al.*, Elettrottica 2002, **93** (2002).
30. A.N. Mansour *et al.*, Phys. Rev. **B65**, 134207 (2002);
31. E.M. Latush *et al.*, Nuclear Instr. & Meth. **A491**, 512 (2002);
32. Z. Wu, J. Zhang *et al.*, Appl. Phys. Lett. **80**, 2973 (2002);
33. S.B. Dabagov *et al.*, Nucl Instr. and Meth. **B187**, 169 (2002);
34. A. Mottana *et al.*, Rev. Miner. & Geochem. **46**, 371 (2002);
35. F. Tombolini *et al.*, Inter. J. Mod. Phys. **B16**, 1673 (2002);
36. E.M. Latush *et al.*, Instr. Exp. Tech. **45**, 819 (2002);
37. T. Polivka *et al.*, Biochemistry **41**, 439 (2002);
38. G. Zucchelli *et al.*, Biophysical Journal **82**, 378 (2002);
39. F. Belloni *et al.*, Radiat. Prot. Dosim., **99**(1-4), 199 (2002);
40. G.F. Grossi *et al.*, LNL INFN Annual Report 2001, LNL INFN rep 182, 87 (2002);
41. F. Belloni *et al.*, LNF INFN Annual Report 2001, LNF-02/024 (IR), 142-144 (2002);
42. Z.Y. Wu *et al.*, Appl. Phys. Lett. **80**, 2973 (2002);
43. N.L. Saini *et al.*, Superconductor Science and Technology **15**, 439 (2002);
44. G. Giuli *et al.*, Eur. J. Mineral. **14**, 429 (2002);
45. Z.Y. Wu *et al.*, Intern. J. Modern Physics **B16**, 1605 (2002);
46. S. Qin *et al.*, Eur. J. Mineral. **14**, 1049 (2002);
47. Z.Y. Wu *et al.*, J. Synchrotron Rad. **9**, 394 (2002);
48. M. Pedio *et al.*, Phys. Rev. **B6**, 144109 (2002);
49. J. Zhang *et al.*, Optical Materials **21**, 573 (2003);
50. N.L. Saini *et al.*, J. Phys.: Condens. Matter **14**, 13543 (2002);
51. Y.L. Ji *et al.*, J. Am. Chem. Society **124**, 14864 (2002);
52. E. Burattini *et al.*, F. Monti, Nuovo Cimento **11** (7), 769 (2002);
53. S.B. Dabagov *et al.*, Nucl. Instr. Meth. **B187** (2) 169 (2002);
54. A.G. Revenko *et al.*, Zavodskaya Laboratoriya **68** (5) 3 (2002);
55. C. Ercole *et al.*, Int. J. Speleol. **30A** (I/4) 69 (2002);
56. S. B. Dabagov *et al.*, Nucl. Instr. and Meth. B **187**, 169 (2002);
57. R.M. Montereali *et al.*, Optics Communications **209**, 201(2002).
58. R.M. Montereali*et al.*, Elettroottica **200**2, 93 (2002).

GILDA

A. Balerna, F. Campolungo (Tecn.), S. Mobilio (Resp.), V. Sciarra (Tecn.)
V. Tullio (Tecn.)

1 Introduction

GILDA (General Purpose Italian BeamLine for Diffraction and Absorption), is the italian CRG beamline (Collaborating Research Group), built to provide the italian scientific community with an easy access to the European Synchrotron Radiation Facility (ESRF) to perform experiments with a high energy and brilliance X-ray photon beam. GILDA is funded by the three italian public research Institutes: Consiglio Nazionale delle Ricerche (CNR), Istituto Nazionale per la Fisica della Materia (INFM) and Istituto Nazionale di Fisica Nucleare (INFN). Experimental stations for X-ray Absorption Spectroscopy, Anomalous X-ray Scattering and X-ray Diffraction (XRD) are present at the GILDA beamline.

2 Activity on the GILDA beamline during 2002

A new software for the alignment of the collimating and focussing mirrors of the beamline was developed. The new software was implemented in the Client/Server philosophy under LABVIEW system and allows a quick and easy alignment of the mirrors; in this way the dead time during configuration changes can be minimized.
A new holder for the first crystal was realized in order to improve its thermal stability; the tests with the beam are foreseen in summer.
Beam monitors in the second and third experimental hutch were installed and successfully tested.
In order to optimize the beamline performances, a new encoder was installed in the monochromator; this encoder is not directly coupled with the crystal movement; its use allows a more smooth movement of the crystal, resulting in an improvement of the overall quality of the spectra.
The standardization of the hardware and software of the beamline to the ESRF requirements was extended to the diffraction hutch and is now continuing with the third hutch.
Great attention was given to the optimization of the fluorescence detection system.
In particular, for what concerns the 13 elements HP-Ge detector, a systematic study was performed in order to understand the procedure to correct the experimental data for the dead time of the detector, when used with high counting rate.
Within the MANU-2 experiment of the INFN Group II, for the first time a micro-calorimeter based on a Transition Edge Sensor (TES) working at 150 mK was tested on a synchrotron source at the GILDA beamline. The aim was to demonstrate the possibility of using cryogenic detectors for hard X-rays, making profit of their high energy resolution. The test was partially successful: a resolution of about 70 eV was achieved at about 10KeV which is 2-3 times better than the one achievable with HP-Ge detectors. The limiting factor were determined, and in the future new tests will be performed in optimized condition, in order to reach the resolution achievable with this kind of detectors of the order of few eV.
A new oven was installed in the X-ray absorption hutch, allowing to study systems at high temperatures up to about 2000 K.

3 Beamtime use during 2002 and scientific outcomes

During 2002, 50 experiments were performed on GILDA, 36 of italian groups and 14 of european groups. Studies and results to be mentioned are:

1. The study on the luster decoration of glasses of renaissance pottery, that has shown the similarity, at a microscopic level, of these ancient materials with modern glasses like ion-exchanged and ion-implanted glasses, studied today for their non linear optical properties.
2. The study of the local structure in III-V semiconductors, like GaAsN and InGaAsN semiconductors; in these systems a tendency towards the chemical ordering as well as a noticeable deviation from the standard behavior of semiconductor alloys was observed.
3. The study of rare earth exchanged cubic manganites like $La_xCa_{1-x}MnO_3$ that have interesting physical properties originating from an interplay between their magnetic, transport and thermal properties. The most popular is the colossal magnetoresistance effect, which consists in a 100% variation of the electrical resistivity with the application of a magnetic field. The microscopic origin of such an effect is still controversial, but a relevant contribution is believed to be due to the coupling of the local structure around the Mn atoms with the conduction electrons. This interaction results in a metal insulator transition at a temperature which is sensitive to the magnetic field. Such coupling and its changes have been measured by means of XAFS (X-ray Absorption Fine Structure) at GILDA.
4. The study of the local structure of the interfaces of Mo/Si multilayers. These systems are of interest for the production of mirrors with high reflectivity in the soft X-ray range, of particular interest both for X-ray astrophysics and soft X-ray lithography. The sharpness of the interfaces and the inter-diffusion of the two elements, crucial parameters for the optimization of the mirrors reflectivity, were measured by using the standing waves generated by Bragg reflection of the multilayer structure to maximize the sensitivity to the Mo-Si interface.

4 2003 - GILDA Foreseen Activity

The activity foresees: 1) the installation of a new second mirror in order to improve the beam homogeneity in the second and third hutch; 2) the design of a new bender for the second monochromator crystal in order to improve the beam dimension in all the three experimental hutches; 3) the test of the improved version of the TES detector. Support will be given to the users, both during the experimental data acquisition and during the data analysis. The continuous upgrade of the instrumentation will be continued, in order to maintain the beamline at the top level it has today.

References

1. G. Faraci, A.R. Pennisi,R. Puglisi, A. Balerna, Phys. Rev. **B 65**, 024101 (2002)
2. G. Faraci, A.R. Pennisi, A. Balerna, Europ. Phys. J. **B 30**, 393 (2002)
3. F. D' Acapito, F. Boscherini, S. Mobilio, A. Rizzi, R. Lantier, Phys. Rev. **B 66**, 205411 (2002)
4. C. Meneghini, C. Castellano, S. Mobilio, A. Kumar, S. Ray, D.D. Sarma, J. of Phys.: Condensed Matter **14**, 1967 (2002)
5. A.Terrasi, S. Scalese, M. Re, E. Rimini, F. Iacona, V. Raineri, F. La Via, S.Colonna, S. Mobilio, J. Applied Phys. **91**, 6754 (2002)

NTA.TTF

L. Cacciotti (Tecn), M. Castellano (Resp), G. Di Pirro, M. Ferrario, G. Fuga (Tecn),
S. Guiducci, R. Sorchetti (Tecn), F. Tazzioli

1 Introduction

The TESLA Test Facility (TTF) is an international effort, based at Desy (Hamburg), aiming at the development of the technologies required for a Superconducting e^+e^- Linear Collider. High-gradient superconducting RF cavities, with their high-power coupling and tuning device, and low cost cryostats were the main goal of the project. The production of a high-power, long-pulse electron beam from an RF gun was an additional requirement. This involved the development of new photocathode, an adequate laser source and new beam diagnostics.

In addition to prove the possibility of producing and accelerating the kind of beam required for the TESLA Lineal Collider, TTF has also demonstrated that this beam was of enough good quality to be successfully used for the production of UV coherent radiation with the Self Amplified Spontaneous Emission (SASE) Free Electron Laser process, that is an important part of the TESLA project.

The INFN contribution comes from LNF, LNL, Sezione di Milano and Sezione di Roma 2.

2 Activity in 2002

In 2002 the first part of the TTF project has been completed.

SC cavities with accelerating gradient larger than 30 MV/m (in vertical cryostat test) have been produced. A full power beam, with an 800 microsecond long pulse has been successfully accelerated at the averaged gradient of 22 MV/m (see Fig. 1).

The Free Electron Laser has reached a steady saturation regime at a wavelength as short as 80 nm.

In summer 2002 the installation of the so called TTF2 has started. The goal is the operating of a 1 GeV machine, with the same beam parameters of TTF, apart from a somewhat smaller emittance. Eventually, the machine will become an "user facility" for the FEL radiation, whose wavelength should reach 6 nm, but in the first stage other experiments will be performed to test components for the TESLA Linear Collider.

Among others, the tests of the new high-gradient SC cavities, with their new tuning system, the powering of many cryostats and the control of the full power, high energy beam. The LNF contribution, in collaboration with Roma 2, is mainly in the beam optical diagnostics. 15 new diagnostic stations, detecting Optical Transition Radiation, will be installed along the beam transfer line to the undulator, as well as on the by-pass line, that will be used for beam commissioning.

For each station an optical system must provide a variable magnification, a variable filtering of radiation, and the control of a digital camera. The system must be robust for prolonged operation, and simple enough to allow its use by non-specialist operators. Meanwhile, its accuracy must be "state of the art" for precise measurements.

A complete new design has been proposed, and a prototype fully tested at LNF. The image acquisition and its analysis is a responsibility of LNF and Roma 2, together with the real time publishing of the images to allow a remote control of the linac. Feasibility tests for this will be performed by LNF.2

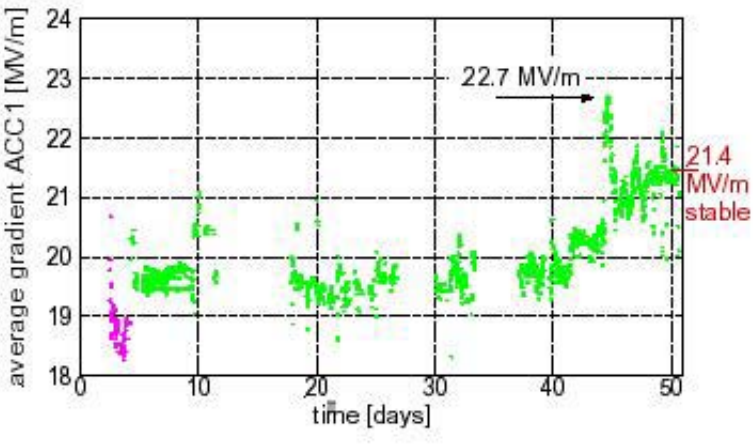

Figure 1: *Average gradient with 800 microsecond long pulse.*

3 Publications

1. V. AYVAZIAN *et al.* Generation Of GW Radiation Pulses From A VUV Free-Electron Laser Operating In The Femtosecond Regime. Phys. Rev. Lett. 88, 104802, (2002).

2. V. AYVAZYAN, N. BABOI, I. BOHNET, R. BRINKMANN, M. CASTELLANO *et al.* A New Powerful Source for Coherent VUV Radiation: Demonstration of Exponential Growth and Saturation at the TTF Free-Electron Laser Eur. Phys. J. D **20**, 149, (2002).

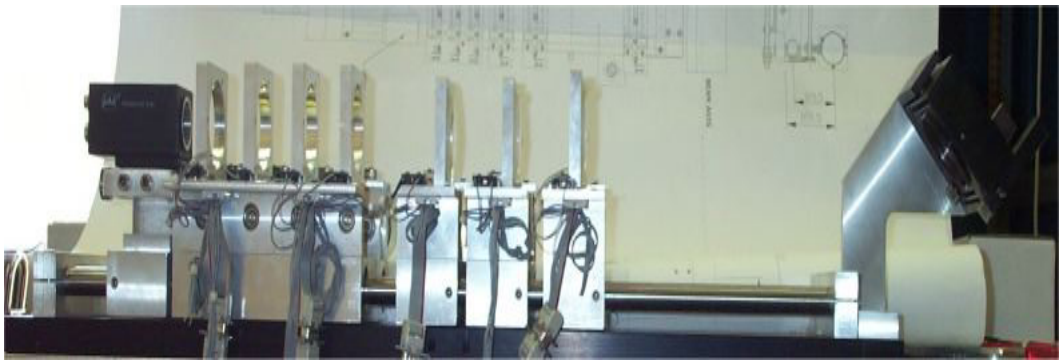

Figure 2: *The prototype of the optical system.*

SPARC

D. Alesini, S. Bertolucci, M.E. Biagini, C. Biscari, R. Boni, M. Boscolo,
M. Castellano, A. Clozza, G. Di Pirro, A. Drago, A. Esposito, M. Ferrario,
V. Fusco, A. Gallo, A. Ghigo, S. Guiducci, M. Incurvati, P. Laurelli, C. Ligi,
F. Marcellini, M. Migliorati, C. Milardi, L. Palumbo (Resp.), L. Pellegrino,
M. Preger, P. Raimondi, R. Ricci, C. Sanelli, M. Serio, F. Sgamma,
B. Spataro, A. Stecchi, A. Stella, F. Tazzioli, C.Vaccarezza,
M. Vescovi, C. Vicario, M. Zobov **(INFN /LNF)**

F. Alessandria, I. Boscolo, F. Broggi, S.Cialdi, C. DeMartinis,
D. Giove, C. Maroli, V. Petrillo, M. Romè, L. Serafini **(INFN /Milano)**

E. Chiadroni, G. Felici, D. Levi, M. Mastrucci, M. Mattioli,
G. Medici, G. S. Petrarca **(INFN /Roma1)**

L. Catani, A. Cianchi, A. D'Angelo, R. Di Salvo, A. Fantini,
D. Moricciani, C. Schaerf, S. Tazzari **(INFN /Roma2)**

1 Aim of the experiment

The Project SPARC (Sorgente Pulsata e Amplificata di Radiazione Coerente), proposed by a collaboration among ENEA-INFN-CNR-Università di Tor Vergata-INFM-ST, was recently approved by the Italian Government and will be built at LNF. The aim of the project is to promote an R&D activity oriented to the development of a coherent ultra-brilliant X-ray source in Italy. This collaboration has identified a program founded on two main issues: the generation of ultra-high peak brightness electron beams and of resonant higher harmonics in the SASE-FEL process.

It is actually well known that the requirements on the electron beam quality, in terms of peak current, energy spread and normalized transverse emittance, imposed by the needs to drive a SASE-FEL instability at very short wavelengths (from 10 nm down to 1 Angstrom), typically exceed the present capability of storage rings by large factors, while they are in perspective attainable by Linacs equipped with advanced photo-injectors and compressor devices (magnetic and/or RF compressors). The benefit of such an effort, i.e. attaining such peak brightness in the electron beam, is the availability of a radiation source emitting coherent X-rays with unprecedented brightness, many orders of magnitude higher than that delivered by (present) third generation light sources.

The overall SPARC project consists of 4 main lines of activity aiming at several goals: their common denominator is to explore the scientific and technological issues that set up the most crucial challenges on the way to the realisation of a SASE-FEL based X-ray source, the SPARX proposal. These are:

1. 150 MeV Advanced Photo-Injector

   Since the performances of X-ray SASE-FEL's are critically dependent on the peak brightness of the electron beam delivered at the undulator entrance, we want to investigate two main issues - generation of the electron beam and bunch compression via magnetic and/or RF velocity bunching - by means of an advanced system delivering 150 MeV electrons, the minimum energy to avoid further emittance dilutions due to time-dependent space charge effects.

2. SASE-FEL Visible-VUV Experiment

   In order to investigate the problems related to matching the beam into an undulator and keeping it well aligned to the radiation beam, as well as the generation of non-linear coherent higher harmonics, we want to perform a SASE FEL experiment with the 150 MeV beam, using a segmented undulator with additional strong focusing, to observe FEL radiation at 530 nm and below.

3. X-ray Optics/Monochromators

   The X-ray FEL radiation will provide unique radiation beams to users in terms of peak brightness and pulse time duration (100 fs), posing at the same time severe challenges to the optics necessary to guide and handle such radiation. This project will pursue also a vigorous R&D activity on the analysis of radiation-matter interactions in the spectral range typical of SASE X-ray FEL's (from 0.1 to 10 nm), as well as the design of new optics and monochromators compatible with these beams.

4. Soft X-ray table-top Source

   In order to test these optics and to start the R&D on applications, the project will undertake an upgrade of the presently operated table-top source of X-rays at INFM-Politecnico Milano, delivering 107 soft X-ray photons in 10-20 fs pulses by means of high harmonic generation in a gas. This will be a very useful bench-test for the activities performed in item 3 above.

2 Group activity in 2002

The activity of the group in 2002 concerned the design of the main devices of the SPARC project, and in particular:

- design of Laser system
- design of RF gun
- design of Linac structure
- design of magnetic components
- design of diagnostics and vacuum

2.1 Advanced Photo-Injector

Two are the main goals of this activity: acquiring an expertise in the construction, commissioning and characterisation of an advanced photo-injector system and performing an experimental investigation of two theoretical predictions that have been recently conceived and presented by members of this study group. These are: the new working point for high brightness RF photo-injectors (Fig. 1) and the velocity bunching technique to apply RF bunch compression through the photo-injector, with emittance preservation (Fig. 2).

The 150 MeV injector will be built inside an available bunker of the Frascati INFN National Laboratories: the general layout of the system is shown in Figs. 3 and 4.

The proposed system to be built consists of: a 1.6 cell RF gun (Fig. 5) operated at S-band (2.856 GHz, of the BNL/UCLA/SLAC type) and high peak field on the cathode (120-140 MeV/m) with incorporated metallic photo-cathode (Copper or Mg), generating a 6 MeV beam which is properly focused and matched into 2 accelerating sections of the SLAC type (S-band, travelling wave) the third section is foreseen for the rectilinear compressor experiment, as explained later.

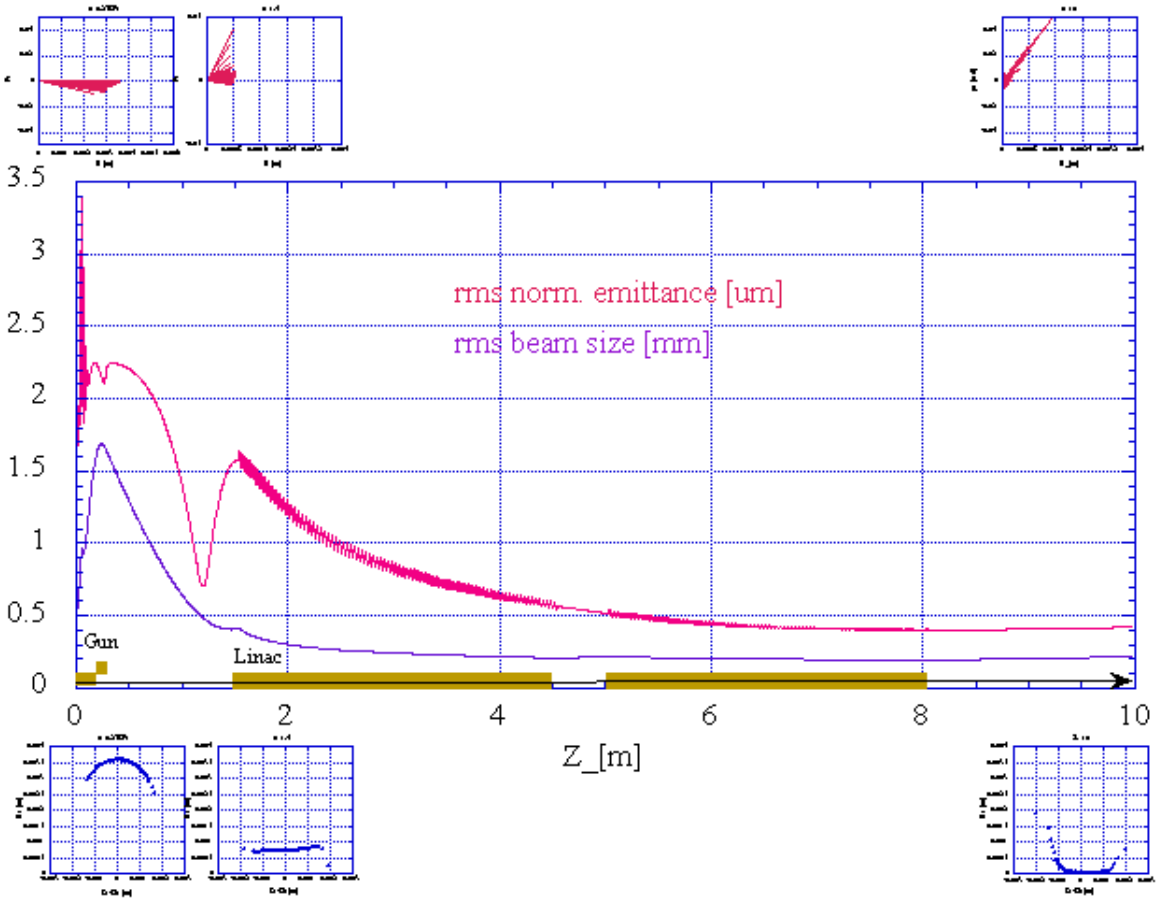

Figure 1: *Rms normalised emittance and beam rms envelope along the SPARC beam line up to 150 MeV (HOMDYN simulation).*

The laser system driving the photocathode will use the radiation from a Ti:Sa laser with the oscillator pulse train locked to the RF. Ti:Sa mode locked oscillator and amplifiers able to produce the requested energy per pulse (500 μJ at 266 nm) are commercially available. To obtain the time pulse shape we are going to test the manipulation of frequency lines in the large bandwidth of Ti:Sa, in order to produce the 10 ps long flat top shape. We can use a liquid crystals mask in the Fourier plane of the non-dispersive optic arrangement or a collinear acusto-optic modulator for line frequency manipulation.

Liquid crystals act as pixels that introduce a controlled phase delay on different parts of the spatially dispersed spectrum. The acusto-optic modulator performs a continous frequency modulation and can operate on a bandwith up to 200 nm, one order of magnitude larger than the capability of liquid crystals. The transverse homogeneity is produced with a pinhole and a position dependent transmission filter. The time and energy stability can be achieved by proper feedback loops and by the control of the laser environment.

The first experiment with the electron beam we have planned to do is the verification of

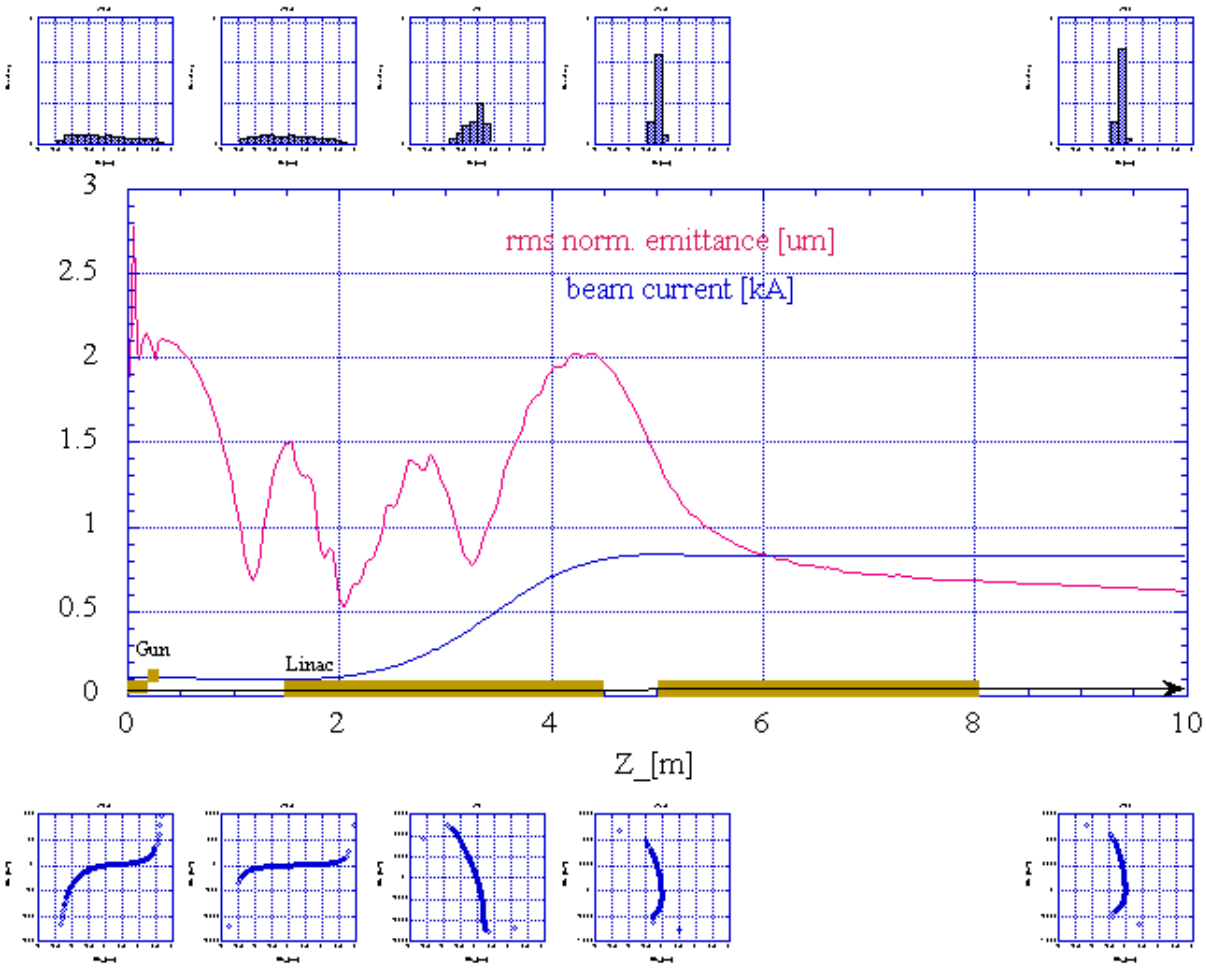

Figure 2: *Rms normalised emittance and beam current along the SPARC beam line when the first cavity is operating in the bunching mode (HOMDYN simulation).*

the beam emittance compensation process predicted by a new working point. The key point is the measurement of the emittance oscillation in the drift after the gun where a double minima behaviour is expected. Since the optimum beam matching to the booster is predicted on the relative emittance maximum, a dedicated mouvable emittance measurement station has been designed.

A pepperpot and a screen are connected with three long bellows in order to scan the emittance along a 1 m long drift and to find experimentally the optimum location of the first TW structure.

The chromatic origin of the double emittance minima behaviour, due to the solenoid energy dependent focal length, and the charge and gun peak field scaling will also be investigated at the beginning of the experimental program.

Our simulations using PARMELA indicate that we can generate with this system a beam like that needed by the FEL experiment at 150 MeV. The rms correlated energy spread over the bunch is 0.14 with a rms normalised emittance of 1.2 mmmrad (at 1 nC bunch charge, 150 A peak current), but the slice energy spread and the slice normalised emittance, calculated over a 300 mm slice length (comparable to the anticipated cooperation length), are well below 0.05% and 0.5

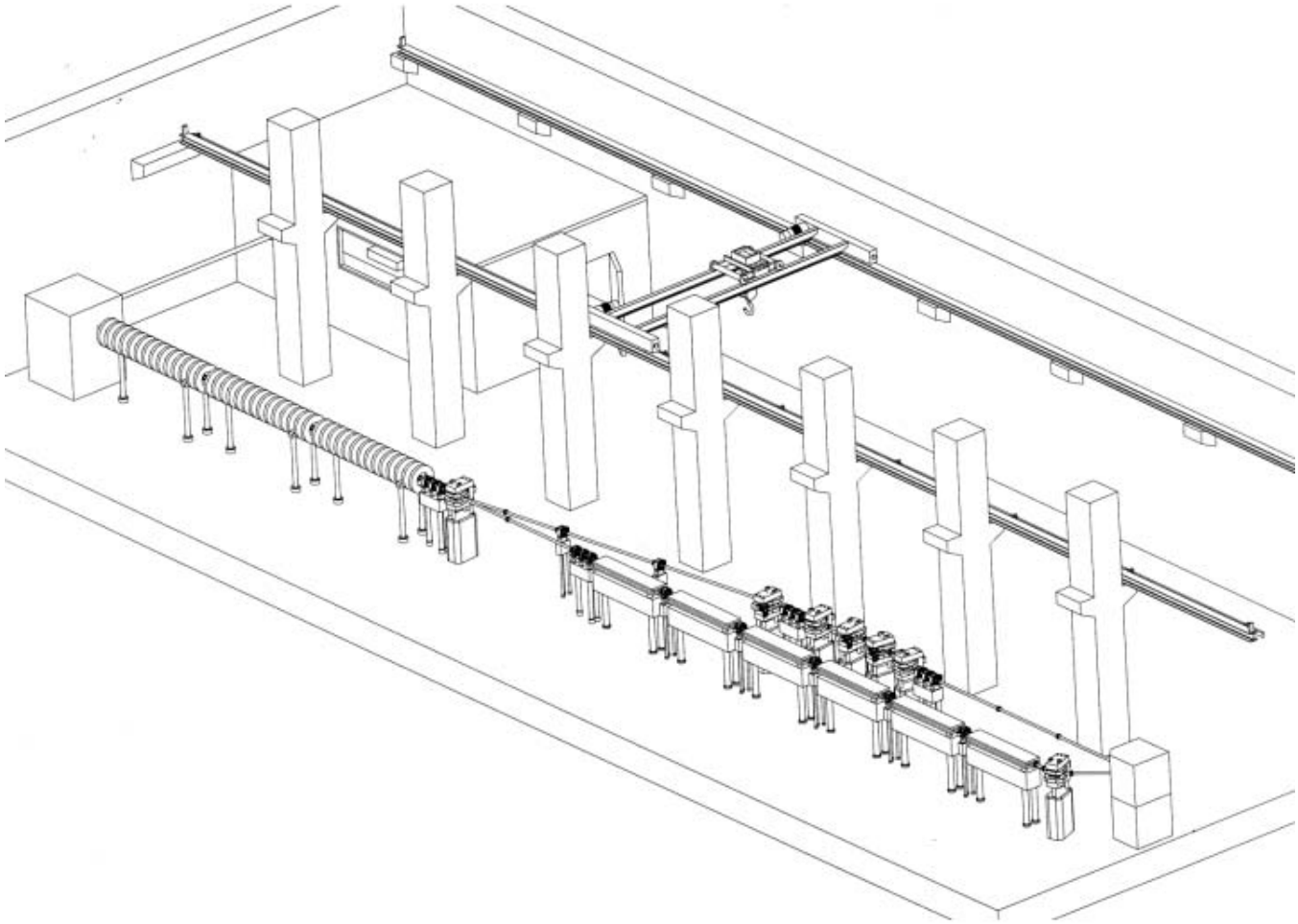

Figure 3: *3D view of the SPARC beam line in its bunker.*

mmmrad respectively all over the bunch (see Fig. 6).

2.2 The FEL SASE Source

The FEL SASE experiment will be conducted using a permanent magnet undulator made of 6 sections, each 2.5 m long, separated by 0.3 m gaps hosting single quadrupoles which focus in the horizontal plane. The undulator period is set at 3.3 cm, with an undulator parameter kw = 1.88 .

Simulations performed with GENESIS shows that the exponential growth of the radiation power at 530 nm along the undulator saturates after 14 m of total undulator length with a power of 108 Watts. Preliminary evaluations of the radiation power generated into the non-linear coherent odd higher harmonics show that 107 and 7x105 W can be reached on the third and fifth harmonics, respectively.

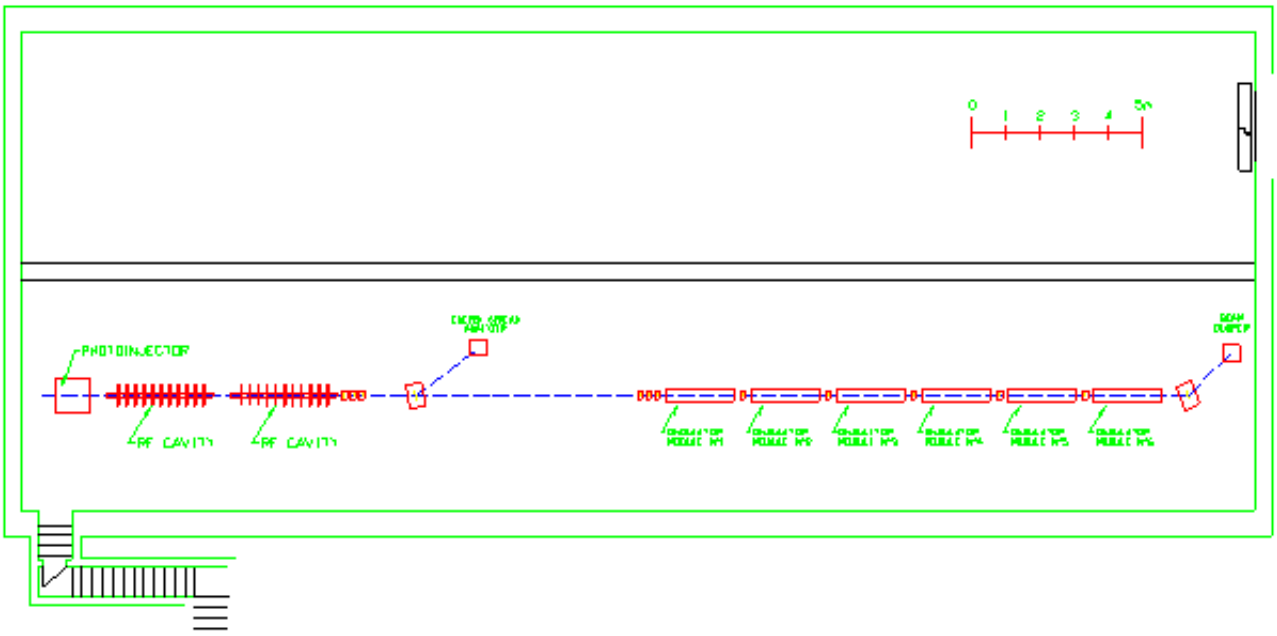

Figure 4: *Lay-out of SPARC Project.*

3 Further Experiments

As shown in Figs. 1 and 2, the SPARC layout displays two main upgrades that will be implemented in a second phase of the project: a third accelerating section which will be inserted downstream the RF gun and a parallel beam line containing a magnetic compressor.

The new section will be designed to study RF compression: it will support traveling waves at an adjustable phase velocity (from v=c down to v=0.999c) in order to exploit the full potentialities of the velocity bunching technique. Its design and construction will proceed in parallel to the commissioning of the SPARC injector system (RF gun + 2 standard SLAC-type 3 m sections). These tests of RF compression assume great relevance in our R&D program since the general lay-out for SPARX foresees the use of a mixed compression scheme, RF compression in the photoinjector up to 700 A and one single stage of magnetic compression at 1 GeV up to the final peak current of 2.5 kA.

The second beam line will allow to conduct experiments on magnetic compression: we want to experimentally investigate CSR induced effects on emittance degradation and surface roughness wake-field effects, without interefering with the ongoing FEL experiment.

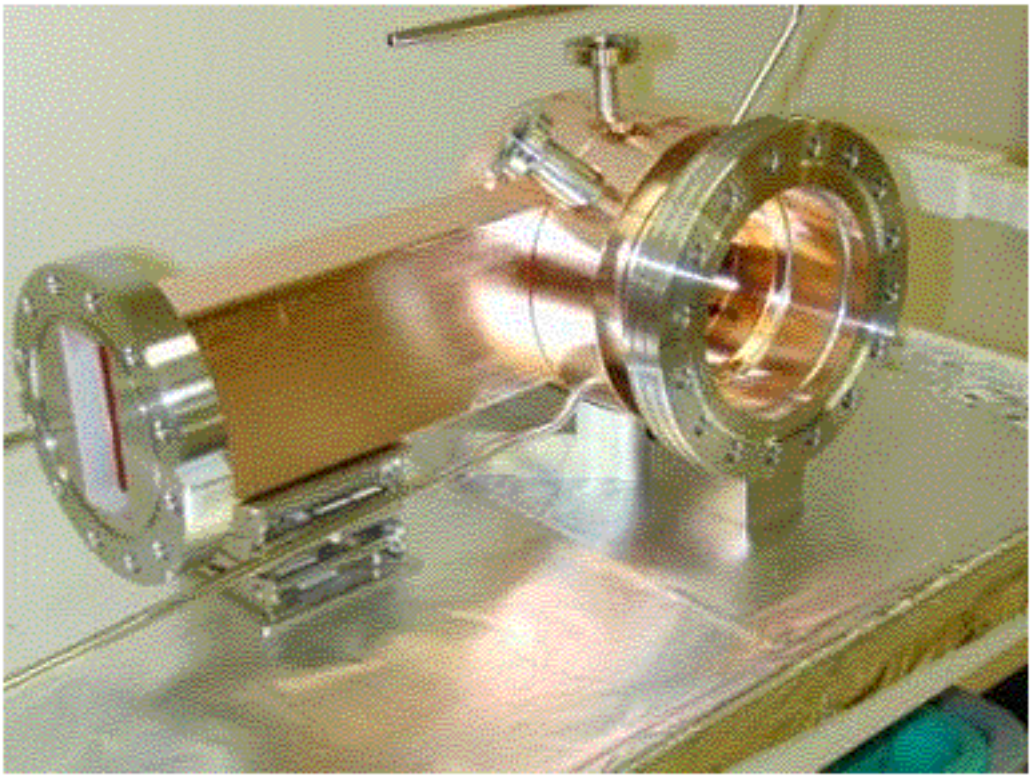

Figure 5: *2856 MHz 1.6 cells RF gun of the BNL/UCLA/SLAC type.*

Rise time: 1 psec, slice analysis

Slice length=300 μm

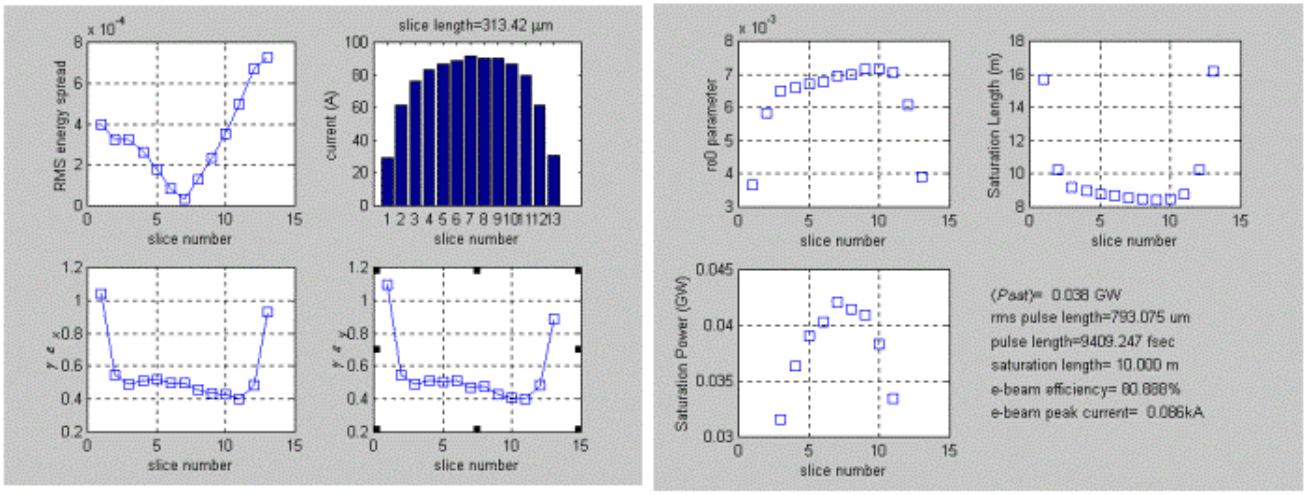

The central slices (81% of the beam) show

ε_n <0.6 mm mrad, σ_e<5e^{-4} => saturation length < 10 m

Figure 6: *Slice analysis of the SPARC beam at the exit of the linac section (PARMELA simulations).*

4 Publications

1. L. Palumbo, et al., *An R&D program for a high brightness electron beam source at LNF*, *European Particle Accelerator Conference 2002*, pp. 1807-1809, Paris, June 2002, anche LNF-02/016 (P), pp. 40-42, Frascati, 12 Luglio 2002.

2. L. Palumbo, et al., *Design study of a soft x-ray SASE-FEL source*, *European Particle Accelerator Conference 2002*, pp. 825-827, Paris, June 2002, anche LNF-02/016 (P), pp. 34-36, Frascati, 12 Luglio 2002.

3. L. Palumbo, et al., *Conceptual design of a soft X-ray SASE-FEL source*, *X-Ray and Inner-Shell Processes: 19^{th} International Conference on X-Ray and Inner-Shell Processes*, AIP Conference Proceedings 652, pp. 53-58.

4. L. Palumbo, et al., *Conceptual Design of a High-Brightness Linac for Soft X-ray SASE-FEL Source*, FEL Conference 2002, to be published on NIM A.

5. L. Palumbo, et al., *The SPARC Project: A High-Brightness Electron Beam Source at LNF to Drive a SASE-FEL Experiment*, FEL Conference 2002, to be published on NIM A.

YEAR 2002 FRASCATI INTERNAL REPORTS

Available at www.lnf.infn.it

1 Frascati Reports

- LNF-02/001 (P)

  The KLOE Collaboration: A. Aloisio, F. Ambrosino, A. Andryakov, A. Antonelli, M. Antonelli, C. Bacci, G. Bencivenni, S. Bertolucci, C. Bini, C. Bloise, V. Bocci, F. Bossi, P. Branchini, S. A. Bulychjov, G. Cabibbo, R. Caloi, P. Campana, G. Capon, G. Carboni, M. Casarsa, V. Casavola, G. Cataldi, F. Ceradini, F. Cervelli, F. Cevenini, G. Chiefari, P. Ciambrone, S. Conetti, E. De Lucia, G. De Robertis , R. De Sangro, P. De Simone, G. De Zorzi, S. Dell'Agnello, A. Denig, A. Di Domenico, C. Di Donato, S. Di Falco, A. Doria, M. Dreucci, O. Erriquez, A. Farilla, G. Felici, A. Ferrari, M. L. Ferrer, G. Finocchiaro, C. Forti, A. Franceschi, P. Franzini, C. Gatti, P. Gauzzi, S. Giovannella, E. Gorini, F. Grancagnolo, E. Graziani, S. W. Hand, M. Incagli, L. Ingrosso, W. Kluge, C. Kuo, V. Kulikov, F. Lacava, G. Lanfranchi, J. Lee-Franzini, D. Leone, F. Lud, M. Martemianov, M. Matsyuk, W. Mei, A. Menicucci, L. Merola, R. Messi, S. Miscetti, M. Moulson, S. Müller, F. Murtas, M. Napolitano, A. Nedosekin, F. Nguyen, M. Palutan, L. Paoluzi, E. Pasqualucci, L. Passalacqua, A. Passeri, V. Patera, E. Petrolo, D. Picca, G. Pirozzi, L. Pontecorvo, M. Primavera, F. Ruggieri, N. Russakovic, P. Santangelo, E. Santovetti, G. Saracino, R. D. Schamberger, B. Sciascia, A. Sciubba, F. Scuri, I. Sfiligoi, T. Spadaro, E. Spiriti, G. L. Tong, L. Tortora, E. Valente, P. Valente, B. Valeriani, G. Venanzoni, S. Veneziano, A. Ventura, Y. Xu, Y. Yu, P. F. Zema

  Measurement of the branching fraction for the decay

  Submitted to Elsevier Science for publication on Phys. Lett. B.

- LNF-02/002 (P)

  The KLOE Collaboration: M. Adinolfi, F. Ambrosino, M. Antonelli, C. Bini, V. Bocci, F. Bossi, P. Branchini, G. Cabibbo, R. Caloi, M. Casarsa, G. Cataldi, P. Ciambrone, E. De Lucia, G. De Robertis, P. De Simone, S. Dell'Agnello, A. Denig, A. Di Domenico, C. Di Donato, S. Di Falco, A. Doria, G. Felici, A. Ferrari, G. Finocchiaro, C. Forti, P. Franzini, C. Gatti, P. Gauzzi, S. Giovannella, E. Graziani, P. Guarnaccia, M. Incagli, C. Kuo, G. Lanfranchi, M. Martemianov, W. Mei, R. Messi, M. Moulson, S. Muller, F. Murtas, L. Pacciani, M. Palutan , E. Pasqualucci, L. Passalacqua, A. Passeri, V. Patera, D. Picca, G. Pirozzi, L. Pontecorvo, M. Primavera, F. Ruggieri, P. Santangelo, E. Santovetti, G. Saracino, C. Schwick, B. Sciascia, A. Sciubba, I. Sfiligoi, T. Spadaro, E. Spiriti, P. Valente, B. Valeriani, G. Venanzoni, A. Ventura

The Trigger System of the KLOE Experiment

Submitted to Nucl. Instr. & Meth.

- LNF-02/003 (P)

  The KLOE Collaboration: A. Aloisio, F. Ambrosino, A. Antonelli, M. Antonelli, C. Bacci, G. Bencivenni, S. Bertolucci, C. Bini, C. Bloise, V. Bocci, F. Bossi,P. Branchini, S. A. Bulychjov, G. Cabibbo, R. Caloi, P. Campana, G. Capon, G. Carboni, M. Casarsa, V. Casavola, G. Cataldi, F. Ceradini, F. Cervelli, F. Cevenini, G. Chiefari, P. Ciambrone, S. Conetti, E. DeLucia, G. DeRobertis, P. DeSimone, G. De Zorzi, S. Dell'Agnello, A. Denig, A. DiDomenico, C. Di Donato, S. Di Falco, A. Doria, M. Dreucci, O. Erriquez, A. Farilla, G. Felici, A. Ferrari, M. L. Ferrer, G. Finocchiaro, C. Forti, A. Franceschi, P. Franzini, C. Gatti, P. Gauzzi, S. Giovannella, E. Gorini, F. Grancagnolo, E. Graziani, S. W. Han, M. Incagli, L. Ingrosso, W. Kim, W. Kluge, C. Kuo, V. Kulikov, F. Lacava, G. Lanfranchi, J. Lee-Franzini, D. Leone, F. Lu, M. Martemianov, M. Matsyuk, W. Mei, L. Merola, R. Messi, S. Miscetti, M. Moulson, S. Muller, F. Murtas, M. Napolitano, A. Nedosekin, F. Nguyen, M. Palutan, L. Paoluzi, E. Pasqualucci, L. Passalacqua, A. Passeri, V. Patera, E. Petrolo, G. Pirozzi, L. Pontecorvo, M. Primavera, F. Ruggieri, P. Santangelo, E. Santovetti, G. Saracino, R. D. Schamberger, B. Sciascia, A. Sciubba, F. Scuri, I. Sfiligoi, T. Spadaro, E. Spiriti, G. L. Tong, L. Tortora, E. Valente, P. Valente, B. Valeriani, G. Venanzoni, S. Veneziano, A. Ventura, Y. Xu, Y. Yu, Y. Wu

  Study of the Decay $\phi \to \pi^0 \pi^0 \gamma$ with the KLOE Detector

  Submitted to Phys. Lett. B

- LNF-02/004 (P)

  The KLOE Collaboratoin: A. Aloisio, F. Ambrosino, A. Antonelli, M. Antonelli, C. Bacci, R. Baldini-Ferroli, G. Bencivenni, S. Bertolucci, C. Bini, C. Bloise, V. Bocci, F. Bossi, P. Branchini, S. A. Bulychjov, G. Cabibbo, R. Caloi, P. Campana, G. Capon, G. Carboni, M. Casarsa, V. Casavola, G. Cataldi, F. Ceradini, F. Cervelli, F. Cevenini, G. Chiefari, P. Ciambrone, S. Conetti, E. De Lucia, G. De Robertis, P. De Simone, G. De Zorzi, S. Dell'Agnello, A. Denig, A. Di Domenico, C. Di Donato, S. Di Falco, A. Doria, M. Dreucci, O. Erriquez, A. Farilla, G. Felici, A. Ferrari, M. L. Ferrer, G. Finocchiaro, C. Forti, A. Franceschi, P. Franzini, C. Gatti, P. Gauzzi, S. Giovannella, E. Gorini, F. Grancagnolo, E. Graziani, S. W. Han, M. Incagli, L. Ingrosso, W. Kluge, C. Kuo, V. Kulikov, F. Lacava, G. Lanfranchi, J. Lee-Franzini, D. Leone, F. Lu, M. Martemianov, M. Matsyuk, W. Mei, L. Merola, R. Messi, S. Miscetti, M. Moulson, S. Mueller, F. Murtas, M. Napolitano, A. Nedosekin, F. Nguyen, M. Palutan, L. Paoluzi, E. Pasqualucci, L. Passalacqua, A. Passeri, V. Patera, E. Petrolo, G. Pirozzi, L. Pontecorvo, M. Primavera, F. Ruggieri, P. Santangelo, E. Santovetti, G. Saracino, R. D. Schamberger, B. Sciascia, A. Sciubba, F. Scuri, I. Sfiligoi, T. Spadaro, E. Spiriti, G. L. Tong, L. Tortora, E. Valente, P. Valente, B. Valeriani, G. Venanzoni, S. Veneziano, A. Ventura, Y. Xu, Y. Yu

Measurement of $\Gamma(K_S \to \pi^+ \pi^- (\gamma))/(K_S \to \pi^0 \pi^0)$

Submitted to Phys. Lett. B

- LNF-02/005 (IR)

  E. Bernieri, A. Balerna, A. Esposito, U. Denni, M. Chiti, M.A. Frani and V. Tullio

  Environment and Nuclear Physics: The GEDI Experiment

- LNF-02/006 (P)

  G. Beer, A.M. Bragadireanu, e ,W. Breunlich, M. Cargnelli, C. Curceanu (Petrascu), J.-P. Egger, H. Fuhrmann, C. Guaraldo, M. Giersch, M. Iliescu, T. Ishiwatari, K. Itahashi, B. Lauss, V. Lucherini, L. Ludhova, J. Marton, F. Mulhauser, T. Ponta, A.C. Sanderson, L.A. Schaller, D.L. Sirghi, F. Sirghi and J. Zmeskal

  A New Method to Obtain a Precise Value of the Mass of the Charged Kaon

  To appear in Phys Lett. B 535 (2002) 52

- LNF-02/007 (P)

  The KLOE Collaboratoin: A. Aloisio, F. Ambrosino, A. Antonelli, M. Antonelli, C. Bacci, G. Bencivenni, S. Bertolucci, C. Bini, C. Bloise, V. Bocci, F. Bossi, P. Branchini, S. A. Bulychjov, G. Cabibbo, R. Caloi, P. Campana, G. Capon, G. Carboni, M. Casarsa, V. Casavola, G. Cataldi, F. Ceradini, F. Cervelli, F. Cevenini, G. Chiefari, P. Ciambrone, S. Conetti, E. De Lucia, G. De Robertis, P. De Simone, G. De Zorzi, S. Dell'Agnello, A. Denig, A. Di Domenico, C. Di Donato, S. Di Falco, A. Doria, M. Dreucci, O. Erriquez, A. Farilla, G. Felici, A. Ferrari, M. L. Ferrer, G. Finocchiaro, C. Forti, A. Franceschi, P. Franzini, C. Gatti, P. Gauzzi, S. Giovannella, E. Gorini, F. Grancagnolo, E. Graziani, S. W. Han, M. Incagli, L. Ingrosso, W. Kim, W. Kluge, C. Kuo, V. Kulikov, F. Lacava, G. Lanfranchi, J. Lee-Franzini, D. Leone, F. Lu, M. Martemianov, M. Matsyuk, W. Mei, L. Merola, R. Messi, S. Miscetti, M. Moulson, S. M\""uller, F. Murtas, M. Napolitano, A. Nedosekin, F. Nguyen, M. Palutan, L. Paoluzi, E. Pasqualucci, L. Passalacqua, A. Passeri, V. Patera, E. Petrolo, G. Pirozzi, L. Pontecorvo, M. Primavera, F. Ruggieri, P. Santangelo, E. Santovetti, G. Saracino, R. D. Schamberger, B. Sciascia, A. Sciubba, F. Scuri, I. Sfiligoi, T. Spadaro, E. Spiriti, G. L. Tong, L. Tortora, E. Valente, P. Valente, B. Valeriani, G. Venanzoni, S. Veneziano, A. Ventura, Y. Xu, Y. Yu, Y. Wu

  Study of the Decay $\phi \to \eta\pi^0 \gamma$ *with the KLOE Detector*

  Submitted Phys. Lett. B

- LNF-02/008 (IR)

  D.Alesini, C.Biscari, R.Boni, A.Clozza, G.Di Pirro, A.Drago, A.Gallo, A.Ghigo, F.Marcellini, C.Milardi, M.A.Preger, C.Sanelli, F.Sannibale, M.Serio, F.Sgamma, A.Stecchi, A.Stella, M.Zobov, R.Bossart, H.Braun, P.Brown, G.Carron, V.Chohan,

R.Corsini, E.D'Amico, S.Deghaye, J.P.Delahaye, F.Di Maio, S.Doebert, B.Dupuy, G.Geschonke, L.Gröning, G.Guignard, H.Hellgren, S.Hutchins, J.H.Lewis, E.Jensen, G.McMonagle, A.Millich, J.Monteiro, J.P.Delahaye, T.Otto, P.Pearce, E.Peschardt, R.Pittin, M.Poehler, J.P.Potier, L.Rinolfi, T.Risselada, G.Rossat, P.Royer, D.Schulte, J.Sladen, G.Suberlucq, I.Syratchev, F.Tecker, H.Trautner, L.Thorndahl, I.Wilson, W.Wünsch, A.Yeremian, R.Miller, R.Ruth, R.Koontz, I.N.Ross, E. Bente, G. Valentine, G.Bienvenu, M.Bernard, M.Omeich, R.Roux, T.Garvey

CTF3 Design report

- LNF-02/009 (P)

  S. Della Longa, M. Benfatto

  Probing the Coordination and Geometry of Heme-iron Ligands in Hemoproteins by XANES (X-ray Absorption Near Edge Structure)

  Submitted to Transword Research Network
- LNF-02/010 (IR)

  M. Aleksa, J.F. Amand, R. Garoby, F. Gerigk, K.Hanke, E.B. Holzer, E.S. Kim, A. Lombardi, M. Migliorati, S. Russenschuck, F. Tazzioli, C. Vaccarezza

  Beam Dynamics Study of a Muon Ionization Cooling Experiment

- LNF-02/011 (IR)

  S. Bartalucci

  High Intensity, Pulsed, Slow Positron and Neutron Sources at INFN – Frascati

- LNF-02/012 (IR)

  AA. VV.
- *LNF Spring School 2002*

- LNF-02/013 (P)

  F. Celani, A. Spallone, P. Marini, V. di Stefano, M. Nakamura, E. Righi, G. Trenta, P. Quercia, A. Mancini, G. D'Agostaro, C. Catena, S. Sandri, C. Nobili, V. Andreassi

  Evidence of Anomalous Tritium Excess in D/Pd Overloading Experiments

  Invited paper at the ICCF9, Beijing (China), 19,25 May 2002, to be published on Conference Proceedings by Springer–Verlag

- LNF-02/014 (P)

  F. Celani, A. Spallone, P. Marini, V. di Stefano, M. Nakamura, A. Mancini, G. D'Agostaro, E. Righi, G. Trenta, P. Quercia, C. Catena

Electrochemical D loading of Palladium wires by heavy ethyl-alcohol and water electrolyte, related to Ralstonia bacteria problematics

Invited paper at the ICCF9, Beijing (China), 19-25 May 2002, to be published on Conference Proceedings by Springer–Verlag

- LNF-02/015 (P)

  A. Spallone, F. Celani, P. Marini, V. Di Stefano

  Experimental studies to achieve H/Pd loading ratio close to 1 in thin wires, using different electrolytic solutions

  Contributed paper, Poster Session at ICCF9 , Beijing 19_25 May 2002 (China), to be published on Proceeedings Conference by Springer-Verlag

- LNF-02/016 (P)

  Accelerator Division

  Papers Presented at EPAC 2002

  Contributions to the: 8th European Particle Accelerator Conference (EPAC 2002), La Villette – Paris, 3 – 7 June 2002

- LNF-02/017 (P)

  F. Tombolini, M.Franca Brigatti, A. Marcelli, G. Cibin, A. Mottana, G. Giuli

  Local and average Fe distribution in trioctahedral micas: Analysis of Fe K-edge XANES spectra in the phlogopite-annite and phlogopite-tetra-ferriphlogopite joins on the basis of single-crystal XRD refinements

  Submitted to European Journal of Mineralogy Vol. 14/6, 2002

- LNF-02/018 (P)

  M. Pedio, Z. Y. Wu, M. Benfatto, A. Mascaraque, E. Michel, C. Ottaviani, C. Crotti, M. Peloi, M. Zacchigna, C. Comicioli

  NEXAFS Experiment and Multiple Scattering Calculations on KO2: effects on the π resonance in the solid phase

  To be published on Phys. Rev. B

- LNF-02/019 (P)

  S. Bellucci, A. Deriglazov, A. Galajinsky

  Geometry of an N=4 Twisted String

  Submitted to Physical Review D

- LNF-02/020 (P)

  S. Bellucci, E. Ivanov, S. Krivonos

  AdS/CFT Equivalence Transformation

  Submitted toPhysical Review D

- LNF-02/021 (P)

  F. Nichitiu, P. Gianotti, C. Guaraldo, A. Lanaro, V. Lucherini, C. Petrascu, A. Rosca, G. Bonomi, M. P. Bussa, A. Donzella, E. Lodi Rizzini, L. Venturelli, A. Zenoni, A. Bertin, M. Bruschi, M. Capponi, S. De Castro, D. Galli, B. Giacobbe, U. Marconi, I. Massa, M. Piccinini, N. Semprini-Cesari, R. Spighi, S. Vecchi, V. Vagnoni, M. Villa, A. Vitale, A. Zoccoli, C. Cicalò, A. De Falco, A. Masoni, S. Mauro, G. Puddu, G. Usai, O. E. Gorchakov, S. N. Prakhov, A. M. Rozhdestvensky, V. I. Tretyak, M. Poli, V. Filippini, A. Fontana, P. Montagna, A. Rotondi, P. Salvini, F. Balestra, L. Busso, P. Cerello, O. Deniso, R. Garfagnini, A. Grasso, A. Maggiora, A. Panzarasa, D. Panzieri, F. Tosello, E. Botta, T. Bressani, D. Calvo, S. Costa, D. D'Isep, A. Feliciello, A. Filippi, S. Marcello, M. Agnello, F. Iazzi, B. Minetti, N. Mirfakhrai, S. Tessaro

  Study of the $K^+K^-\pi^+\ \pi\ \pi^0$ *final state in antiproton annihilation at rest in gaseous hydrogen at NTP with the OBELIX spectrometer*

  Submitted to Phys. Lett. B

- LNF-02/022 (P)

  Editors in Chief: W. Chou and J.M. Jowett - Editors: C. Biscari, S. Chattopadhyay, S. Ivanov, H. Mais, J. Wei, and C. Zhang

  ICFA - International Committee for Future Accelerators

  Sponsored by the Particles and Fields Commission of IUPAP

  Beam Dynamics, Newsletter, No. 28

- LNF-02/023 (P)

  V. Lucherini, A. M. Bragadireanu, G. Beer, C. Curceanu (Petrascu), J.-P. Egger, C. Guaraldo, M. Iliescu, T. Ponta, D.L. Sirghi, F. Sirghi, J. Zmeskal

  The DEAR Kaon Monitor at DAΦNE

  Submitted to Elsevier Science

- LNF-02/024 (P)

  AA.VV

  Activity Report 2001

- LNF-02/025 (P)

  M. Benfatto S. Della Longa C.R. Natoli

  The MXAN Procedure: a new Metod for Analysing the Xanes Spectra of Metalloproteins to Obtain Structural Quantitative Information

  Journal of Synhrotron Radiation

- LNF-02/026 (P)

  C.R. Natoli, M. Benfatto S. Della Longa, K. Hatada

  X-Ray Absorption Spectroscopy: State-of-the-art Analysis

  Journal of Synhrotron Radiation

- LNF-02/027 (Thesis)

  Manuela Boscolo

  Beam-Beam Interaction Effects in DAΦNE

- LNF-02/028 (P)

  F. Ronga

  Experimental Review of Atmospheric Neutrino Oscillations

  Invited talk: Vulcano Workshop 2002, Vulcano 20-25 May, 2002 (Italy)

- LNF-02/029 (P)

  Stefano Bianco on behalf of the FOCUS and E687 Collaborations:. L. Agostino, G. Alimonti, J.C. Anjos, V. Arena, R. Baldini-Ferroli, S. Barberis, I. Bediaga, G. Bellini, L. Benussi, J.M. Bishop, G. Boca, G. Bonomi, M. Boschini, D. Brambilla, D. Buchholz, J.N. Butler, B. Caccianiga, A. Calandrino, S. Carrillo, E. Casimiro, N.M. Cason, C. Castoldi, C. Cawlfield, A. Cerutti, H.W.K. Cheung, G. Chiodini, K. Cho, Y.S. Chung, S. Cihangir, L. Cinquini, L. Cinquini, D. Claes, N. Copty, R. Culbertson, J.P. Cumalat, C. Dallapiccola, P. D'Angelo, T.F. Davenport III J.M. de Miranda, M. DiCorato, P. Dini, A.C. dos Reis, L. Edera, D. Engh, C.J. ennedy, S. Erba, F.L. Fabbri, P.L. Frabetti, I. Gaines, P.H. Garbincius, R. Gardner, L.A. Garren, M. Giammarchi, G. Gianini, J.F. Ginkel, B. Gobbi C. Göobel, E. Gottschalk, S.A. Gourlay, R. Greene, T. Handler D.J. Harding, H. Hernandez, M. Hosack, P. Inzani, W.E. Johns, J.S. Kang, P.H. Kasper, D.Y. Kim, G.N. Kim, B.R. Ko, A.E. Kreymer, A. Kryemadhi R. Kutschke, J.W. Kwak, Y. Kwon P. Lebrun, K.B. Lee, F. Leveraro, G. Liguori, T.F. Lin, J.M. Link, A.M. Lopez, J. Magnin, S. Malvezzi, A. Massafferri, D. Menasce, H. Mendez, L. Mendez, M. Merlo, E. Meroni, M. Mezzadri, L. Milazzo, A. Mirles, E. Montiel, L. Moroni, S.S. Myung M.S. Nehring, D. Olaya, B. O'Reilly, D. Pantea, V.S. Paolone, K.S. Park, H. Park, D. Pedrini, I.M. Pepe, L. Perasso, C. Pontoglio, F. Prelz, M. Purohit, D.L. Puseljic, J. Quinones, A. Rahimi, J.E.

Ramirez, S.P. Ratti, M. Reyes, C. Riccardi, C. Rivera, M. Rovere, R.C. Ruchti, S. Sala A. Sala, M. Sales, A. Sánchez-Hernández, I. Segoni M. Sheaff P.D. Sheldon, W.D. Shephard, S. Shukla, F. Simõ, K. Stenson, J.A. Swiatek, P. Torre, D. Torretta, C. Uribe, E.W. Vaandering F. Vasquez L. Viola, M. Vittone, P. Vitulo, M.S. Webster, J.R. Wilson, J. Wiss, Z.Y. Wu, P.M. Yager, A. Zallo, Y. Zhang

Light Quark Spectroscopy Results from FOCUS and E687

Proc. International Conference on High-Energy Physics (ICHEP02), Amsterdam, The Nederlands, 2002

- LNF-02/030 (P)

  M. Incurvati, F.Terranova

  Modeling Skin Effect in Larrge Magnetized Iron Detectors

\Submitted to Nucl. Instr. & Meth.

- LNF-02/031 (P)

  F. Celani, A. Spallone, P. Marini, V. di Stefano, M. Nakamura, A. Mancini, G. D'Agostaro, E. Righi, G. Trenta, P. Quercia, C. Catena, V. Andreassi, F. Fontana, D. Garbelli, L. Gamberale, D. Azzarone, E. Celia, F. Falcioni, M.Marchesini, E. Novaro

  Unexpected Detection of New Elements in Electrolytic Experiments with Deuterated Ethyl-alcohol, Pd Wire, Sr and Hg Salts

  Proc.of 4th Meeting of Japan CF Research Society, Morioka, (Japan) October 17-18, (2002), Ed.: by Hiroshi Yamada, pp. 17-21

2 Frascati Physics Series

Volume XXIV

International School of Space Science –2001 Course on: Astroparticle and Gamma-ray Physics in Space

Eds. A. Morselli, P. Picozza

L'Aquila, Italy, August 30 –September 7, 2000

Volume XXV

TRDs for the 3rd Millennium Workshop on Advanced Transition Radiation Detectors for Accelerator and Space Applications

Eds. N. Giglietto, P. Spinelli

Bari, Italy, September 20-23, 2001

Volume XXVI

KAON 2001, International Conference on CP Violation

Eds. F. Costantini, G. Isidori, M. Sozzi

Pisa Italy, June 12th –17th, 2001

Volume XXVII – *Special Issue*

Les Rencontres de Physique de la Vallée d'Aoste -Results and Perspectives in Particle Physics

Ed. M. Greco

La Thuile, Aosta Valley, March 3-9, 2002

Volume XXVIII

Heavy Quarks at Leptons 2002

Eds. G.Cataldi, F.Grancagnolo, R Perrino, S.Spagnolo

Vietri sul mare (Italy), May 27th – June 1st, 2002

Volume XXIX

Workshop on Radiation Dosimetry: Basic Technologies, Medical Applications, Environmental Applications

Ed. A. Zanini

Rome (Italy), February 5–6, 2002

Glossary

These are the acronyms used in each status report to describe personnel qualifications other than Staff Physicist:

Art. 15	Term Contract (Technician)
Art. 23	Term Contract (Scientist)
Ass.	Associated Scientist
Ass. Ric.	Research Associate
Bors.	Fellowship holder
Bors. PD	Post–Doc Fellow
Dott.	Graduate Student
Laur.	Undergraduate Student
Osp.	Guest Scientist
Perfez.	Post–Laurea Student
Resp.	Local Spokesperson
Resp. Naz.	National Spokesperson
Specializ.	Post–Laurea Student
Tecn.	Technician